

A STOCHASTIC FRAMEWORK FOR EVALUATING
FOREST MANAGEMENT IMPACTS ON WATER
QUALITY FROM WATERSHEDS IN THE
OUACHITA MOUNTAINS

By

KENNETH W. TATE

Bachelor of Science
Oklahoma State University
Stillwater, Oklahoma
1989

Master of Science
Oklahoma State University
Stillwater, Oklahoma
1991


Submitted to the Faculty of the
Graduate College of the
Oklahoma State University
in partial fulfillment of
the requirements for
the Degree of
DOCTOR OF PHILOSOPHY
May, 1995

A STOCHASTIC FRAMEWORK FOR EVALUATING
FOREST MANAGEMENT IMPACTS ON WATER
QUALITY FROM WATERSHEDS IN THE
OUACHITA MOUNTAINS


Thesis Approved:

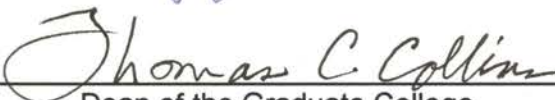


Thesis Adviser









Dean of the Graduate College

ACKNOWLEDGMENTS

I wish to thank my major advisor, Dr. D.J. Turton for the support he provided throughout my degree. I would like to thank Drs. C.T. Haan, E.L. Miller, and D.L. Nofziger for serving as members of my graduate committee. I also thank Dr. G.J. Sabbagh for his assistance in this project.

I am thankful for the USDA National Needs Fellowship program which provided the financial support enabling me to pursue this degree. I am appreciative of the OSU Department of Forestry, the OSU Department of Biosystems and Agricultural Engineering, and Weyerhaeuser Company for additional support throughout my degree.

The support and encouragement of my family, Kenneth, Carolyn, and Pamela, has been the foundation of all that I have achieved. Special thanks go to Brock and Sheila, John, Edward, Lisa, and Julie for their support and friendship.

To my wife, Ghisleli. There cannot exist a more patient, enduring, caring, or loving person. Thank you for putting up with me, I would not be here today if it were not for you.

TABLE OF CONTENTS

Chapter	Page
I. INTRODUCTION	1
Total Maximum Daily Load	2
Forest Management and NPS Pollution in the Ouachita Mountains	6
Large Clear Cut Watersheds and TMDLs in the Ouachita Mountains	7
Objectives	9
II. METHODS.....	12
Clayton Lake and Clayton Lake Watershed.....	12
Definitions	13
Management Unit.....	14
Clearcutting.....	14
Management Cycle	14
Active Clearcutting Period.....	15
Clearcutting Level	15
Recovery Period.....	15
Recovery Status.....	16
Clearcutting Management Scenario	16
Worst Case Condition	17
General Description of the Stochastic Framework	17
Application of the Stochastic Framework to Clayton Lake Watershed.....	18
Model Selection.....	18
Clearcutting Management Scenarios and Identification of the Worst Case Condition	19
Clearcutting Management Scenario	19
Worst Case Condition	21
Monte Carlo Simulation Techniques	23
Analysis.....	27
Weather	27
Annual Maximum Daily Q, TSS, PHOS, and NO3N	27
Forest Roads.....	29
III. MODEL CALIBRATION	37
Introduction	37

Model Performance Evaluation Methods.....	38
Observed Data	39
EPIC System File Structure.....	41
Basic User-Supplied Data File	41
Crop Parameter File.....	42
Tillage Parameter File	43
Parameter Selection.....	43
Tillage and Crop Parameter Files.....	44
Basic User-Supplied Data Files.....	44
Clear Cut Watershed.....	45
Initial Parameter Estimates	45
Calibration and Model Performance Evaluation	47
Initial and Subsequent Model Runs.....	47
Hydrology.....	47
TSS.....	47
PHOS	48
NO3N.....	48
Final Model Run.....	49
Daily Evaluation of the Final Model	49
Annual Maximum Daily Q and TSS, PHOS, and NO3N Loading.....	50
Undisturbed Watershed	50
Initial Parameter Estimates	51
Calibration and Model Performance Evaluation	51
Initial and Subsequent Model Runs.....	51
Hydrology.....	51
TSS.....	52
PHOS	52
NO3N.....	53
Final Model Run.....	53
Daily Evaluation of the Final Model	54
Annual Maximum Daily Q and TSS, PHOS, and NO3N Loading.....	54
Discussion.....	54
Conclusion	60
 IV. RESULTS AND DISCUSSION: APPLICATION OF THE STOCHASTIC FRAMEWORK TO CLAYTON LAKE WATERSHED.....	 88
Simulated Weather.....	88
Quantification of Worst Case Daily Loading.....	93
Descriptive Statistics	93
Population Distribution Information	94
Risk Assessment.....	97
 V. CONCLUSIONS	 130
 LITERATURE CITED	 133
 APPENDIXES	 137

APPENDIX I - EPIC: MODEL DEVELOPMENT AND DOCUMENTATION.....	137
APPENDIX II - CLEAR CUT WATERSHED: RESULTS OF MODEL PERFORMANCE EVALUATIONS.....	168
APPENDIX III - UNDISTURBED WATERSHED: RESULTS OF MODEL PERFORMANCE EVALUATIONS.....	205

LIST OF TABLES

Table	Page
1. Annual NPS loads reported in the Ouachita Mountains. CC indicates a clear cut treatment and UN indicates a control watershed.....	11
2. Regional estimates of average annual P, Q, ET, and PRK as well as the percentage of P lost to Q, ET, and PRK for north-central Pushmataha County	31
3. Area (A), percent of Clayton Lake Watershed (%), average land slope (S), maximum travel distance (L) for each management unit	31
4. Management units ranked from most to least erosive based first upon average land slope (S) and area (A).....	31
5. Allocation of management units for each clearcutting level. A is the area (ha) in each recovery status and % is the percent of Clayton Lake Watershed in each recovery status	32
6. Parameters contained in the Basic-User-Supplied data File	61
7. Parameters contained within the Crop Parameter File	65
8. Parameters contained within the Tillage File	66
9. Tillage operations available within the Tillage Parameter File	67
10. Parameters determined to be candidates for modification during model calibration	68
11. Initial estimates for program control codes	68
12. Initial estimates for general information parameters.....	69
13. Estimates of monthly weather parameters provided for Smithville, OK.....	70
14. Wind erosion parameters set to default values (Dumesnil 1993)	71
15. Initial estimates of soil parameters for soil layers 1 through 8 of the Camasaw Soil Series	72

16.	Initial estimates of general soil profile parameters for the Camasaw Soil Series	73
17.	Default values for parameters NIRR through FDSF	73
18.	Management operation schedule used to simulate recovery period.....	73
19.	Observed and simulated annual maximum daily Q (mm), TSS ($t\ ha^{-1}$), PHOS ($kg\ ha^{-1}$), and NO ₃ N ($kg\ ha^{-1}$) on WS-I for the recovery period.....	74
20.	Initial estimates for program control codes.....	75
21.	Initial estimates for general information parameters.....	75
22.	Initial estimates of general soil profile parameters for the Camasaw Soil Series	76
23.	Management operation schedule used to simulate U/R recovery period.....	76
24.	Observed and simulated annual maximum daily Q (mm), TSS ($t\ ha^{-1}$), PHOS ($kg\ ha^{-1}$), and NO ₃ N ($kg\ ha^{-1}$) on WS-III	77
25.	Descriptive statistics for simulated and observed weather records	100
26.	Descriptive statistics for annual rainfall, annual maximum daily TSS, PHOS, and NO ₃ N loadings at the CC00 clearcutting level resulting from non-random selection of IGN	101
27.	Descriptive statistics for output variables of the stochastic framework.....	102

LIST OF FIGURES

Figure	Page
1. Clayton Lake Watershed divided into 11 management units	33
2. Allocation of management units on Clayton Lake Watershed for the CC33 clearcutting management scenario.....	34
3. Allocation of management units on Clayton Lake Watershed for the CC66 clearcutting management scenario.....	35
4. Allocation of management units on Clayton Lake Watershed for the CC100 clearcutting management scenario.....	36
5. Location of WS-I and WS-III on Clayton Lake Watershed	78
6. EPIC system file structure (Dumesnil 1993)	79
7. Observed and simulated annual maximum daily Q for WS-I	80
8. Observed and simulated annual maximum daily TSS loading for WS-I.....	81
9. Observed and simulated annual maximum daily PHOS loading for WS-I.....	82
10. Observed and simulated annual maximum daily NO3N loading for WS-I.....	83
11. Observed and simulated annual maximum daily Q for WS-III	84
12. Observed and simulated annual maximum daily TSS loading for WS-III.....	85
13. Observed and simulated annual maximum daily PHOS loading for WS-III.....	86
14. Observed and simulated annual maximum daily NO3N loading for WS-III.....	87
15. Simulated annual rainfall versus Monte Carlo run	103

16.	Correlogram for simulated annual rainfall.....	104
17.	Correlogram for simulated annual maximum daily TSS loading.....	105
18.	Correlogram for simulated annual maximum daily PHOS loading.....	106
19.	Correlogram for simulated annual maximum daily NO3N loading.....	107
20.	Simulated annual rainfall under non-random IGN selection versus Monte Carlo run	108
21.	Correlogram for simulated annual rainfall under non-random IGN selection.....	109
22.	Correlogram for simulated annual maximum daily TSS loading under non-random IGN selection.....	110
23.	Correlogram for simulated annual maximum daily PHOS loading under non-random IGN selection.....	111
24.	Correlogram for simulated annual maximum daily NO3N loading under non-random IGN selection.....	112
25.	Simulated annual rainfall under random IGN selection versus Monte Carlo run	113
26.	Correlogram for simulated annual rainfall under random IGN selection.....	114
27.	Correlogram for simulated annual maximum daily TSS loading under random IGN selection.....	115
28.	Correlogram for simulated annual maximum daily PHOS loading under random IGN selection.....	116
29.	Correlogram for simulated annual maximum daily NO3N loading under random IGN selection.....	117
30.	Mean annual maximum daily Q at the CC33 clearcutting management scenario	118
31.	Mean annual maximum daily TSS loading at the CC33 clearcutting management scenario.....	119
32.	Mean annual maximum daily PHOS loading at the CC33 clearcutting management scenario.....	120

33.	Mean annual maximum daily NO ₃ N loading at the CC33 clearcutting management scenario.....	121
34.	Relative frequency of Q at the CC00, CC33, CC66, and CC100 clearcutting management scenario. Class interval equals 500,000 m ³	122
35.	Relative frequency of TSS at the CC00, CC33, CC66, and CC100 clearcutting management scenario. Class interval equals 200 t	123
36.	Relative frequency of PHOS at the CC00, CC33, CC66, and CC100 clearcutting management scenario. Class interval equals 100 kg.....	124
37.	Relative frequency of NO ₃ N at the CC00, CC33, CC66, and CC100 clearcutting management scenario. Class interval equals 100 kg.....	125
38.	Probability plot for annual maximum daily Q at the CC00, CC33, CC66, and CC100 clearcutting management scenarios.....	126
39.	Probability plot for annual maximum daily TSS at the CC00, CC33, CC66, and CC100 clearcutting management scenarios.....	127
40.	Probability plot for annual maximum daily PHOS at the CC00, CC33, CC66, and CC100 clearcutting management scenarios.....	128
41.	Probability plot for annual maximum daily NO ₃ N at the CC00, CC33, CC66, and CC100 clearcutting management scenarios.....	129

CHAPTER I

INTRODUCTION

Forest watershed managers are often interested in quantifying the potential nonpoint source (NPS) pollution generation from different management practices. NPS pollution generation is often a major consideration when selecting a management plan for a large forest watershed. NPS pollution generation from forest watersheds is in large part a function of rainfall. Thus, NPS pollution generation from forest watersheds is a stochastic process. When estimating potential NPS pollution generation from different watershed management plans one should account for the variability due to different but equally likely weather sequences. In reality, watershed management decisions are often based upon the results of short-term, small-scale experimental study results. Haan et al. (1994) discuss the characterization of variability due to natural weather sequences as well as the care which must be taken when basing conclusions on results representing single weather sequences.

A method of quantifying NPS loading and the variability in NPS loading from large clear cut watersheds in the Ouachita Mountains would be a valuable tool for forest managers in the region. The concept of total maximum daily load (TMDL) has focused attention on quantifying daily NPS loading from large watersheds. Thus, a method of quantifying daily NPS loading and the variability in daily NPS loading due to natural weather sequences is needed for the Ouachita Mountains.

Total Maximum Daily Load

The TMDL concept was introduced in the Clean Water Act of 1972 (PL 92-500 Sec. 303 (d)). A TMDL is a tool for implementing State water quality standards and is based on the relationship between pollution sources and in-stream water quality conditions. A TMDL establishes the allowable loadings or other quantifiable parameters for a waterbody and thereby provides the basis for States to establish water quality-based controls (USEPA 1991). TMDLs are developed based upon the assimilative capacity of a given waterbody. Point and nonpoint source (NPS) pollution contributors must be managed such that they do not combine to generate daily pollutant loadings in exceedance of estimated TMDLs.

The TMDL concept is one portion of the water quality-based approach to pollution control. A brief description of the water quality-based approach to pollution control directed by the Clean Water Act of 1987, and the role TMDLs play in it is warranted. The USEPA (1991) states that a water quality-based approach to pollution control emphasizes the overall quality of water within a waterbody and provides a mechanism (TMDL) through which the amount of pollution entering a waterbody is controlled based upon the intrinsic conditions of that body of water and the standards set to protect it. A water quality standard defines the water quality goals of a waterbody by designating the use or uses to be made of the water, by setting criteria necessary to protect the uses, and by preventing degradation of water quality through antidegradation provisions. The water quality-based approach to pollution control is comprised of the following steps: 1. identification of waterbodies in the State which are water quality-limited in terms of the State's water quality standards; 2. prioritization of waterbodies from most to least water quality-limited; 3. development of TMDLs for the

water quality-limited waterbodies in the order of priority; 4. implementation of the control actions identified during the TMDL development; 5. assessment of the success of the water quality-based pollution control actions through monitoring programs.

Development of a working definition of TMDL first requires the definition of several associated terms. All definitions are taken from the United States Environmental Protection Agency (USEPA 1991). Daily loading capacity (LC) is the greatest amount of loading of a given pollutant that a water can receive on a daily basis without violating water quality standards. Loading allocation (LA) is the portion of a receiving water's daily loading capacity that is attributed either to one of its existing or future nonpoint sources of pollution or to natural background sources. Wasteload allocation (WLA) is the portion of a receiving water's daily loading capacity that is allocated to one of its existing or future point sources of pollution. A TMDL serves as a means of assigning portions of the daily loading capacity to WLAs and LAs contributing to a water quality-limited waterbody. A TMDL is the sum of the loadings contributed from the WLAs and LAs, and cannot exceed the LC. A margin of safety (MOS) is incorporated into the estimated TMDL to account for uncertainty in the estimates of LC, LA, and WLA. A TMDL can be represented as shown in the following equation.

$$\text{TMDL} = \text{LC} = \text{WLA} + \text{LA} + \text{MOS} \quad 1.1$$

LC = Loading Capacity

WLA = Point Source Contribution

LA = Nonpoint Source Contribution

MOS = Margin of Safety

The TMDL development process involves the following steps: 1. definition of the pollutant types (identification of the cause of the water quality impairment); 2. quantification of pollutant loadings from all sources (identification of the source of the water quality impairment); 3. estimation of the waterbody's assimilative capacity for the identified pollutants (LC); 4. analysis of the potential to reduce loading from point and nonpoint sources under alternate management; 5. allocation of the LC among pollution sources on the watershed (WLAs and LAs) based upon reductions estimated in step 4 and some MOS; 6. USEPA approval of the TMDL; 7. establishment of monitoring programs to assess water quality following implementation; 8. determination of compliance with water quality standards (if not then revise the TMDL, if so then proceed to step 9); 9. removal of waterbody from water quality-limited list; and 10. continuation of the monitoring program. The USEPA recommends that State's develop TMDLs on a watershed basis.

A significant amount of information about daily loading is required to develop meaningful TMDLs. The amount of information available on the sources, fate, and transport of the pollutant of interest will be extremely limited for most water quality-limited waterbodies. Such information may often be nonexistent. This is especially the case when nonpoint source pollution is involved. However, the USEPA (1991) specifically states that lack of information about certain types of pollution problems (for example, those associated with nonpoint sources or with certain toxic pollutants) should not be used as a reason to delay implementation of water quality-based pollution control measures.

In the absence of adequate information, emphasis is placed upon developing a monitoring program which will begin to provide the information in question, upon the use of water quality models to simulate daily loading in lieu of forthcoming data, and

upon the development of a MOS to account for the uncertainty introduced by modeling. Modeling schemes may be used to simulate loading from nonpoint sources on the watershed, to evaluate the effectiveness of potential Best Management Practices (BMPs), and to evaluate alternative pollution allocation scenarios. A MOS is often incorporated by using conservative assumptions and by considering reasonable worst case conditions during TMDL development (USEPA 1991). In addition, Monte Carlo simulation techniques can be utilized during the modeling process. The water quality model is run a large number of times based upon random input, and model outputs are ranked to determine a frequency distribution which may be compared to in-stream criteria to determine if water quality standards are met (USEPA 1991).

On a watershed with both point and nonpoint sources contributing loadings to a water quality-limited waterbody, the only Federally enforceable pollution controls are those for point sources through National Pollutant Discharge Elimination System (NPDES) permitting (USEPA 1991). Thus, when allocating loads among point and nonpoint sources on a watershed, assurances must be obtained from those managing the nonpoint sources that they will implement the BMPs determined most effective during TMDL development. If such assurances cannot be obtained, the point source operators on the watershed must accommodate the entire load reduction required to meet water quality standards. State and local laws may be utilized to enforce the installation of BMPs. Also, funds from Federal, State, and local subsidy programs may be withheld until BMPs are installed. It is ultimately the State's responsibility to establish TMDLs such that water quality standards are attained for all water quality-limited waters in the State.

Forest Management and NPS Pollution in the Ouachita Mountains

Land use in the Ouachita Mountains of southeastern Oklahoma is dominated by silviculture. Clear cut harvesting and forest roads have been identified as silvicultural practices which generate nonpoint source pollution in the region (Scoles et al. 1994). In general, research conducted on small experimental watersheds in the Ouachita Mountains indicates that the impacts of clearcutting on water quality are short lived. Miller (1984) reported a significant increase in sediment yield during the first three years following clearcutting on three small watersheds in southeast Oklahoma. No significant increase in sediment yield was realized in the fourth year. Miller et al. (1988) reported a significant increase in sediment yield during the first year following clearcutting on small watersheds in west-central Arkansas. Sediment yields from clear cut watersheds were not significantly different from control watersheds during the remaining two years of the study. Clear cut watershed to control watershed sediment yield ratios were 20:1, 6:1, and 2.6:1 for the first, second, and third year following clearcutting, respectively.

Naseer (1992) reports clear-cut watershed to control watershed yield ratios for sediment, total phosphorus, and nitrate-nitrogen from small watersheds in southeast Oklahoma. Clear cut to control sediment yield ratios were 11:1, 2:1, 2.5:1, and 1.8:1 for the first, second, third, and fourth year following clearcutting, respectively. Clear cut to control total phosphorus yield ratios were 6:1, 3:1, 3:1, 1.5:1 for the first, second, third, and fourth year following clearcutting, respectively. Clear cut to control nitrate-nitrogen yield ratios were 138:1, 12:1, 10:1, 37:1 for the first, second, third, and fourth year following clearcutting, respectively. Table 1 summarizes annual NPS loadings observed in each year of the three studies discussed above.

Rogerson (1971) reports an average annual sediment loss of 0.0025 t ha^{-1} based upon nine years of data from three undisturbed watersheds in the Ouachita Mountains of central Arkansas. Annual sediment loss ranged from 0.0010 to 0.0040 t ha^{-1} . Scoles et al. (1994) summarize many of the watershed studies conducted in the Ouachita Mountains (including Miller 1984 and Miller et al. 1988). Scoles et al. (1994) estimate sediment delivery rates of $0.157 \text{ t ha}^{-1} \text{ yr}^{-1}$ due to harvesting, site preparation, and erosion from forest roads. The authors also concluded that clearcutting increases the loss of phosphorus and nitrogen the first year following harvest, but that nutrient losses return to natural levels by the fourth year after harvesting.

Scoles et al. (1994) attribute relatively low soil losses from clear cut watersheds to the low erodibility of forest soils, to sediment trapping due to harvest and site preparation activities, and to the rapid re-vegetation of clear cut sites. Following a typical clearcutting operation in the Ouachita Mountains, a wide range of plant species immediately establish themselves on the disturbed site. This is the beginning of a process known as secondary succession. The plant community found on a "young" clear cut site is a mixture of competing pine seedlings, grasses, forbs, and woody species. This is a complex plant community which can be expected to rapidly cover the soil surface, utilize soil water at a high rate, and tie up most available nutrients on the site.

Large Clear Cut Watersheds and TMDLs in the Ouachita Mountains

A well-defined scientific framework does not exist to guide TMDL development efforts in the Ouachita Mountains. One certainty is that one must be able to quantify daily NPS loading due to current and alternative management plans on large clear cut

watersheds. Quantifying daily NPS loading from large clear cut watersheds in the Ouachita Mountains is a complex problem. Land use patterns are commonly mosaics of undisturbed, freshly clear cut, recovering clear cut, and recovered clear cut sites. Daily NPS pollution loading realized from a large clear cut watershed depends upon the temporal and spatial arrangement of undisturbed, freshly clear cut, recovering clear cut, and recovered clear cut sites, as well as upon the weather occurring during the time period of interest. On any given large watershed, there are a large number of possible temporal and spatial combinations of undisturbed, freshly clear cut, recovering clear cut, and recovered clear cut sites. Considering the countless number of weather scenarios that could coincide with each temporal and spatial combination one can see that a countless number of daily NPS loadings are possible due to clearcutting on large watersheds.

Ideally, observed data from the particular watershed and waterbody of interest would be used in combination with some modeling scheme during TMDL development. The availability and applicability of such data is limited. The next best source of information for use during TMDL development efforts would be data from large experimental watersheds in the region. Such data would be of value for investigating the source, fate, and transport of NPS pollution from large clear cut watersheds in the region, as well as for calibrating water quality models to simulate daily NPS pollution from clear cut watersheds in the region.

For several reasons, large watershed studies are essentially nonexistent in the Ouachita Mountains. First, it is difficult to locate large watersheds on which the experimenter can attain complete control of the activities occurring on the watershed. Second, forest management cycles range from 30 to 50 years, thus large watershed experiments are longer than most research careers. Third, traditional statistical and

experimental design concepts such as repetition over time and space are difficult to incorporate into large-scale watershed studies for three basic reasons: 1. locating comparable large watersheds is difficult; 2. once a watershed is clear cut it will be a long time, if ever, before the experiment can be repeated on that particular watershed; and 3. time, funding, and labor requirements limit sample size.

Limited amounts of daily NPS loading data from short-term, small-scale watershed studies does exist in the region. It is important to note that small watershed data often reflects watershed response generated by a single storm, a series of storms, or several years of rainfall at one location. Thus, data from small-scale, short-term watershed studies is of limited value for quantifying daily NPS loading and the variability due in daily NPS loading. Whatever its short-comings, small watershed data forms the basis of our understanding of NPS pollution generation from clear cut and undisturbed forest watersheds in the Ouachita Mountains.

Objectives

The purpose of this project was to develop a stochastic framework for evaluating forest management impacts on water quality from watersheds in the Ouachita Mountains. The framework was developed to allow characterization of the variability in NPS loading due to natural weather sequences. One possible application of the framework would be during TMDL development (step 4 of the TMDL development process) to quantify daily NPS loading from large clear cut watersheds. The framework would quantify daily NPS loading as well as allow assessment of the risk of daily NPS loading exceeding estimated waterbody loading capacity under various clearcutting management schemes.

As a case study, the framework was applied to Clayton Lake Watershed to evaluate daily NPS loading under four hypothetical clearcutting management scenarios. Conservative assumptions and worst case conditions were used to account for the MOS.

The objectives of this study are listed below.

1. Develop a stochastic framework which quantifies worst case daily total suspended solid (TSS), total phosphorus (PHOS), and nitrate-nitrogen (NO₃N) loading from large clear cut watersheds in the Ouachita Mountains in such a manner as to allow assessment of the risk of exceeding estimated waterbody loading capacity for TSS, PHOS, and NO₃N.
2. Apply the stochastic framework to Clayton Lake Watershed to quantify worst case daily TSS, PHOS, and NO₃N loading under four hypothetical clearcutting levels and demonstrate the potential of the stochastic framework.

Table 1. Annual NPS loads reported in the Ouachita Mountains. CC indicates a clear cut treatment and UN indicates a control watershed.

Report	Pollutant	TRT	Year After Harvest			
			1	2	3	4
Miller (1984)	Sediment (t ha ⁻¹)	CC	0.28	0.04	0.02	0.04
		UN	0.04	0.01	0.01	0.02
Miller (1988)	Sediment (t ha ⁻¹)	CC	0.24	0.09	0.18	-
		UN	0.01	0.02	0.07	-
Naseer (1992)	Sediment (t ha ⁻¹)	CC	1.95	0.37	0.14	0.14
		UN	0.18	0.19	0.05	0.08
	Total Phosphorus (kg ha ⁻¹)	CC	1.20	0.35	0.13	0.09
		UN	0.20	0.13	0.04	0.06
	Nitrate-nitrogen (kg ha ⁻¹)	CC	7.40	1.04	0.18	0.96
		UN	0.05	0.09	0.02	0.02

CHAPTER II

METHODS

Clayton Lake and Clayton Lake Watershed

Clayton Lake and Clayton Lake Watershed are located in Pushmataha County in the Ouachita Mountains of southeastern Oklahoma. Clayton Lake is found on Peal Creek at latitude 34° 32' 30" by longitude 95° 22' 18", approximately 6.44 km southeast of Clayton, Oklahoma. Clayton Lake has a normal pool surface area of 163 ha, storage capacity of 1,176,002 m³, shoreline of 3.2 km, and surface elevation of 202 m (OWRB 1990). The lake was constructed in 1935 and is owned by the State of Oklahoma. Clayton Lake is currently used for public recreation.

The following description of the climate at Clayton Lake is based upon a 23-year climatic record at Antlers, OK, which is approximately 42 km southwest of Clayton Lake. Average annual precipitation is 1194 mm and sixty percent of the total annual precipitation falls from April to September. The maximum recorded 24-hour rainfall is 157 mm. Average annual snowfall is 75 mm, with accumulations generally less than 25 mm. Regional estimates of average annual streamflow, evapotranspiration and percolation are listed in Table 2. Average daily temperatures range from 5.2° C in January to 27.8° C in July. Average minimum and maximum daily temperatures are -1.6° C and 34.6° C in January and July, respectively. Average relative humidity at dawn and at mid-afternoon is 82 and 50 %, respectively.

The area of Clayton Lake Watershed is approximately 2097 ha. Soils on the watershed were formed from highly weathered, thin, tilted interlamination of sandstones and shales. Soil properties are highly spatially variable over short distances. Three soil associations are found on the watershed (Bain and Watterson 1979). In order of dominance they are the Carnasaw-Pirum-Clebit association (12 to 20 % slopes), the Clebit-Pirum-Carnasaw association (20 to 45 % slopes), and the Carnasaw-Stapp association (8 to 12 % slopes). All three associations have high (≈ 25 %) rock content throughout their profile. The Carnasaw, Clebit, and Pirum soil series are found on upland sites such as mountain sides, benches, and ridge tops. Stapp soils are found on gently sloping to strongly sloping areas. The reaction of the four soil series range from acidic to extremely acidic. Soils on Clayton Lake Watershed are typical of those found on hillslopes throughout the Ouachita Mountains.

Native vegetation on the watershed is a pine-hardwood complex. The overstory is composed primarily of shortleaf pine (*Pinus echinata*), hickory (*Carya* sp.), and oaks (*Quercus* sp.). The understory is composed primarily of elms (*Ulmus* sp.), flowering dogwood (*Cornus florida*), blueberry (*Vaccinium* sp.), poison ivy (*Rhus radicans*), and bluestem grasses (*Andropogon* sp.) (Turton 1989).

Definitions

Certain terms require definition prior to introduction of the stochastic framework and its application to Clayton Lake Watershed.

Management Unit

A management unit is the basic land area of a commercial forest landscape. An analogy would be a field in an agricultural landscape. Management practices are uniform across a management unit. Typical management unit size in the Ouachita Mountains is 65 ha.

Clearcutting

The stages typically involved in clearcutting a management unit in the Ouachita Mountains are: 1. harvesting of all merchantable pine trees (Jun); 2. lodging and chopping of all remaining vegetation (Jul); 3. prescribed burning (Aug); 4. subsoiling (Oct); and 5. regeneration with loblolly pine seedlings (Feb). In general, pine trees are cut using either chain-saws or harvesting machines. Cut trees are dragged by wheeled or tracked skidders along temporary skid trails to a landing and removed from the management unit. Site preparation starts with a bull-dozer pulling a drum chopper through the management unit, lodging and crushing all slash and remaining vegetation. Following a drying period, the management unit is burned. Site preparation is completed by subsoiling, which consists of a bull-dozer pulling a chisel-like implement along the contour at 2.5 m intervals. Pine seedlings are planted in the furrows at about a 2 m spacing.

Management Cycle

A management cycle is the basic time unit in commercial forest management. For large watersheds, management cycle is defined as the period of time required for

the pine crop planted on to the first clear cut management unit to reach maturity. In the Ouachita Mountains this time period can range from 30 to 50 years.

Active Clearcutting Period

The active clearcutting period is the period of time (years) within a management cycle during which clearcutting is occurring on a large watershed. The duration of the active clearcutting period depends upon the number of management units on the watershed (watershed size), and how many management units are clear cut per year.

Clearcutting Level

Clearcutting level is the number of management units which are clear cut per year during the active clearcutting period. Clearcutting level may or may not be constant throughout the active clearcutting period. Year to year variation in economics, timber demand, social perceptions, multiple use demands, and weather cause year to year variation in clearcutting level.

Recovery Period

The recovery period for a clear cut management unit is the 4 year period following clearcutting. This is the period of time required for the hydrologic, erosion, and nutrient transport dynamics of the management unit to return to near undisturbed levels (Miller 1984, Miller et al. 1988, Naseer 1992, and Scoles et al. 1994).

Recovery Status

The recovery status of a management unit refers to the number of years since that management unit was clear cut. The R1 recovery status indicates a management unit is in the first year following clearcutting. The R2 recovery status indicates a management unit is in the second year following clearcutting. The R3 recovery status indicates a management unit is in the third year following clearcutting. The R4 recovery status indicates a management unit is in the fourth year following clearcutting. The U/R recovery status indicates the management is either undisturbed or has recovered (> 4 years since clearcutting) from the clearcutting activity.

Clearcutting Management Scenario

Each clearcutting management scenario represents a different clearcutting scheme for a large forest watershed. Clearcutting management scenarios may vary in clearcutting level, size of streamside management zones, size of clear cut management units, etc. An almost endless number of clearcutting management scenarios could be implemented on a large forested watershed.

This project addresses step 4 of the TMDL development process. Step 4 involves the investigation of alternative clearcutting management scenarios to replace the current clearcutting management scenario, thus reducing NPS loading from the watershed. When applying the stochastic framework to complete step 4, the forest manager is interested in quantifying daily NPS pollution due to hypothetical clearcutting scenarios.

Worst Case Condition

The USEPA (1991) suggests that one component of the MOS associated with a given TMDL be the consideration of worst case conditions during the development of the TMDL. Daily TSS, PHOS, and NO₃N loadings estimated for step 4 of the TMDL development process should be calculated under the worst case condition. The worst case condition is different for each clearcutting management scenario applied to a given watershed. There are three components to the worst case condition for any clearcutting management scenario on any watershed.

The first component is the timing of clearcutting activities. For the worst case condition to occur, the maximum number of disturbed management units possible under a given clearcutting management scenario must be present on the watershed. The second component is the location of the R1, R2, R3, and R4 recovery status management units (disturbed management units) on the watershed. For the worst case condition to occur, the disturbed management units must be arranged on the watershed to provide the greatest opportunity for NPS pollution generation. The third component is rainfall. The timing and location of disturbed management units may be such that the greatest opportunity for daily NPS pollution generation exists under a given clearcutting management scenario, but NPS pollution will not be generated unless it rains.

General Description of the Stochastic Framework

The stochastic framework is based upon stochastic weather input to a water quality model to simulate worst case daily TSS, PHOS, and NO₃N loading under one or more clearcutting management scenarios. The worst case temporal and spatial

arrangement of disturbed management units must be determined for each clearcutting management scenario. The model is applied to estimate worst case daily TSS, PHOS, and NO₃N loading under each clearcutting management scenario of interest on the large watershed. Monte Carlo simulation techniques are used to account for the stochastic influence of weather and to generate samples of worst case daily TSS, PHOS, and NO₃N loading populations. Descriptive statistics and relative frequency plots are computed to quantify worst case daily TSS, PHOS, and NO₃N loading under each clearcutting management scenario. Frequency analysis are employed to examine the probability of LA exceeding LC under each clearcutting management scenario.

Application of the Stochastic Framework to Clayton Lake Watershed

Model Selection

Proper model selection was identified as the most crucial component of the framework. Inadequate model selection would result in unsatisfactory performance of the stochastic framework. In general, a model selected for use in the framework should: 1. be designed for the application it is to be employed for; 2. be designed for the region in which it is to be applied; 3. simulate daily TSS, PHOS, and NO₃N loading; 4. be continuous; 5. be well documented; 6. be relatively easy to use; and 7. be well suited for the application of Monte Carlo techniques.

For the application of the framework to Clayton Lake Watershed it was determined that the water quality model selected must be able to simulate daily TSS, PHOS, and NO₃N loading from R1, R2, R3, R4, and U/R recovery status management units on Clayton Lake Watershed. Unfortunately, a water quality model designed specifically to simulate daily TSS, PHOS, and NO₃N loading from large forested

watersheds in the Ouachita Mountains does not exist. The following field-scale agricultural water quality models were examined: 1. GLEAMS (Groundwater Loading Effects of Agricultural Management Systems); 2. AGNPS (Agricultural Nonpoint Source); 3. HSPF (Hydrologic Simulation Program Fortran); 4. ANSWERS (Aerial, Nonpoint Source Watershed Environment Response Simulation); 5. SWRRB (Simulator for Water Resources in Rural Basins); and 6. EPIC (Erosion / Productivity Impact Calculator).

EPIC was chosen for this project because it: 1. simulates daily TSS, PHOS, and NO₃N loading; 2. is continuous; 3. is well documented; 4. accounts for lateral subsurface flow; 5. has a component for the simulation of TSS, PHOS, and NO₃N loading from pine tree plantations; 6. is relatively easy to use; 7. was designed to be applicable to a wide range of soils, crops, and climates; 8. contains a stochastic weather generator; and 9. is well suited for the application of Monte Carlo techniques. EPIC is a lumped parameter model. EPIC model components are weather, hydrology, erosion, nutrients (nitrogen and phosphorus), soil temperature, crop growth, tillage, plant environmental controls, and economics. Details of the calibration of EPIC to simulate daily TSS, PHOS, and NO₃N loading from R1, R2, R3, R4, and U/R management units on Clayton Lake Watershed are presented in Chapter 3. A review of the pertinent components of EPIC is given in Appendix I.

Clearcutting Management Scenarios and Identification of Worst Case Conditions

Clearcutting Management Scenarios

The four hypothetical clearcutting management scenarios selected for examination on Clayton Lake Watershed represented an incremental increase in the

percentage of the watershed disturbed by clearcutting activities. This set of clearcutting management scenarios was selected so that the performance of the stochastic framework could be compared with the generally accepted concept that watershed response (flow and NPS pollution) increases proportionally with the percentage of a watershed that is clear cut. The four hypothetical clearcutting management scenarios were defined in terms of clearcutting level. It was assumed that clearcutting level was constant throughout the active clearcutting period. Definitions of the worst case condition for each of the four clearcutting management scenarios are discussed in the next section.

Clayton Lake Watershed was divided into 11 management units (Figure 1) using a digital terrain model (Sabbagh et al. 1994). The area, percent of Clayton Lake Watershed, average land slope, and maximum travel distance for each management unit was determined (Table 3). Management unit size was larger than commonly found in the Ouachita Mountains. Examination of the four clearcutting management scenarios did not require high spatial resolution, so the largest reasonable management unit sizes were selected.

The first clearcutting level investigated was $n = 0$ (CC00). This level reflects background or natural daily TSS, PHOS, and NO₃N loading. At this level 0% of Clayton Lake Watershed would be disturbed under the worst case condition. Note that (n) is the number of management units clear cut each year of the active clearcutting period, and that disturbed refers to management units in the R1, R2, R3, and R4 recovery status. The second clearcutting level investigated was $n = 1$ (CC33). At this level approximately 33% of Clayton Lake Watershed would be disturbed under the worst case condition. The active clearcutting period would be 11 years. The third clearcutting level investigated was $n = 2$ (CC66). At this level approximately 66% of

Clayton Lake Watershed would be disturbed under the worst case condition. The active clearcutting period would be 6 years. The final clearcutting level investigated was $n = 3$ (CC100). At this level 100% of Clayton Lake Watershed would be disturbed under the worst case condition. The active clearcutting period would be 4 years.

Worst Case Condition

Recall that clearcutting management scenarios were defined in terms of increasing clearcutting level, and that a clear cut management unit recovers in 4 years. Under a constant clearcutting level, the period of time from 4 years into the management cycle until the end of the active clearcutting period represents the period during which the maximum amount of Clayton Lake Watershed would be disturbed under each of the four hypothetical clearcutting management scenarios. During this period of the management cycle, an equilibrium would be achieved between the percent of the watershed in the disturbed and in the undisturbed/recovered condition. During this equilibrium period there would be (n) R1 units, (n) R2 units, (n) R3 units, and (n) R4 units. The remaining (k) management units would be in the U/R recovery status. On Clayton Lake Watershed the equilibrium period would last 7, 3, and 1 years for the CC33, CC66, and CC100 clearcutting management scenarios, respectively.

The worst case spatial arrangement of clear cut units for each clearcutting management scenario occurs when the (n) R1 management units are located on the most erodible set of units, the (n) R2 management units on the second most erodible set of units, the (n) R3 management units on the third most erodible set of units, the (n) R4 management units on the fourth most erodible set of units, and the (k) U/R

management units are located on the least erodible set of units on Clayton Lake Watershed.

Management units on Clayton Lake watershed were ranked in order of most to least erodible. The ranking would normally be based upon the soil characteristics and slope of each management unit. However, uniform soils were assumed across all management units on Clayton Lake Watershed. Soils found on Clayton Lake Watershed are associations of the Carnasaw, Clebit, Pirum, and Stapp soils. The dominant soil series on Clayton Lake Watershed, as well as within Pushmataha County, is the Carnasaw Soil Series (Bain and Watterson 1979). During this project, a relatively large amount of soil survey and research data was found for the Carnasaw soil series, while little information was available for the other three soil series. For these reasons, the physical and chemical characteristics of the Carnasaw Soil Series were applied to all management units. Due to the application of the Carnasaw Soil Series to all management units, estimation of individual management unit erodibility could not be based upon soil characteristics.

Management units on Clayton Lake Watershed were ranked from most to least erodible based upon average land slope (S) and area (A) (Table 4). Erodible was defined as having characteristics which facilitate sediment generation. It was assumed that those characteristics which facilitate sediment generation also facilitate PHOS and NO₃N generation. The erosion component of EPIC is defined by equation A.84 in Appendix I. Given that K (USLE K-factor) and CE (USLE C-factor) are computed automatically within EPIC based upon user defined soil characteristics, and that PE (USLE P-factor) and ROKF (rock content of the soil) are constant, only LS (USLE slope-length factor) and q_p (peak overland flow rate) vary among management units. Examination of equations A.39, A.42, and A.43 indicates that as management unit area

and average land slope increase, simulated sediment yield increases. Also, examination of equations A.103, and A.104 indicate as S increases, simulated sediment yield increases. Thus, management units were ranked from most to least erodible based first upon S, and second upon A. Table 5 lists the allocation of management units to present the worst case spatial and temporal arrangement of management units on Clayton Lake Watershed for each of the four hypothetical clearcutting management scenarios. Figures 2, 3, and 4 indicate the location of R1, R2, R3, R4, and U/R management units for the CC33, CC66, and CC100 clearcutting management scenarios, respectively.

Finally, the worst case condition for daily TSS, PHOS, and NO₃N loading only occurs when the worst case daily rainfall event coincides with the worst case temporal and spatial arrangement of disturbed management units. It is often difficult to quantify the worst case daily rainfall event, and thus the worst case condition. The occurrence of extreme daily rainfall events was incorporated into the stochastic framework using synthetic weather records and Monte Carlo simulation techniques. The worst case temporal and spatial arrangement of management units for each clearcutting management scenario was held constant over Monte Carlo simulation.

Monte Carlo Simulation Techniques

Prior to a description of the Monte Carlo simulation techniques employed during application of the stochastic framework to Clayton Lake Watershed, a limited discussion of the functioning of EPIC is required. At the beginning of a simulation, EPIC assumes that bare, unprotected soil exists on the site to be modeled. EPIC was designed to simulate the planting, growth, and harvesting of a crop. Thus, a pine crop

must be planted and grown to obtain daily TSS, PHOS, and NO₃N loading estimates from management units in any recovery status.

Because EPIC is a spatially lumped model, daily TSS, PHOS, and NO₃N loading were simulated individually for each management unit. Daily TSS, PHOS, and NO₃N loading from a management unit in the R1 recovery status was simulated by planting the pine crop, simulating for one year, and recording daily TSS, PHOS, and NO₃N loading from that one year. Daily TSS, PHOS, and NO₃N loading from a management unit in the R2 recovery status was simulated by planting the pine crop, simulating for two years, and recording daily TSS, PHOS, and NO₃N loading from the second year. Daily TSS, PHOS, and NO₃N loading from a management unit in the R3 recovery status was simulated by planting the pine crop, simulating for three years, and recording daily TSS, PHOS, and NO₃N loading from the third year. Daily TSS, PHOS, and NO₃N loading for a management unit in the R4 recovery status was simulated by planting the pine crop, simulating for four years, and recording daily TSS, PHOS, and NO₃N loading from the fourth year. Daily TSS, PHOS, and NO₃N loading for a management unit in the U/R recovery status was simulated by planting the pine crop, simulating for twenty years, and recording daily TSS, PHOS, and NO₃N loading from the twentieth year.

The recovery status assigned to each management unit was dependent upon the clearcutting management scenario (Table 5). For example, the simulation of one year of daily TSS, PHOS, and NO₃N loading from Clayton Lake Watershed under CC33 for one possible weather scenario requires simulation of the R1, R2, R3, and R4 recovery status on Units 8, 9, 3, and 11, respectively. The U/R recovery status would be simulated on Units 1, 2, 4 through 7, and 10. Simulations would be timed such that

the year-long data set recorded for the R1, R2, R3, R4, and U/R management units resulted from the same year of synthetic weather record.

Daily TSS, PHOS, and NO₃N loading from Clayton Lake Watershed under each clearcutting management scenario was found as the sum of daily loading from each of the management units on the watershed. In order for annual maximum daily TSS, PHOS, and NO₃N loading estimates for the CC00, CC33, CC66, and CC100 clearcutting management scenarios to be comparable, the estimates had to be generated under common weather. Due to the method required to simulate daily loading from management units in the R1, R2, R3, R4, and U/R recovery status, five weather files were necessary to simulate one year of daily loading from Clayton Lake Watershed. The last year of each weather file had to be identical.

The following is an explanation of the process used to develop one weather set containing the five weather records required to simulate one year of daily TSS, PHOS, and NO₃N loading from Clayton Lake Watershed. The EPIC weather generator (described in Appendix I and by Sharpley and Williams 1990) was used to generate a 20-year (WTH20) daily weather record to simulate the U/R recovery status. The generated WTH20 contained average daily solar radiation (RAD) as MJ m⁻², maximum daily temperature (TMAX) in °C, minimum daily temperature (TMIN) in °C, daily rainfall (RAIN) in mm, and average daily relative humidity (RHD) in a fraction. The last 1, 2, 3, and 4 years of data in the WTH20 daily weather record were extracted and duplicated to generate 1-year (WTH1), 2-year (WTH2), 3-year (WTH3), and 4-year (WTH4) daily weather records. In this manner, a total of five daily weather records were obtained such that WTH1 matched year 20 of WTH20 (for simulation of the R1 recovery status), WTH2 matched years 19 and 20 of WTH20 (for simulation of the R2 recovery status), WTH3 matched years 18, 19, and 20 of WTH20 (for simulation of the R3 recovery

status), and WTH4 matched years 17, 18, 19, and 20 of WTH20 (for simulation of the R4 recovery status). Daily weather files WTH1, WTH2, WTH3, WTH4, and WTH20 are collectively referred to as a weather set.

Monte Carlo simulation techniques simply involved the repetition of the process to generate one year of daily TSS, PHOS, and NO₃N loading from Clayton Lake Watershed. This process was repeated 1500 times. A single repetition in the Monte Carlo simulation was defined as a Monte Carlo run. A different and independent weather set was developed for each Monte Carlo run. Initial conditions were identical at the beginning of each Monte Carlo run. Each of the four hypothetical clearcutting management scenarios were considered during each Monte Carlo run. In this manner 1500 independent, directly comparable year-long records of daily Q and daily TSS, PHOS, and NO₃N loading estimates for Clayton Lake Watershed were generated for each clearcutting management scenario. Annual maximum daily Q and annual maximum daily TSS, PHOS, and NO₃N loading were extracted from each of the 1500 independent year-long daily records to develop four data sets (annual maximum daily Q, TSS, PHOS, and NO₃N) for each clearcutting management scenario (a total of 16 data sets). Based upon worst case conditions and the selection of annual maximum daily estimates, these synthetic data sets are samples of the worst case populations for daily Q and daily TSS, PHOS, and NO₃N loading from Clayton Lake Watershed under each clearcutting management scenario. Monte Carlo runs were conducted on a Pentium 66-mhz personal computer.

Analysis

Weather

Annual rainfall, maximum daily rainfall, mean daily solar radiation, maximum daily solar radiation, minimum daily solar radiation, maximum daily temperature, minimum daily temperature, and mean daily relative humidity were calculated for the year common within each weather set (i.e. year 20 of WTH20, year 4 of WTH4, etc.). The grand minimum, maximum, and mean were calculated for the 1500 weather sets and compared to statistics computed from long-term observed weather records.

Annual Maximum Daily Q, TSS, PHOS, and NO3N

Descriptive statistics and relative frequency plots were computed to quantify annual maximum daily flow (Q) as well as annual maximum daily TSS, PHOS, and NO3N loading from Clayton Lake Watershed under each clearcutting management scenario. Frequency analysis in the form of probability plotting was conducted on the 1500 annual maximum daily Qs and annual maximum daily TSS, PHOS, and NO3N loadings for each clearcutting management scenario.

Frequency analysis is generally applied to time series of data. Although the synthetic data sets generated for Clayton Lake Watershed were not time series, frequency analysis could be employed as long as certain assumptions were met. The main assumptions were: 1. the observations within a data set were statistically independent of each other; 2. the observations were from a stationary time series. Considering annual maximum daily Q and annual maximum daily TSS, PHOS, and NO3N loading satisfied the first assumption of frequency analysis. The second

assumption was satisfied because the scope was limited to the worst case condition for each clearcutting management scenario, and the worst case condition did not change from Monte Carlo run to Monte Carlo run.

The steps followed during the development of the probability plots were: 1. ranking of the estimates in each data set from largest to smallest; 2. calculation of the plotting position for each estimate in each data set; and 3. plotting annual maximum daily Q, TSS, PHOS, or NO₃N on the y-axis and plotting position on the x-axis of log-normal probability paper. The plotting position (p) for each estimate was determined using the Weibull plotting position formula (Haan 1977).

$$p = m / (n + 1) \qquad 2.1$$

Where m was the rank of the estimate in relation to the other estimates in the sample, and n was the sample size. By ranking the estimates from largest to smallest the plotting position corresponded to $1 - P_x(x)$, the probability of the occurrence of a daily load with a magnitude equal to or greater than the event in question (Haan 1977). This probability is the exceedance probability. Exceedance probability is equal to the reciprocal of the return period for a T-year event. A T-year event is defined as an event of such magnitude that over a long period of time (much longer than T years), the average time between events having a magnitude greater than the T year event is T years (Haan et al. 1994). Return period was displayed on the secondary x-axis of the probability plot.

Forest Roads

EPIC cannot simulate the generation and transport of TSS, PHOS, and NO₃N from forest road networks. Thus, the annual maximum daily TSS, PHOS, and NO₃N loading estimates from Clayton Lake Watershed generated under the stochastic framework will not account for contributions from forest roads. This is a major shortcoming of the framework because the construction and maintenance of roads, trails, and landings associated with clearcutting have been identified as major sources of NPS pollution (Scoles et. al. 1994).

Miller et al. (1985) conducted a 17 month study (1-Jun-1982 to 31-May-1983 and 1-Aug-1984 to 31-Dec-1984) to characterize the erosion rates and sediment delivery potential of a road system on a large watershed in the Ouachita Mountains. Precipitation during the study period was 143 % above normal. A single storm exceeding the 100 year 24 hour rainfall amount occurred during the study, and total monthly rainfall for Oct-1984 was the greatest on record. The authors present 56.05 t ha⁻¹ as an upper limit estimate of the erosion rate which can be expected from unpaved roads on large forest watersheds in the Ouachita Mountains. This translated to 40.59 t km road⁻¹ yr⁻¹. Sediment delivery rate to the stream was estimated to be 0.085 t ha⁻¹ yr⁻¹, or 4.45 t km road⁻¹ yr⁻¹.

In the batholith of Idaho, Megahan and Kidd (1972) determined that 85% of the soil loss due to road construction occurred in the first year following construction while Fredricksen (1970) reported a 250 X, 2 X, and 3 X increase in TSS compared to the control for the first, second, and third year following road construction. An estimated 245 t ha⁻¹ of soil erosion occurred in the first year. Average erosion rate over eight years was 27 t ha⁻¹ yr⁻¹. Anderson and Potts (1987) reported an average TSS

concentration of 6.7 mg L^{-1} and a 7.7 X increase in annual sediment yield during the first year following the construction of 2.5 km of logging road on a small watershed in west-central Montana. Based upon observations of low levels of soil disturbance and overland flow following timber harvest the authors concluded that erosion from roads contributed more to the total watershed soil loss than did timber harvest. This supports observations by McCashion and Rice (1983) that on a 12,262 ha of commercial forest land in northwest California, 40% of the total erosion associated with the management of the area was due to a road system which comprised only 6% of the land surface. Average road related erosion was approximately 17 X that due to the timber harvest operation.

Forest roads associated with clearcutting activities are a major source of NPS pollution generation, and may in fact be responsible for more NPS pollution generation than the clearcutting activity. Although significant NPS pollution can be generated from forest roads, simple BMP's can be installed to effectively reduce the amount of NPS pollution which reaches waterbodies. Simulation of NPS pollution from forest roads must eventually be incorporated into the framework. No attempt was made to account for forest roads on Clayton Lake Watershed.

Table 2. Regional estimates of average annual P, Q, ET, and PRK as well as the percent of P lost to Q, ET, and PRK for north-central Pushmataha County (Pettyjohn et al. 1983).

	Average Annual (mm)	Percent of Average Annual P
P	1219	100.0
Q	356	29.2
ET	788	64.6
PRK	75	6.2

Table 3. Area (A), percent of Clayton Lake Watershed (%), average land slope (S), maximum travel distance (L) for each management unit.

Unit	A (ha)	%	S (%)	L (km)
1	151	7.1	13.8	2.08
2	180	8.5	13.3	2.47
3	121	5.7	16.2	2.23
4	189	8.9	15.5	2.36
5	210	9.9	13.4	2.75
6	108	5.1	14.8	2.22
7	275	12.9	12.6	4.10
8	276	13.0	19.1	3.52
9	273	12.8	17.2	3.29
10	208	9.8	15.7	3.00
11	106	5.0	16.2	2.03

Table 4. Management units ranked from most to least erosive based first upon average land slope (S) and area (A).

Unit	A (ha)	%	S (%)	L (km)
8	276	13.0	19.1	3.52
9	273	12.8	17.2	3.28
3	121	5.7	16.2	2.22
11	106	5.0	16.2	2.02
10	208	9.8	15.7	3.00
4	189	8.9	15.5	2.36
6	108	5.1	14.8	2.22
1	151	7.1	13.8	2.07
5	210	9.9	13.4	2.74
2	180	8.5	13.3	2.47
7	275	12.9	12.6	4.10

Table 5. Allocation of management units for each clearcutting management scenario. A is the area (ha) in each recovery status and % is the percent of Clayton Lake Watershed in each recovery status.

Scenario	Recovery Status	Management Units	A	%
CC00	R1	-	0	0
	R2	-	0	0
	R3	-	0	0
	R4	-	0	0
	U/R	1 - 11	2097	100.0
CC33	R1	8	276	13.2
	R2	9	273	13.0
	R3	3	121	5.8
	R4	11	106	5.0
	U/R	10, 4, 6, 1, 5, 2, 7	1321	63.0
CC66	R1	8, 9	549	26.2
	R2	3, 11	227	10.8
	R3	10, 4	397	18.8
	R4	6, 1	259	12.5
	U/R	5, 2, 7	665	31.7
CC100	R1	8, 9, 3	670	32.0
	R2	11, 10, 4	503	24.0
	R3	6, 1, 5	469	22.4
	R4	2, 7	455	21.6
	U/R	-	0	0

Figure 1. Clayton Lake Watershed divided into 11 management units.

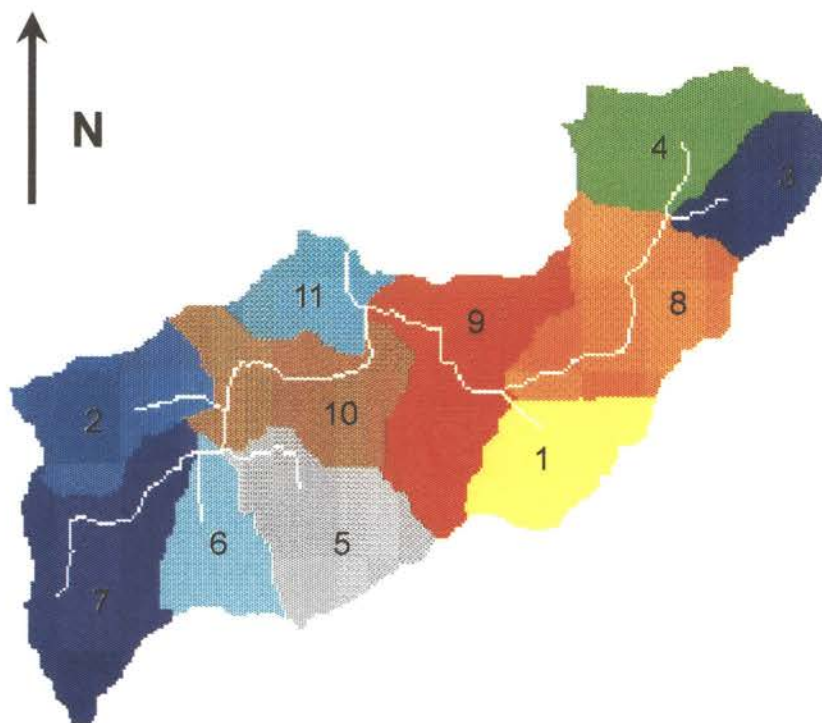


Figure 2. Allocation of management units on Clayton Lake Watershed for the CC33 clearcutting management scenario.

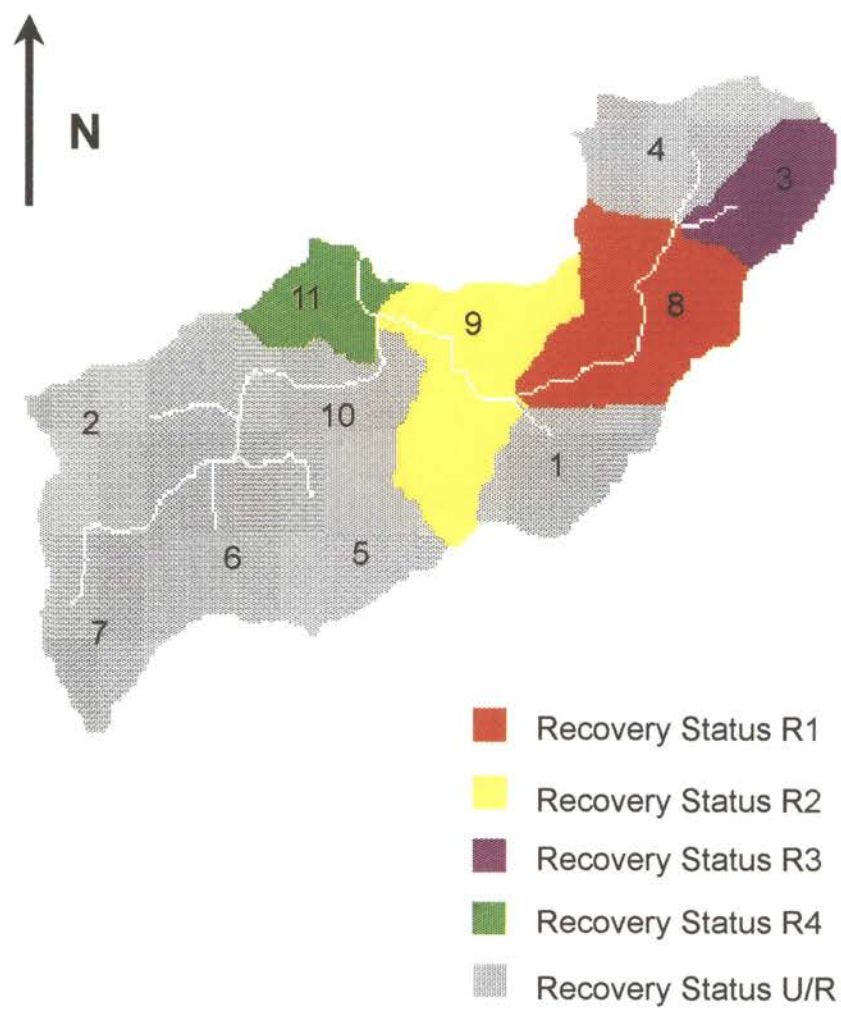


Figure 3. Allocation of management units on Clayton Lake Watershed for the CC66 clearcutting management scenario.

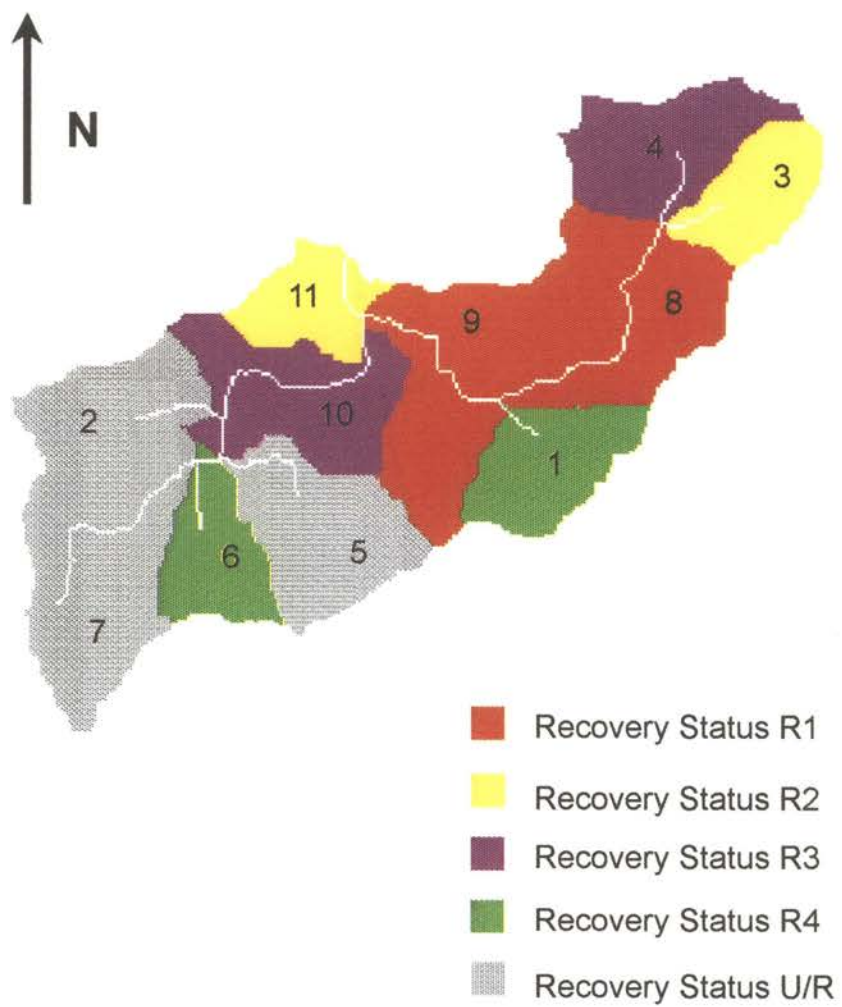
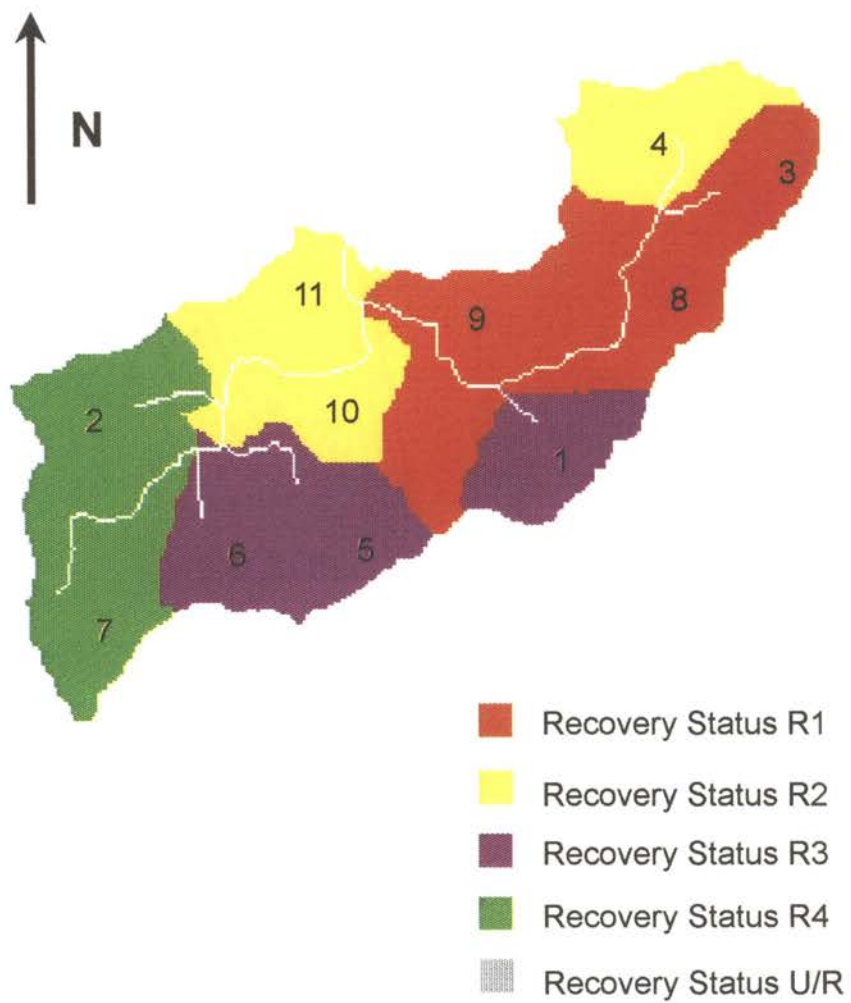


Figure 4. Allocation of management units on Clayton Lake Watershed for the CC100 clearcutting management scenario.



CHAPTER III

MODEL CALIBRATION

Introduction

For this project, parameter estimation is referred to as calibration. Haan et al. (1994) define parameter estimation as the process by which the parameters of a model are estimated for a particular application, and state that rational parameter estimation must be based upon some criterion in order to identify a unique set of parameter estimates. The parameter estimation criteria applied in this effort can be described as personal judgment optimization univariately by trial and error. Initial parameter estimates were developed based upon research data, soil survey information, monthly weather data available in EPIC, topographic data, suggestions within the EPIC documentation, and the judgment of the model user. Model performance evaluation was conducted following each model run. Based upon that evaluation, the estimate for a selected parameter was modified and the model was run again. This process was continued until satisfactory model performance was attained. Satisfactory model performance will be defined later in this chapter.

Recall that annual maximum daily TSS, PHOS, and NO₃N loadings are the quantities of interest. Unfortunately, limited observed annual maximum daily loading data was available for model performance evaluation. Upon identification of the final

parameter set, EPIC's performance was evaluated on its ability to simulate monthly and daily Q, TSS, PHOS, and NO₃N loading as well as to simulate annual maximum daily Q, TSS, PHOS, and NO₃N loading. Model performance evaluation methods included linear regression analysis, graphical analysis, and comparison of simulated and observed annual summaries. Although evaluating EPIC based upon monthly and daily loadings does not directly evaluate EPIC's ability to simulate annual maximum daily loadings, it does provide insight to EPIC's overall performance.

In the interest of space, a condensed format was developed for the presentation of model performance evaluation results for daily TSS, PHOS, and NO₃N loading. The presentation format consists of the following per final model run: 1. one page containing the tabular results of linear regression analysis (i.e. ANOVA, coefficients, etc.) and tests of the slope and intercept of the linear regression model; 2. a plot of observed and simulated values over time; and 3. a scatter plot of the linear regression line through the data. Results of day-to-day model performance evaluations of the final models are presented in Appendix II and III.

Model Performance Evaluation Methods

Several simple methods of comparing simulated and observed values were employed during the calibration process. Linear regression analysis was applied to predict observed values by simulated values. The slope of the regression line (b) provides a measure of the bias in the model estimates, while the coefficient of determination (r^2) is a measure of how model output tracks observed values in a relative sense (Haan et al. 1994). The coefficient of determination is the ratio of the sum of squares due to regression to the total sum of squares corrected for the mean

and can be used as a measure of the ability of the regression line to explain variations in the dependent variable (Haan 1977). If EPIC output exactly matched observed data, r^2 would equal 1, b would equal 1, and the intercept of the regression line (a) would equal 0. Graphical evaluation of model performance was conducted using plots of simulated and observed values over time. Annual sums of simulated and observed values were computed and compared.

Monthly values for Q, TSS, PHOS, and NO₃N loading were used for evaluation of model performance during the initial and subsequent model runs of the parameter estimation process. Daily values of Q, TSS, PHOS, and NO₃N loading were used for evaluation of final model performance (the model determined to be the "best" based upon evaluation of monthly values). Graphical evaluation was employed to examine the relationship between simulated and observed annual maximum daily TSS, PHOS, and NO₃N loadings.

In order to evaluate model performance, some standard of model performance must be established. Few guidelines exist to aid in the development of such a standard. In the absence of guidelines, satisfactory model performance was defined as follows: 1. $r^2 \geq 0.70$; 2. b not significantly different from 1; and 3. a not significantly different from 0.

Observed Data

Two small-scale experimental watersheds, WS-I and WS-III, are located on Clayton Lake Watershed (Figure 5). WS-I was clear cut in Sep-83. Site preparation for pine establishment consisted of lodging hardwoods and drumchopping slash in Jul-84, prescribed burning in Aug-84, and subsoiling in Jan-85 (Naseer 1992). WS-I was

planted to a monoculture of loblolly pine in Mar-85. WS-III was left undisturbed to serve as a control watershed.

Streamflow was measured using 1.2 m concrete H-flumes (Naseer 1992). ISCO (Instrument Specialties Company) Model 1680 automatic pumping samplers (28 sample capacity) were installed 1 m upstream of the flume inlet to collect discrete water quality samples. Floats equipped with mercury switches were used to activate the automatic pumping samplers during runoff events. During runoff events, discrete water quality samples were collected by the ISCO Model 1680 at 0.25 to 0.30 hr intervals. Rainfall was measured using one weighing-bucket recording rain gage per watershed.

TSS concentrations were determined by vacuum filtering through 0.45 μm filters, oven drying the filtrate at 110 $^{\circ}\text{C}$, and weighing the dry filtrate (Naseer 1992). PHOS concentrations were determined by persulfate digestion and the ascorbic acid colorimetric method (APHA 1976). NO_3N concentrations were determined by the cadmium reduction method (APHA 1976).

Rainfall charts were digitized and a digital precipitation record developed. Streamflow charts were digitized and a digital record of streamflow developed. Water quality samples were matched with streamflow data. Digital files containing stormflow volume (Q) as well as TSS, PHOS, and NO_3N concentrations were developed for all stormflow events during the study period.

For the purposes of this project, a continuous record of daily rainfall (RAIN) in mm, daily Q in mm, daily TSS loading in t ha^{-1} , daily PHOS loading in kg ha^{-1} , and daily NO_3N loading in kg ha^{-1} was developed for WS-I and WS-III. The record extends from 1-Oct-83 to 30-Sep-88. Annual maximum daily Q as well as annual maximum daily TSS, PHOS, and NO_3N loading for the R1, R2, R3, and R4 recovery status were

computed (water years 1985, 1986, 1987, and 1988 on WS-1). This resulted in one observation each of annual maximum daily Q, TSS, PHOS, and NO₃N for the R1, R2, R3, and R4 recovery status. Annual maximum daily Q as well as annual maximum daily TSS, PHOS, and NO₃N loadings for the U/R recovery status were computed (water years 1984, 1985, 1986, 1987, and 1988 on WS-III). This resulted in five observations of annual maximum daily Q, TSS, PHOS, and NO₃N for the U/R recovery status.

EPIC System File Structure

Throughout this chapter parameters are categorized and discussed based upon their location within the EPIC system file structure, thus a brief description of the EPIC system file structure is warranted. EPIC system files are text files which contain the estimates for the parameters of EPIC. Figure 6 illustrates the EPIC system file structure. The Basic-User-Supplied Data File, the Crop Parameter File, and the Tillage Parameter File are discussed in the following sections. The reader is referred to Dumesnil (1993) for a detailed description of the remaining files, and to Appendix I for complete descriptions of the parameters discussed in this chapter.

Basic User-Supplied Data File

As the name indicates, the Basic User-Supplied Data File must be developed by the user. The EPIC User's Guide (Dumesnil 1993) identifies 9 categories of user-supplied data: title; program control codes; general data; water erosion data; weather data; wind erosion data; soil data; management information; and daily weather data.

A total of 617 values must be estimated to develop a Basic User-Supplied Data File (Table 6) (149 parameters, assuming 8 soil horizons, and 12 months of monthly weather statistics). Parameters NBYR through IHUS are program control codes (Table 6). Parameters WSA through CHD provide general data about the site to be modeled, while parameters SL through DRV provide the water erosion data required by the EPIC erosion component.

Monthly weather data files for over 137 sites in the United States are available within EPIC. These files contain estimates for parameters YWI through RH and WWL through DIR16 in Table 6. These parameters supply the basic information required by EPIC to simulate daily weather and evapotranspiration. Parameters FL through ACW relate to the simulation of wind erosion. Soil data files containing estimates for parameters SALB through WP are available for 737 soil series found within the United States are available within EPIC. Parameters NRO through PAR comprise the management information data. These parameters define the management scenario associated with the production of the crop(s) of interest. Observed daily weather data for one or more of the six driving weather variables can be incorporated by inserting the name and location of the Daily Weather Data File at the end of the Basic User-Supplied Data File.

Crop Parameter File

The Crop Parameter File stores estimates of the crop parameters of EPIC. Table 7 lists the 45 parameters required per crop contained in the Crop Parameter File. During a simulation EPIC reads crop parameter estimates from the Crop Parameter File based upon the crop type specified in the Basic User-Supplied Data File. The EPIC

Crop Parameter File contains information for 22 crops, one of which is pine trees (PINE).

Tillage Parameter File

The Tillage Parameter File stores information about tillage, planting, harvesting, and other operations. During a simulation EPIC reads tillage parameter estimates from the Tillage Parameter File based upon the tillage operation specified in the Basic User-Supplied Data File. Table 8 lists the 12 parameters required for each tillage operation contained in the Tillage Parameter File. Table 9 lists the tillage operations contained in the EPIC Tillage Parameter File.

Parameter Selection

In the previous section, 205 parameters are identified for which a total of 674 estimates must be determined. Within EPIC a parameter can represent a physical / chemical characteristic, a ratio, or a code to specify the use of a particular calculation / evaluation technique. Only a limited number of the parameters in EPIC are of value for calibration. Parameters not employed for calibration purposes were set to values suggested within the EPIC User's Guide, to values determined by research on the study site, or to values determined from the literature. The initial task was to determine which of the 205 parameters were to be considered as candidates for parameter estimate modification during the model calibration process.

Tillage and Crop Parameter Files

All parameters contained within the Tillage Parameter File were excluded from modification. With the exception of the CVM parameter (minimum daily USLE C-factor value), those parameters contained in the Crop Parameter File were excluded from modification. CVM is a factor in the calculation of CE and thus TSS (equations A.102 and A.84 in Appendix I). There are two reasons for the exclusion of the remaining parameters within the Crop and Tillage Parameter Files. First, other than those estimates provided within EPIC data files, it is extremely difficult to obtain estimates for most of the parameters contained within the Crop and Tillage Parameter Files. Second, the effect that manipulating crop and tillage parameters has upon the functioning of the crop growth model is difficult to assess.

Basic User-Supplied Data File

The majority of parameters within the Basic User-Supplied Data File were excluded as candidates for modification. Referring to Table 6, program control codes NBYR through LPYR, ISCN through ICODE, and ISTA through IHUS were excluded as candidates for modification. General information parameters WSA, CHL through SN, and YLT through S were not modified during model calibration. Monthly weather parameters YWI through RH and WWL through DIR16 were not modified during model calibration. Wind erosion parameters FL, FW, ANG, UXP, DIAM, and ACW were not modified during model calibration. Soil property parameters SALB through XIDS, Z through SIL, PH through ROK, RSD, BDD, and SC were not modified during model calibration because soil survey and research data were available for the estimation of

these parameters. All management information parameters were excluded as candidates for modification.

A total of 14 parameters were identified as candidates for parameter estimate modification during model calibration (Table 10). Based upon this particular parameter selection, the calibration of EPIC amounts to the development of one Basic User-Supplied Data File for clear cut management units and another for undisturbed management units.

Clear Cut Management Unit

EPIC was calibrated to simulate the entire four year recovery period following clearcutting on WS-I. Simulation began 1-Oct-84 and ended 30-Sep-88. Observed data from water years 1985 (R1), 1986 (R2), 1987 (R3), and 1988 (R4) was used for model performance evaluation. Daily rainfall data for the period 1-Jan-84 to 12-Dec-88 was input and the remaining required daily weather variables were estimated. The transplant tillage operation was applied to plant a pine crop at the beginning of the simulation. Parameter estimates provided within EPIC for the transplant tillage operation and the pine crop were utilized. Results of final model performance evaluations are presented in Appendix II.

Initial Parameter Estimates

The first step was to identify initial estimates for the 149 parameters contained in the Basic User-Supplied Data File. Initial parameter estimates are based upon research data, soil survey information, monthly weather data available in EPIC, topographic data, suggestions within the EPIC documentation, and the judgment of the

model user. A portion of the parameters were set to default values. CVM was initially set at its default value of 0.001. Initial program control code settings are listed in Table 11. Initial estimates for general information parameters are listed in Table 12.

Estimates for monthly weather parameters are listed in Table 13. Monthly weather parameter estimates are based upon 7 years of daily weather data recorded at Smithville, OK, approximately 56 km east of Clayton Lake Watershed. Wind erosion parameters were set to their default values (Table 14). STD (standing dead residue) was set to 3 t ha^{-1} in an attempt to represent the residue found on clear cut sites.

Soil parameters fall into two categories, those requiring an estimate for each soil layer and those requiring one estimate for the entire soil profile. Initial estimates for soil parameters in the first category are listed in Table 15. Initial estimates for general soil parameters are listed in Table 16.

Management operation parameters NIRR through FDSF do not pertain to this project and were assigned default values (Table 17). The management operation schedule used for clear cut simulations is shown in Table 18. Operation 4 represents the transplanting of a crop, and crop ID number 23 indicates that pine trees were the crop transplanted. MAT (years until the pine trees reach maturity) was set at 40. Operation 72 represents irrigation of the site. EPIC requires that at least one management operation be performed within each year of simulation. Irrigation of the site with 1 mm of water in years other than the transplanting year was determined to be a operation that could be employed with minimal impact upon model performance.

Calibration and Model Performance Evaluation

Initial and Subsequent Model Runs

Hydrology. The initial hydrology model run was conducted using the initial Basic User-Supplied Data File described above. Monthly simulated Q estimates were calculated as the sum of daily overland and lateral subsurface flow for each month. Model performance evaluation results indicated that EPIC initially over-predicted monthly Q. Hydrology model run two was conducted with subsurface travel time (RFTT) set to 2 days. Examination of equations A.48 through A.56 indicated that increasing RFTT would increase soil water retention time which increases evapotranspiration (ET) and percolation (PRK), decreasing Q. Evaluation of hydrology model run two indicated that EPIC satisfactorily estimated monthly Q.

TSS. The initial TSS model run, TSS model run two, and TSS model run three were conducted using the Basic User-Supplied Data File developed in hydrology model run two with the equation for water erosion (DRV) equal to the Modified Universal Soil Loss Equation (MUSLE), the small watershed version of MUSLE (MUSS), and the Universal Soil Loss Equation (USLE), respectively. Evaluation of the first three model runs indicated that EPIC initially under-predicted TSS, but did not indicate which erosion model was most appropriate.

Examination of equations A.84 and A.102 showed that increasing CVM increases CE and thus TSS. TSS model run four was conducted with CVM equal to 0.002 and DRV equal to MUSLE. TSS model run five was conducted with CVM equal to 0.002 and DRV equal to MUSS. TSS model run six was conducted with CVM equal to 0.002, and DRV equal to USLE. Evaluation of model runs three through six

indicated USLE was not well-suited for predicting TSS from WS-I. The evaluation also indicated that EPIC under-predicted TSS in year 1 (R1).

Examination of equations A.84 and A.102 showed that reducing STD would reduce CE in year 1 and thus increase TSS in year 1 (R1). TSS model run seven was conducted with STD equal to 2 t ha^{-1} , CVM equal to 0.002, and DRV equal to MUS. TSS model run eight was conducted with STD equal to 2.5 t ha^{-1} , CVM equal to 0.002, and DRV equal to MUSLE. Model performance evaluation indicated that MUSLE was the most appropriate erosion model. Evaluation also indicated that EPIC unsatisfactorily estimated monthly TSS. Subsequent parameter modification and model runs did not improve upon the model fit realized under TSS model run eight. Model run eight provided the best model fit achieved.

PHOS. The initial PHOS model run was conducted using the Basic User-Supplied Data File developed in TSS model run eight. The results of model performance evaluation indicated EPIC initially under-predicted PHOS. Setting AP1 and AP2 to a low value reduced PHOS by reducing the amount of phosphorus available to be transported from the site. PHOS model run two was conducted with AP1 and AP2 set to 5 g t^{-1} . Evaluation indicated that EPIC satisfactorily estimated monthly PHOS.

NO3N. The initial NO3N model run was conducted using the Basic User-Supplied Data File developed in PHOS model run two. The results of model performance evaluation indicated EPIC initially over-predicted NO3N. Setting WN1-8 to a low value reduced NO3N by reducing the amount of NO3N available to be transported from the site. NO3N model two was conducted with WN1-8 equal to 1 g t^{-1} .

Evaluation indicated EPIC over-predicted NO₃N. NO₃N model three was conducted with WN1-8 equal to 0.1 g t⁻¹. Evaluation indicated EPIC satisfactorily estimated monthly NO₃N.

Final Model. Monthly Q, as well as monthly TSS, PHOS, and NO₃N loading estimates were generated using the final Basic User-Supplied Data File developed in NO₃N model run three. Model performance evaluation indicated EPIC did not satisfactorily estimate monthly PHOS and TSS. The change in EPIC's ability to satisfactorily simulate monthly PHOS was probably due to an interaction between the nitrogen and phosphorus components of EPIC. Thus, it was necessary to continue the calibration of EPIC for PHOS.

PHOS model run three was conducted with organic phosphorus concentration in all soil layers (WP1-8) set to 500 g t⁻¹. WP1-8 were set to 500 g t⁻¹ to increase the amount of PHOS available for transport. Evaluation indicated that EPIC over-predicted annual PHOS. PHOS model four was conducted with WP1-8 equal to 450 g t⁻¹. Evaluation indicated that EPIC satisfactorily estimated monthly PHOS.

The final model performance evaluation indicated EPIC satisfactorily estimated monthly Q, PHOS, and NO₃N loading from WS-I during the four year recovery period. EPIC did not satisfactorily estimate monthly TSS ($r^2=0.68$). No further parameter estimate modification was conducted.

Daily Evaluation of the Final Model

The final model developed above was evaluated based upon simulated and observed daily Q, as well as daily TSS, PHOS, and NO₃N loading (Appendix II).

Evaluations were conducted individually for recovery status R1, R2, R3, and R4. Model performance evaluations were less favorable for Q, TSS, PHOS, and NO₃N at the daily time step than at the monthly time step. Low coefficients of determination indicated that simulated values inadequately tracked observed values. Regression line slopes and intercepts indicated bias in the model estimates. Model performance evaluations indicated that EPIC unsatisfactorily estimated day-to-day Q, as well as day-to-day TSS, PHOS, and NO₃N loading.

Annual Maximum Daily Q and TSS, PHOS, and NO₃N Loading

Simulated and observed annual maximum daily Q as well as annual maximum daily TSS, PHOS, and NO₃N loading were compared for the R1, R2, R3, and R4 recovery status. These values, as well as the day of record on which they were realized, are listed in Table 19. Figures 7 through 10 illustrate simulated and observed values.

Undisturbed / Recovered Management Unit

EPIC was calibrated to simulate Q as well as TSS, PHOS, and NO₃N loading from WS-III, an undisturbed watershed. The simulation period was 20 years, beginning 1-Oct-69 and ending 30-Sep-88. Initially, both a 40 and 20 year simulation duration were examined. Improved model performance was not realized at the 40 year duration, while computation time was significantly increased. Observed and simulated values for water years 1984 through 1988 were used for model performance evaluation. Daily rainfall data was input directly and the remaining required daily weather variables were estimated. The daily rainfall record was constructed such that the last five years

matched that realized on WS-III for the period 1-Jan-83 to 12-Dec-88. The transplant tillage operation was applied to plant pine trees at the beginning of the simulation. Parameter estimates provided within EPIC for the transplant tillage operation and the pine crop were utilized. Results of final model performance evaluations are presented in Appendix III.

Initial Parameter Estimates

Initial parameter estimates were based upon research data, soil survey information, monthly weather data available in EPIC, topographic data, suggestions within the EPIC documentation, and the judgment of the model user. A portion of the parameters were set to default values. CVM was initially set to its default value of 0.001. Initial program control code settings are listed in Table 20. Initial estimates for general information parameters are listed in Table 21. Estimates for monthly weather parameters are listed in Table 13. Wind erosion parameters are listed in Table 14. STD was assigned an initial estimate of 2.5 t ha^{-1} . Initial estimates for soil parameters are listed in Tables 21 and 22. Management operation parameters NIRR through FDSF are listed in Table 17. The management operation schedule used for undisturbed simulations is shown in Table 23. MAT was set to 40.

Calibration and Model Performance Evaluation

Initial and Subsequent Model Runs

Hydrology. The initial hydrology model run was conducted using the initial Basic User-Supplied Data File described above. Model performance evaluation results

indicated EPIC initially over-predicted annual Q. Decreasing CN would decrease the amount of RAIN lost as surface runoff, thus increasing the amount of water entering the soil profile. This would allow a greater portion of RAIN to be lost as ET or PRK, decreasing Q (equations A.22 and A.23). Hydrology model run two was conducted with CN set to 25. Evaluation indicated that EPIC unsatisfactorily estimated monthly Q during model run two ($r^2=0.63$). Subsequent parameter modification and model runs did not improve upon the model fit realized under hydrology model run two. Model run two provided the best model fit achieved.

TSS. The initial TSS model run was conducted using the Basic User-Supplied Data File developed in hydrology model run two with DRV equal to MUSLE. Model performance evaluation results indicated EPIC did not satisfactorily estimate monthly TSS. TSS model run two was conducted with DRV set to USLE and CVM set to 0.002. Evaluation indicated a better model fit than under the initial TSS model run. The evaluation also indicated EPIC over-predicted annual TSS. TSS model run three was conducted with DRV set to USLE, CVM set to 0.002, and the USLE P-factor (PE) equal to 0.06. Reducing PE reduced TSS (equation A.84). Results of model performance evaluations indicated EPIC still unsatisfactorily estimated monthly TSS. Subsequent parameter modification and model runs did not improve upon the model fit realized under TSS model run three. Model run three provided the best model fit achieved.

PHOS. The initial PHOS model run was conducted using the Basic User-Supplied Data File developed in TSS model run three. Results of model performance evaluation indicated EPIC initially under-predicted PHOS. PHOS model run 2 was conducted with WP1-8 set to 1000 g t^{-1} . Evaluation indicated that EPIC unsatisfactorily

estimated monthly PHOS during model run two. Subsequent parameter modification and model runs did not improve upon the model fit realized under PHOS model run two. Model run two provided the best model fit achieved.

NO3N. The initial NO3N model run was conducted using the Basic User-Supplied Data File developed in PHOS model run two. The results of model performance evaluation indicated EPIC initially over-predicted NO3N. NO3N model two was conducted with WNO31-8 set to 20 g t^{-1} . Evaluation indicated EPIC over-predicted NO3N. It was suspected that the over-prediction was due to nitrogen contributions to WS-III from rainfall. NO3N model run three was conducted with the average concentration of nitrogen in rainfall (RCN) reduced to 0.015 ppm. Evaluation indicated that EPIC unsatisfactorily estimated monthly NO3N during model run three, but was improved over model run two. Subsequent parameter modification and model runs did not improve upon the model fit realized under NO3N model run three. Model run three provided the best model fit achieved.

Final Model. The final model was run and model performance evaluation conducted. Results of model performance evaluation indicate that EPIC unsatisfactorily estimated monthly Q, TSS, PHOS, and NO3N. Additional efforts to calibrate for Q were not successful. No further parameter estimate modification was conducted.

Daily Evaluation of the Final Model

The final model was evaluated based upon simulated and observed daily Q, as well as daily TSS, PHOS, and NO₃N loading (Appendix III). Evaluations were conducted for the period beginning 1-Oct-83 and ending 30-Sept-88. In general, model performance evaluations were less favorable at the daily time step than they were at the monthly time step. The exception being PHOS, for which model performance evaluations were more favorable at the daily time step. Low coefficients of determination indicated that simulated values inadequately tracked observed values. Regression line slopes and intercepts indicated bias in the model estimates. Model performance evaluations indicate that EPIC unsatisfactorily estimated day-to-day Q, as well as day-to-day TSS, PHOS, and NO₃N loading.

Annual Maximum Daily Q and TSS, PHOS, and NO₃N Loading

Simulated and observed annual maximum daily Q as well as annual maximum daily TSS, PHOS, and NO₃N loading were compared for water years 1984, 1985, 1986, 1987, and 1987. These values, as well as the day of record on which they were realized, are listed in Table 24. Figures 11 through 14 illustrate simulated and observed values.

Discussion

There are several possible explanations for EPIC's failure to predict observed values. The majority of these explanations are rooted in the fact that EPIC was not designed for forested watersheds in the Ouachita Mountains.

The first possible explanation is that EPIC does not adequately represent the hydrologic regime of forested watersheds in the Ouachita Mountains. EPIC employs the SCS Curve Number approach to estimate the amount of rainfall lost as overland flow (equations A.22 through A.31 of Appendix I). EPIC determines the amount of rainfall entering the soil profile as the difference between total rainfall and the amount of rainfall lost as overland flow. EPIC simultaneously calculates the loss of soil water as lateral subsurface flow and percolation (equations A.50 through A.58). Overland flow is the principle stormflow generation mechanism on thinly vegetated or disturbed watersheds located in arid to sub-humid climates (Dunne 1983). This description encompasses most agricultural lands. Thus, overland flow-based stormflow models have been widely accepted and incorporated into agricultural field-scale water quality models such as EPIC.

Attempts to estimate stormflow generation from heavily vegetated forest watersheds located in humid regions using overland flow -based runoff models have met with limited success (Dunne and Black 1970a, Medina and Helfrich 1979, Hewlett 1982, and Bras 1990). Extensive calibration must be conducted to achieve satisfactory model performance (Dunne 1983, Hewlett and Hibbert 1967). Horton (1943) stated that "owing to somewhat unusual conditions, surface runoff rarely occurs from soil well protected by forest cover." The fact that there was often no observable overland flow on forested watersheds (Muller 1966, Tsukamoto 1966, and Dunne and Black 1970a) coupled with observed infiltration rates on forest soils ranging from 14 to 50 in hr^{-1} (Trimble et al. 1958) cast serious doubt on the applicability of overland flow-based runoff models to heavily vegetated watersheds.

Despite the fact that overland flow rarely occurs on well protected forest soils, significant stormflows are generated from forest watersheds. Numerous intensive field

studies have been conducted in an attempt to identify the mechanisms of stormflow generation on heavily vegetated, humid watersheds (Dunne and Black 1970b, Freeze 1974, Mosley 1979, Abdul and Gillham 1989, Turton 1989, Pearce 1990, Wels et al. 1991, Barnes 1992, Navar 1992, and Turton et al. 1992). The current consensus is that the major stormflow generating processes on undisturbed, heavily vegetated, humid watersheds are shallow lateral subsurface flow through highly permeable soil horizons and saturation overland flow from near-stream areas of the watershed.

The variable source area concept was developed to explain stormflow generation from forested watersheds (Hewlett and Hibbert 1967, Hewlett and Troendle 1975, Troendle 1985, and Hibbert and Troendle 1988). Hibbert and Troendle (1988) state that the central precept of the variable source area concept is that water generally infiltrates undisturbed forest soils, migrates downslope, and maintains saturation or near saturation at lower slope positions. These lower slope positions readily contribute subsurface flow to stormflow as the zone of saturated soil surface expands laterally and longitudinally. The degree to which saturation and subsequent expansion would occur for a given slope varies as a function of antecedent soil moisture, precipitation volume, and duration of input.

More specifically, a small but spatially variable portion of an undisturbed forest watershed will generate stormflow in a given storm. The stormflow generating area is fed water as subsurface flow from up slope areas of the watershed. As the water table near the stream builds or "mounds" during a storm, the soil surface will become saturated from below. This area of saturation will grow in size as the storm continues, and decrease as the storm subsides. Precipitation which falls onto the saturated area becomes saturation overland flow and contributes to stormflow. Infiltrated stormflow traveling as subsurface flow can exfiltrate at the boundary of the saturation zone and

contribute to stormflow as return flow. Saturated subsurface flow can contribute to stormflow at the stream channel face. Hortonian overland flow can only contribute to stormflow if the impervious source of the flow is connected to the stream, otherwise it is infiltrated on its path to the stream and becomes subsurface flow.

Given the current theories of stormflow generation from forested watersheds, it is likely that use of the SCS Curve Number model in EPIC does not adequately represent the hydrology of forest watersheds in the Ouachita Mountains. EPIC does attempt to simulate lateral subsurface flow, and is one of the few water quality models which does. However, there is no way of determining if EPIC's lateral subsurface flow component is accurately depicting lateral subsurface flow from WS-I or WS-III. The hydrology component of EPIC drives all other EPIC model components.

A second possible explanation for EPIC's inability to estimate monthly and day-to-day Q, TSS, PHOS, and NO₃N is inadequate simulation of the water, energy, and nutrients dynamics of the pine "crop" found on WS-I and WS-III. Unfortunately, the EPIC documentation does not discuss the development of the parameter estimates for the pine crop contained in the Crop Parameter File. It is known that the parameter estimates are intended for a pine plantation setting. The species of pine, nor the ecosystem, which the pine crop parameter estimates represent is not identified. The presence or absence of a forest understory is not specified in the model documentation.

Because there is no description of the pine crop contained in the Crop Parameter File, it is not known if that crop is representative of the plant community found on clear cut management units in the Ouachita Mountains (Chapter 1). Nor is it known if it is representative of a mature pine plantation plant community found in the Ouachita Mountains. No crop production data exists for WS-I or WS-III, so the EPIC

crop model could not be evaluated for pine production. Within EPIC the crop model impacts evapotranspiration, percolation, lateral subsurface flow, erosion, and nutrient transport estimates.

A third possible explanation for EPIC's inability to satisfactorily estimate day-to-day Q, TSS, PHOS, and NO₃N deals with the timing of rainfall and subsequent stormflow. In reality, the majority of stormflow realized from a day's rainfall may not occur in the same day the rainfall occurred. For instance, if a storm began in the evening of day 1 and the majority of the rainfall in that storm fell prior to 12:00 p.m., the majority of stormflow could well be realized during the early hours of day 2. This phenomena was present in the observed data. Within EPIC, daily rainfall is assumed to fall at the beginning of the day and all surface runoff occurs in the day of question. The timing of lateral subsurface flow depends upon the porosity (PO), field capacity (FC), and saturated conductivity (SC) of each soil layer as well as upon RTTN (equations A.50 and A.53).

A fourth possible explanation for EPIC's inability to satisfactorily estimate day-to-day Q, TSS, PHOS, and NO₃N is the calibration process followed in this project. Improper parameter selection and estimation will of course lead to unsatisfactory model performance. There exists some optimal combination of parameter estimates which will provide the best possible model fit. However, there is no guarantee that parameter estimates under this optimal combination will be within some realistic range. That depends in part upon the quality of the model and its suitability for the task assigned.

Several decisions made prior to and during the calibration of EPIC for this project certainly influenced model performance. First, personal judgment parameter estimation methods were employed during model calibration. Haan et al. (1994) discuss the advantages and disadvantages of the personal judgment parameter

estimation method. Perhaps the use of an objective parameter optimization method would have lead to a better model fit than the personal judgment method. Second, a select group of parameters were chosen for use during the calibration of EPIC. Limiting the number of parameters certainly lead to a worse model fit than if the entire set of parameters contained in EPIC had been used. Third, optimization was based on monthly Q, TSS, PHOS, and NO₃N loading. This decision was made in part to limit the amount of time spent on computing, data processing, and model performance evaluation. It was the judgment of the model user that these were acceptable optimization functions. Better model performance might have been realized if the optimization had been based on daily Q, TSS, PHOS, and NO₃N loading. Finally, parameter estimation was based upon a univariate optimization process, while a multivariate optimization process would have made better use of the information contained in the observed data sets (Haan et al. 1994). The reader is referred to Yan and Haan (1991a and 1991b) as well as Allred and Haan (1991) for further information on parameter estimation procedures.

A fifth possible explanation for EPIC's inability to satisfactorily estimate day-to-day Q, TSS, PHOS, and NO₃N is the presence of errors in the calibration data. There will of course be errors in any data set. Error can be introduced into a data set by poor experimental design, poor sampling technique, faulty equipment, and human imperfection. Although experimental design and sampling technique were sound, error could have been introduced into either data set during data processing.

The actual explanation for EPIC's inability to satisfactorily estimate day-to-day Q, TSS, PHOS, and NO₃N is probably a combination of all five possible explanations discussed above. How large a role, if any role at all, each played cannot be determined.

Conclusion

In general, EPIC did a better job of estimating monthly and day-to-day Q, TSS, PHOS, and NO₃N from WS-I than from WS-III. This is logical because WS-I more closely resembles the agricultural scenarios for which EPIC was designed than does WS-III. Using the parameter estimates selected in this effort, EPIC failed to satisfactorily estimate certain monthly, as well as all daily Q, TSS, PHOS, and NO₃N loading. Conclusions about EPIC's ability to simulate annual maximum daily TSS, PHOS, and NO₃N loading can only be based upon a limited set of observations. However, EPIC's inability to predict the day of occurrence for the annual maximum daily Q, TSS, PHOS, and NO₃N cannot be over-looked. Results indicate that fundamental problems exist concerning the application of EPIC to simulate daily Q, TSS, PHOS, and NO₃N from forested watersheds in the Ouachita Mountains. EPIC did simulate the rapid recovery (reduction in TSS, PHOS, and NO₃N across R1, R2, R3, and R4) of clear cut sites.

It was decided to utilize EPIC in this project despite its short-comings estimating day-to-day Q, TSS, PHOS, and NO₃N loading. EPIC is an interchangeable component of the stochastic framework. Further investigation of the application of EPIC to forested watersheds must be conducted before any management or regulatory decisions in the region can, if ever, be confidently based upon EPIC model predictions.

Table 6. Parameters contained within the Basic-User-Supplied Data File.

Parameter	Description
NBYR	number of years of simulation duration
IYR	beginning year of the simulation
IMO	beginning month of the simulation
IDA	beginning day of the simulation
NIPD	printout interval
IPD	print code to select type of output
NGN	weather input code
IGN	number of times the random number generator cycles
IGSD	day weather generator stops generating same weather
LPYR	leap year considered
IET	potential evapotranspiration equation
ISCN	stochastic CN estimation code
IGRAF	graph display code
ICODE	output conversion code
ITYP	peak runoff rate estimate code
ISTA	static soil profile code
IHUS	automatic heat unit scheduling
WSA	watershed area (ha)
CN2	SCS curve number for moist soil conditions
CHL	distance from outlet to most distant point on watershed (km)
CHS	average channel slope ($m\ m^{-1}$)
CHN	channel roughness factor (Manning's N)
SN	surface roughness factor (Manning's N)
APM	peak runoff rate-rainfall energy adjustment factor
YLT	latitude of watershed
ELEV	average watershed elevation (m)
SNO	water content of snow on ground at start of simulation (frac.)
RCN	average concentration of nitrogen in rainfall (ppm)
RTN	number of years of cultivation before simulation
CO2	CO ₂ concentration in the atmosphere (ppm)
CNO3i	CNO ₃ concentration in irrigation water (ppm)
CHD	mean channel depth (m)
SL	slope length (m)
S	slope steepness ($m\ m^{-1}$)
PEC	erosion control practice factor
DRV	equation for water erosion
YWI	years of maximum monthly 0.5-h rainfall data available
BTA	coefficient used to estimate wet-dry probabilities
EXPK	coefficient used to modify exponential distribution of R
OBMX (1-12) ^a	average monthly maximum air temperature (C)
OBMN (1-12)	average monthly minimum air temperature (C)
STDMX (1-12)	monthly standard deviation for OBMX (C)
STD MN (1-12)	monthly standard deviation for OBMN (C)
RMO (1-12)	average monthly rainfall amount (mm)
RST2 (1-12)	monthly standard deviation of RMO (mm)
RST3 (1-12)	monthly skew coefficient of RMO

PRW1 (1-12)	monthly probability of wet day after a dry day
PRW2 (1-12)	monthly probability of wet day after a wet day
UAVM (1-12)	average number of wet days per month
WI (1-12)	monthly maximum 0.5 h rainfall (mm)
OBSL (1-12)	average monthly solar radiation (MJ m^{-2})
RH (1-12)	monthly average solar radiation (frac.)
FL	field length (km)
FW	field width (km)
ANG	clockwise angle of field length from north
STD	standing dead crop residue (t ha^{-1})
UXP	coefficient of the modified, exponential wind-speed distribution
DIAM	soil particle diameter (μm)
ACW	wind erosion adjustment factor
WVL (1-12) ^a	average monthly wind velocity
DIR1 (1-12)	percent of the month a N wind is realized (%)
DIR2 (1-12)	percent of the month a NNE wind is realized (%)
DIR3 (1-12)	percent of the month a NE wind is realized (%)
DIR4 (1-12)	percent of the month a ENE wind is realized (%)
DIR5 (1-12)	percent of the month a E wind is realized (%)
DIR6 (1-12)	percent of the month a ESE wind is realized (%)
DIR7 (1-12)	percent of the month a SE wind is realized (%)
DIR8 (1-12)	percent of the month a SSE wind is realized (%)
DIR9 (1-12)	percent of the month a S wind is realized (%)
DIR10 (1-12)	percent of the month a SSW wind is realized (%)
DIR11 (1-12)	percent of the month a SW wind is realized (%)
DIR12 (1-12)	percent of the month a WSW wind is realized (%)
DIR13 (1-12)	percent of the month a W wind is realized (%)
DIR14 (1-12)	percent of the month a WNW wind is realized (%)
DIR15 (1-12)	percent of the month a NW wind is realized (%)
DIR16 (1-12)	percent of the month a NNW wind is realized (%)
SALB	soil albedo
TSLA	maximum number of soil layers
ZQT	minimum soil layer thickness (cm)
ZTK	initial soil layer splitting thickness (cm)
ZF	profile thickness at which to stop simulation (cm)
FFC	initial soil water capacity, or fraction of field capacity
WTMN	minimum water table depth (m)
WTMX	maximum water table depth (m)
WTBL	initial water table depth (m)
XIDS	soil weathering code
RFTT	subsurface flow travel time (d)
Z (1-8) ^b	depth from surface to bottom of soil layer (m)
BD (1-8)	bulk density of soil layer (t m^{-3})
U (1-8)	wilting point of soil layer (m m^{-1})
FC (1-8)	field capacity of soil layer (m m^{-1})
SAN (1-8)	sand content of soil layer (%)
SIL (1-8)	silt content of soil layer (%)
WN (1-8)	organic N concentration (g t^{-1})
PH (1-8)	pH of soil layer

SMB (1-8)	sum of bases in soil layer (cmol kg^{-1})
CBN (1-8)	organic carbon content of soil layer (%)
CAC (1-8)	calcium carbonate content of soil layer (%)
CEC (1-8)	cation exchange capacity of soil layer
ROK (1-8)	coarse fragment content of soil layer (% by vol.)
WNO3 (1-8)	nitrate concentration of soil layer (g t^{-1})
AP (1-8)	labile phosphorus concentration of soil layer (g t^{-1})
RSD (1-8)	crop residue in soil layer (t ha^{-1})
BDD (1-8)	oven-dry bulk density of soil layer (t m^{-3})
PSP (1-8)	phosphorus sorption ratio of soil layer
SC (1-8)	saturated hydraulic conductivity of soil layer (mm hr^{-1})
WP (1-8)	organic phosphorus concentration of soil layer (g t^{-1})
NRO	crop rotation duration
NIRR	rigidity of irrigation code
IRR	irrigation code
IRI	minimum automatic irrigation application interval
IFA	minimum automatic fertilizer application interval
LM	liming control code
IFD	furrow diking code
IDR	drainage code
IFFR	automatic fertilization rigidity code
BIR	water stress factor to trigger automatic irrigation
EFI	irrigation runoff ratio
VIMX	maximum allowable irrigation volume per crop (mm)
ARMN	minimum irrigation volume per application (mm)
ARMX	maximum irrigation volume per application (mm)
BFT	N stress factor to trigger automatic fertilization
FNP	fraction of maximum N fertilizer potentially applied at plant
FMX	maximum annual N fertilizer rate per crop (kg ha^{-1})
DRT	time required for drainage to eliminate aeration stress (d)
FDSF	fraction of water in furrow dike available for soil storage
MON (n) ^c	month of operation
DAY (n)	day of operation
COD (n)	operation/tillage code number
CRP (n)	crop ID number
GRZ (n)	grazing duration (d)
MAT (n)	number of years necessary for crop to mature
PHU (n)	potential heat units
CND (n)	curve number after this operation
WSF (n)	plant water stress factor
FPP (n)	fraction of original plant population
MCF (n)	maximum annual N fertilizer applied to crop (kg ha^{-1})
HUSC (n)	timing of operation as a fraction of the growing season
FN (n)	fertilizer ID number
FAP (n)	fertilizer application rate (kg ha^{-1})
FDP (n)	depth of fertilizer placement (mm)
IA (n)	irrigation volume applied (mm)
QVOL (n)	runoff ratio for irrigation water (manual application only)
PST (n)	pesticide ID number
PCF (n)	pest control factor

PAR (n) pesticide application rate (kg ha^{-1})

- ^a Parameter estimate required for month 1 through 12.
- ^b Parameter estimate required for soil layer 1 through 8.
- ^c Parameter estimate required for management operation 1 through n.

Table 7. Parameters contained within the Crop Parameter File.

Parameter	Description
WA	potential energy to biomass conversion factor
HI	normal harvest index (crop yield / aboveground biomass)
TB	optimal temperature for plant growth
TG	minimum or base temperature for plant growth
DMLA	maximum potential leaf area index
DLAI	point in the growing season when leaf area begins to decline
DLP1	defines S-shaped curve relating percent maximum leaf area development to percent of the growing season
DLP2	defines S-shaped curve relating percent maximum leaf area development to percent of the growing season
RLAD	leaf-area-index decline rate parameter
RBMD	biomass-energy decline rate parameter
ALT	index of crop tolerance to aluminum saturation
GSI	maximum stomatal conductance at high solar radiation and low vapor pressure deficit.
CAF	critical aeration factor
SDW	normal planting rate
HMX	maximum crop height
RDMX	maximum root depth
WAC2	describes the effect of atmospheric [CO ₂] on the parameter WA
CVM	minimum value of water erosion C factor (CE)
CNY	normal fraction nitrogen in yield
CPY	normal fraction P in yield
WSYF	lower limit of harvest index (lowest level of HI expected due to water stress)
PST	pest damage factor (fraction of yield remaining after damage)
COSD	seed cost
PRY	price of yield
WCY	fraction of water in yield
BN1	normal fraction of N in crop biomass at emergence
BN2	normal fraction of N in crop biomass at mid-season
BN3	normal fraction of N in crop biomass at maturity
BP1	normal fraction of P in crop biomass at emergence
BP2	normal fraction of P in crop biomass at mid-season
BP3	normal fraction of P in crop biomass at maturity
BW1	wind erosion factor for standing live biomass
BW2	wind erosion factor for standing standing dead crop residue
BW3	wind erosion factor for flat residue
IDC	crop category number
FRS1	point on the frost damage curve relating minimum temperatures to fraction of biomass lost each day that the specified minimum temperature occurs.
FRS2	point on the frost damage curve relating minimum temperatures to fraction of biomass lost each day that the specified minimum temperature occurs.
WAVP	rate of decline in WA per unit increase in vapor pressure deficit (VPD)

VPTH	threshold VPD (leaf conductance is insensitive to VPD until VPD exceeds VPTH)
VPD2	relates a value of VPD above VPTH to a corresponding fraction of the maximum leaf conductance at that value of VPD.
SM42	crop number
RWPC1	fraction of root weight at emergence
RWPC2	fraction of root weight at maturity
CONV	metric to english conversion factor
UNTC	identifies English units for use with crop yield

Table 8. Parameters contained in Tillage Parameter File.

Parameter	Description
TILL	type of tillage operation (equipment)
COTL	cost of tillage operation per hectare
EMX	mixing efficiency of tillage operation
RR	surface random roughness created by operation
TLD	tillage depth (+ is below ground, - indicates aboveground harvest)
RHT	ridge height
RIN	ridge interval
DKH	furrow dike height
DKI	furrow dike interval
IHC	operation code (-2 desroys furrow dikes, -1 builds furrow dikes, 1 kills crop, 2 harvests w/o killing crop, 3 applies manual irrigation, 4 applies fertilizer, 5, plants in rows, 6 plants w/ drill, 7 applies pesticides)
HE	harvest efficiency (fraction of the harvested material removed from the field)
ORHI	override of harvest index

Table 9. Tillage operations available within the Tillage Parameter File.

Operation	Description
LISTPLT	lister planter
ROW PLT	row planter
PLANT DR	drill planter
TRSPLANT	transplant trees
INJ-PEST	inject pesticide
SPREADER	apply fertilizer
SPRYER	apply pesticides
ANHYD AP	anhydrous ammonia applicator
LISTER	lister
DISK BED	disk bedder
ROWBUILD	row builder for sugar cane
CULTIPACK	culti-packer
ROW CULT	row cultivator
FLD CULT	field cultivator
ROT HOE	rotary hoe
ROD WEED	rod weeder
SWEEP	sweep
NOBLE PL	noble plow
SPIK HAR	spike harrow
SAND F	sand fighter (for wind erosion control)
MB PLOW	mold board plow
TAN DISK	tandom disk
PT-CHS	point chisel
TWPT-CHS	twisted point chisel
SWP-CHS	sweep chisel
OFFSET-D	offset disk
SUBSOIL	deep tillage device
KILL	use after harvest to kill crop
HARV2.95	harvest with 95% efficiency - does not kill crop
HAROR85	harvest with 95% efficiency - does not kill crop (harvest index override 85% - used for forage crop)
HARVOR95	harvest with 95% efficiency - does not kill crop (harvest index override 95% - used for forage crop)
SWATHER	harvests - does not kill crop
BALER	bale hay or crop residue
P NUT DIG	peanut digger
SHREDDER	shredder
BURNED	burning operation - does not kill crop
CLEARCUT	harvests trees in a clearcut operation
BAGMOWER	bagmower
MULCHMOW	mulchmower
GRAZE1	cattle grazing - 50 kg of biomass removed per day
GRAZE2	cattle grazing - 5 kg of biomass removed per day
GRZ2-AUM	25 kg consumed and 25 kg trampled, daily; feed conversion 10:1
GRZ1-AUM	12.5 kg consumed and 12.5 kg trampled, daily; feed conversion 10:1
FERTILIZE	applies user-specified dates and amounts of fertilizer

IRRIGATE	applies user-specified dates and amounts of irrigation water
BDIKE100	builds 100 mm tall furrow dikes
BDIKE300	builds 300 mm tall furrow dikes
RMV-DIKE	removes furrow dikes
PADDYBD	rice paddy simulation - builds paddy borders

Table 10. Parameters determined to be candidates for modification during model calibration.

Parameter	Description
IET	potential evapotranspiration equation
ITYP	peak runoff rate estimate code
CN2	SCS curve number for moist soil conditions
APM	peak runoff rate-rainfall energy adjustment factor
PEC	erosion control practice factor
DRV	equation for water erosion
STD	standing dead crop residue (t ha^{-1})
RFTT	subsurface flow travel time (d)
WN (1-8)	organic N concentration (g t^{-1})
WNO3 (1-8)	nitrate concentration of soil layer (g t^{-1})
AP (1-8)	labile phosphorus concentration of soil layer (g t^{-1})
PSP (1-8)	phosphorus sorption ratio of soil layer
WP (1-8)	organic phosphorus concentration of soil layer (g t^{-1})
CVM	minimum value of water erosion C factor (CE)

Table 11. Initial estimates for program control codes.

Parameter	Units	Initial Estimate
NBYR	-	5
IYR	-	84
IMO	-	10
IDA	-	1
NIPD	-	0
IPD	-	3
NGN	-	1
IGN	-	0
IGSD	-	0
LPYR	-	0
IET	-	1
ISCN	-	1
IGRAF	-	1
ICODE	-	1
ITYP	-	0
ISTA	-	0
IHUS	-	0

Table 12. Initial estimates for general information parameters.

Parameter	Units	Initial Estimate	Source
WSA	ha	7.7	Naseer (1992)
CN2	-	70	Dumesnil (1993)
CHL	km	0.48	USGS (1971)
CHS	m m ⁻¹	0.15	USGS (1971)
CHN	-	0.10	Dumesnil (1993)
SN	-	0.59	Ogden (1992)
APM	-	1.0	Dumesnil (1993)
YLT	degrees	34.5	USGS (1971)
ELEV	m	277	Turton (1989)
SNO	fraction	0	Dumesnil (1993)
RCN	ppm	0.8	Dumesnil (1993)
RTN	yr	0	Dumesnil (1993)
CO2	ppm	350	Dumesnil (1993)
CNO3i	ppm	0	Dumesnil (1993)
CHD	m	0	Dumesnil (1993)
SL	m	31	Young et al. (1987)
S	m m ⁻¹	0.15	USGS (1971)
PEC	-	1	Dumesnil (1993)
DRV	-	4	Dumesnil (1993)
YWI	yr	7	EPIC Monthly Weather File ^a
BTA	-	0	EPIC Monthly Weather File ^a

^a Corresponds to the estimates of monthly weather parameters provided for Smithville, OK.

Table 13. Estimates of monthly weather parameters provided for Smithville, OK.

Parameters	Units	Month											
		1	2	3	4	5	6	7	8	9	10	11	12
OBMX	C	10.66	13.23	18.03	23.19	26.84	30.93	33.75	33.55	29.68	24.47	17.37	12.47
OBMN	C	-2.82	-0.91	3.55	8.71	13.19	17.39	19.31	18.23	14.78	8.34	2.84	-1.35
STDMX	C	6.63	6.51	5.94	4.29	3.46	3.29	3.26	3.42	4.28	4.74	5.76	6.02
STDMN	C	6.51	5.97	6.22	5.73	4.56	3.31	2.30	2.66	4.74	5.87	6.17	6.29
RMO	mm	80.0	85.1	99.9	112.4	144.7	102.9	112.2	87.2	89.9	110.2	72.0	91.1
RST2	mm	14.7	17.8	17.8	15.0	21.8	19.0	20.8	17.3	19.6	28.2	18.5	22.1
RST3	mm	1.21	3.24	1.48	0.67	1.59	0.91	2.24	1.23	2.05	3.71	1.93	3.92
PRW1	-	0.16	0.18	0.18	0.21	0.20	0.15	0.16	0.16	0.14	0.14	0.14	0.13
PRW2	-	0.42	0.37	0.40	0.47	0.46	0.45	0.43	0.37	0.44	0.41	0.34	.40
UAVM	d	6.70	6.44	7.15	8.51	8.38	6.43	6.79	6.36	6.00	5.95	5.25	5.52
WI	mm	10.7	17.5	21.6	25.9	33.8	32.5	31.2	34.0	34.0	24.4	25.9	12.4
OBSL	MJ m ⁻²	197.0	269.0	364.0	451.0	528.0	574.0	564.0	529.0	448.0	352.0	253.0	195
RH	frac.	0.72	0.68	0.65	0.66	0.70	0.70	0.65	0.66	0.64	0.67	0.62	0.65
WVL	m s ⁻¹	4.43	4.51	5.08	4.90	4.21	3.94	3.58	3.55	3.62	3.86	4.24	4.28
DIR1	%	12	10	8	8	5	3	4	4	6	8	8	8
DIR2	%	7	6	6	6	5	3	4	5	7	6	5	5
DIR3	%	7	8	7	7	8	7	10	11	13	10	8	8
DIR4	%	8	8	7	7	7	7	9	10	11	9	7	8
DIR5	%	6	7	8	7	8	8	9	10	11	7	7	7
DIR6	%	3	3	4	4	5	5	6	6	6	4	3	3
DIR7	%	5	5	7	7	9	10	9	10	8	8	5	5
DIR8	%	6	6	8	11	12	14	11	10	9	10	8	7
DIR9	%	11	9	9	13	14	20	16	14	12	12	11	10
DIR10	%	5	4	5	6	6	9	8	7	5	5	5	5
DIR11	%	4	4	4	4	4	5	6	5	3	3	4	4
DIR12	%	4	4	3	2	2	2	3	2	2	2	4	4
DIR13	%	7	6	6	4	4	2	2	2	2	4	6	7
DIR14	%	5	5	5	4	4	1	1	1	1	3	5	6
DIR15	%	5	6	6	5	3	2	2	2	2	4	7	6
DIR16	%	8	8	7	6	4	2	2	2	3	5	7	6

Table 14. Wind erosion parameters set to default values (Dumesnil 1993).

Parameter	Units	Estimate
EXPK	-	0
FL	km	0
FW	km	0
ANG	degrees	0
UXP	-	0
DIAM	μm	0
ACW	-	0

Table 15. Initial estimates of soil parameters for soil layers 1 through 8 of the Carnasaw Soil Series.

Parameter	Units	Soil Layer								Source
		1	2	3	4	5	6	7	8	
Z	m	0.10	0.09	0.15	0.36	0.69	0.91	1.35	1.78	Bain and Watterson (1979)
BD	t m ⁻³	1.30	1.30	1.30	1.45	1.35	1.35	1.35	1.35	Abernathy et al. (1983)
U	m m ⁻¹	0.05	0.05	0.05	0.05	0.05	0.18	0.18	0.27	Turton (1989)
FC	m m ⁻¹	0.25	0.25	0.25	0.23	0.23	0.36	0.31	0.40	Turton (1989)
SAN	%	20.0	20.0	14.6	6.0	5.7	1.4	1.7	1.3	Abernathy et al. (1983)
SIL	%	59.3	59.3	67.8	47.8	43.5	31.8	51.7	68.3	Abernathy et al. (1983)
WN	g t ⁻¹	0.0	0.0	0.0	0.0	0.0	0.0	0.0	0.0	Dumesnil (1993)
PH	-	5.1	5.1	5.1	5.0	5.0	5.0	4.9	5.0	Abernathy et al. (1983)
SMB	cmol kg ⁻¹	4.1	4.1	1.5	4.3	5.1	8.4	8.8	10.9	Abernathy et al. (1983)
CBN	%	5.1	5.1	1.2	0.8	0.6	0.6	0.6	0.8	Abernathy et al. (1983)
CAC	%	0.0	0.0	0.0	0.0	0.0	0.0	0.0	0.0	Dumesnil (1993)
CEC	cmol kg ⁻¹	19.3	19.3	11.7	20.7	24.3	36.5	30.0	21.4	Abernathy et al. (1983)
ROK	% vol.	25.0	25.0	25.0	25.0	25.0	25.0	5.0	5.0	Turton (1989)
WNO3	g t ⁻¹	0.0	0.0	0.0	0.0	0.0	0.0	0.0	0.0	Dumesnil (1993)
AP	g t ⁻¹	0.0	0.0	0.0	0.0	0.0	0.0	0.0	0.0	Dumesnil (1993)
RSD	t ha ⁻¹	0.0	0.0	0.0	0.0	0.0	0.0	0.0	0.0	Dumesnil (1993)
BDD	t m ⁻³	1.6	1.6	1.6	1.6	1.7	1.6	1.6	1.6	Bain and Watterson (1979)
PSP	frac.	0.0	0.0	0.0	0.0	0.0	0.0	0.0	0.0	Dumesnil (1993)
SC	mm hr ⁻¹	1461.0	1461.0	1461.0	1461.0	1461.0	1461.0	2.32	2.32	Williams (1990)
WP	g t ⁻¹	0.0	0.0	0.0	0.0	0.0	0.0	0.0	0.0	Dumesnil (1993)

Table 16. Initial estimates of general soil profile parameters.

Parameter	Units	Initial Estimate	Source
SALB	-	0.13	EPIC Soil Data File ^a
TSLA	-	0	Dumesnil (1993)
ZQT	cm	0	Dumesnil (1993)
ZTK	cm	0	Dumesnil (1993)
ZF	cm	0	Dumesnil (1993)
FFC	fraction	0	Dumesnil (1993)
WTMN	m	0	Dumesnil (1993)
WTMX	m	0	Dumesnil (1993)
WTBL	m	0	Dumesnil (1993)
XIDS	-	0	Dumesnil (1993)
RFTT	d	1	Turton (1989)

^a Data provided for the Camasaw Soil Series within EPIC's soil data file.

Table 17. Default values for parameters NIRR through FDSF.

Parameter	Units	Default Value
NIRR	-	0
IRR	-	0
IRI	d	0
IFA	-	0
LM	-	0
IFD	-	0
IDR	-	0
IFFR	-	0
BIR	-	0
EFI	-	0
VIMX	mm	0
ARMN	mm	0
ARMX	mm	0
BFT	-	0
FNP	fraction	0
FMX	kg ha ⁻¹	0
DRT	d	0
FDSF	fraction	0

Table 18. Management operation schedule used to simulate recovery period.

Year	Management Operation Parameters				
	MON	DAY	COD	CRP	IA (mm)
H	1	1	72	-	1
R1	2	1	4	23	-
R2	1	1	72	-	1
R3	1	1	72	-	1
R4	1	1	72	-	1

Table 19. Observed and simulated annual maximum daily Q (mm), TSS (t ha⁻¹), PHOS (kg ha⁻¹), and NO3N (kg ha⁻¹) on WS-I for the recovery period.

	R1		R2		R3		R4	
	Value	Day	Value	Day	Value	Day	Value	Day
Obs Q	55.04	49	53.80	201	23.98	168	33.30	86
Sim Q	85.34	20	60.80	57	33.31	253	28.47	86
Obs TSS	0.2581	49	0.0932	57	0.0648	354	0.0121	86
Sim TSS	0.2201	20	0.1450	57	0.0501	353	0.0267	46
Obs PHOS	0.2266	6	0.0873	201	0.0152	35	0.0093	86
Sim PHOS	0.2110	6	0.0848	57	0.0638	350	0.0322	46
Obs NO3N	0.6119	49	0.2039	126	0.0203	168	0.0097	80
Sim NO3N	0.4894	20	0.1252	57	0.0565	35	0.0313	46

Table 20. Initial estimates for program control codes.

Parameter	Units	Initial Estimate
NBYR	-	20
IYR	-	69
IMO	-	1
IDA	-	1
NIPD	-	0
IPD	-	3
NGN	-	1
IGN	-	0
IGSD	-	0
LPYR	-	0
IET	-	1
ISCN	-	1
IGRAF	-	1
ICODE	-	1
ITYP	-	0
ISTA	-	1
IHUS	-	0

Table 21. Initial estimates for general information parameters.

Parameter	Units	Initial Estimate	Source
WSA	ha	7.9	Naseer (1992)
CN2	-	30	Dumesnil (1993)
CHL	km	0.61	USGS (1971)
CHS	m m ⁻¹	0.12	USGS (1971)
CHN	-	0.10	Dumesnil (1993)
SN	-	0.59	Ogden (1992)
APM	-	1.0	Dumesnil (1993)
YLT	degrees	34.5	USGS (1971)
ELEV	m	277	Turton (1989)
SNO	fraction	0	Dumesnil (1993)
RCN	ppm	0.8	Dumesnil (1993)
RTN	yr	0	Dumesnil (1993)
CO2	ppm	350	Dumesnil (1993)
CNO3i	ppm	0	Dumesnil (1993)
CHD	m	0	Dumesnil (1993)
SL	m	31	Young et al. (1987)
S	m m ⁻¹	0.15	USGS (1971)
PEC	-	1	Dumesnil (1993)
DRV	-	4	Dumesnil (1993)
YWI	yr	7	EPIC Monthly Weather File ^a
BTA	-	0	EPIC Monthly Weather File ^a

^a Corresponds to the estimates of monthly weather parameters provided for Smithville, OK.

Table 22. Initial estimates of general soil profile parameters for the Carnasaw Soil Series.

Parameter	Units	Initial Estimate	Source
SALB	-	0.13	EPIC Soil Data File ^a
TSLA	-	0	Dumesnil (1993)
ZQT	cm	0	Dumesnil (1993)
ZTK	cm	0	Dumesnil (1993)
ZF	cm	0	Dumesnil (1993)
FFC	fraction	0	Dumesnil (1993)
WTMN	m	0	Dumesnil (1993)
WTMX	m	0	Dumesnil (1993)
WTBL	m	0	Dumesnil (1993)
XIDS	-	0	Dumesnil (1993)
RFTT	d	2	-

^a Data provided for the Carnasaw Soil Series within EPIC's soil data file.

Table 23. Management operation schedule used to simulate the U/R recovery period.

Year	Management Operation Parameters				
	MON	DAY	COD	CRP	IA (mm)
69	1	1	4	23	-
70	1	1	72	-	1
71	1	1	72	-	1
72	1	1	72	-	1
73	1	1	72	-	1
74	1	1	72	-	1
75	1	1	72	-	1
76	1	1	72	-	1
77	1	1	72	-	1
78	1	1	72	-	1
79	1	1	72	-	1
80	1	1	72	-	1
81	1	1	72	-	1
82	1	1	72	-	1
83	1	1	72	-	1
84	1	1	72	-	1
85	1	1	72	-	1
86	1	1	72	-	1
87	1	1	72	-	1
88	1	1	72	-	1

Table 24. Observed and simulated annual maximum daily Q (mm), TSS (t ha⁻¹), PHOS (kg ha⁻¹), and NO₃N (kg ha⁻¹) on WS-III.

	1984		1985		1986		1987		1988	
	Value	Day	Value	Day	Value	Day	Value	Day	Value	Day
Obs Q	24.46	150	44.25	205	28.65	228	23.98	24	29.89	87
Sim Q	17.61	361	45.34	21	27.72	58	22.16	241	17.57	46
Obs TSS	0.0044	150	0.0122	205	0.0090	228	0.0077	169	0.0064	87
Sim TSS	0.0049	361	0.0172	21	0.0046	237	0.0105	241	0.0042	317
Obs PHOS	0.0085	176	0.0538	21	0.0154	237	0.0199	152	0.0071	47
Sim PHOS	0.0048	361	0.0633	21	0.0159	228	0.0205	102	0.0041	317
Obs NO ₃ N	0.0016	176	0.0086	21	0.0034	237	0.0035	169	0.0014	185
Sim NO ₃ N	0.0030	297	0.0066	21	0.0034	58	0.0032	241	0.0017	46

Figure 5. Location of WS-I and WS-III on Clayton Lake Watershed.

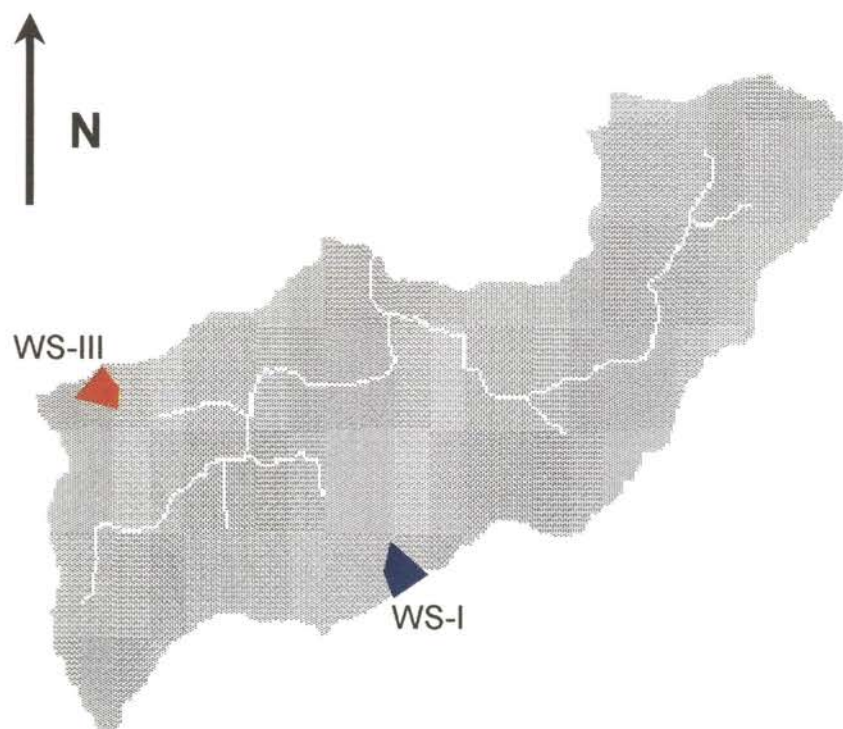


Figure 6. EPIC system file structure (Dumesnil 1993).

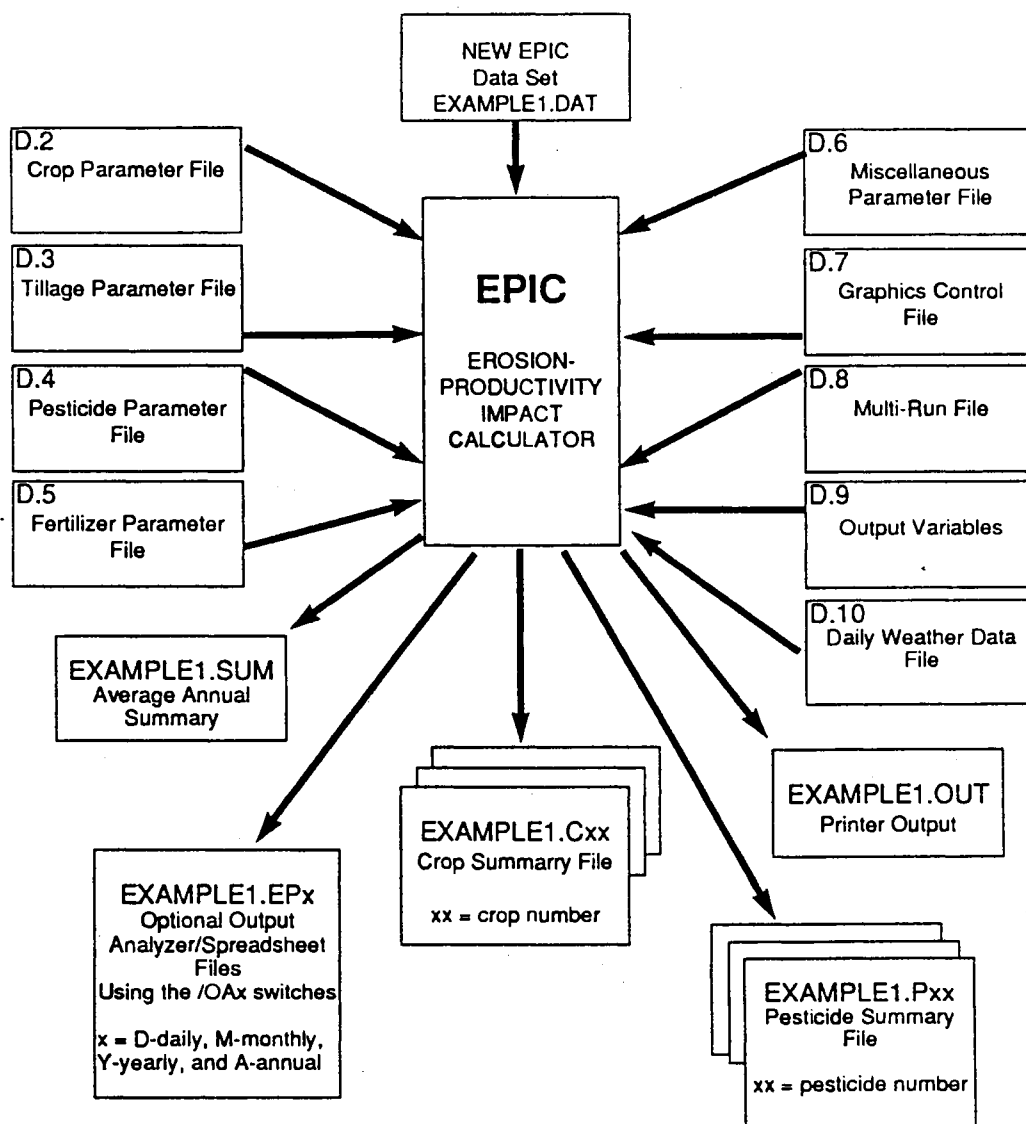


Figure 7. Observed and simulated annual maximum daily Q for WS-I.

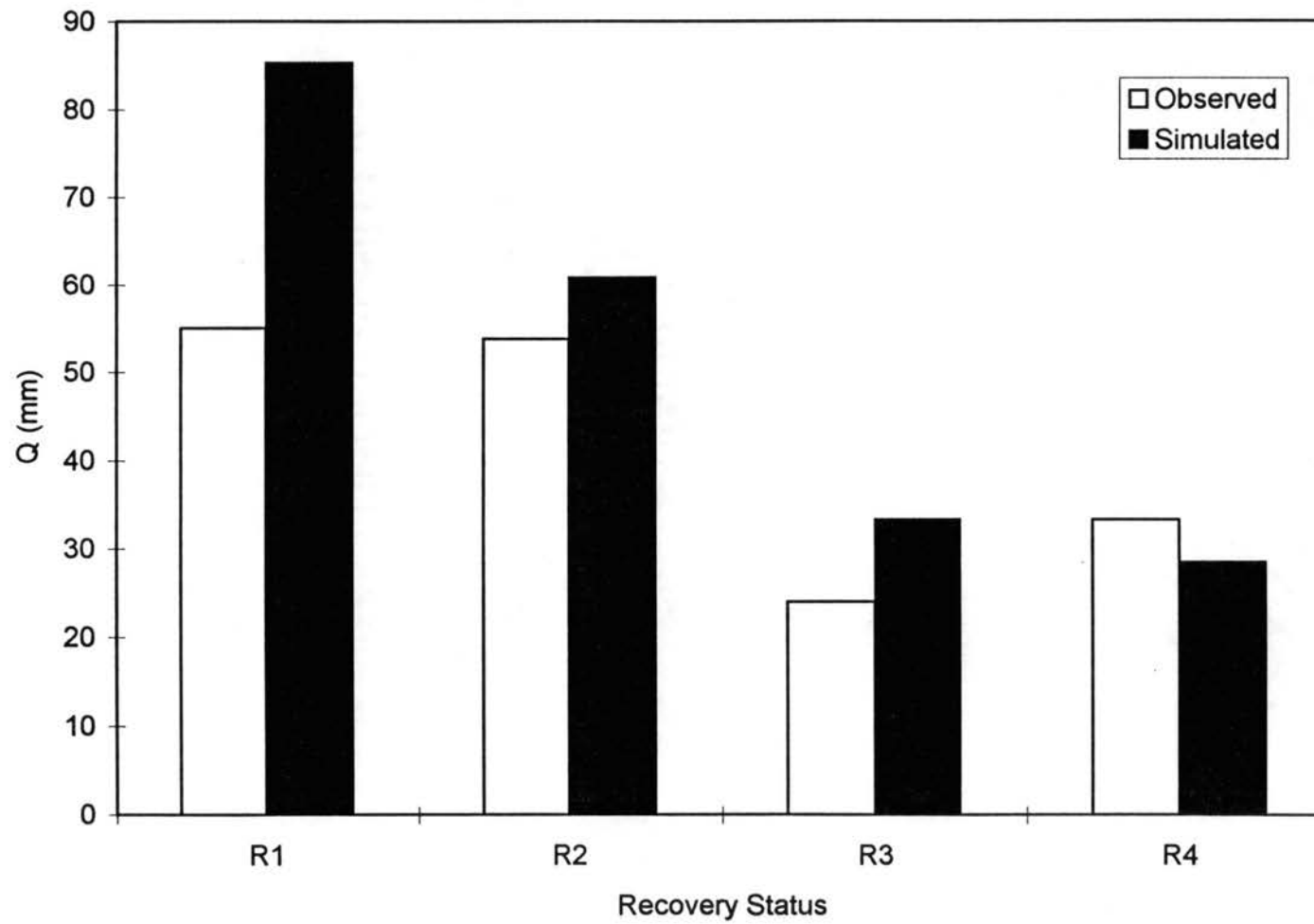


Figure 8. Observed and simulated annual maximum daily TSS loading for WS-I.

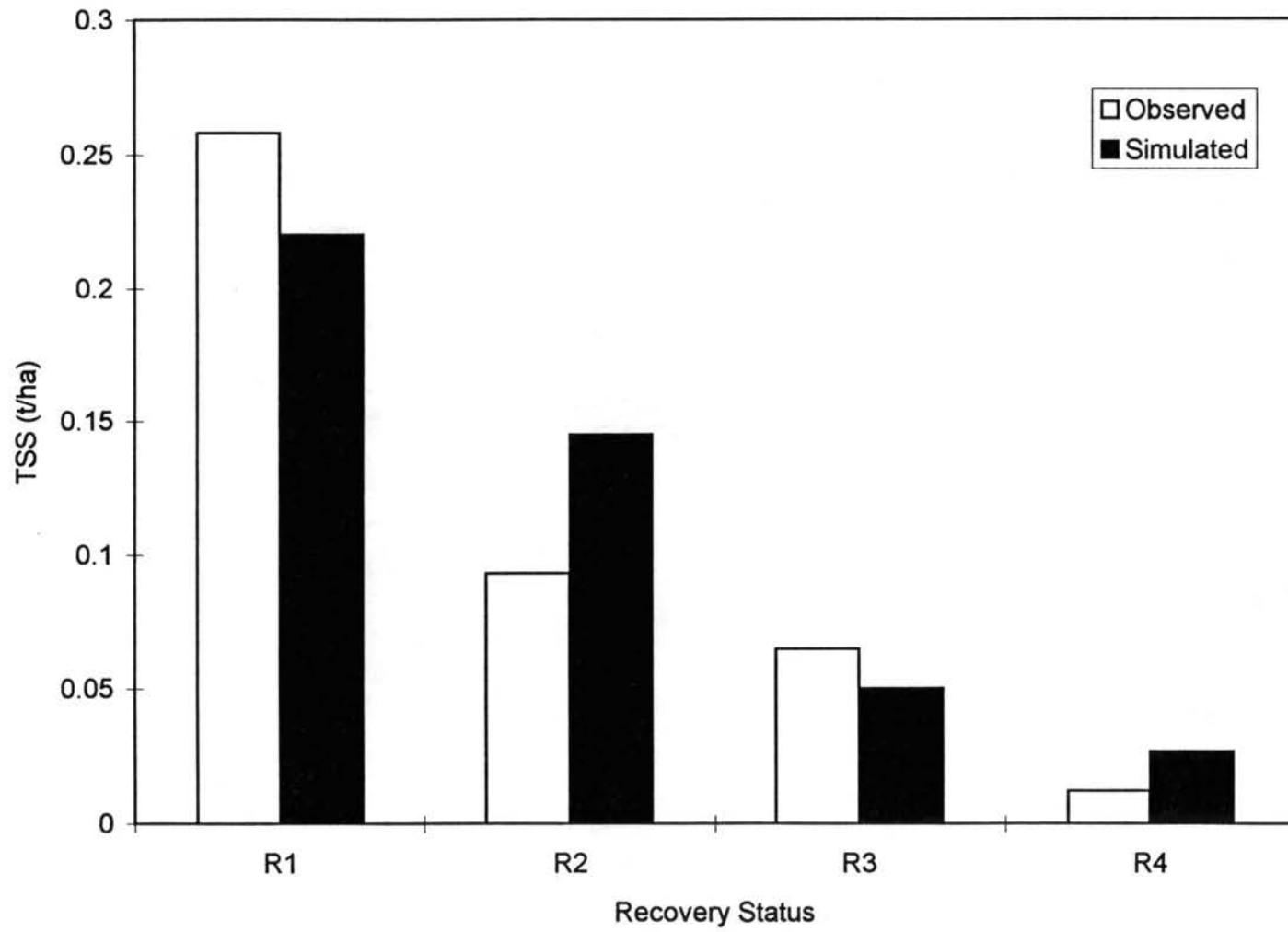


Figure 9. Observed and simulated annual maximum daily PHOS loading for WS-I.

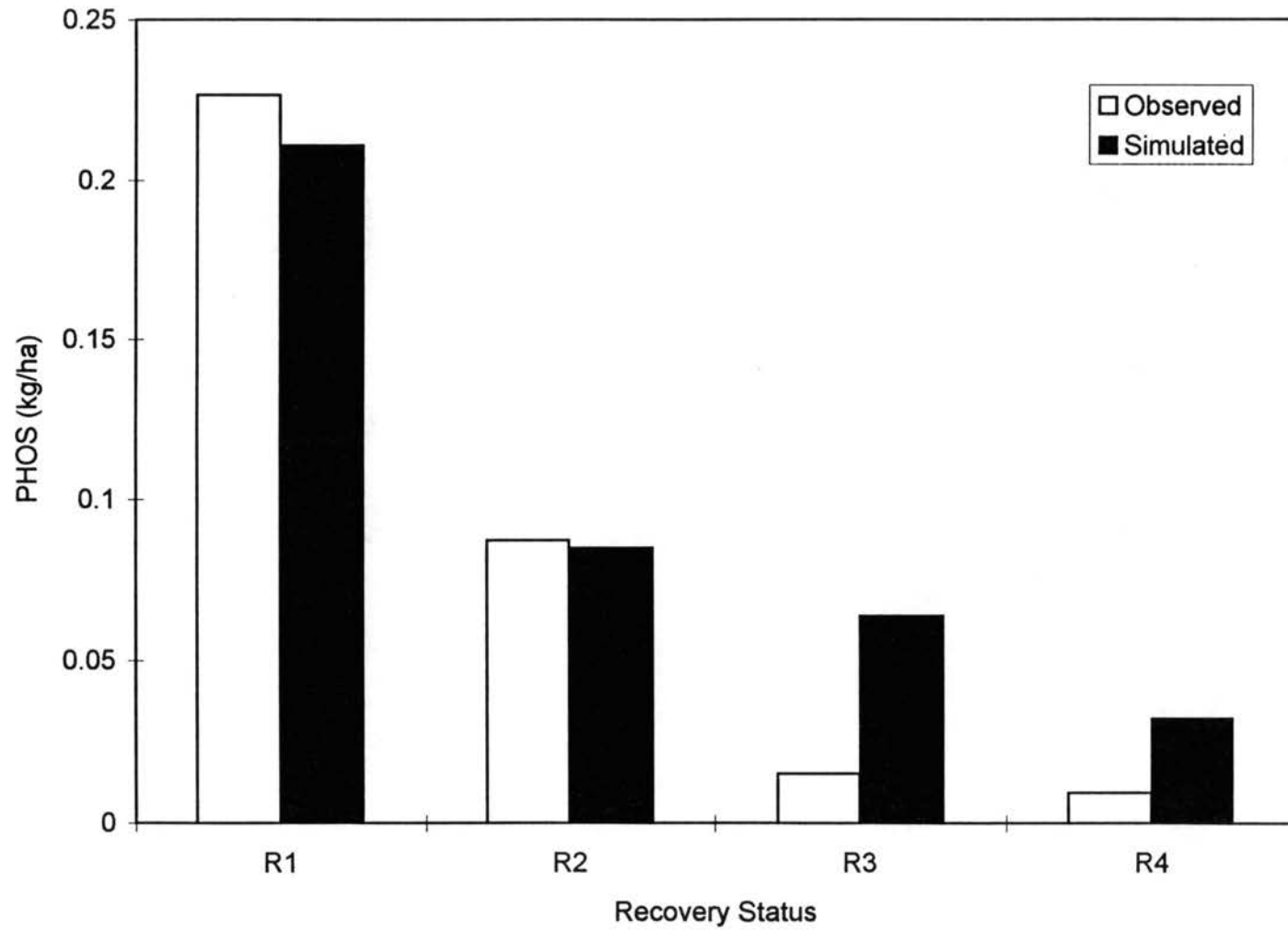


Figure 10. Observed and simulated annual maximum daily NO₃N loading for WS-I.

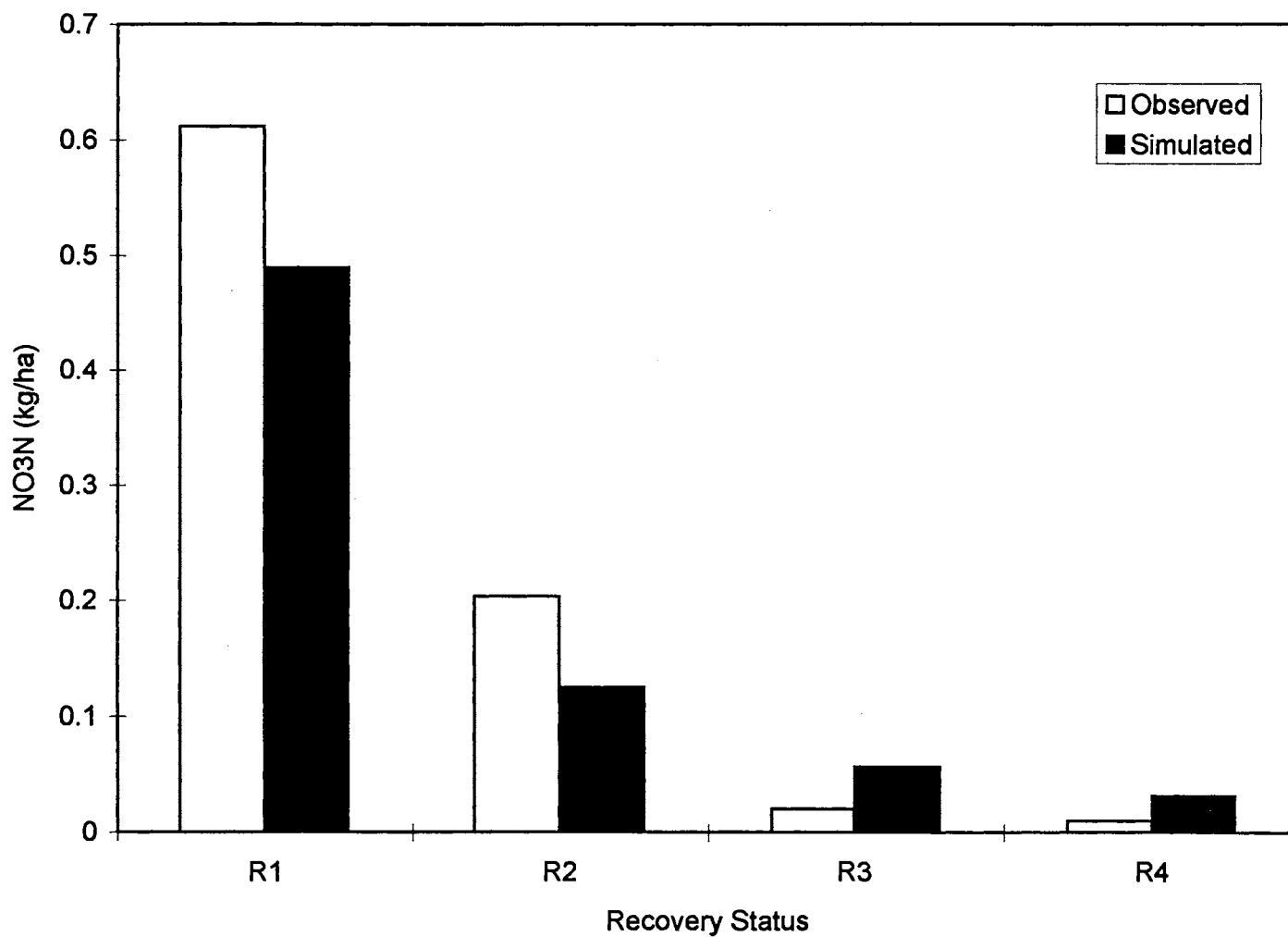


Figure 11. Observed and simulated annual maximum daily Q for WS-III. Each water year represents the U/R recovery status.

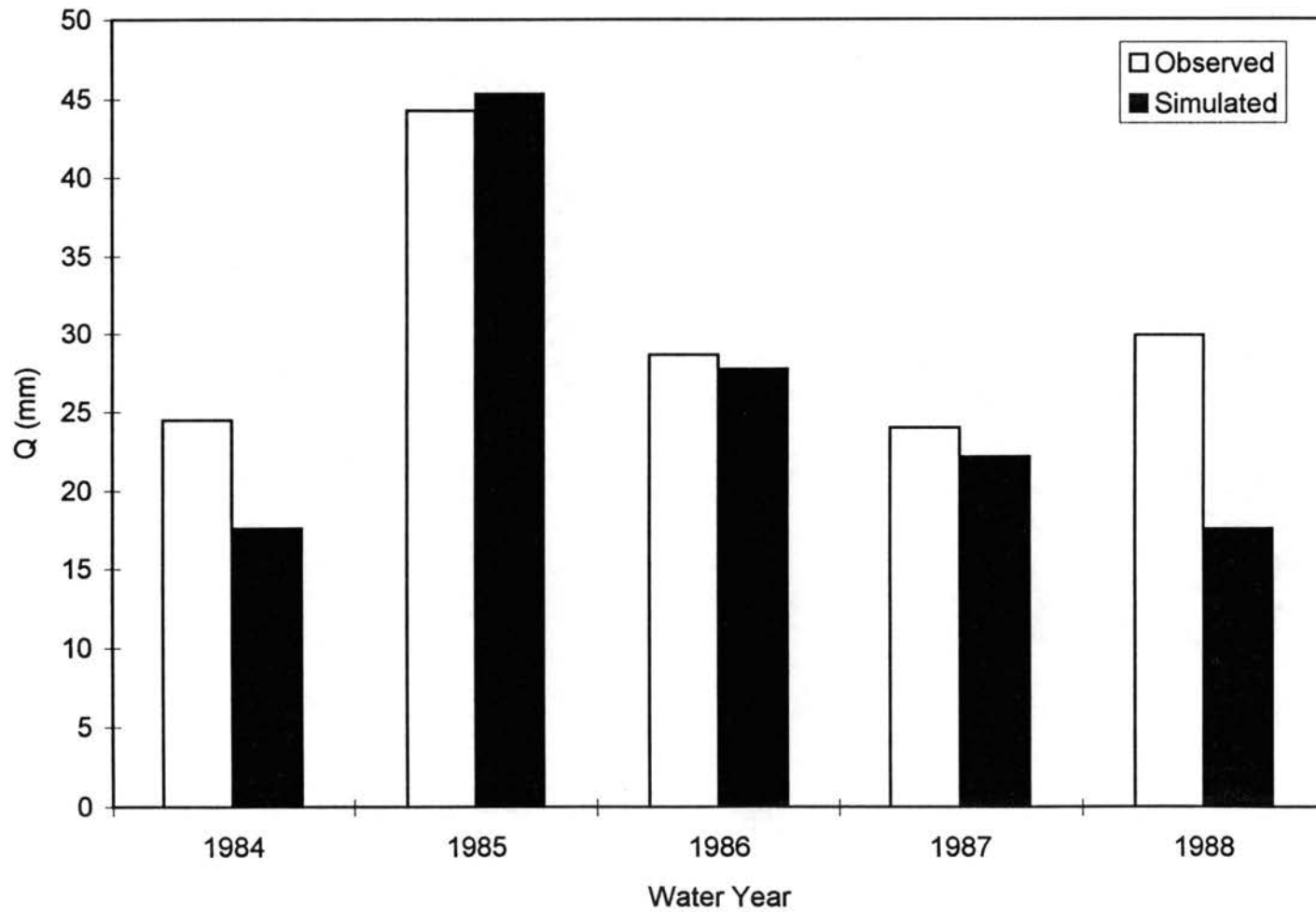


Figure 12. Observed and simulated annual maximum daily TSS loading for WS-III. Each water year represents the U/R recovery status.

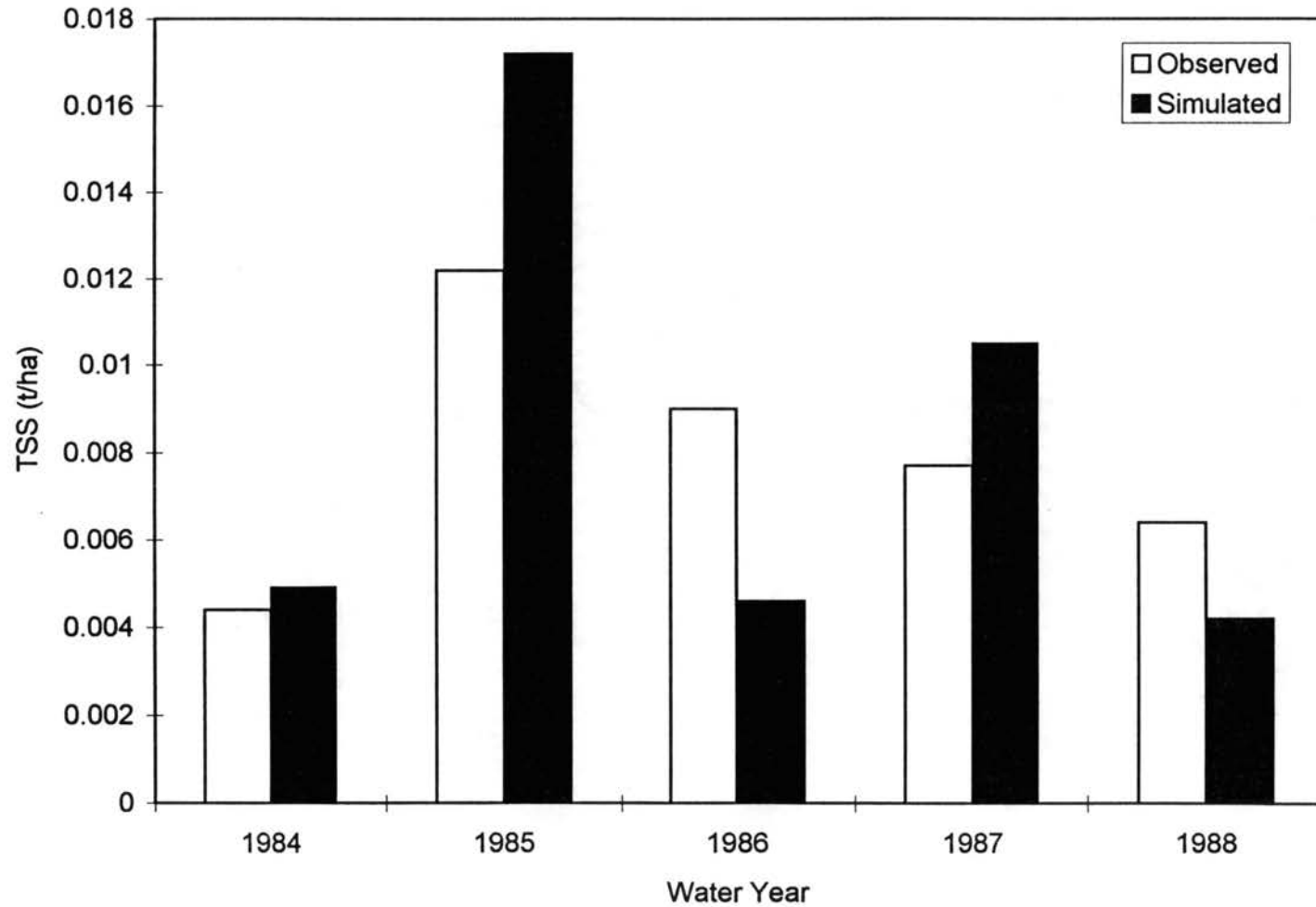


Figure 13. Observed and simulated annual maximum daily PHOS loading for WS-III. Each water year represents the U/R recovery status.

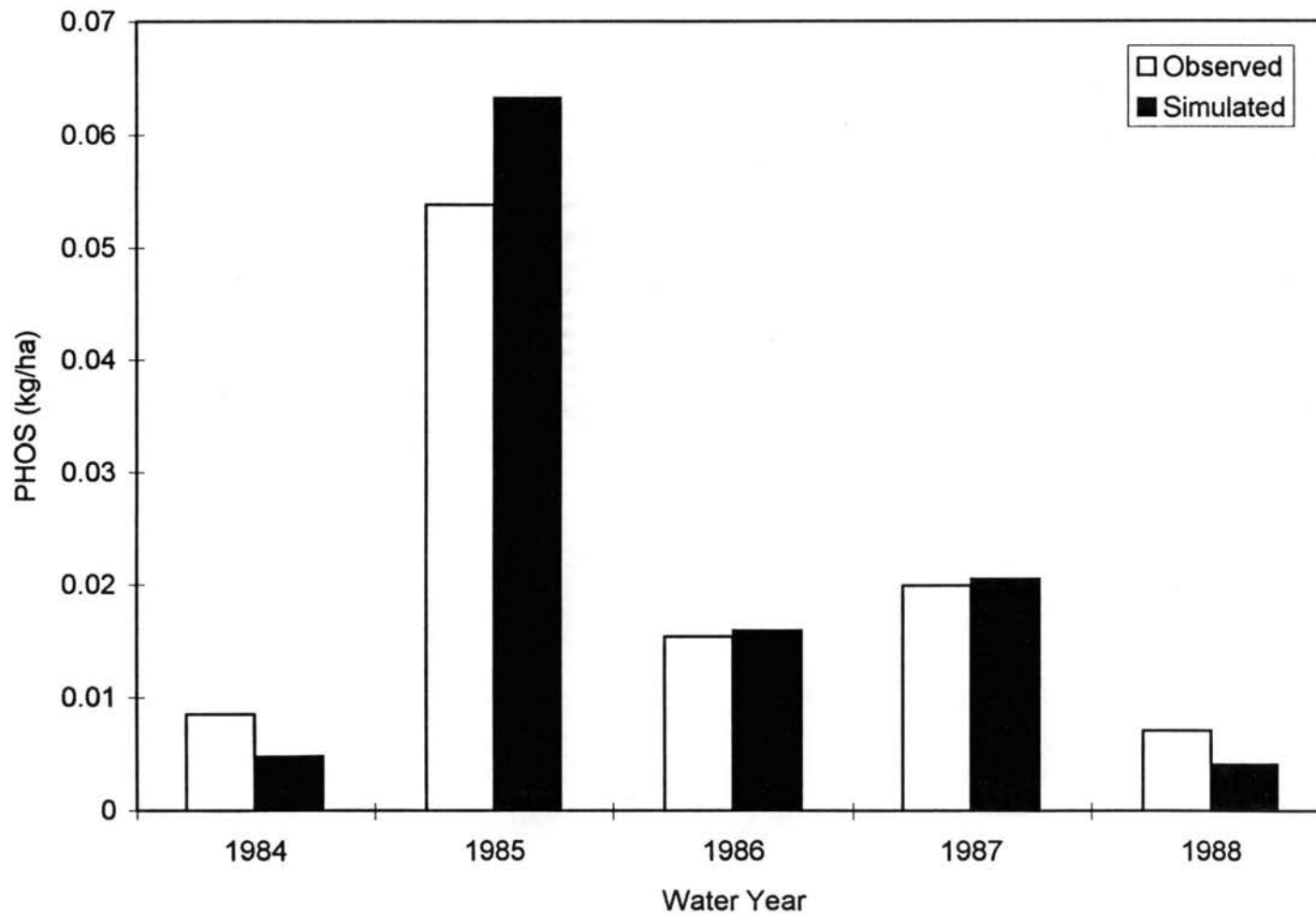
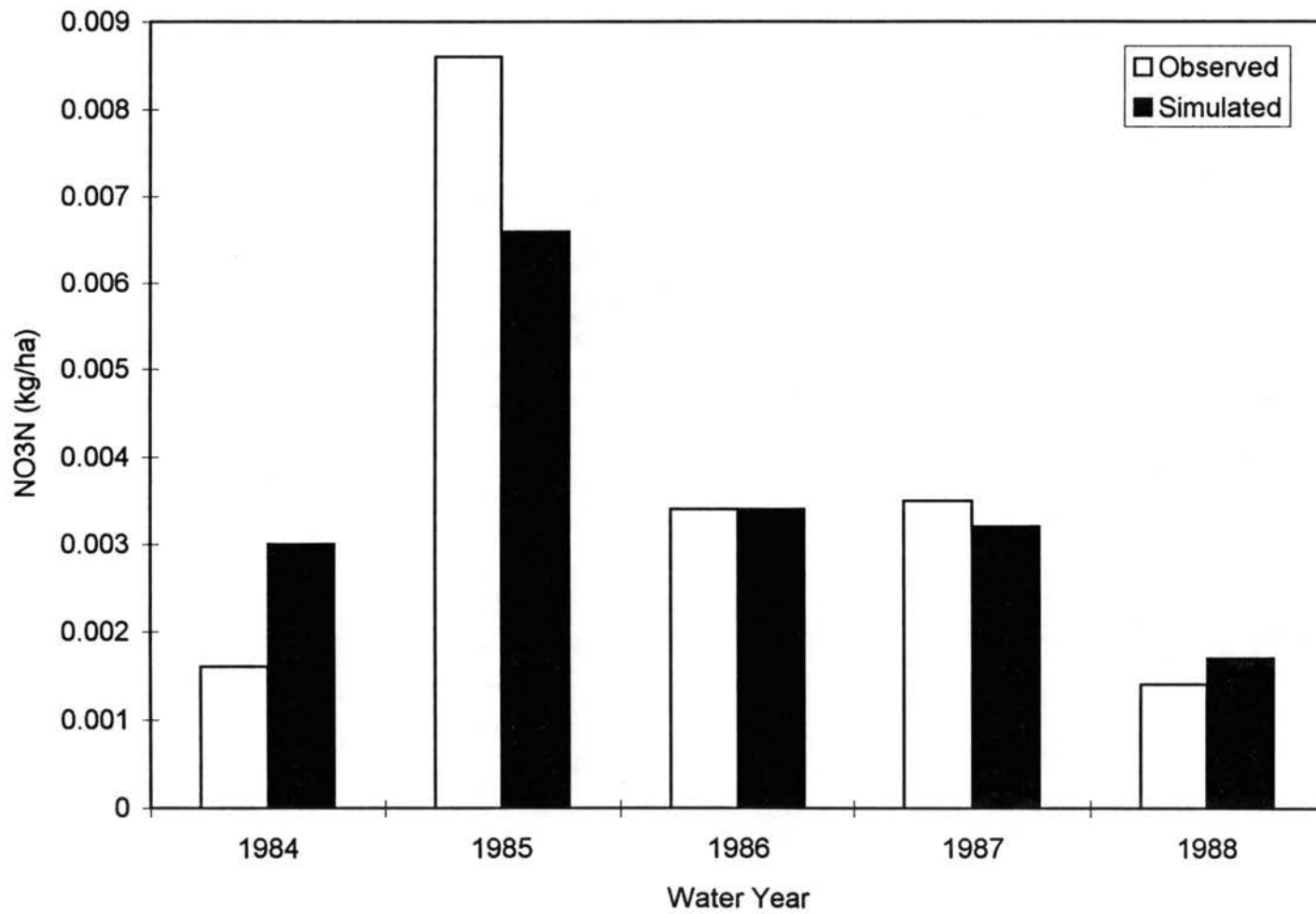


Figure 14. Observed and simulated annual maximum daily NO₃N loading for WS-III. Each water year represents the U/R recovery status.



CHAPTER IV

RESULTS AND DISCUSSION: APPLICATION OF THE STOCHASTIC FRAMEWORK TO CLAYTON LAKE WATERSHED

Simulated Weather

It was important to test the assumption that the simulated weather utilized during the Monte Carlo process was representative of the climate at Clayton Lake Watershed. Annual rainfall, maximum daily rainfall, mean daily solar radiation, maximum daily solar radiation, minimum daily solar radiation, maximum daily temperature, minimum daily temperature, and mean daily relative humidity were calculated for the year common within each weather set (i.e. year 20 of WTH20, year 4 of WTH4, etc.). The grand minimum, maximum, and mean were calculated for the 1500 weather sets and compared to statistics calculated from 23 years of observed daily weather record at Antlers, OK (Bain and Watterson 1979) (Table 25). Long-term observed and simulated grand mean annual rainfall, maximum and minimum recorded daily temperature, and mean daily relative humidity compared well. Grand simulated maximum daily rainfall was more than double the long-term observed maximum daily rainfall. This indicates that synthetic storms much larger than those contained within the 23 year observed weather record were generated. The assumption that simulated weather was representative of the long-term observed weather near Clayton Lake Watershed was accepted.

A scatter plot of simulated annual rainfall versus Monte Carlo run (Figure 15) was developed during examination of the 1500 daily weather sets. This plot does not represent a time sequence of annual rainfall. Each data point represents the output of one Monte Carlo run, and the sequence of data points over Monte Carlo runs has no bearing upon the independence of the data points with respect to time. Figure 15 implies that simulated annual rainfall realized from one Monte Carlo run is correlated with the simulated annual rainfall realized from the previous Monte Carlo run. This correlation was unexpected and required investigation.

During Monte Carlo simulation, a different daily weather set was developed for each Monte Carlo run. This was accomplished by utilizing a different IGN value for the generation of each weather set. IGN is an EPIC program control code which defines the number of times the random number generator cycles before a uniform random number (u) between (0.0 - 1.0) is generated. The uniform random number, u , is used to stochastically generate a series of daily weather data to drive EPIC during each Monte Carlo run. Changing IGN will alter the sequence of generated weather data without changing its long-term statistical properties (Dumesnil 1993). If IGN were not changed the same daily weather data would have been generated for each Monte Carlo run. Based upon the selection of a different IGN value for Monte Carlo run, the author expected the scatter plot of annual rainfall versus Monte Carlo run (Figure 15) to be random in nature.

In a time series, correlation from one observation to the next is called serial correlation or autocorrelation. Autocorrelation in a time series can be examined by comparing data points at 1, 2, 3, ..., k time lags (where k is less than sample size). A correlation coefficient and its associated confidence intervals can be calculated for

each time lag comparison. If the correlation coefficient for a given time lag comparison falls outside the confidence intervals, one can reject the hypothesis that the correlation coefficient is equal to 0. This implies that autocorrelation exists for that time lag. The process described above will be referred to as autocorrelation analysis. The results of autocorrelation analysis are often displayed as correlograms. Correlograms are plots of correlation coefficients plus their associated confidence intervals over lag.

Autocorrelation analysis was applied to examine the correlation of annual rainfall over Model Carlo run. The lag in this analysis was not a lag in time step, but a lag in Monte Carlo run. Figure 16 displays the results of autocorrelation analysis for simulated annual rainfall, confirming that correlation existed within the annual rainfall data set with respect to Monte Carlo run. The author was interested in knowing if the correlation with respect to Monte Carlo run found in annual rainfall had been transmitted through EPIC to the output variables. Figures 17 through 19 display the results of autocorrelation analysis conducted for annual maximum daily TSS, PHOS, and NO₃N loading at the CC00 clearcutting level. Correlation with respect to Monte Carlo run did exist in each of these data sets. It was assumed that correlation with respect to Monte Carlo run existed for the CC33, CC66, and CC100 clearcutting level data sets.

The obvious question is what caused this correlation. It is the author's contention that the correlation is a figment of the process by which IGN values were selected for each Monte Carlo run. IGN values for each Monte Carlo run were selected incrementally. IGN for Monte Carlo run 1 was 1, IGN for Monte Carlo run 2 was 2,....., IGN for Monte Carlo run 1499 was 1499, and IGN for Monte Carlo run 1500 was 1500. It appears that by incrementally increasing IGN value for each Model run, correlation with respect to Monte Carlo run was built into the weather data sets. Why this caused

the correlation cannot be explained because the relationship between IGN, selection of u , and daily weather series generation is not adequately defined in the EPIC model documentation. It is not known if the correlation represents the cyclic nature found in long-term weather data, or if it represents some procedural or “looping” step within EPIC.

In the absence of model documentation the author decided to conduct an investigation of the significance of the correlation with respect to Monte Carlo run for this project. The author theorized that the correlation with respect to Monte Carlo run could be removed by conducting the Monte Carlo process with IGN values (as integers) selected randomly, without replacement, from a uniform distribution (1 - 1500). It was also theorized that the exact same data sets would be generated under random IGN selection as under non-random IGN selection, given that the same set of IGN values was chosen. The data points contained in the data sets generated under random IGN selection would occur in a random order, and no correlation with respect to Monte Carlo run would exist. If this were the case, one can see from the frequency analysis process detailed in Chapter 2 that the probability plots developed under random and non-random IGN selection would be identical.

To test these theories, a small study was conducted to compare data sets generated under non-random IGN selection to data sets generated under random IGN selection. Annual rainfall, annual maximum daily TSS, PHOS, and NO₃N loadings at the CC00 clearcutting level were generated under each IGN selection scheme and evaluated for correlation with respect to Monte Carlo run. Descriptive statistics were developed to determine if the data sets generated under each IGN selection scheme were identical. Monte Carlo runs/IGN values 451 through 550 were used for this study.

These Monte Carlo runs/IGN values were chosen because they represent one of the more pronounced cycles in the annual rainfall data reported in Figure 15.

The data sets for non-random IGN selection were extracted from the larger data sets (output from Monte Carlo runs 451 to 550). Figure 20 is a scatter plot of simulated annual rainfall generated under non-random IGN selection versus Monte Carlo run. Figures 21 through 24 are correlograms for annual rainfall and annual maximum daily TSS, PHOS, and NO₃N loading under non-random IGN selection. Table 26 reports descriptive statistics for annual rainfall, and annual maximum daily TSS, PHOS, and NO₃N loadings.

Under random IGN selection, an integer between 451 and 550 was selected randomly without replacement for each Monte Carlo run. Utilizing the Monte Carlo process described in Chapter 2, 100 estimates of annual rainfall and annual maximum daily TSS, PHOS, and NO₃N loading were generated. Figure 25 is a scatter plot of simulated annual rainfall generated under random IGN selection versus Monte Carlo run. Figures 26 through 29 are correlograms for annual rainfall and annual maximum daily TSS, PHOS, and NO₃N loading under random IGN selection. Table 26 reports descriptive statistics for annual rainfall, as well as annual maximum daily TSS, PHOS, and NO₃N loadings.

Correlation with respect to Monte Carlo run is implied in Figure 20 while Figure 25 implies that annual rainfall is random over Monte Carlo run. Correlograms presented in Figures 21 through 24 indicate the data sets generated under non-random IGN selection contained correlation with respect to Monte Carlo run. Correlograms presented in Figures 26 through 29 indicate the data sets generated under random IGN selection contained no correlation with respect to Monte Carlo run. Examination of Table 26 shows that the data sets generated under random and non-random IGN

selection were identical. The proposed theories are supported by the results of this investigation. The correlation with respect to Monte Carlo run detected in Figures 15 through 19 is a function of the IGN selection process, and does not affect the suitability of the data sets for probability plotting.

Although not critical for this project, the problem identified above could have been critical under different circumstances. This case brings to light the need for complete and detailed model documentation on the part of the model developer. It also brings to light the responsibility of the model user to insure that the modeling process he/she is employing is doing what he/she thinks it is. This requires an understanding of the relationships, assumptions, and limitations of the model being used. If the model developer has neglected to properly document some component of the model which influences the modeling process being employed, the model user should evaluate the influence of that model component on said modeling process. The investigation above is one such example. Ideally, such evaluations should be conducted before the fact to avoid wasted time and effort.

Quantification of Worst Case Daily Loading

Descriptive Statistics

Descriptive statistics for annual maximum daily Q, as well as annual maximum daily TSS, PHOS, and NO₃N loading from Clayton Lake Watershed under each clearcutting management scenario are reported in Table 27. Minimum, maximum, and mean annual maximum daily Q, and annual maximum daily TSS, PHOS, and NO₃N loading increased as clearcutting level increased. This is logical because as clearcutting level increased the amount of the watershed generating elevated levels of

Q, TSS, PHOS, and NO₃N increased. Variance and standard deviation of the four output variables also increased as clearcutting level increased. Coefficient of Variation (Cv), a dimensionless measure of dispersion, of each of the four output variables tended to decrease as clearcutting level increased. The coefficient of skew (SKEW), a measure of the symmetry of the data, was positive in all cases and decreased as clearcutting level increased. Cv and SKEW were noticeably larger at the CC00 clearcutting level than at any other clearcutting level for all output variables. The reduction of Cv as clearcutting level increased indicates that the standard deviation of simulated annual maximum daily Q, and annual maximum daily TSS, PHOS, and NO₃N loading decreased faster than the mean increased as more of the watershed became disturbed. In a sense, watershed response became more predictable as the watershed became more disturbed. The output of the stochastic framework agrees with the generally accepted concept that watershed response (flow and NPS pollution) increases proportionally with the percentage of a watershed that is clear cut (Bosch and Hewlett 1982).

Population Distribution Information

The data sets developed under the stochastic framework contain more information for quantifying worst case daily TSS, PHOS, and NO₃N loading than can be revealed by descriptive statistics alone. There exists some population probability distribution which describes the populations of worst case annual maximum daily Q and annual maximum daily TSS, PHOS, and NO₃N loading at the CC00, CC33, CC66, and CC100 clearcutting management scenarios on Clayton Lake Watershed. The form and parameters of these probability distributions must be estimated from samples taken

from the populations. The data sets generated within this project are such samples. The point should be made that these samples are representative of the population of worst case daily loading from Clayton Lake Watershed as predicted by EPIC. Whether or not these samples are representative of the populations of actual worst case daily loading from Clayton Lake Watershed depends upon how well EPIC represented "reality" on Clayton Lake Watershed.

In general, the reliability of sample statistics for estimating population parameters depends upon how representative the sample is of the population and the sample size. In this case sample size was certainly large. The descriptive statistics reported in Table 27 are estimates of some of the parameters of the unknown underlying populations. Figures 30 through 33 illustrate the change in mean annual maximum daily Q and mean annual maximum daily TSS, PHOS, and NO₃N as predicted by EPIC at the CC33 clearcutting management scenario as sample size increased. These figures provide information on the reliability of the sample means to predict the population means as sample size increases. Note that each sample mean approached some value as sample size increases. The value approached is the population mean. Similar plots at the CC00, CC66, and CC100 clearcutting levels displayed the same form.

Insight to the form of a probability distribution describing a population can often be obtained by developing relative frequency plots. Developing a relative frequency plot involves partitioning the observations in a sample into classes and determining the relative frequency of observations in each class. In this case, relative frequency plots are plots of the frequency of occurrence of annual maximum daily Q, and annual maximum daily TSS, PHOS, and NO₃N loading per class interval versus the class interval midpoint. The equation presented by Sturges (1926) was used as a guideline

for class size selection. A constant class interval was chosen for each output variable to allow examination of changes in the relative frequency distribution over clearcutting level.

Figure 34, 35, 36, and 37 display relative frequency plots for simulated annual maximum daily Q and annual maximum daily TSS, PHOS, and NO₃N at the CC00, CC33, CC66, and CC100 clearcutting levels. The class interval was set to 500,000 m³, 200 t, 100 kg, and 100 kg for Q, TSS, PHOS, and NO₃N, respectively. The relative frequency plots displayed in Figures 34 through 37 reflect the SKEW estimates reported in Table 27. As clearcutting level increased the relative frequency distributions shifted to the right as the frequency of large values increased. In the case of annual maximum daily Q, annual maximum daily PHOS and NO₃N the relative frequency distributions became less positively skewed and more symmetrical in nature as clearcutting level increased. Annual maximum daily TSS became less positively skewed as clearcutting level increased, but did not approach a symmetrical shape as rapidly as the other output variables. Figures 34 through 37 imply that some probability distribution with a strong positive skew describes the populations of worst case annual maximum daily loading from Clayton Lake Watershed as simulated by EPIC.

No attempt was made to identify probability distributions which describe worst case annual maximum daily loading from Clayton Lake Watershed. The discussion above was solely intended to point out that the stochastic framework developed in this project can provide a large amount of information about a given hydrologic variable. Again, this information is only representative of reality if the model employed in the stochastic framework is representative of the system being modeled. Unfortunately, the ability of EPIC to represent annual maximum daily loading from Clayton Lake Watershed could only be evaluated based upon the comparison of a small number of

observed and simulated samples. The reader is referred to Figures 30 through 33 as evidence of the variability which can be expected in statistics based upon small sample numbers.

Risk Assessment

Probability plots for annual maximum daily Q and annual maximum daily TSS, PHOS, and NO₃N loading under the CC00, CC33, CC66, and CC100 clearcutting management scenarios are presented in Figures 38, 39, 40, and 41, respectively. As clearcutting level increased the magnitude associated with each exceedance probability increased. Considering a single magnitude, the probability of the occurrence of an event of equal or greater magnitude increased as clearcutting level increased. The increase from CC00 to CC33 was noticeably greater than the increase from CC33 to CC66 or CC66 to CC100.

The probability plots displayed in Figures 39 through 41 are the end products for the risk assessment component of this project. Figure 38 contains valuable information concerning annual maximum daily flows, but is not of direct interest to this project. The question being asked is what is the probability of LA (nonpoint source pollution from clear cut management units) exceeding the estimated LC (daily loading capacity) for Clayton Lake under the four hypothetical clearcutting levels. The application of the probability plots to assess the risk of LAs from Clayton Lake Watershed exceeding LCs for Clayton Lake is detailed in Chapter 2.

Daily loading capacity estimates are unknown for Clayton Lake. For the sake of illustration, assume that LC was estimated to be 120 t, 120 kg, and 120 kg for TSS, PHOS, and NO₃N, respectively. Examining Figure 39 reveals that under the

assumptions made in this project the risk of daily TSS loading exceeding the estimated LC for TSS would be 0 %, approximately 7 %, approximately 21 %, and approximately 31 % at the CC00, CC33, CC66, and CC100 clearcutting management scenarios, respectively. The risk of daily PHOS loading exceeding the estimated LC for PHOS would be approximately 0.5 %, 10 %, 23 %, and 43 % at the CC00, CC33, CC66, and CC100 clearcutting levels, respectively (Figure 40). The risk of daily NO₃N loading exceeding the estimated LC for NO₃N would be 0 %, approximately 1.1 %, approximately 40 %, and approximately 88 % at the CC00, CC33, CC66, and CC100 clearcutting levels, respectively (Figure 41).

The forest manager must determine what level of risk he/she is willing to accept, or what level of risk State and local law will allow him/her to accept. If that level of risk is low, then his/her management options are limited to either the CC00 or the CC33 clearcutting level. If these options are unacceptable to the manager for reasons other than water quality related (i.e. economic), he/she must develop a different set of management scenarios and reapply the stochastic framework to determine if any of those proposed management scenarios would be suitable.

An important side-note is that the LC estimated for a given waterbody will most likely be the result of simulations conducted using a lake response model. As such, the LC may or may not be realistic. Comparing estimated natural loading levels from a large forest watershed to the estimated LC for the waterbody of interest can provide valuable information about the quality of the LA and LC estimate as well as about the attainability of water quality standards.

For example, assume that the LC for PHOS at Clayton Lake is estimated to be 40 kg. The risk of daily PHOS loading exceeding 40 kg is approximately 43 %, 99 %, 99.6 %, and > 99.95 % at the CC00, CC33, CC66, and CC100 clearcutting level,

respectively (Figure 39). One might conclude that either the LC was under-predicted or LA was over-predicted. Both cases would lead to the development of a conservative TMDL, one which would mandate that little or no point and nonpoint source pollution generating activities be allowed on Clayton Lake Watershed. Conversely, one might conclude that the LC and LA estimates were realistic. In this case, acceptable water quality in the waterbody would not be sustainable under natural loading conditions and the water quality standards developed for that waterbody are too stringent.

Faced with such a situation one would need to evaluate all three possible explanations. A reliable framework for estimating natural loading is an important, but often ignored part of TMDL development. Without an understanding of natural loading levels, unrealistic water quality standards might well lead to the development of TMDLs which cannot be attained under any watershed management plan.

Table 25. Descriptive statistics for simulated and observed weather records.

Annual Weather Parameter	Unit		Min.	Max.	Mean
Rainfall	mm	Simulated	623	2372	1193
		Observed	-	-	1194
Maximum Daily Rainfall	mm	Simulated	37	375	93
		Observed	-	157	-
Average Daily Solar Radiation	MJ m ²	Simulated	15.5	17.4	16.5
		Observed	-	-	-
Maximum Daily Solar Radiation	MJ m ²	Simulated	28.0	32.0	27.7
		Observed	-	-	-
Minimum Daily Solar Radiation	MJ m ²	Simulated	0.0	4.0	0.7
		Observed	-	-	-
Maximum Daily Temperature	C	Simulated	38.1	47.2	42.2
		Observed	-	43.9	-
Minimum Daily Temperature	C	Simulated	-28.1	-8.9	-16.0
		Observed	-23.3	-	-
Average Daily Relative Humidity	frac.	Simulated	0.64	0.68	0.66
		Observed	-	-	0.66

Table 26. Descriptive statistics for annual rainfall, annual maximum daily TSS, PHOS, and NO3N loadings at the CC00 clearcutting level resulting from non-random and random selection of IGN.

IGN Selection	Output	Units	MIN	MAX	MEAN	VAR	ST DEV	C _v	SKEW
Non-Random	Rainfall	mm	883	1800	1159	33259	182	0.16	1.36
	TSS	t	2.39	51.18	10.89	58.84	7.67	0.71	2.31
	PHOS	kg	7.50	259.37	55.63	2563.41	50.63	0.91	1.77
	NO3N	kg	1.31	19.17	5.39	11.15	3.34	0.62	1.50
Random	Rainfall	mm	883	1800	1159	33259	182	0.16	1.36
	TSS	t	2.39	51.18	10.89	58.84	7.67	0.71	2.31
	PHOS	kg	7.50	259.37	55.63	2563.41	50.63	0.91	1.77
	NO3N	kg	1.31	19.17	5.39	11.15	3.34	0.62	1.50

Table 27. Descriptive statistics for output of the Monte Carlo procedure. TRT = clearcutting management scenario.

Output	Unit	TRT	MIN	MAX	MEAN	VAR	ST DEV	C _v	SKEW
Q	m ³	CC00	133171	5100000	627397	179862000000	424101	0.68	3.61
		CC33	204790	5991000	897148	289002000000	537589	0.60	2.96
		CC66	253151	6548000	1061780	380322700000	616707	0.58	2.73
		CC100	293000	7400000	1289648	549610000000	741357	0.57	2.53
TSS	t	CC00	2.4	150.5	12.4	125.8	11.2	0.90	4.61
		CC33	6.9	1077.6	136.8	13399.8	115.8	0.85	2.73
		CC66	9.3	1718.0	217.3	33571.7	183.2	0.84	2.60
		CC100	10.6	2183.5	275.6	55918.6	236.5	0.86	2.65
PHOS	kg	CC00	5.5	403.0	59.1	2882.3	53.7	0.91	2.09
		CC33	30.1	723.0	173.4	9087.0	95.3	0.55	1.83
		CC66	45.5	955	245.5	15776.5	125.6	0.51	1.75
		CC100	61.3	1210.0	319.0	24075.3	155.2	0.49	1.71
NO3N	kg	CC00	0.8	44.6	6.1	21.5	4.6	0.76	2.81
		CC33	76.2	460.1	160.5	1778.1	42.2	0.26	1.72
		CC66	137.0	810.9	291.4	5517.0	74.3	0.25	1.58
		CC100	190.0	1114.0	389.0	10085.2	100.4	0.26	1.74

Figure 15. Simulated annual rainfall versus Monte Carlo run.

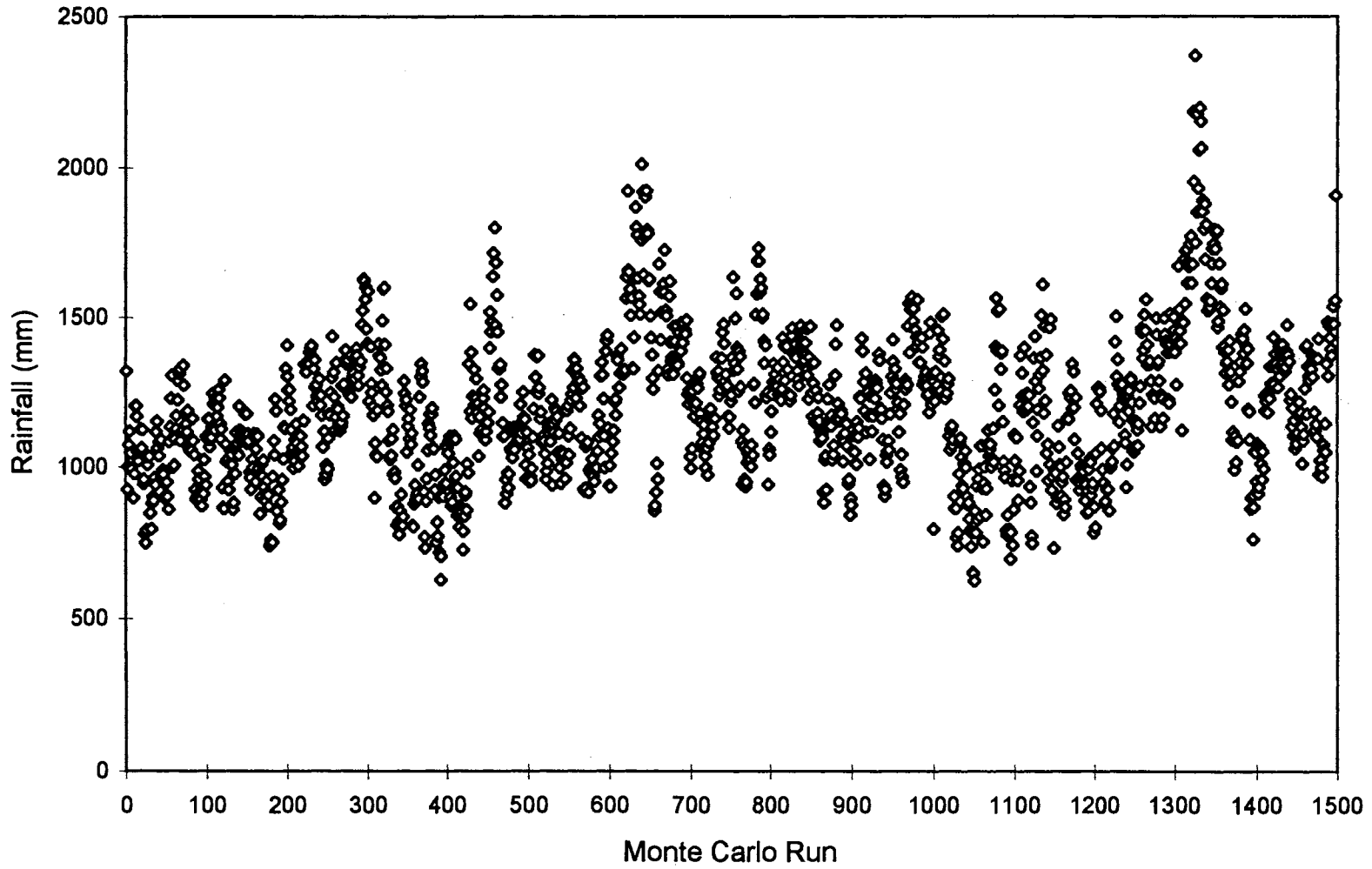


Figure 16. Correlogram for simulated annual rainfall.

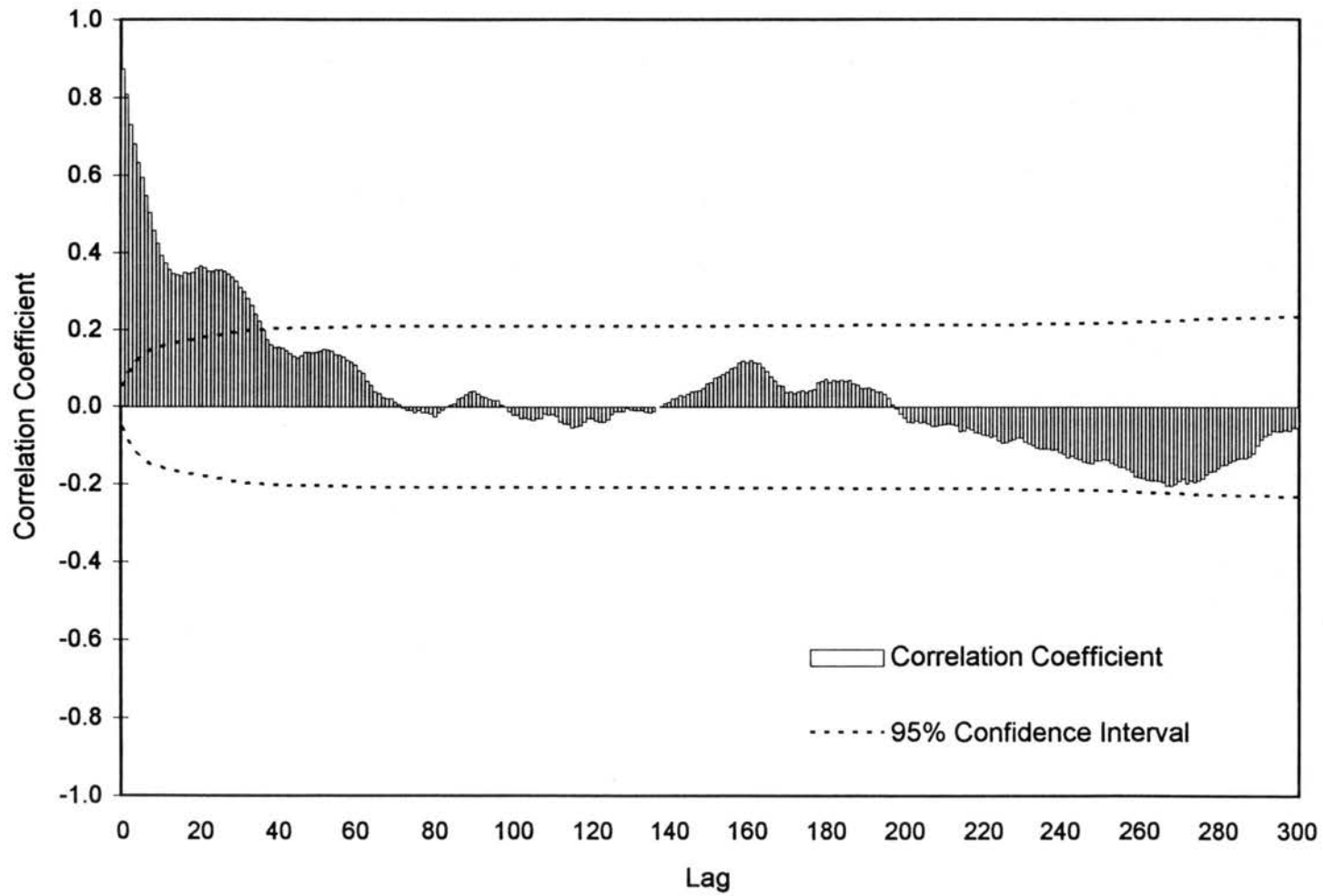


Figure 17. Correlogram for simulated annual maximum daily TSS loading.

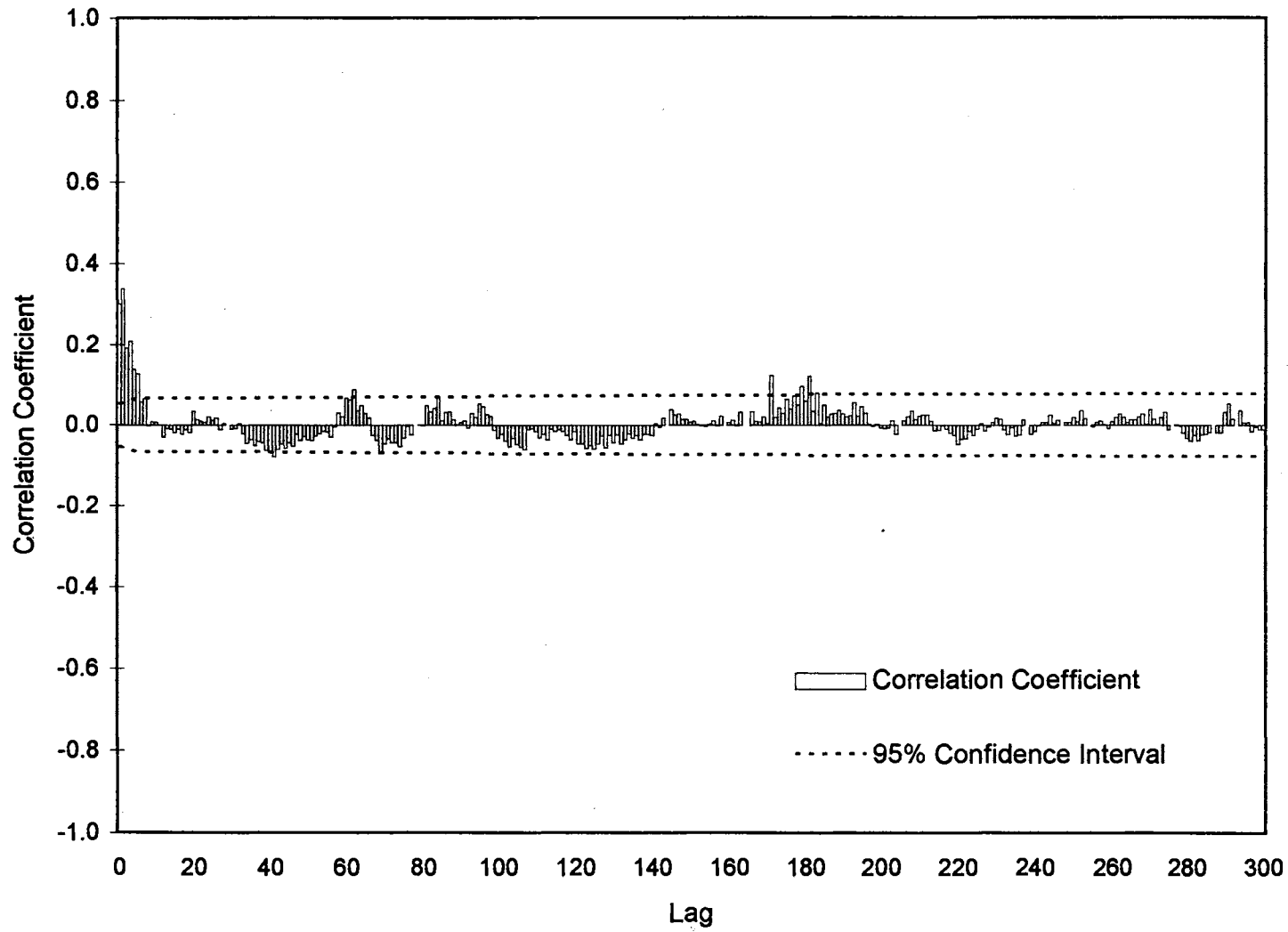


Figure 18. Correlogram for simulated annual maximum daily PHOS loading.

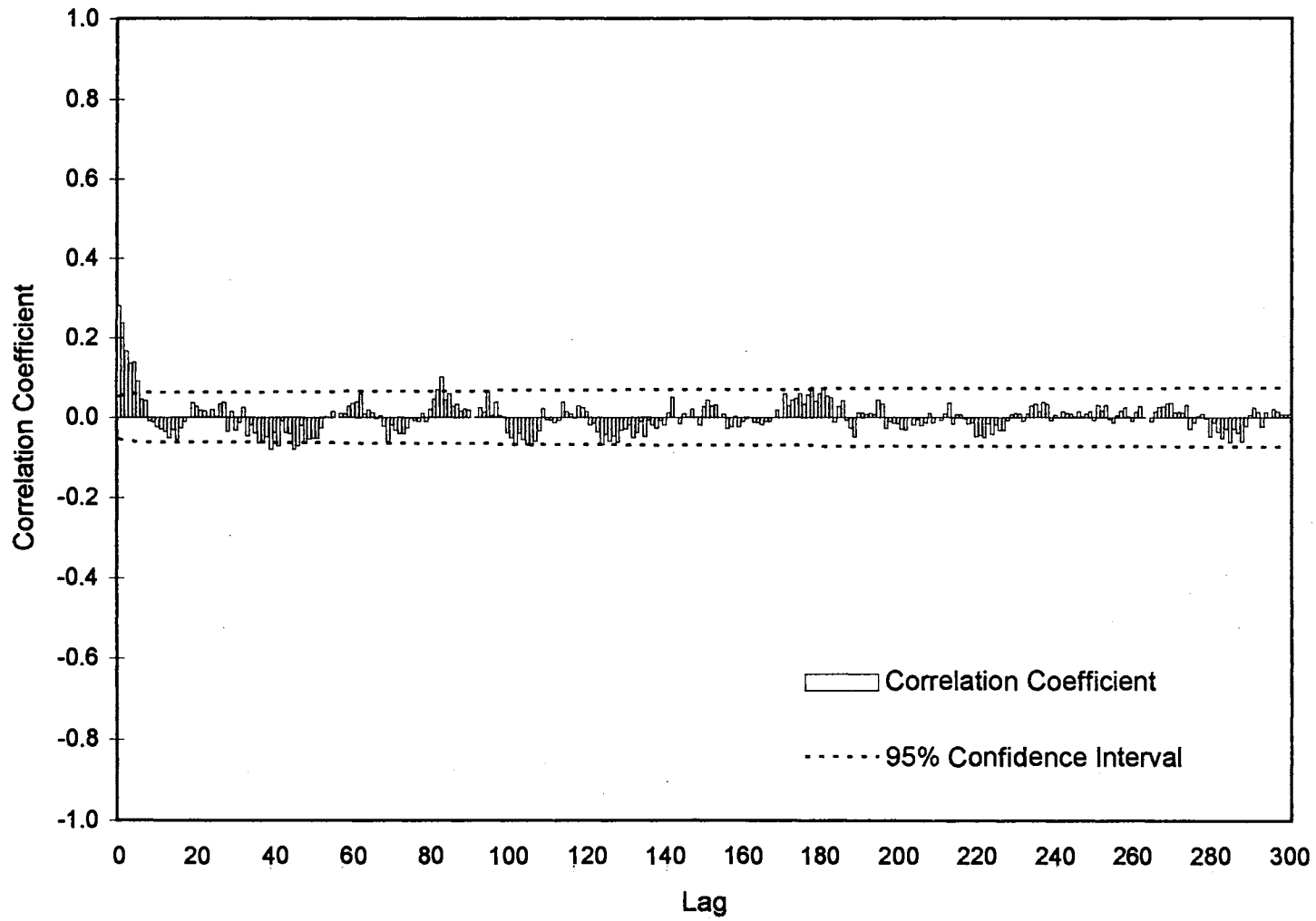


Figure 19. Correlogram for simulated annual maximum daily NO₃N loading.

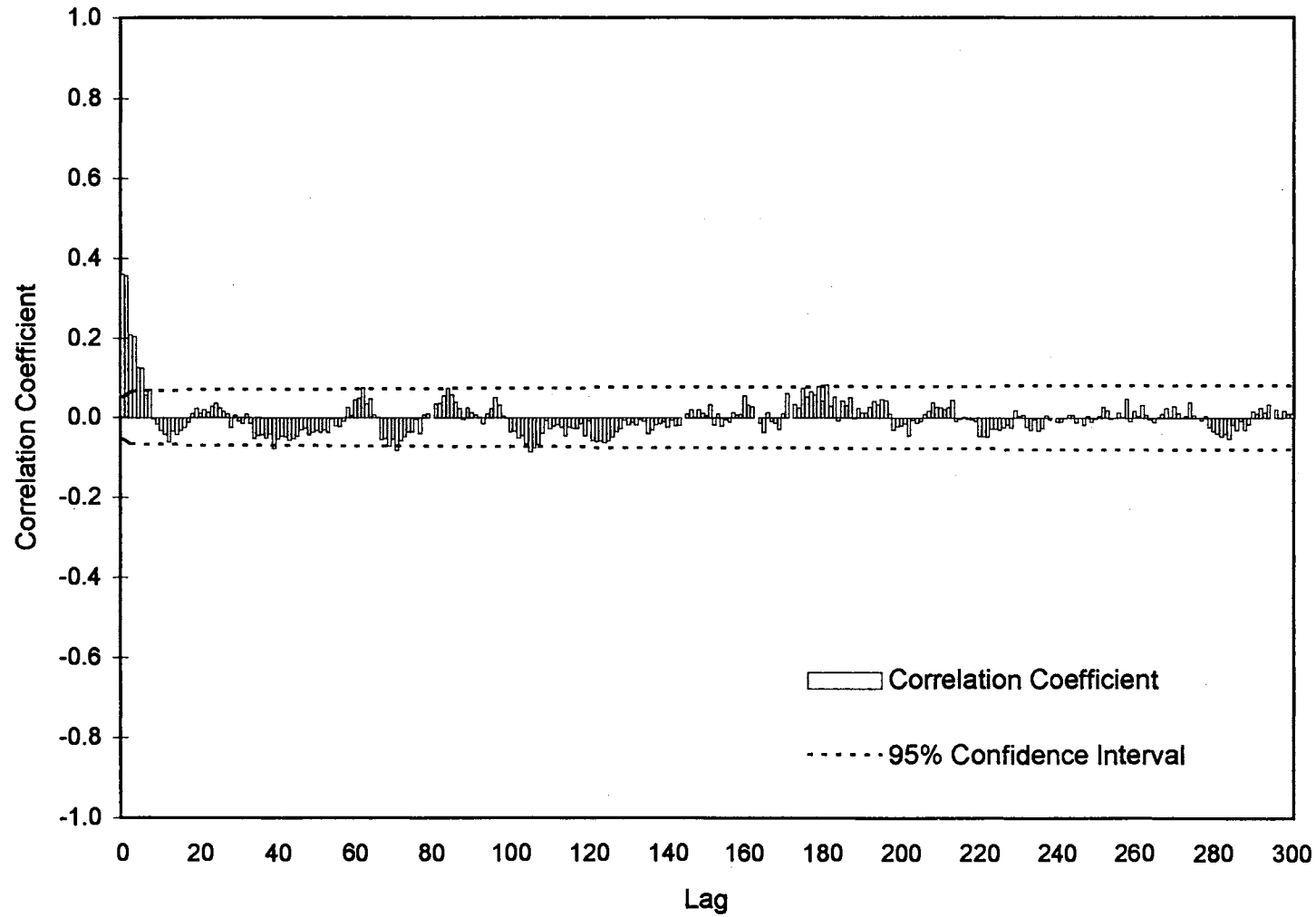


Figure 20. Simulated annual rainfall under non-random IGN selection versus Monte Carlo run.

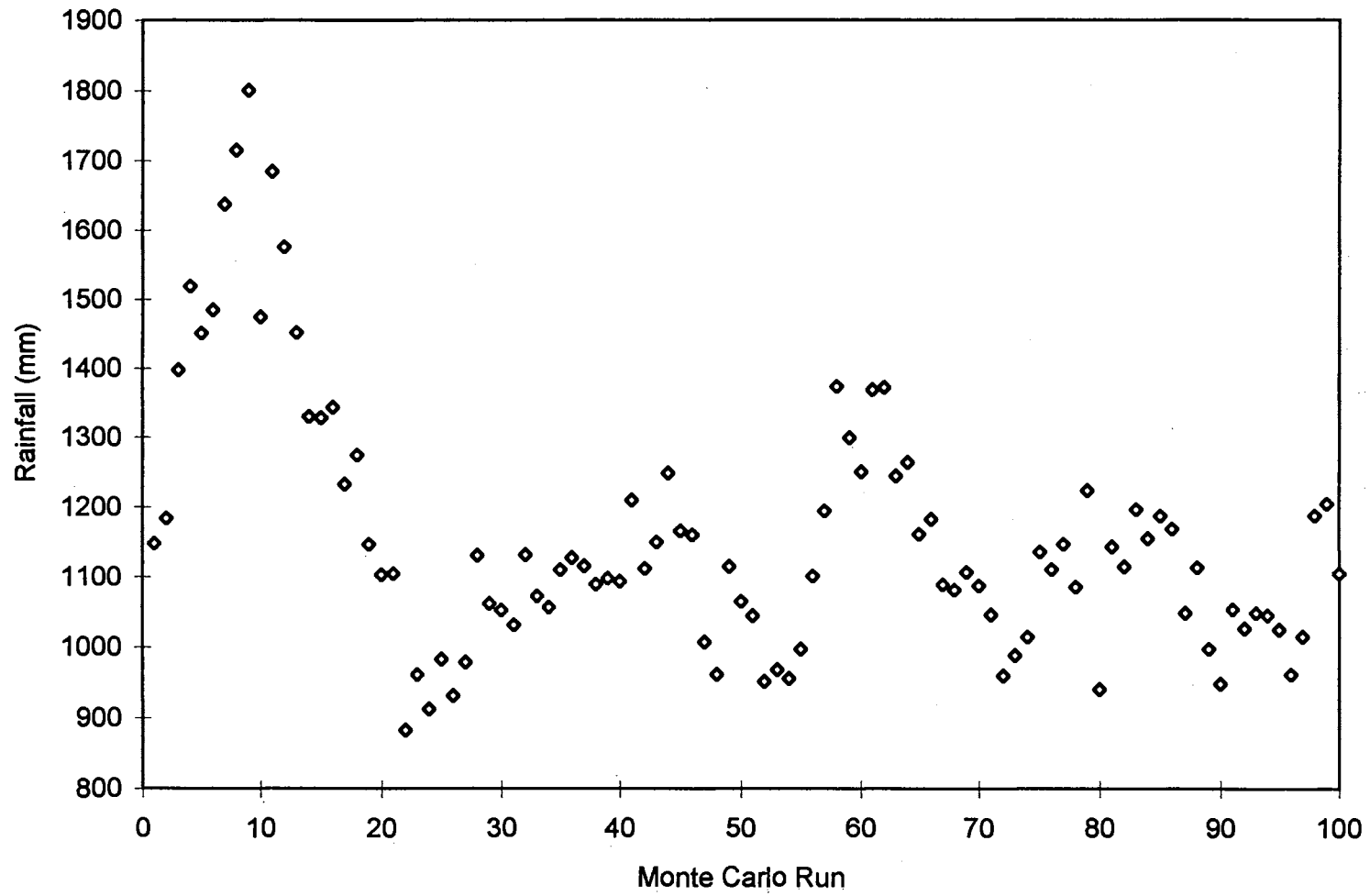


Figure 21. Correlogram for simulated annual rainfall under non-random IGN selection.

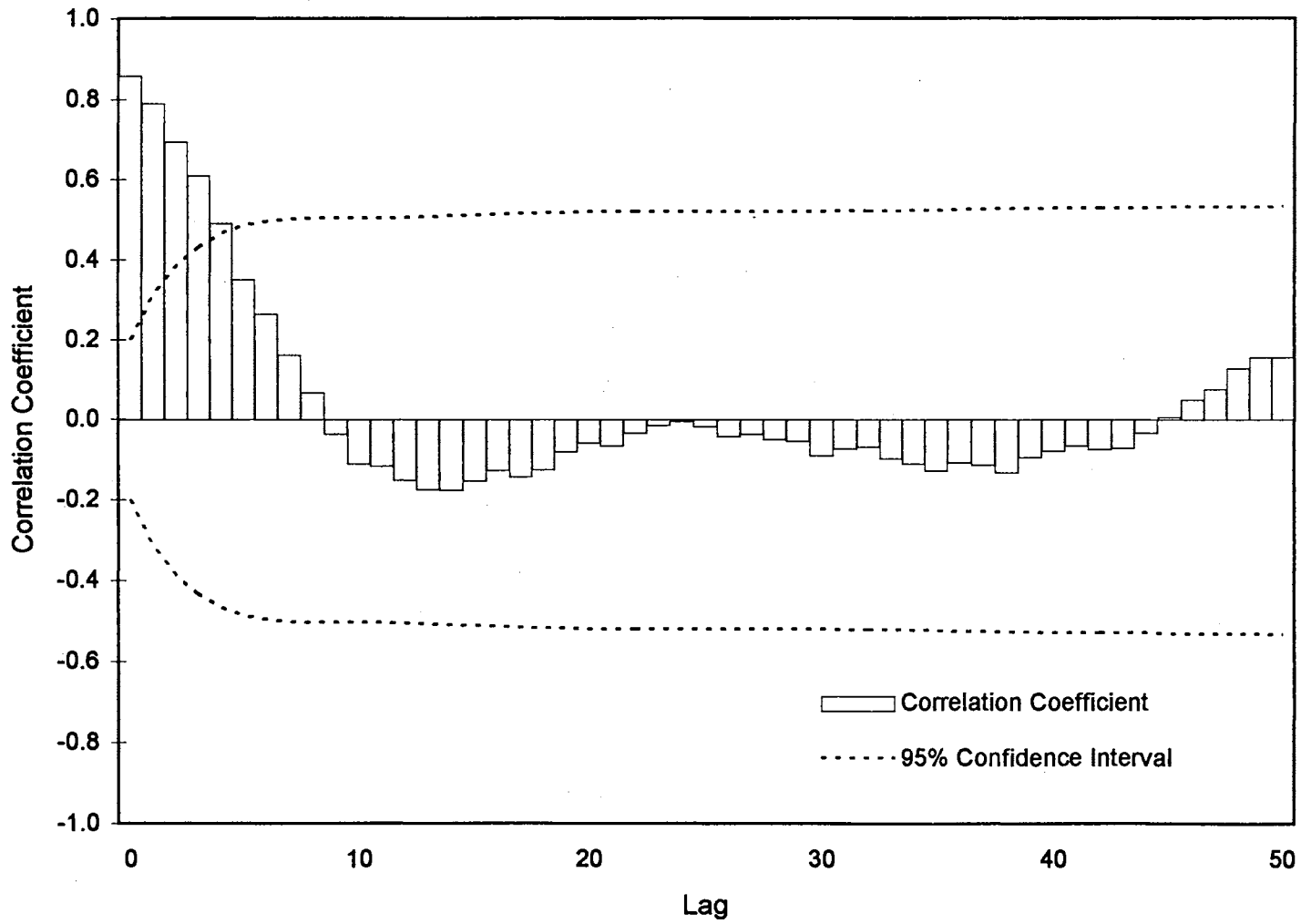


Figure 22. Correlogram for simulated annual maximum daily TSS loading under non-random IGN selection.

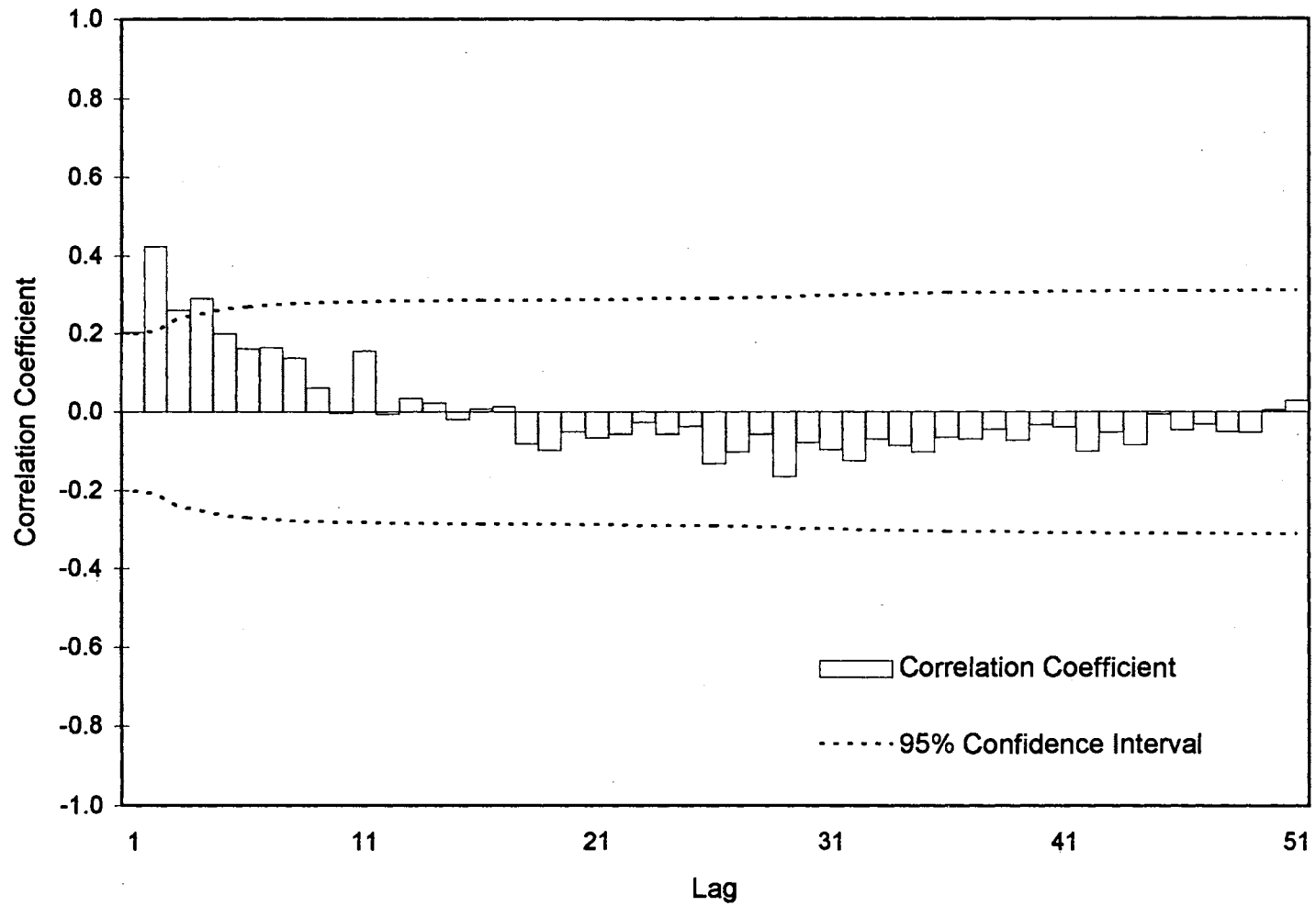


Figure 23. Correlogram for simulated annual maximum daily PHOS loading under non-random IGN selection.

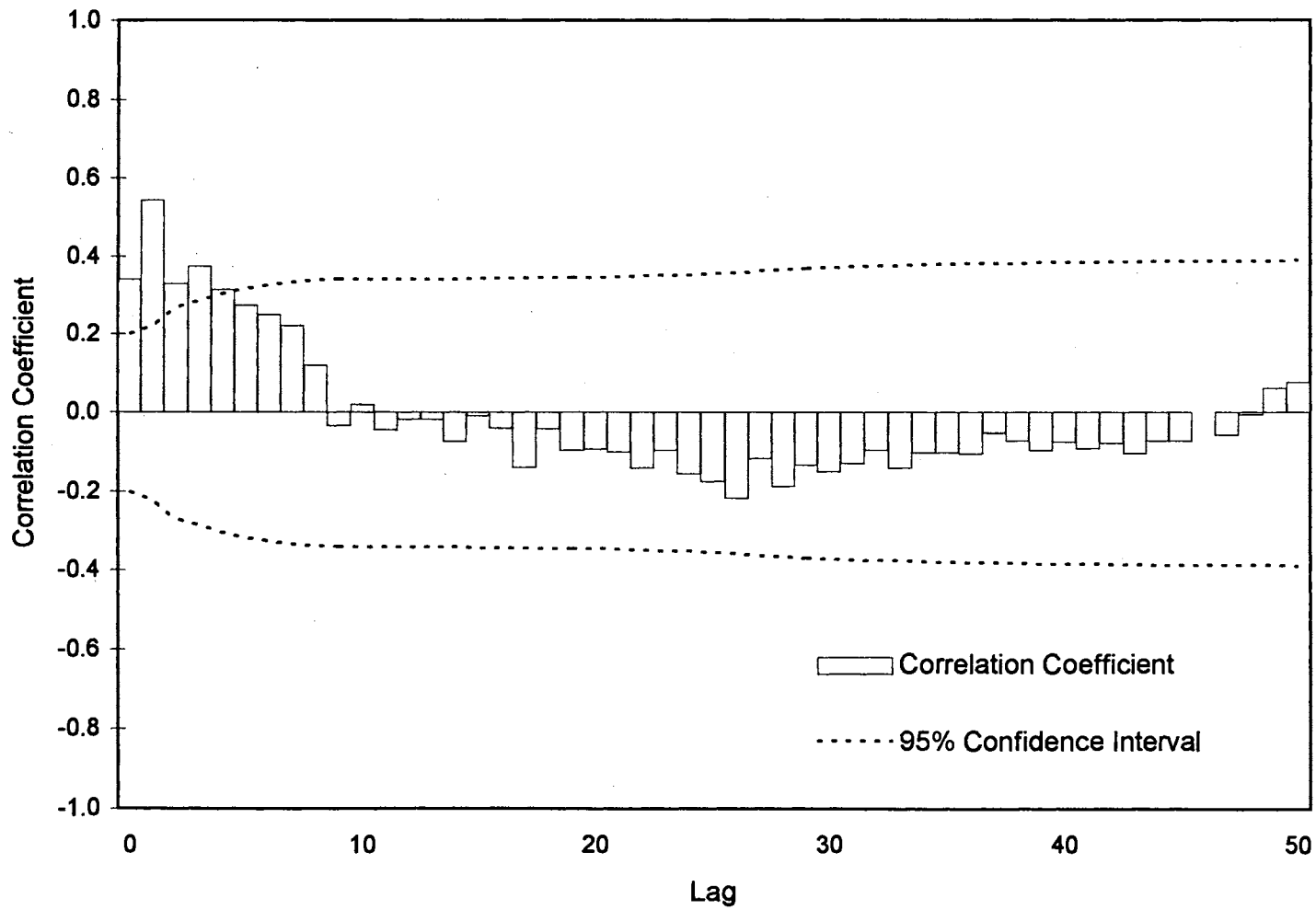


Figure 24. Correlogram for simulated annual maximum daily NO₃N loading under non-random IGN selection.

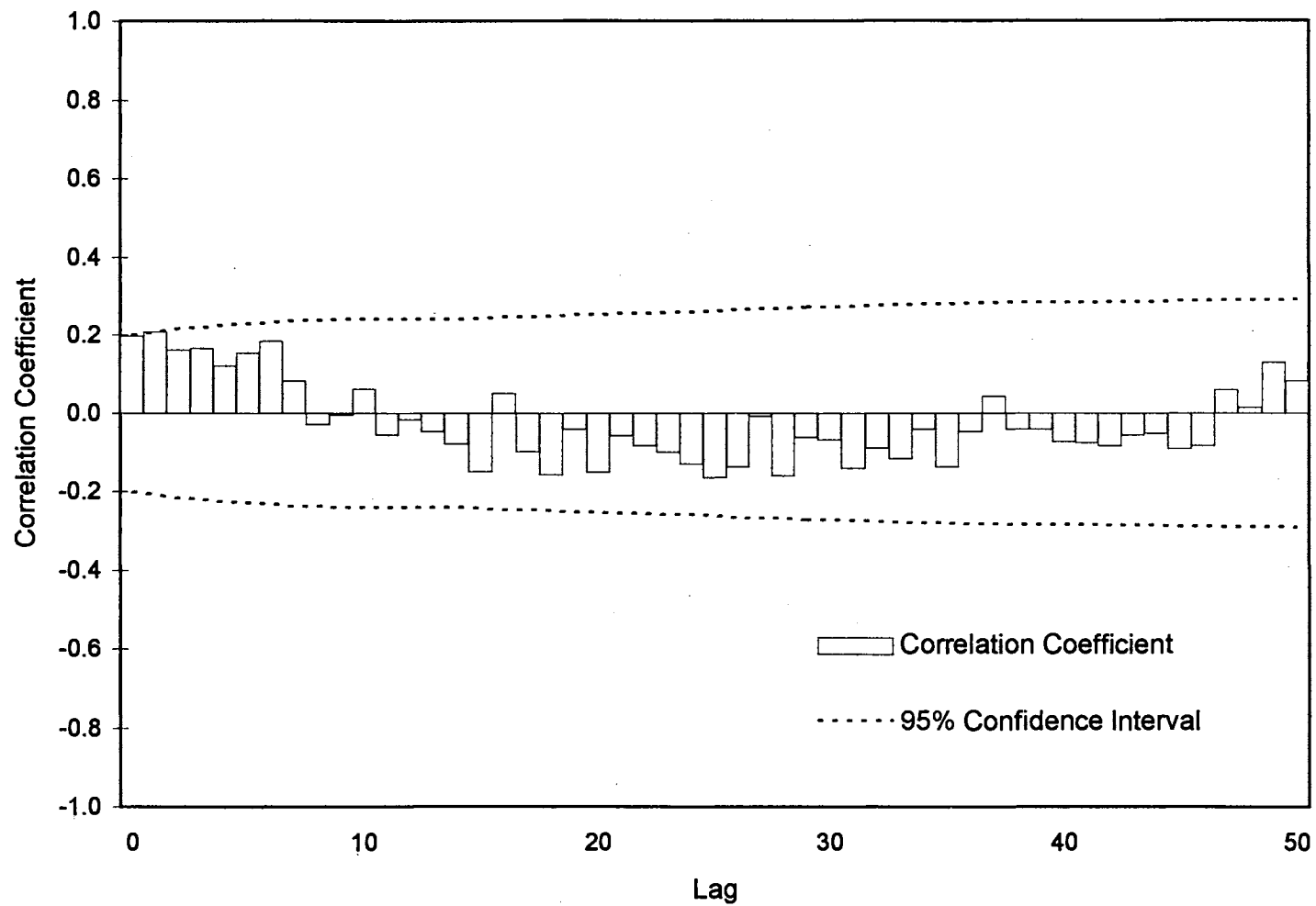


Figure 25. Simulated annual rainfall under random IGN selection versus Monte Carlo run.

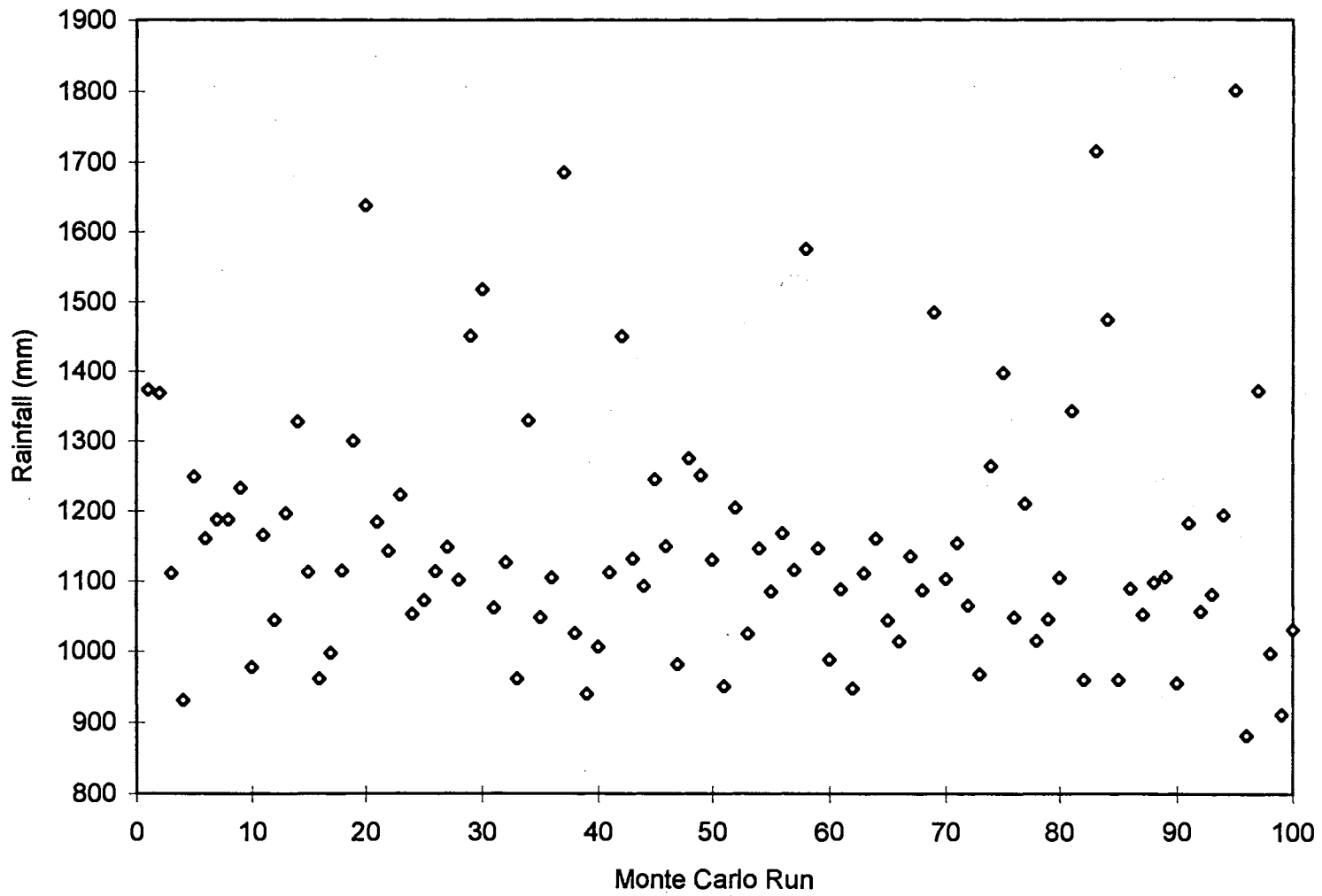


Figure 26. Correlogram for simulated annual rainfall under random IGN selection.

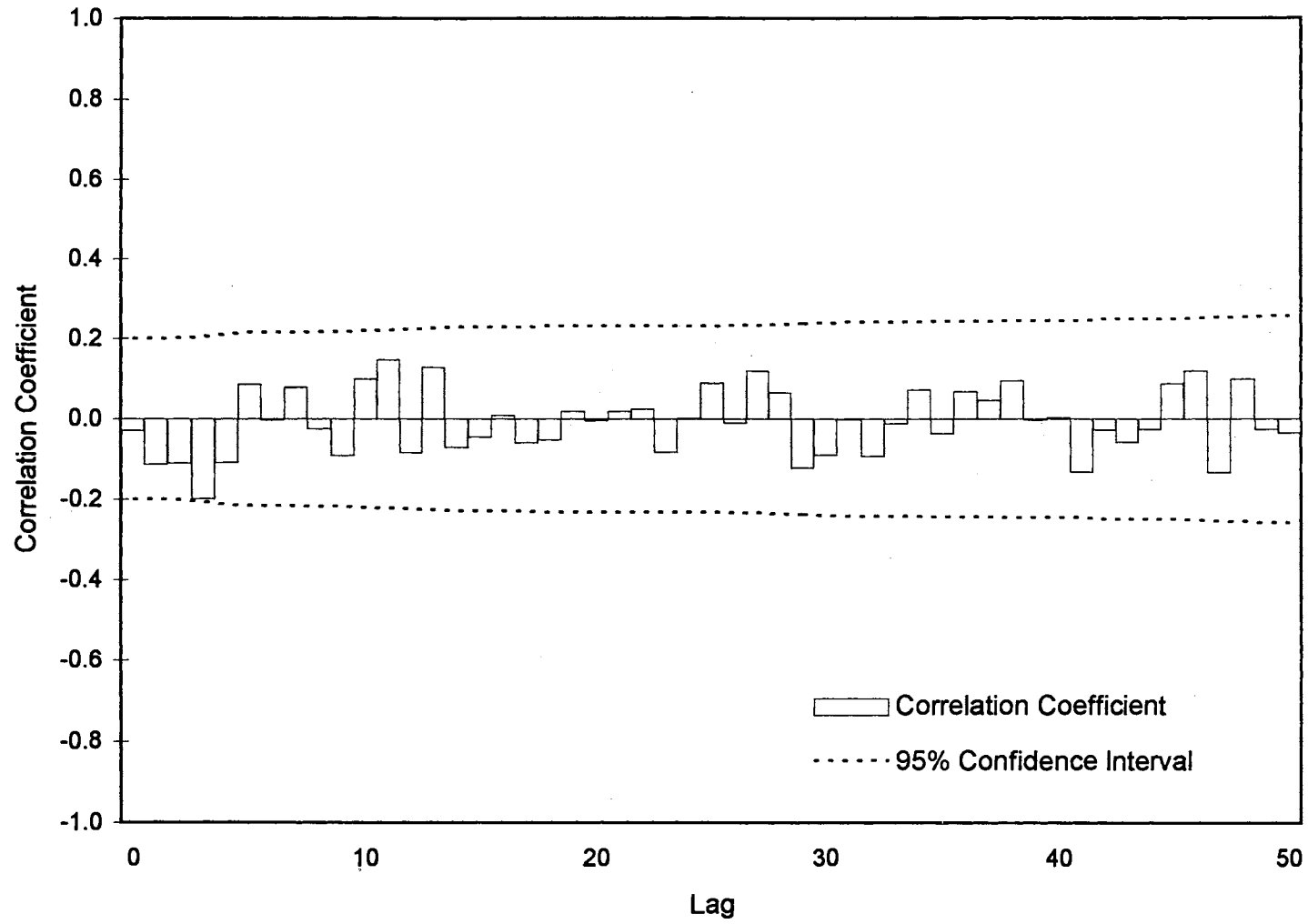


Figure 27. Correlogram for simulated annual maximum daily TSS loading under random IGN selection.

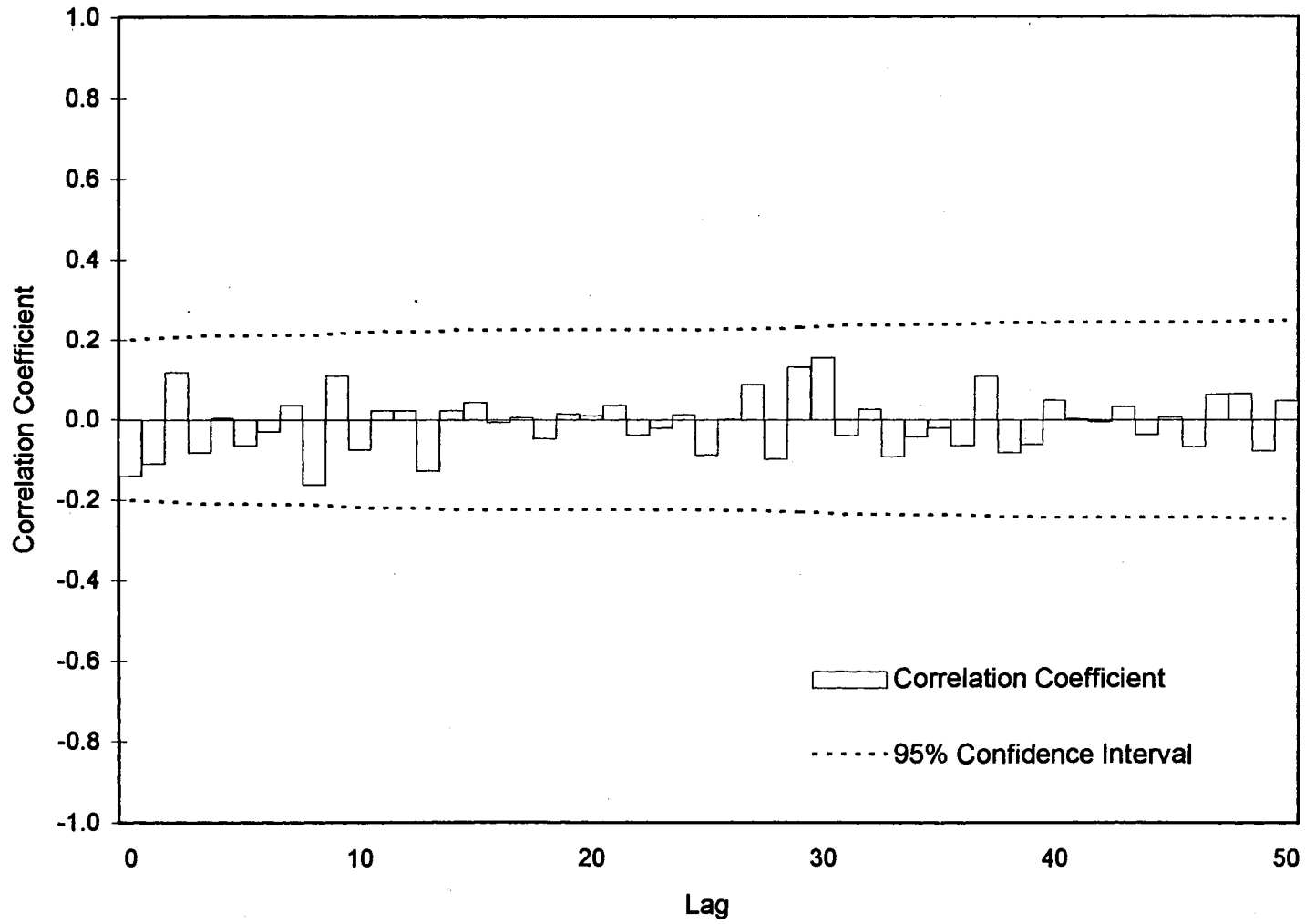


Figure 28. Correlogram for simulated annual maximum daily PHOS loading under random IGN selection.

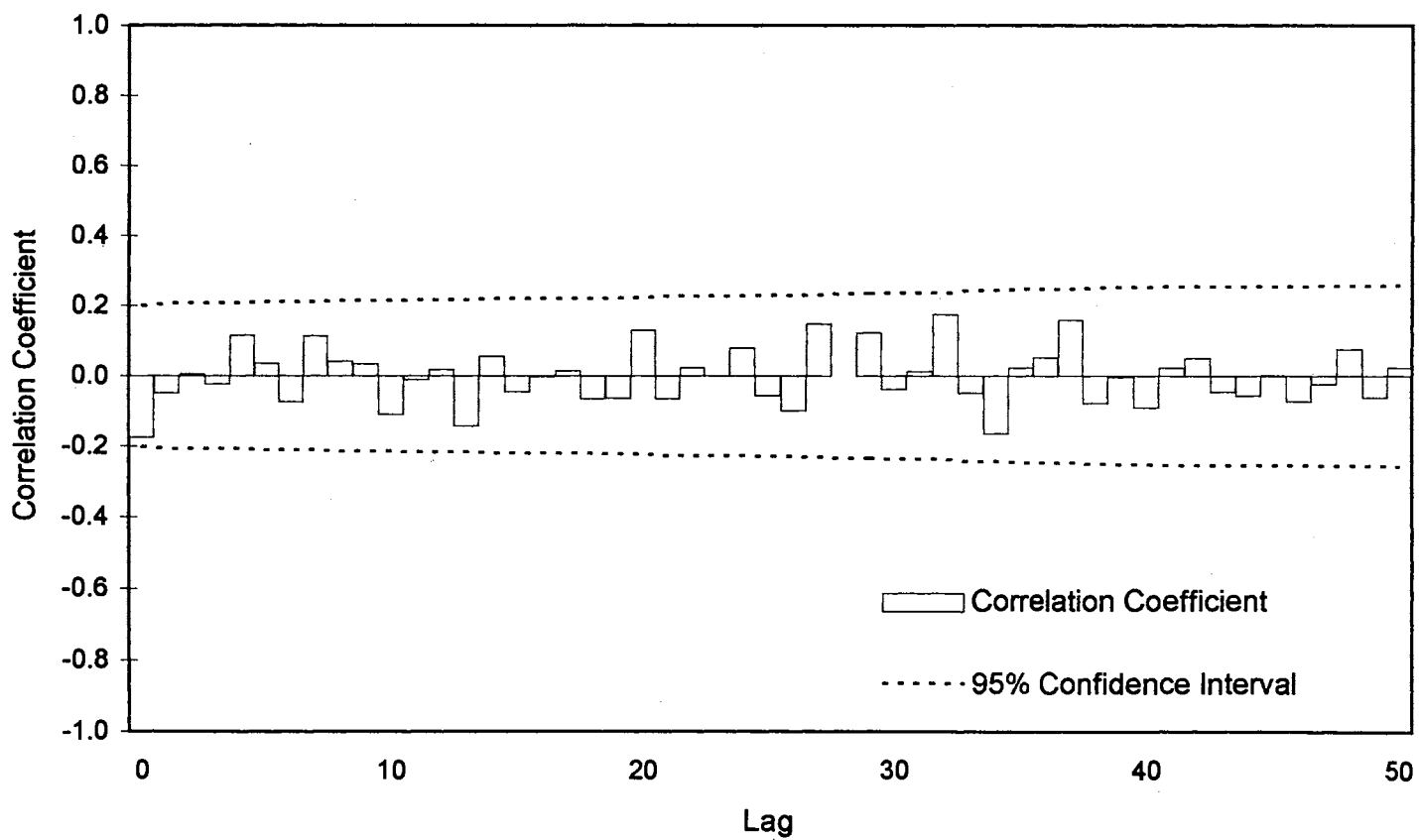


Figure 29. Correlogram for simulated annual maximum daily NO₃N loading under random IGN selection.

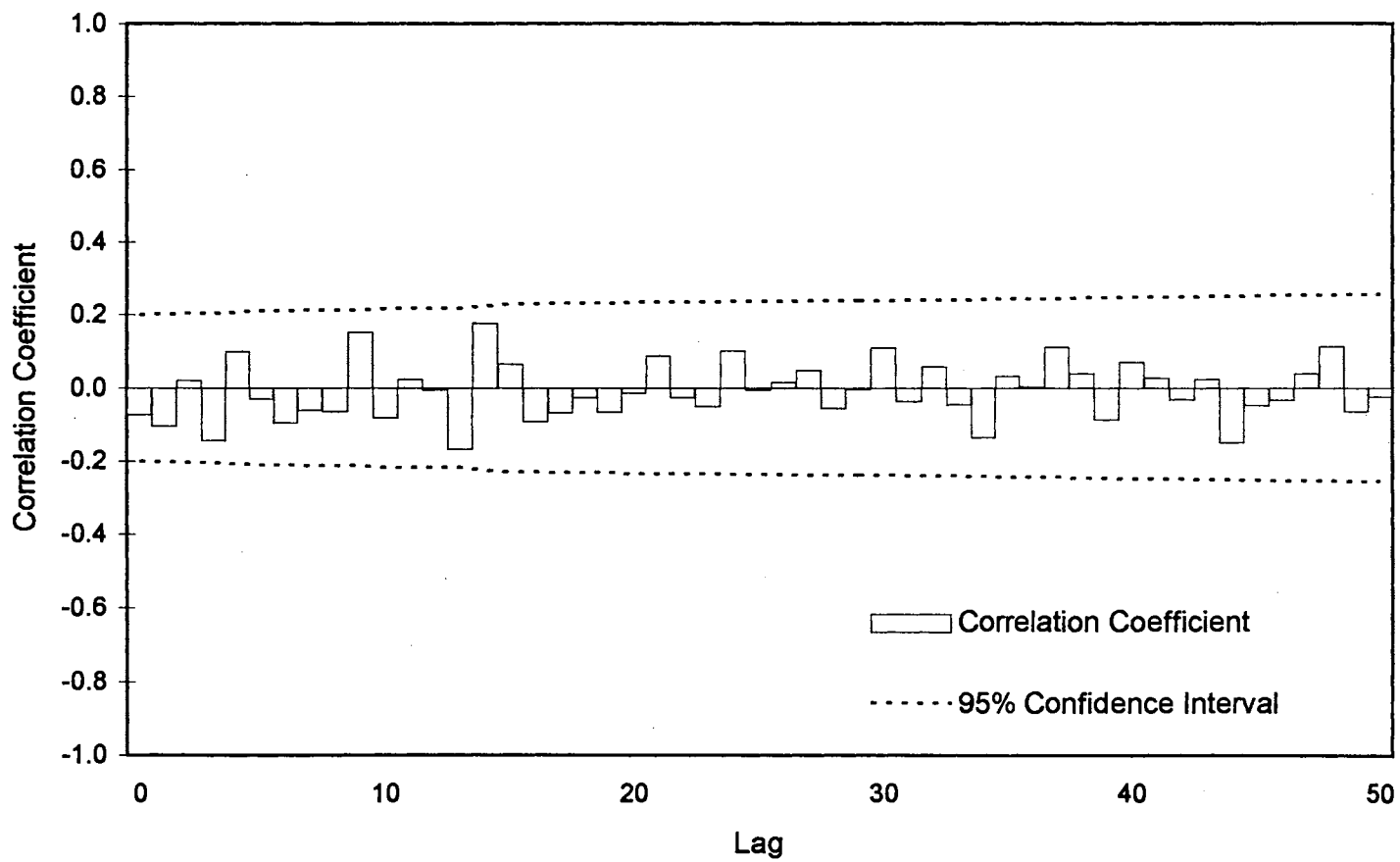


Figure 30. Mean annual maximum daily Q under the CC33 clearcutting management scenario.

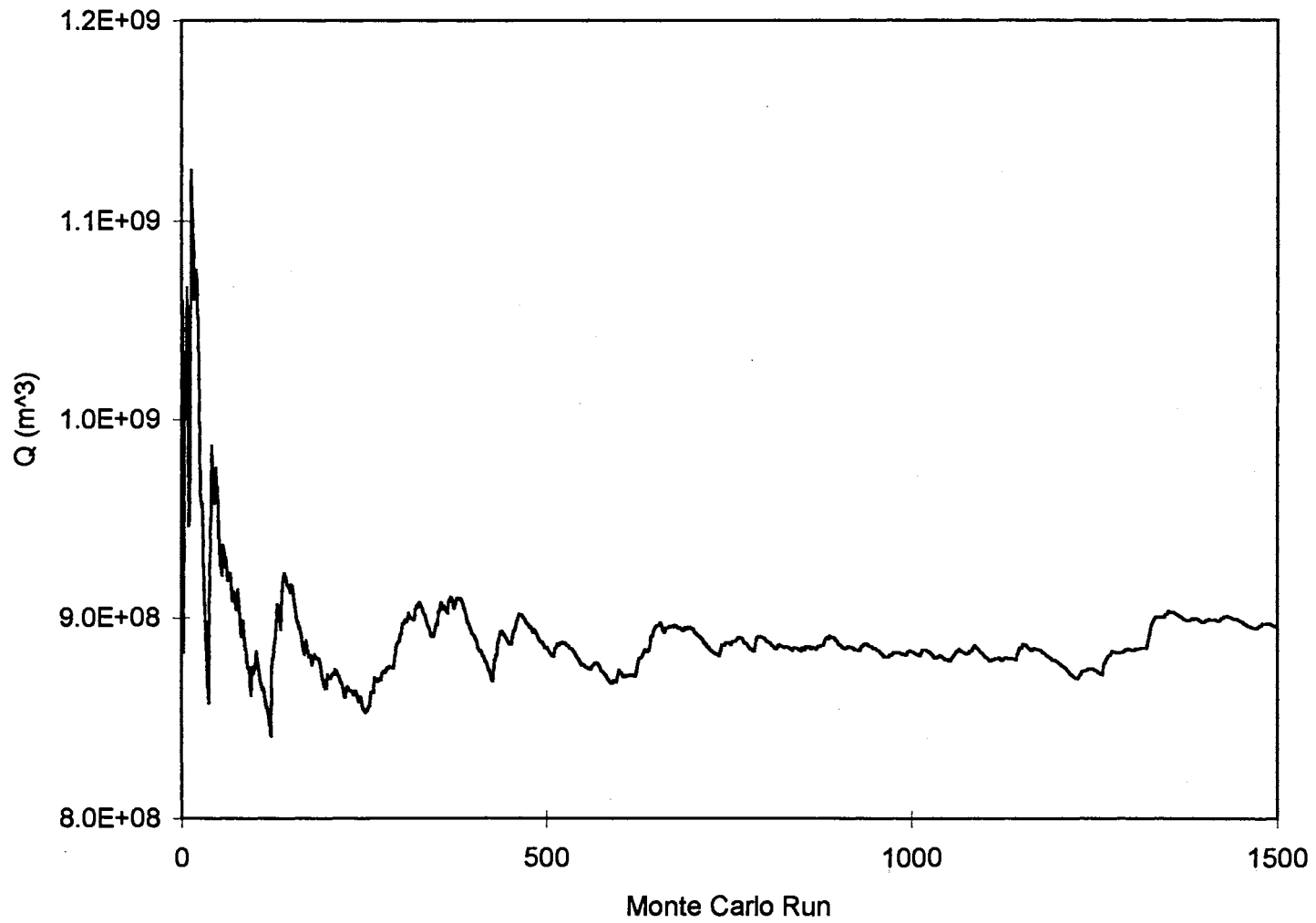


Figure 31. Mean annual maximum daily TSS loading at the CC33 clearcutting management scenario.

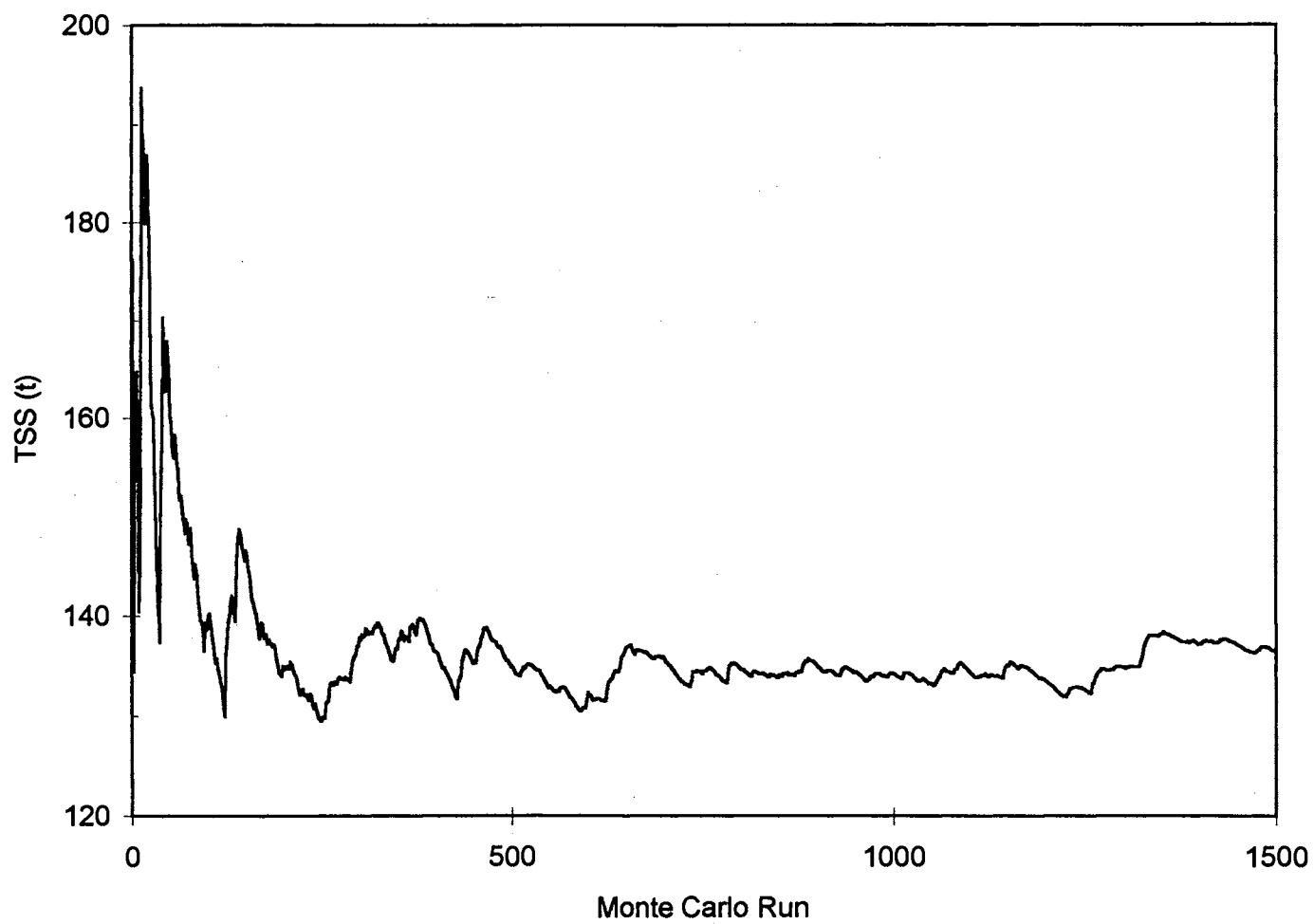


Figure 32. Mean annual maximum daily PHOS at the CC33 clearcutting management scenario.

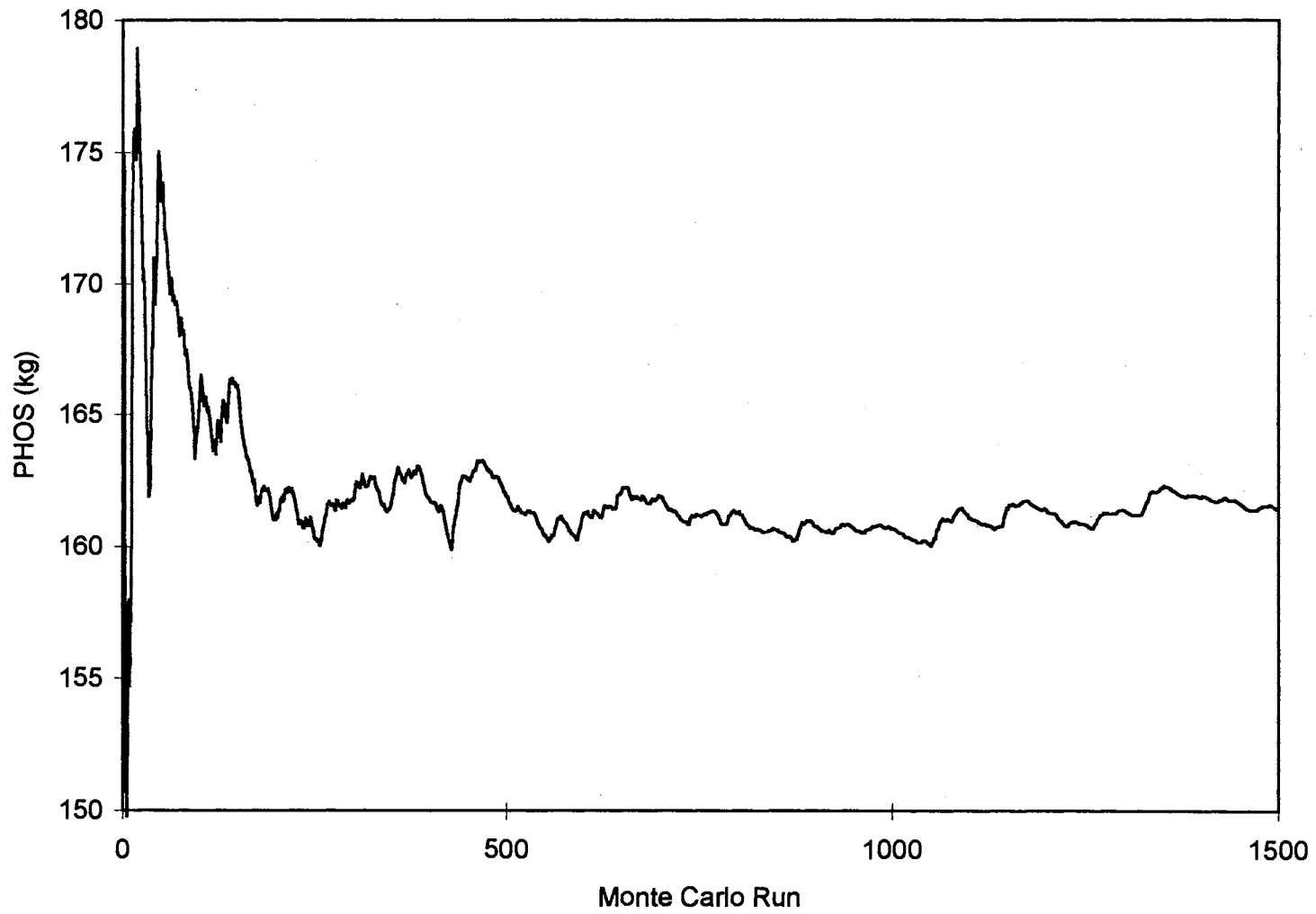


Figure 33. Mean annual maximum daily NO₃N loading at the CC33 clearcutting management scenario.

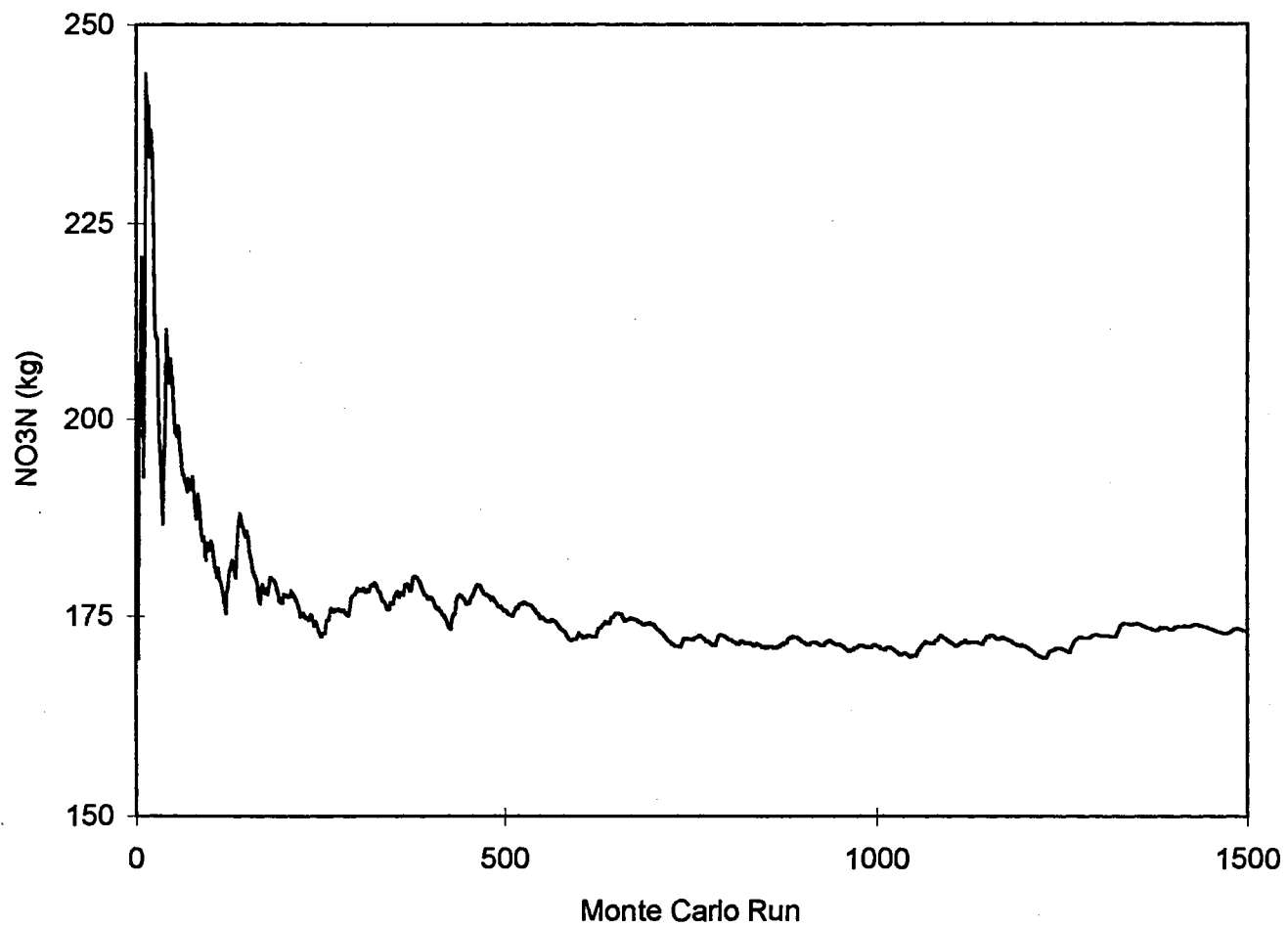


Figure 34. Relative frequency of Q at the CC00, CC33, CC66, and CC100 clearcutting level. Class interval equals 500,000 m³.

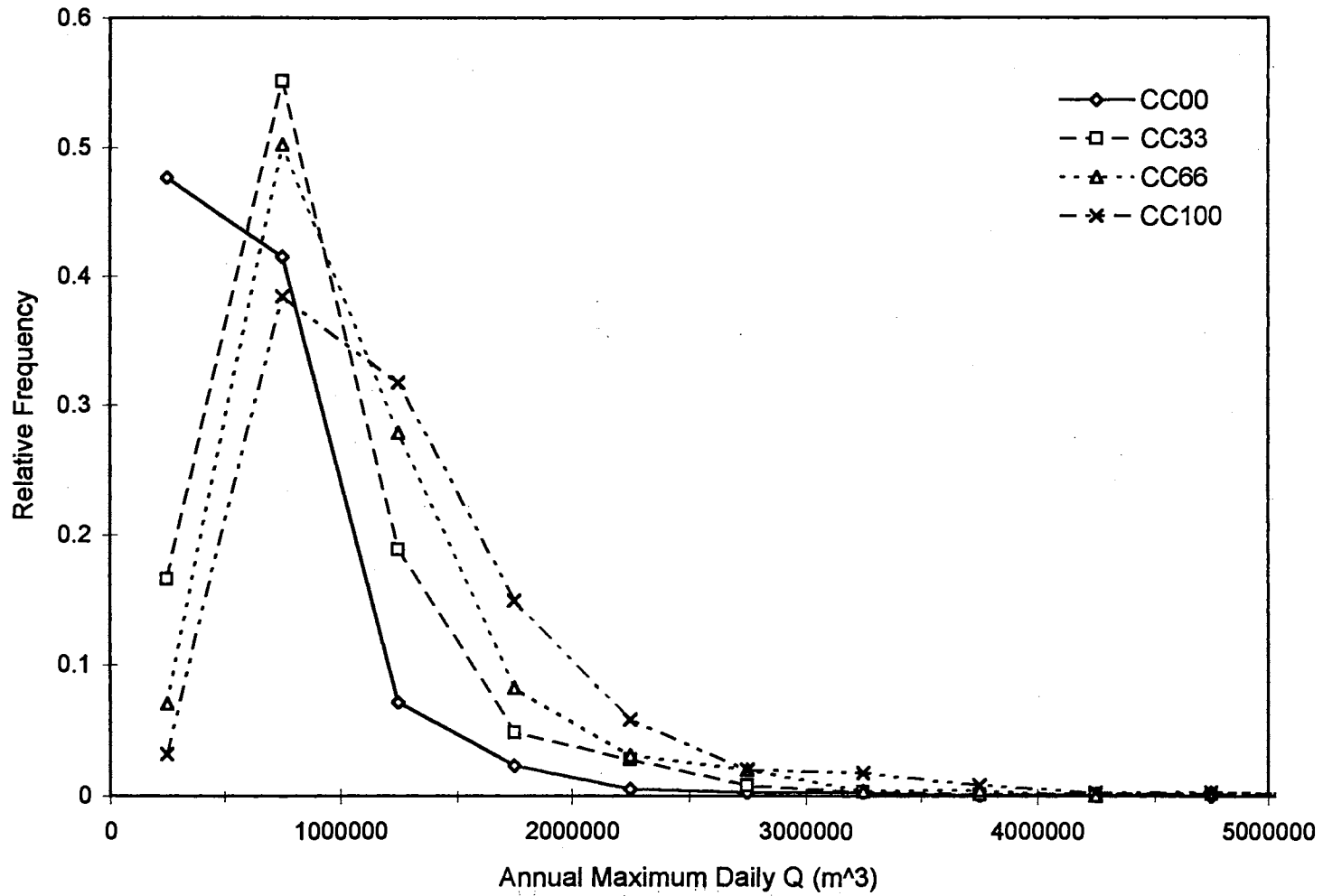


Figure 35. Relative frequency of TSS at the CC00, CC33, CC66, and CC100 clearcutting level. Class interval equals 200 t.

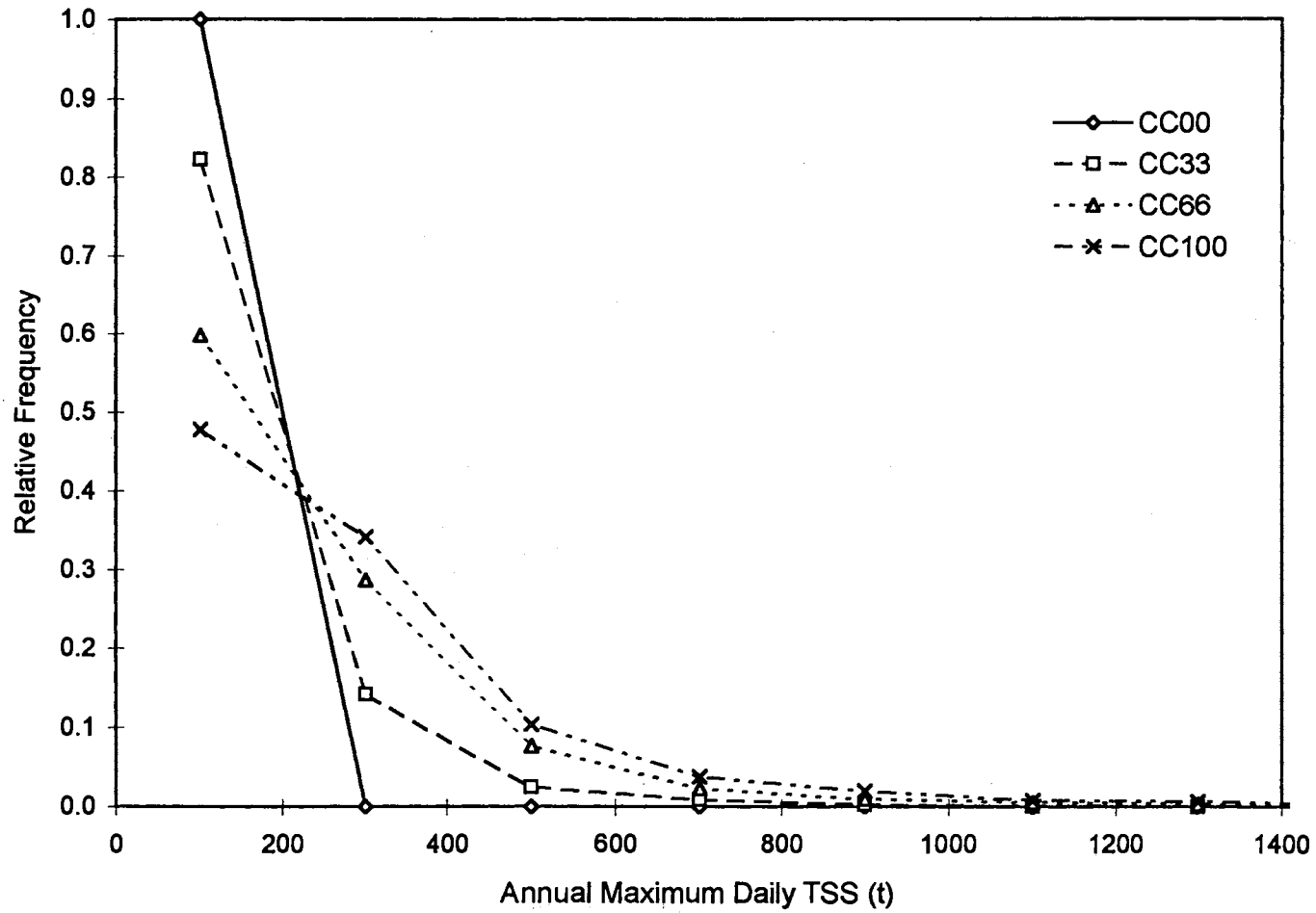


Figure 36. Relative frequency of PHOS at the CC00, CC33, CC66, and CC100 clearcutting level. Class interval equals 100 kg.

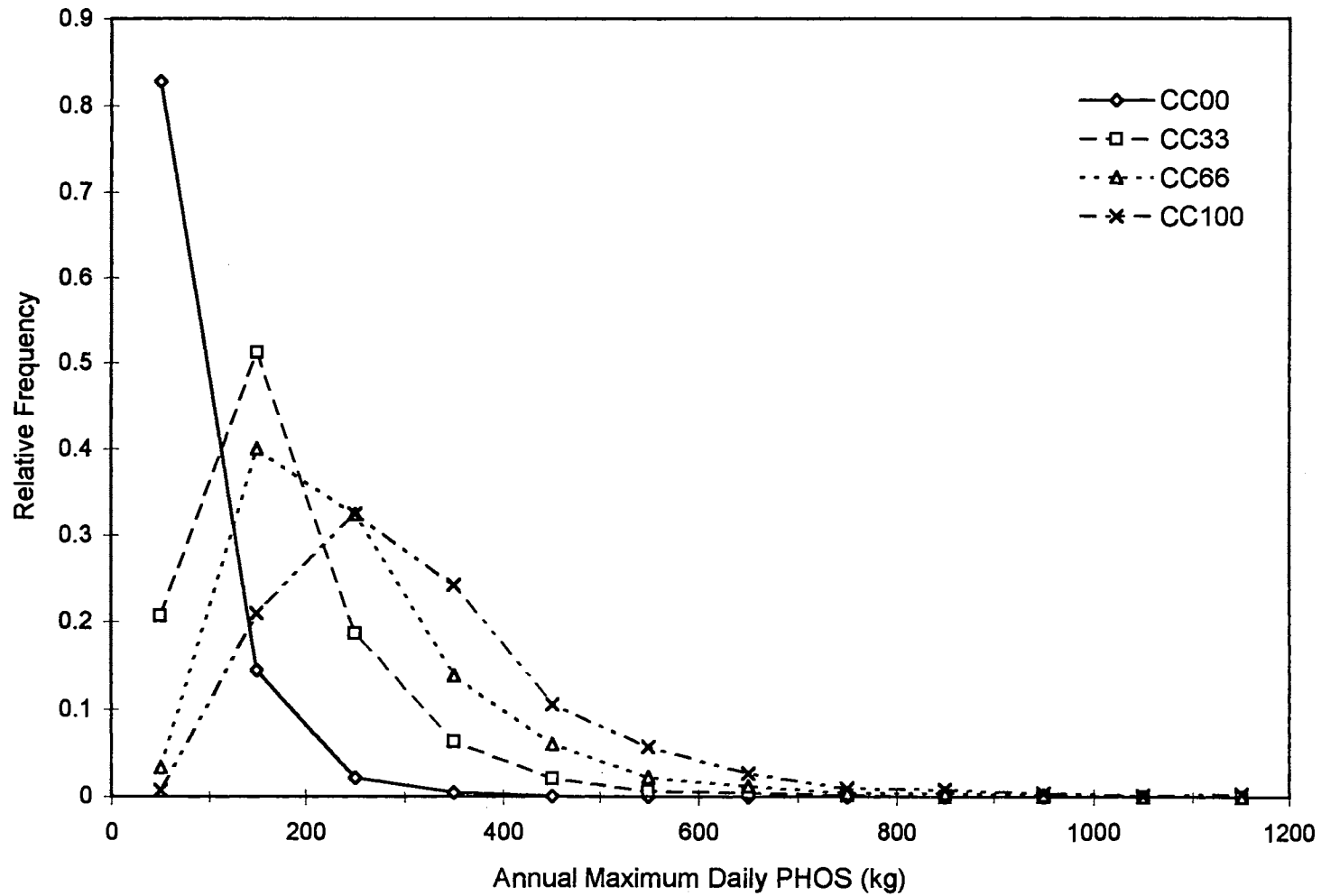


Figure 37. Relative frequency of NO₃N at the CC00, CC33, CC66, and CC100 clearcutting level. Class interval equals 100 kg.

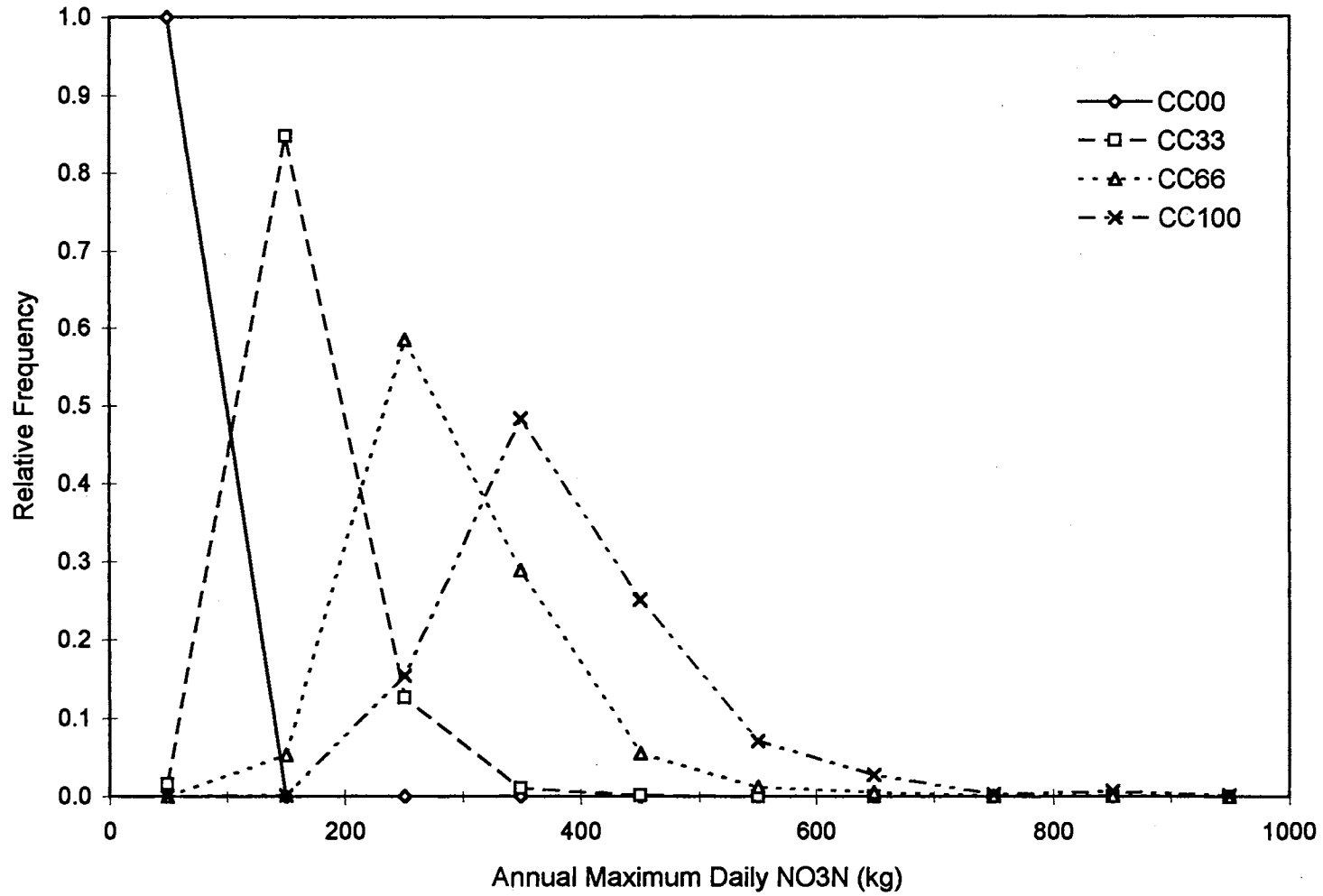


Figure 38. Probability plot for annual maximum daily Q at the CC00, CC33, CC66, and CC100 clearcutting management scenario.

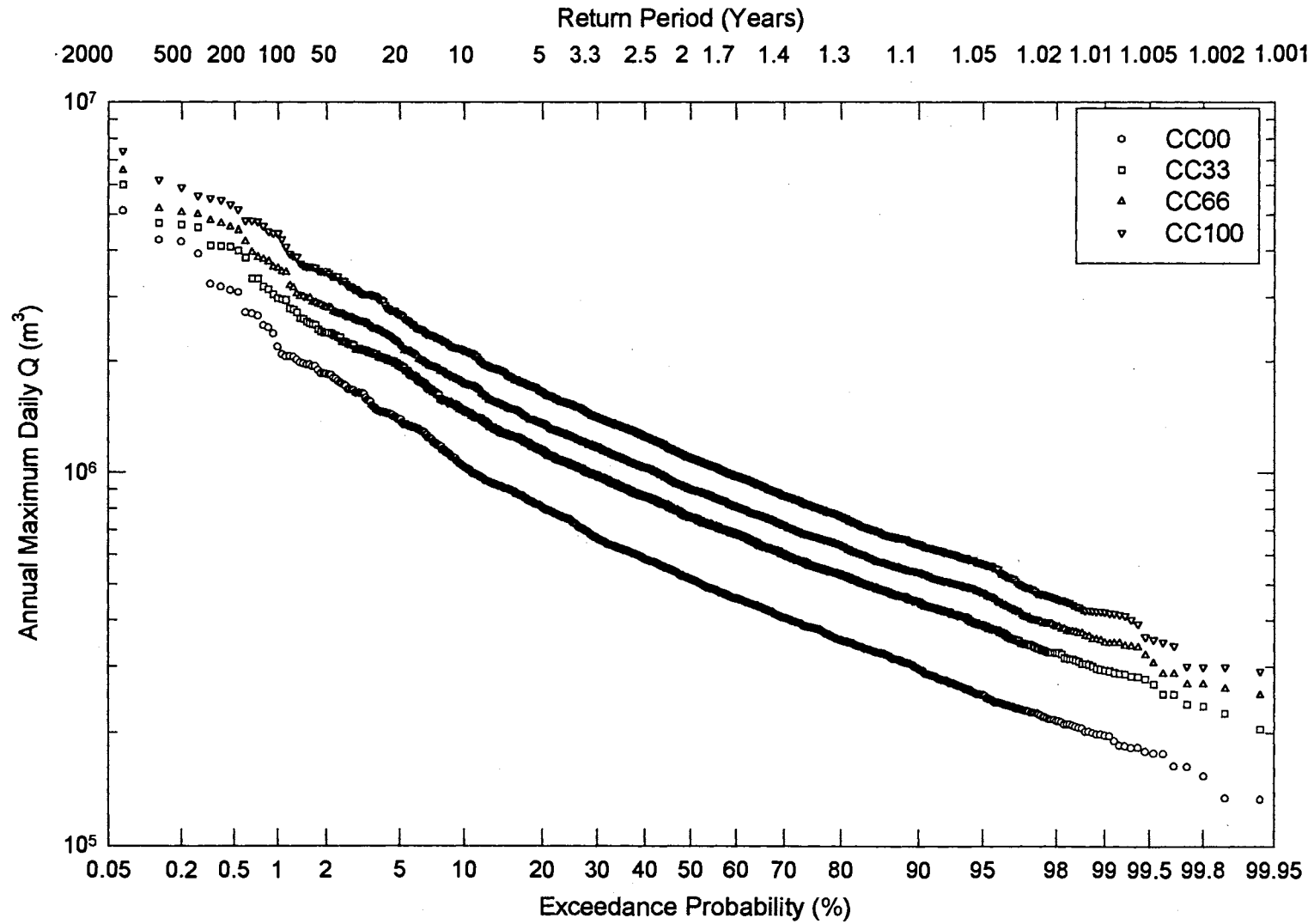


Figure 39. Probability plot for annual maximum daily TSS at the CC00, CC33, CC66, and CC100 clearcutting management scenario.

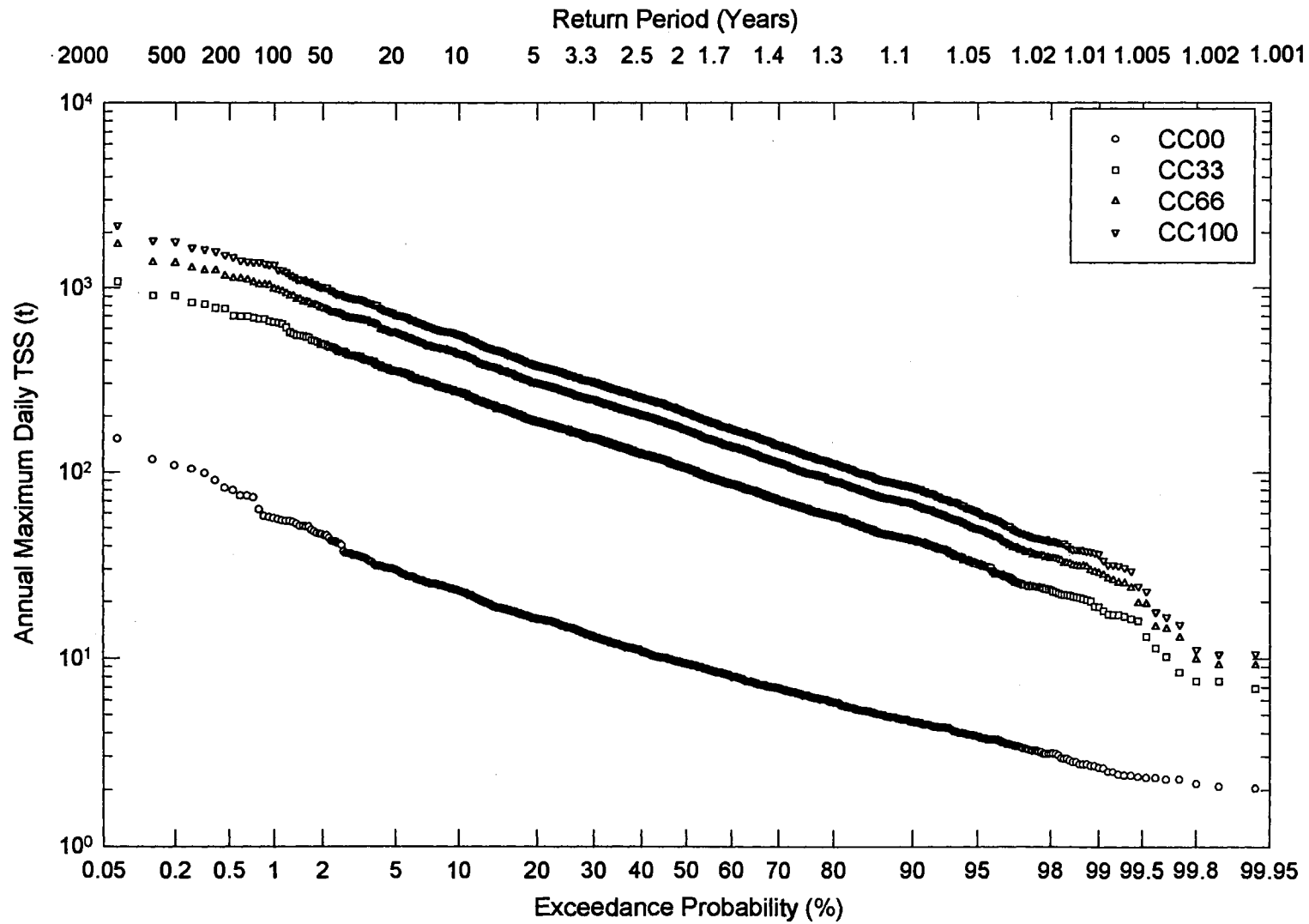


Figure 40. Probability plot for annual maximum daily PHOS at the CC00, CC33, CC66, and CC100 clearcutting management scenario.

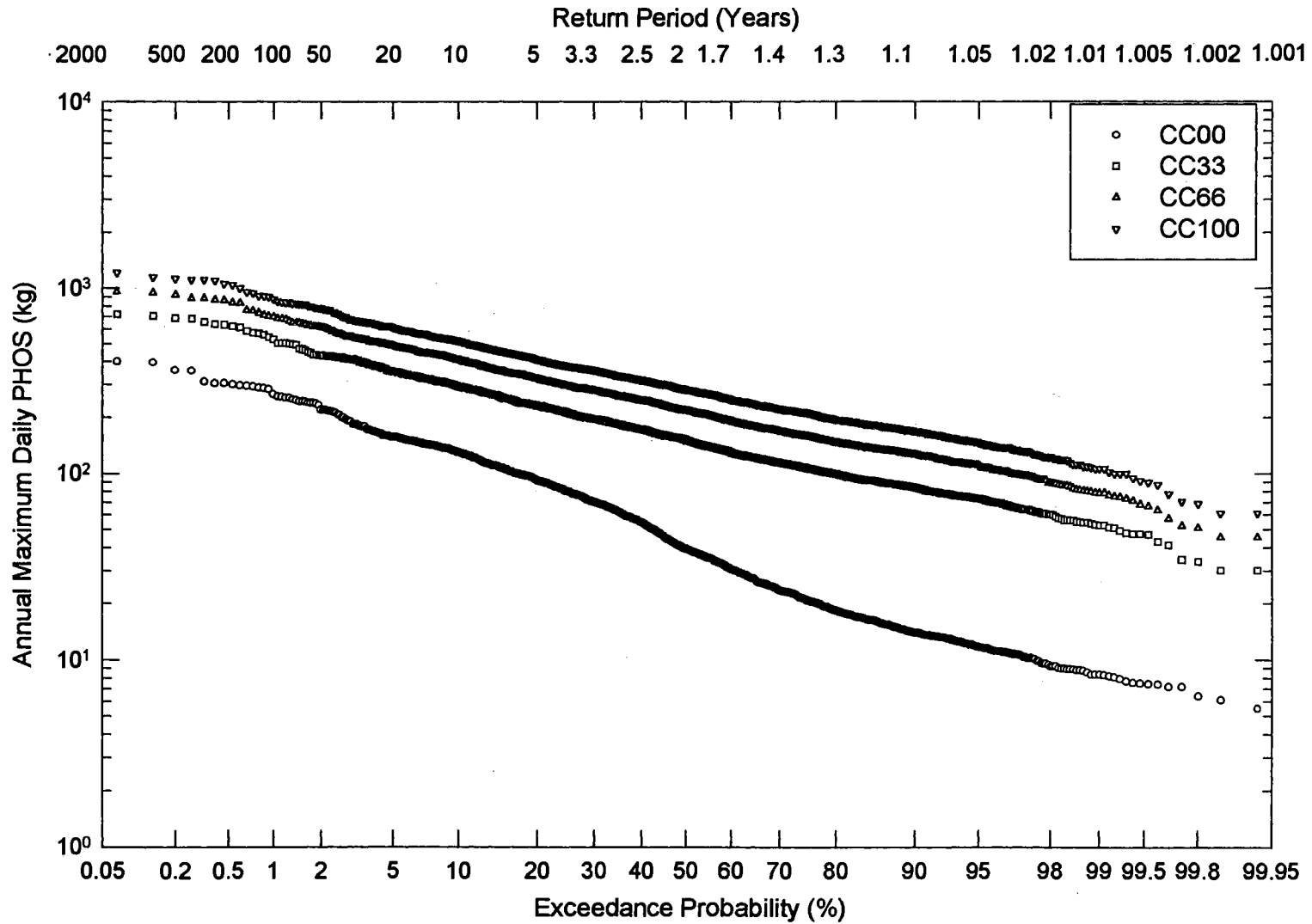
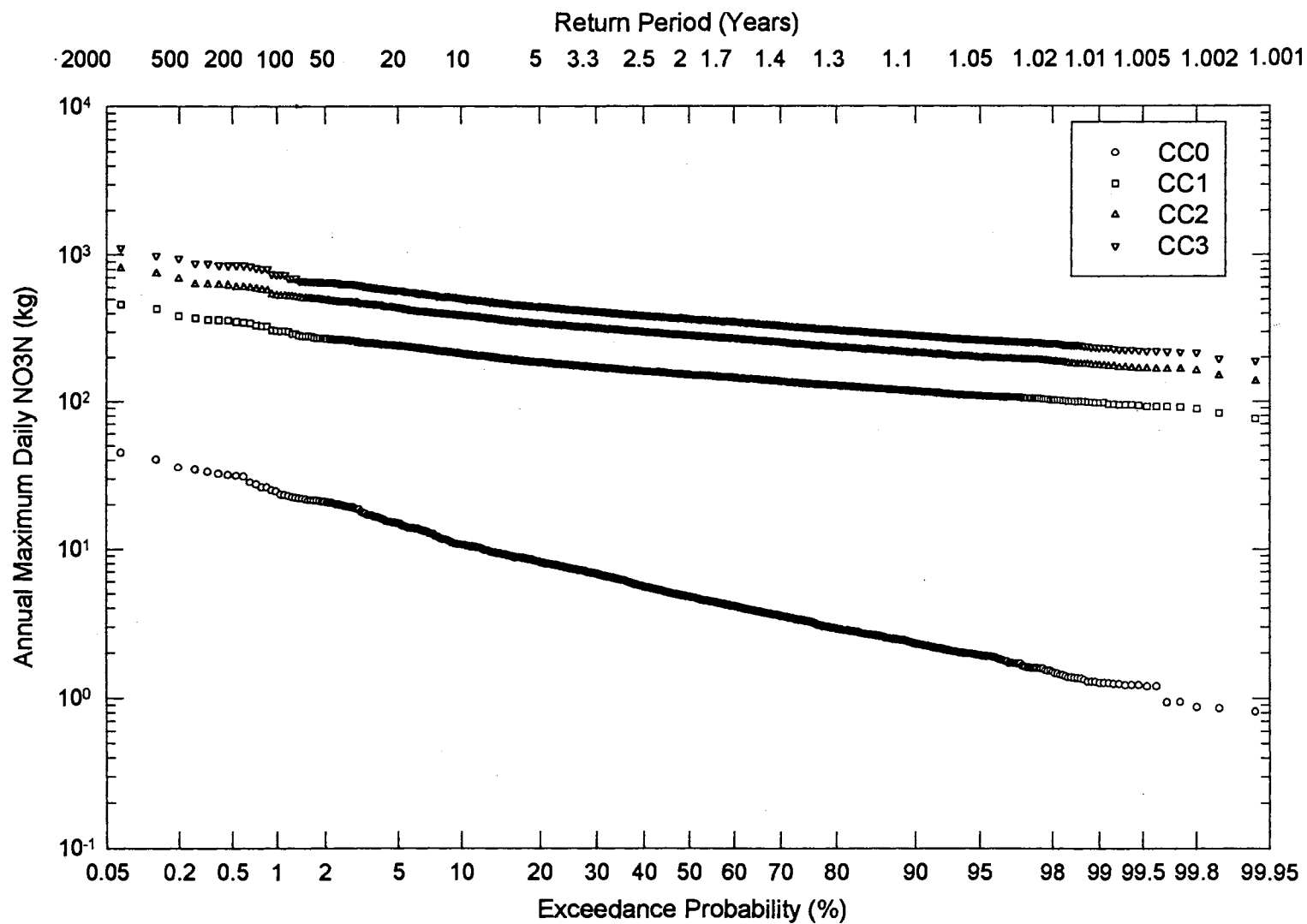


Figure 41. Probability plot for annual maximum daily NO₃N at the CC0, CC1, CC2, and CC3 clearcutting levels.



CHAPTER V

CONCLUSIONS

The Clean Water Act of 1987 has focused attention on the restoration and maintenance of the chemical, physical, and biological integrity of the Nation's waters. The Act specifically addressed the issue of nonpoint source pollution (Sec. 101a(7)). A water quality-based approach to pollution control was mandated, and the TMDL concept developed as a means to achieve this mandate. Quantifying daily NPS loading contributions from large clear cut watersheds is an important component for developing TMDLs for water quality-limited waterbodies in the Ouachita Mountains.

The first objective of this project was to develop a stochastic framework to quantify worst case daily total suspended solid (TSS), total phosphorus (PHOS), and nitrate-nitrogen (NO₃N) loading from large clear cut watersheds in the Ouachita Mountains in such a manner as to allow assessment of the risk of exceeding estimated waterbody loading capacity for TSS, PHOS, and NO₃N. The second objective was to apply the stochastic framework to Clayton Lake Watershed to quantify worst case daily TSS, PHOS, and NO₃N loading under four hypothetical clearcutting levels, and demonstrate the risk analysis potential of the stochastic framework.

The first objective was not satisfied because of EPIC's inability to simulate daily NPS loading from clear cut and undisturbed forest watersheds. This application of EPIC was well beyond the use intended by the model developers, so the failure of EPIC in this application does not call into question the quality or value of the model for

other applications. Also, the failure of EPIC does not imply that the stochastic framework is a failure. The framework is a valuable tool for quantifying NPS loading at any time step. The water quality model employed during a particular application of the framework is an interchangeable component of the framework. A model better suited for simulating daily NPS loading from large clear cut watersheds in the Ouachita Mountains must be identified for use in the framework. The second objective was satisfied in this project. However, due to the short-comings of EPIC the model results and thus the results of the framework have questionable value.

The stochastic framework developed in this study is dependent upon predictions from a water quality model. Thus, the value of the output from the stochastic framework for real world application is dependent upon the model selected for use in the framework. If an unsuitable model is selected, or if model parameters are improperly estimated, the framework output will have little value. If an appropriate model is selected and model parameters are estimated correctly, the framework output will be of value for TMDL development efforts.

This project served to introduce the stochastic framework and to demonstrate its potential for use during TMDL development efforts. However, the stochastic framework will not be complete until a method of accounting for NPS pollution loading from forest road networks is incorporated. The construction and maintenance of roads, trails, and landings associated with clearcutting have been identified as major sources of NPS pollution. NPS loading from large clear cut watersheds will be underestimated if contributions from forest road networks are not considered.

The framework needs to be expanded to incorporate point source as well as nonpoint source contributions. A TMDL applies to both nonpoint and point sources of pollution. Clearcutting management plans must be developed with consideration of

the needs of point source contributors on the watershed. In addition, some form of assessing the long-term economic feasibility of clearcutting management scenarios must be incorporated into the framework. A clearcutting management scenario which has desirable impacts on water quality may or may not be a viable option from the land owner's point of view. The land owner will not have much incentive to implement BMPs if he/she is losing money.

The conclusions reached in this study are as follows:

1. The framework proposed in this study is a viable procedure for quantifying worst case daily TSS, PHOS, and NO₃N loading from large clear cut watersheds in the Ouachita Mountains. However, EPIC is not a suitable water quality model for incorporation into the framework.

2. The framework proposed in this study allows assessment of the risk of estimated daily NPS loadings (LAs) exceeding the daily loading capacities (LCs) of water quality-limited waterbodies.

3. EPIC did not satisfactorily simulate day-to-day Q and TSS, PHOS, and NO₃N loading realized from a small clear cut and a small undisturbed sites on Clayton Lake Watershed. Further examination of the suitability of EPIC for simulating daily Q and TSS, PHOS, and NO₃N loading should be conducted prior to employing EPIC as a decisions making tool on forested watersheds in the Ouachita Mountains. Additional models should be investigated for use in the stochastic framework.

Future research should be directed towards either identifying or developing a water quality model suitable for simulating daily NPS loading from large watersheds in the Ouachita Mountains. Also, some method of accounting for stochastic NPS pollution contributions from forest road systems must be identified.

LITERATURE CITED

- Abernathy, E.J., K.M. Olszewski, and R. Peters. 1983. Soil survey of LeFlore County, Oklahoma. USDA-SCS. 211 pp.
- Abdul, A.S., and R.W. Gillham. 1989. Field studies of the effects of capillary fringe on streamflow generation. *J. Hydrology*. 112:1-18.
- Allred, B., and C.T. Haan. 1991. Variability of optimized parameter estimates based on observed record length. *Trans. ASAE*. 34:2421-2426.
- Anderson, B., and D.F. Potts. 1987. Suspended sediment and turbidity following road construction and logging in western Montana. *Water Resources Bulletin*. 23:681-690.
- Bain, W.R., and A. Watterson, Jr. 1979. Soil survey of Pushmataha County, Oklahoma. USDA-SCS. 153 pp.
- Barnes, D.J. 1992. Release of old and new water from an undisturbed forest pedon in the Ouachita National Forest. M.S. Thesis, Oklahoma State University, Department of Forestry.
- Bras, R.L. 1990. *Hydrology: an introduction to hydrologic science*. Addison-Wesley Pub. Co., N.Y., NY. 643 pp.
- Bosch, J.M. and J.D. Hewlett. 1982. A review of catchment experiments to determine the effect of vegetation changes on water yield and evapotranspiration. *J. Hydrology*. 55:3-23.
- Dumesnil, D. 1993. EPIC user's guide-draft. USDA-ARS.
- Dunne, T. 1983. Relation of field studies and modeling in the prediction of storm runoff. *J. Hydrology*. 65:25-48.
- Dunne, T., and R.D. Black 1970a. An experimental investigation of runoff production in permeable soils. *Water Res. Res.* 6:478-490.
- Dunne, T., and R.D. Black 1970b. Partial area contributions to storm runoff in a small New England watershed. *Water Res. Res.* 6:1296-1311.
- Fredricksen, R.L. 1970. Erosion and sedimentation following road construction and timber harvest on unstable soils in three small western Oregon watersheds. USDA-FS. Res. Pap. PNW-104.

- Freeze, A.R. 1974. Streamflow generation. *Rev. Geophys. and Space Physics*. 12:627-647.
- Haan, C.T., B.J. Barfield, and J.C. Hayes. 1994. *Design hydrology and sedimentology for small catchments*. Academic Press. San Diego, CA. 588 pp.
- Haan, C.T., D.L. Nofziger, and F.K. Ahmed. 1994. [?] *J. Environmental Quality*. 23:349-354.
- Haan, C.T. 1977. *Statistical methods in hydrology*. Iowa State Univ. Press. 378 pp.
- Hewlett, J.D. 1982. *Principles of forest hydrology*. Univ. Georgia Press. 183 pp.
- Hewlett, J.D., and C.A. Troendle. 1975. Non-point and diffused water sources: a variable source area problem. pp. 21-46 in: *Watershed Management*. Amer. Soc. Civil Engin. 781 pp.
- Hewlett, J.D. and A.R. Hibbert. 1967. Factors affecting the response of small watersheds to precipitation in humid areas. pp. 275-290 in: W.E. Sopper and H.W. Lull (eds) *Forest Hydrology*. Pergamon Press, N.Y., NY.
- Hibbert, A.R., and C.A. Troendle. 1988. Streamflow generation by variable source area. pp. 111-127 in: W.T. Swank and D.A. Crossley Jr. (eds) *Forest Hydrology and Ecology at Coweeta*.
- Horton, R.E. 1943. Discussion of "Infiltration capacities of some plant-soil complexes on Utah range watershed lands" by L. Woodward. *trans. Am. Geophys. Union*. 24:473-475.
- Leonard, R.A., W.G. Knisel, and D.A. Still. 1987. GLEAMS: groundwater loading effects of agricultural management systems. *Trans. ASAE*. 30:1401-1418.
- McCashion, J.D. and R.M. Rice. 1983. Erosion on logging roads in northwestern California: how much is avoidable. *J. Forestry*. 81:23-26.
- Medina, M.A. Jr., and K. Helfrich. 1979. Evaluation of infiltration models in kinematic wave approximation to forested watershed overland flow. pp. 218-233 in: *Proc. Hydrol. Transport Modeling Symp.* New Orleans, LA. Amer. Soc. Ag. Engin.
- Megahan, W.F., and W.J. Kidd. 1972. Effect of logging roads on sediment production rates in the Idaho batholith. *USDA-FS. Res. Pap. INT-123*. pp.14.
- Miller, E.L., R.S. Beasley, and E.R. Lawson. 1988. Forest harvest and site preparation effects on erosion and sedimentation in the Ouachita Mountains. *J. Environ. Qual.* 17:219-225.
- Miller, E.L., R.S. Beasley, and J.C. Covert. 1985. Forest road sediments: production and delivery to streams. pp. 164-176 in: B.G. Blackmon (ed) *Proceedings of forestry and water quality: a mid-south symposium*.

- Miller, E.L. 1984. Sediment yield and storm flow response to clear-cut harvest and site preparation in the Ouachita Mountains. *Water Res. Res.* 20:471-475.
- Mosley, M.P. 1979. Streamflow generation in a forested watershed, New Zealand. *Water Res. Res.* 15:795-806.
- Muller, R.A. 1966. The effects of reforestation on water yield. *Pu. Climatol.* 19:251-304.
- Naseer, M. 1992. Timber harvest and site preparation impacts on erosion and sediment and nutrient yields from forested watersheds in Clayton Oklahoma. M.S. Thesis. Oklahoma State University.
- Oklahoma Water Resources Board. 1990. Oklahoma Water Atlas. Publication 135. 360 pp.
- Pearce, A.J. 1990. Streamflow generation processes: an Austral view. *Water Res. Res.* 26:3037-3047.
- Pettyjohn, W.A., H. White, and S. Dunn. 1983. Water atlas of Oklahoma. Okla. State Univ., Univ. Center Water Res. Stillwater, OK. 72 pp.
- Rogerson, T.L. 1971. Hydrologic characteristics of small headwater catchments in the Ouachita Mountains. USDA-FS, Research Note SO-117.
- Sabbagh, G.J., D.E. Storm, and C.T. Haan. 1994. Digital terrain model to estimate watershed characteristics for hydrologic and water quality modeling. ASAE International Summer Meeting. Kansas City, MO.
- Scoles, S., S. Anderson, D. Turton, and E. Miller. 1994. Forestry and water quality: a review of watershed research in the Ouachita Mountains. Oklahoma Coop. Ext. Serv. Circular E-932. 29 pp.
- Sharpley, A.N., and J.R. Williams. 1990. EPIC-erosion/productivity impact calculator: 1. model documentation. USDA Tech. Bull. No. 1768.
- Sturges, H.A. 1926. The choice of a class interval. *J. American Statistical Association* 21:65-66.
- Trimble, G.R., Jr., C.E. Hale, and H. S. Potter. 1951. Effect of soil and cover conditions on soil water relationships. USDA-FS-NE Paper 39. 44 pp.
- Troendle, C.A. 1985. Variable source area models. pp. 347-403. In: M.G. Anderson and T.P. Burt (eds) *Hydrological Forecasting*. Wiley and Sons Ltd, N.Y., NY.
- Tsukamoto, Y. 1966. Analysis of hydrologic phenomena occurring in mountain watersheds. Tokyo Univ. Agr. and Tech. Exp. Forest Bull. 6. 79 pp.
- Turton, D.J., C.T. Haan, and E.L. Miller. 1992. Subsurface flow responses of a small catchment in the Ouachita Mountains. *Hydro. Processes.* 6:111-125.

- Turton, D.J. 1989. Measurement and modeling of water quality from a forested watershed in southeastern Oklahoma. Ph.D. Dissertation. Oklahoma State University.
- USEPA. 1991. Guidance for water quality-based decisions: the TMDL process. EPA 440/4-91-001. 59 pp.
- Wels, C., C.H. Taylor, R.J. Cornett, and B.D. Lazerte. 1991. Streamflow generation in a headwater basin on the Precambrian Shield. *Hydrol. Processes*. 5:185-199.
- Williams, J.R., P.T. Dyke, W.W. Fuchs, V.W. Benson, O.W. Rice, and E.D. Taylor. 1990. EPIC-erosion/productivity impact calculator: 2. user manual. USDA-ARS Technical Bulletin Number 1768.
- Williams, M.A. 1990. Saturated interflow and water table response of a small forested watershed in the Ouachita Mountains of central Arkansas. M.S. Thesis. Oklahoma State University. 142 pp.
- Yan, J., and C.T. Haan. 1991a. Multiobjective parameter estimation for hydrologic models - weighting of errors. *Trans ASAE*. 34:135-141.
- Yan, J., and C.T. Haan. 1991b. Multiple parameter estimation for hydrologic models- multiobjective programming. *Trans. ASAE*. 34:848-856.

APPENDIX I

EPIC: MODEL DEVELOPMENT AND DOCUMENTATION

APPENDIX I

EPIC: MODEL DEVELOPMENT AND DOCUMENTATION

Introduction

The purpose of this appendix is to bring together several documentation publications for EPIC to provide a reference for use during this project. Only those model components and relationships which are pertinent to this project are discussed. Following a 1980 United States Department of Agriculture (USDA) workshop focusing on improving the understanding of the crop yield / soil loss relationship a national Agricultural Research Service (ARS) modeling team was organized and began developing EPIC (Williams 1990). Team objectives were to develop a continuous, physically based model that is: 1. capable of simulating the biophysical processes relevant to the crop yield / soil loss relationship simultaneously and realistically using readily available inputs; 2. capable of simulating these processes for hundreds of years; 3. applicable to a wide range of soils, crops, and climates; and 4. efficient, convenient to use, and capable of assessing the effects of management changes on erosion and soil productivity.

Weather Generator

General Description

EPIC is driven by precipitation, air temperature, solar radiation, wind speed, wind direction, and relative humidity. Daily observations of these weather variables can be input directly into the model. If data for one or more of these variables is not available, EPIC can simulate daily estimates for the missing variables. It is possible to utilize a combination of observed data and simulated values (ex. utilize daily precipitation data and simulate the remaining five variables). Richardson and Nicks (1990) report that the EPIC weather generator is designed to preserve the dependence in time, the internal correlation, and the seasonal characteristics that exist in the actual weather data. Precipitation, wind speed, and wind direction are generated independent of the other variables. Maximum and minimum temperature, solar radiation, and relative humidity are dependent upon the occurrence of precipitation on the day in question. Nicks et al. (1990) concluded that the EPIC weather generator was adequate to meet the requirements of the model. The techniques for generating daily estimates for the six weather variables are discussed below.

Precipitation

EPIC utilizes a first-order Markov chain model to simulate daily precipitation (Nicks 1974). The probability of precipitation on day i is dependent upon the wet or dry status of day $i-1$. A wet day is defined as a day during which at least 0.2 mm of precipitation is realized.

$$P(D / W) = 1 - P(W / W) \quad A.1$$

$$P(D / D) = 1 - P(W / D) \quad A.2$$

$P(D/W)$ is the probability of a dry day following a wet day, $P(W/W)$ is the probability of a wet day following a wet day, $P(D/D)$ is the probability of a dry day following a dry day, and $P(W/D)$ is the probability of a wet day following dry day. Given $P(W/W)$ and $P(W/D)$ the transitional probabilities can be defined.

If $P(W/W)$ and $P(W/D)$ are not available, the average number of rainy days in each month may be utilized to estimate them (Williams et al. 1990).

$$PW = \frac{NWD}{ND} \quad A.3$$

PW is the probability of a wet day during the month, NWD is the number of wet days in the month, and ND is the number of days in the month. $P(W/D)$ is estimated as a fraction of PW .

$$P(W / D) = \beta * PW \quad A.4$$

Where β is usually ranges from 0.6 to 0.9. $P(W/W)$ is calculated directly.

$$P(W / W) = 1.0 - \beta + P(W / D) \quad A.5$$

When $\beta=1.0$, the effect of wet days on the probability of precipitation is minimized ($P(W/D) = P(W/W) = PW$). When $\beta=0.0$ wet days have maximum effect upon the probability of precipitation ($\beta \rightarrow 0.0, P(W/D) \rightarrow 0.0, P(W/W) \rightarrow 1.0$).

Following input or estimation of the wet-dry probabilities, a random number ranging from 0.0 to 1.0 is generated and compared with the appropriate wet-dry probability. If the random number is less than or equal to the wet-dry probability,

precipitation occurs on that day. No precipitation occurs if the random number is greater than the wet-dry probability (Williams et al. 1990).

The amount of precipitation realized during a rainfall event is generated from a skewed normal daily precipitation distribution.

$$R_i = \left(\frac{(\text{SND}_i - \frac{\text{SCF}_k}{6.0}) * \frac{\text{SCF}_k}{6.0} - 1.0}{\text{SCF}_k} \right) * \text{RSDV}_k + \bar{R}_k \quad \text{A.6}$$

R is the rainfall amount for day i (mm), SND is the standard normal deviate for day i , SCF is the skew coefficient, RSDV is the standard deviation of daily rainfall (mm), and \bar{R} is the mean daily rainfall in month k .

If the standard deviation and skew coefficient are not available, the weather generator estimates daily rainfall amount using a modified exponential distribution (Williams et al. 1990).

$$R_i = \frac{(-\ln \mu)^\zeta * \bar{R}_k}{\int_{0.0}^{1.0} (-\ln x)^\zeta dx} \quad \text{A.7}$$

Where μ is a uniform random number between 0.0 and 1.0, and ζ is a parameter usually ranging from 1.0 to 2.0. As the value of ζ increases, so does the simulated rainfall amount. If the average daily air temperature is 0°C or below, the precipitation is snowfall. Otherwise, it is rainfall.

Air Temperature and Solar Radiation

The EPIC air temperature and solar radiation model generates the residuals of maximum and minimum temperature, and solar radiation from a multivariate normal

distribution (Richardson 1981). It is assumed that the residuals of maximum and minimum temperature as well as solar radiation are normally distributed, and that the serial correlation of each variable may be described by a first-order linear autoregressive model (Williams et al. 1990). The reader is referred to Richardson (1981) and Richardson and Nicks (1990) for details of the multivariate generation model. Richardson (1982) describes the dependence structure of daily maximum temperature, minimum temperature, and solar radiation.

Monthly means and standard deviations for the maximum and minimum temperature are required to generate daily temperature and solar radiation estimates. If the standard deviations are not available, the long-term observed extreme monthly minimums and maximums may be substituted (Williams et al. 1990).

$$\text{SDTMX}_k = 0.25 * (\text{TE}_{\text{mx},k} - \bar{\text{T}}_{\text{mx},k}) \quad \text{A.8}$$

SDTMX is the standard deviation of the daily maximum temperature, TE is the extreme daily maximum temperature, and $\bar{\text{T}}_{\text{mx}}$ is the average daily maximum temperature for month k. The standard deviation of the daily minimum temperature can be found by equation A.8 where minimum values (mn) are substituted for maximum (mx) values.

The solar radiation model is based on observed long-term monthly extremes.

$$\text{SDRAMX}_k = 0.25 * (\text{RAMX}_k - \overline{\text{RA}}_k) \quad \text{A.9}$$

SDRAMX is the standard deviation of the maximum daily solar radiation (MJ m^{-2}), RAMX is the maximum daily solar radiation at mid-month, and $\overline{\text{RA}}$ is the mean daily solar radiation for month k. The standard deviation of the daily minimum solar radiation can be found by equation A.9 where minimum values (MN) are substituted for maximum (MX) values.

Mean maximum temperature and solar radiation are adjusted downward for rainy days. To adjust T_{mx} it is assumed that wet day values are less than dry day values by some fraction of $T_{mx} - T_{mn}$ (Williams et al. 1990)

$$TW_{mx,k} = TD_{mx,k} - \Omega_T * (T_{mx,k} - T_{mn,k}) \quad A.10$$

TW_{mx} is the daily mean maximum temperature for wet days ($^{\circ}C$) in month k , TD_{mx} is the daily mean maximum temperature for dry days, Ω is a scaling factor ranging from 0.0 to 1.0, T_{mx} is the daily mean maximum temperature, and T_{mn} is the daily mean minimum temperature. Observed data indicate that Ω_T usually lies between 0.5 and 1.0 (Williams et al. 1990). Since equation A.10 generally gives lower mean maximum temperature values for wet days, a companion equation was developed to slightly increase mean maximum temperature for dry days. The companion equation is based upon the continuity equation.

$$T_{mx,k} * ND_k = TW_{mx,k} * NWD_k + TD_{mx,k} * NDD_k \quad A.11$$

Where NDD is the number of dry days in the month. Substitute equation A.10 into A.11 and solve for TD for the final form of the companion equation .

$$TD_{mx,k} = T_{mx,k} + \frac{NWD_k}{ND_k} * \Omega_T * (T_{mx,k} - T_{mn,k}) \quad A.12$$

Solar radiation for wet and dry days is adjusted in a similar fashion. The radiation on wet days is a fraction of the dry day radiation.

$$RAW_k = \Omega_R * RAD_k \quad A.13$$

Where RAW is the daily mean solar radiation on wet days ($MJ m^{-2}$), Ω_R is a scaling factor ranging from 0.0 to 1.0, and RAD is the mean daily solar radiation on dry days.

The dry day equation is developed by replacing temperature with radiation in equation A.11 and substituting equation A.13 for RAW (Williams et al. 1990).

$$RAD_k = \frac{RA_k * ND_k}{\Omega_R * NWD_k + NDD_k} \quad A.14$$

Where RAD is the daily mean solar radiation on dry days ($MJ m^{-2}$), and RA is the daily mean solar radiation for month k ($MJ m^{-2}$).

Wind Velocity

The wind simulation model was designed by Richardson and Wright (1984) specifically for EPIC. Average daily wind velocity is generated. Average daily wind velocity is estimated from a two-parameter gamma distribution (Williams et al. 1990).

$$U = \left(\frac{V}{V_p}\right)^{\eta-1} * e^{-(\eta-1)*\left(1-\frac{V}{V_p}\right)} \quad A.15$$

U is a dimensionless variable (0-1) expressing the frequency with which wind velocity V ($m s^{-1}$) occurs, V_p is the wind velocity at the peak frequency, and η is the gamma distribution shape parameter.

$$\eta = \frac{\bar{V}^2}{SDV^2} \quad A.16$$

Where \bar{V} is the annual average wind velocity ($m s^{-1}$) and SDV is the standard deviation of daily wind velocity ($m s^{-1}$). This data can be difficult to find. Values for the average annual wind velocity and the standard deviation of hourly wind can be obtained from the USDC (1968). A correction factor of 0.7 was determined to be appropriate for converting hourly standard deviations to daily (Williams et al. 1990).

Relative Humidity

The relative humidity model simulates average daily relative humidity from the monthly average based upon a triangular distribution. The mean daily relative humidity is adjusted to account for wet and dry day effects. The assumed relation between relative humidity on wet and dry days is as follows (Williams et al. 1990)

$$RHW_k = RHD_k + \Omega_H * (1.0 - RHD_k) \quad A.17$$

Where RHW is the daily mean relative humidity on wet days for month k, RHD is the daily mean relative humidity on dry days, and Ω_H is a scaling factor ranging from 0.0 to 1.0. Using the continuity equation as described in the temperature and solar radiation section produces the following equation.

$$RHD_k = \frac{RH_k - \Omega_H * \frac{NWD}{ND}}{1.0 - \Omega_H * \frac{NWD}{ND}} \quad A.18$$

RH is the long-term average relative humidity for month k. Either RHW or RHD is used as the peak of a triangular distribution from which daily relative humidity is generated. The upper limit of the triangular distribution is set with the following equation.

$$RHU_i = RHP_i + (1.0 - RHP_i) * e^{RHP_i - 1.0} \quad A.19$$

RHU is the largest relative humidity value that can be generated on day i, and RHP is the peak of the triangular distribution (RHW or RHD). The lower limit of the triangular distribution is set with the following equation.

$$RHL_i = RHP_i * (1.0 - e^{-RHP_i}) \quad A.20$$

Where RHL is the lowest relative humidity that can be generated on day i.

Williams et al. (1990) state that to be assured the simulated long-term mean relative humidity value agrees with input RH, the simulated value is adjusted.

$$RHG_i^* = RHG_i * \frac{RHP_i}{\overline{RH}_i} \quad A.21$$

RHG* is the simulated relative humidity value for day i adjusted to the mean of the triangle, RHG is the relative humidity generated from the triangle, and \overline{RH} is the mean of the triangle.

Hydrology

Surface Runoff

Runoff Volume. Surface runoff volume (Q) is estimated using a modification of the Soil Conservation Service (SCS) curve number (CN) method.

$$Q = \frac{(R - 0.2s)^2}{R + 0.8s}, \quad R > 0.2s \quad A.22$$

$$Q = 0.0, \quad R \leq 0.2s$$

Where Q is daily surface runoff (mm), and s (mm) is a retention parameter.

$$s = 254 * \left(\frac{100}{CN} - 1 \right) \quad A.23$$

Based upon the assumption that the CN_2 values, CN values for moist soil conditions, listed in the SCS Hydrology Handbook (USDA-SCS 1972) are appropriate for a 5% slope, Williams et al. (1990) developed the following equation for adjusting that CN value for use on other slopes.

$$CN_{2s} = \frac{1}{3}(CN_3 - CN_2) * (1 - 2e^{-13.86S}) + CN_2 \quad A.24$$

CN_{2s} is the SCS Hydrology Handbook CN_2 value adjusted for slope, CN_3 is the CN for wet soil conditions, and S is the average slope of the watershed.

$$CN_1 = CN_2 - \frac{20(100 - CN_2)}{100 - CN_2 + e^{2.533 - 0.0636(100 - CN_2)}} \quad A.25$$

$$CN_3 = CN_2 e^{0.00673(100 - CN_2)} \quad A.26$$

The retention parameter, s , fluctuates over time with soil water content.

$$s = s_1 \left(1 - \frac{FFC}{FFC + e^{w_1 - w_1(FFC)}} \right) \quad A.27$$

Where s_1 is the value of s with CN_1 , FFC is the fraction of field capacity, and w_1 and w_2 are shape parameters.

$$FC = \frac{SW - WP}{FC - WP} \quad A.28$$

Where SW is the soil water content in the root zone, WP is the wilting point water content, and FC is the field capacity water content. Values for w_1 and w_2 are obtained from a simultaneous solution of equation A.27 according to the assumptions that $s = s_2$ when $FFC = 0.5$ and $s = s_3$ when $FFC = 1.0$.

$$w_1 = \ln\left(\frac{1}{1 - \frac{s_3}{s_1}} - 1\right) + w_2 \quad A.29$$

$$w_2 = 2\left(\ln\left(\frac{0.5}{1 - \frac{s_2}{s_1}}\right) - 0.5 - \ln\left(\frac{1}{1 - \frac{s_3}{s_1}} - 1\right)\right) \quad A.30$$

Where s_3 is the CN_3 retention parameter. Equations A.29 and A.30 assure that CN_1 corresponds with the wilting point and that the CN cannot exceed 100 (Williams et al. 1990).

The FFC value obtained in equation A.28 represents soil water uniformly distributed through the top 1.0 m of soil. EPIC estimates water content for each soil layer daily, thus providing the means to estimate runoff based upon a depth distribution of soil water. The effect of depth distribution on runoff is expressed in the depth weighting function Williams et al. (1990).

$$FFC^* = \frac{\sum_{x=1}^M FFC_x \left(\frac{Z_x - Z_{x-1}}{Z_x} \right)}{\sum_{x=1}^M \frac{Z_x - Z_{x-1}}{Z_x}}, \quad Z_x \leq 1.0 \text{ m} \quad \text{A.31}$$

FFC^* is the depth weighted FFC value for use in equation A.27, Z is the depth to the bottom of soil layer x and M is the number of soil layers.

Stochasticity may be incorporated into the runoff estimate procedure through stochastic CN selection. Stochastic CN generation is optional. If chosen, the final curve number estimate is generated from a triangular distribution, the mean of which is the best estimate of CN based upon equations A.23, A.24, A.27, A.28 and A.31, and the extremes of which are ± 5 curve numbers from the mean (Williams et al. 1990). The stochastically generated curve number is substituted into equation A.23.

Peak Runoff Rate. Peak runoff rate (q_p) estimation is based upon a modification of the Rational Formula (Lloyd-Davis 1906).

$$q_p = \frac{(\rho) * (r) * (A)}{360}, \quad \text{A.32}$$

Where q_p is the peak daily runoff rate ($m^3 s^{-1}$), ρ is a runoff coefficient expressing the watershed infiltration characteristics, r is the rainfall intensity ($mm hr^{-1}$) for the watershed's time of concentration, and A is the drainage area (ha).

$$\rho = \frac{Q}{R} \quad A.33$$

$$r = \frac{R_{tc}}{t_c} \quad A.34$$

R_{tc} is the amount of rainfall (mm) during the watershed's time of concentration, t_c (h).

$$R_{tc} = \alpha R_{24} \quad A.35$$

Where α is the ratio of the maximum rainfall amount during a period equal to the watershed time of concentration to the total rainfall for the storm, and R_{24} is the 24-h duration accumulated rainfall from the Weather Service's TP-40 (Hershfield 1961).

Williams et al. (1990) state that to properly evaluate α , variation in rainfall pattern must be considered. Storms with uniform intensity (pattern) cause α to approach a minimum value. Storms of other rainfall patterns (i.e. not uniform rainfall intensity for the duration of the storm) cause higher α values because R_{tc} is greater than R_{24} for all patterns except the uniform. For some short duration storms, most or all the rain occurs during t_c , causing α to approach its upper limit of 1.0. Substituting the products of intensity and time into equation A.34 provides an expression for the minimum value of α , α_{mn} , (Williams et al. 1990).

$$\alpha_{mn} = \frac{t_c}{24} \quad A.36$$

Thus α has limits of

$$\frac{t_c}{24} \leq \alpha \leq 1.0$$

Williams et al. (1990) state that the value of α is assigned with considerable uncertainty when only daily rainfall and simulated runoff amounts are given. To account for some of this uncertainty, α is generated from a gamma distribution having a base ranging from $t_c/24$ to 1.0. The USLE and AOF water erosion models, to be discussed in the Erosion section of this chapter, utilize the maximum 0.5-h amount of each daily rainfall, thus α is computed with the following equation.

$$\alpha = \alpha_{0.5} * \frac{R_{t_c}}{R_{0.5}} \quad \text{A.37}$$

$R_{0.5}$ is the maximum 0.5-h rainfall amount (mm), and $\alpha_{0.5}$ is the ratio of the maximum rainfall amount during 0.5 h to the total rainfall for the storm.

$$R_t = R_6 * \left(\frac{t}{6}\right)^b \quad \text{A.38}$$

Where R_t is the rainfall amount (mm) for any time t , R_6 is the 10-year, 6-h rainfall amount (mm) from Hershfield (1961), and b is a parameter used to fit the TP-40 relationship (Hershfield 1961) at any location. Note that t of R_t is set to 0.5 h in equation A.37. The estimation of $\alpha_{0.5}$ is discussed in the Erosion section of this chapter.

Substituting equations A.33, A.34, and A.35 into equation A.32 provides the peak runoff equation.

$$q_p = \frac{(\alpha) * (Q) * (A)}{360 (t_c)} \quad \text{A.39}$$

Time of concentration is calculated by the following equation.

$$t_c = t_{cc} + t_{cs} \quad \text{A.40}$$

Where t_{cc} is the time of concentration for channel flow and t_{cs} is the time of concentration for surface flow (h). Time of concentration for surface flow is estimated as follows.

$$t_{cs} = \frac{\lambda}{V_s} \quad \text{A.41}$$

Where λ is the surface slope length (m) and V_s is the surface flow velocity (m s^{-1}).

Using Manning's Equation (Manning 1891) to estimate V_s gives the following.

$$V_s = \frac{q_s^{0.4} * S^{0.3}}{n^{0.6}} \quad \text{A.42}$$

Where q_s is the average surface flow rate (mm hr^{-1}) and S is the land surface slope (m m^{-1}). Williams et al. (1990) assume that the average surface flow rate is about 6.35 mm hr^{-1} , and make substitutions into equations A.41 and A.42 to convert from $\text{m}^3 \text{ s}^{-1}$ to mm hr^{-1} and seconds to hours to develop the final equation for estimating t_{cs} .

$$t_{cs} = \frac{(\lambda * n)^{0.6}}{18 * S^{0.3}} \quad \text{A.43}$$

The t_{cc} is estimated as follows.

$$t_{cc} = \frac{L_c}{V_c} \quad \text{A.44}$$

L_c is the average channel flow length (km) for the watershed, and V_c is the average channel velocity (m s^{-1}).

$$L_c = \sqrt{L * L_{ca}} \quad \text{A.45}$$

L is the channel length from the most distant point to the watershed outlet (km), and L_{ca} is the distance along the channel to the watershed centroid (km). Average velocity is

estimated by Manning's Equation, assuming a trapezoidal channel with 2:1 side slopes and a 10:1 bottom width/depth ratio (Williams et al. 1990). Substitution of A.45 for L_c and Manning's Equation for V_c into equation A.44 gives the following equation.

$$t_{cc} = \frac{\sqrt{L * L_{ca}} * n^{0.75}}{0.489 * (q_c)^{0.25} * (\sigma)^{0.375}} \quad A.46$$

Where n is Manning's n , q_c is the average channel flow rate ($m^3 s^{-1}$), and σ is the average channel slope ($m m^{-1}$). Assuming that $L_{ca}=0.5L$, that the average flow rate is about 6.35 mm hr^{-1} , and that the average flow rate is a function of the square root of drainage area yields the final equation for t_{cc} .

$$t_{cc} = \frac{1.1 * (L) * n^{0.75}}{A^{0.125} * \sigma^{0.375}} \quad A.47$$

Percolation

A storage routing technique is used to simulate vertical flow through each soil layer. Flow from a soil layer occurs when the soil water content exceeds the field capacity of the soil layer, and water flows from the layer until field capacity is attained (Williams et al. 1990). The following equation estimates reduction in soil water.

$$SW_x = (SW_{Ox} - FC_x) * e^{\frac{-\Delta t}{TT_x}} + FC_x \quad A.48$$

SW and SW_o are the soil water contents at $t = 0$ and $t = 24 \text{ h}$, respectively. TT is the travel time through layer x (h). Daily percolation rate for layer x (O_x) is computed in mm d^{-1} .

$$O_x = (SW_{Ox} - FC_x) * (1.0 - e^{\frac{-\Delta t}{TT_x}}) \quad A.49$$

$$TT_x = \frac{PO_x - FC_x}{SC_x} \quad A.50$$

PO is the porosity (mm), FC is the field capacity (mm), and SC is the saturated hydraulic conductivity (mm hr⁻¹). This process is applied to the soil profile layer by layer from the surface to the deepest layer. If a layer's porosity is exceeded, the excess water is transferred to the layer above.

SC may be input or estimated for each soil layer. If data are not available, SC is calculated as follows.

$$SC_x = \frac{12.7 * (100 - CLA_x) * (SS_x)}{100 - CLA_x * e^{11.45 - 0.097 * (100 * CLA_x)}} \quad A.51$$

Where CLA is the percentage of clay in soil layer x, and SS is the soil strength factor (described in the Growth Constraints section of this chapter).

Lateral Subsurface Flow

Lateral subsurface flow rate (SSF) in mm d⁻¹ is calculated simultaneously with percolation.

$$SSF_x = (SW_{Ox} - FC_x) * (1.0 - e^{\frac{-1.0}{TT_{Rx}}}) \quad A.52$$

TT_{Rx} is the lateral flow time (d) for soil layer x.

$$TT_{Rx} = \frac{1000 * CLA_x * SS_x}{CLA_x + e^{10.047 - 0.148 * CLA_x}} + 10 \quad A.53$$

Equations A.49 and A.52 are solved simultaneously. The sum of percolation and lateral subsurface flow is found as follows (Williams et al. 1990).

$$O_x + SSF_x = (SW_{Ox} - FC_x) * (1.0 - e^{\frac{-\Delta t}{TT_x}} * e^{\frac{-1.0}{TT_{Rx}}}) \quad A.54$$

Considering the ratio of SSF to O and substituting the resulting SSF into equation A.54.

$$O + O * \left(\frac{1.0 - e^{-\frac{-1.0}{T_{Rx}}}}{1.0 - e^{-\frac{-\Delta t}{T_x}}} \right) = (SW_{Ox} - FC_x) * (1.0 - e^{-\frac{-\Delta t}{T_x}} * e^{-\frac{-1.0}{T_{Rx}}}) \quad A.55$$

Solving for O gives the final percolation equation.

$$O = \frac{(SW_{Ox} - FC_x) * (1.0 - e^{-\frac{-\Delta t}{T_x}} * e^{-\frac{-1.0}{T_{Rx}}}) * (1.0 - e^{-\frac{-\Delta t}{T_x}})}{2.0 - e^{-\frac{-\Delta t}{T_x}} - e^{-\frac{-1.0}{T_{Rx}}}} \quad A.56$$

The calculated O value is substituted into equation A.54 to obtain the final estimate of SSF (Williams et al. 1990).

Evapotranspiration

Potential Evaporation. In EPIC, one of four methods of estimating potential evaporation (E_o) can be used per simulation. The Hargraves and Samani (1985) method, the Priestly-Taylor (1972) method, the Penman (1948) method, and the Penman-Monteith (Monteith 1965) method. The Penman-Monteith method serves as the default PET estimation method. Only the Penman and the Priestly-Taylor methods are detailed in the model documentation (Williams et al. 1990).

The Penman (1948) option for estimating potential evaporation is based upon the following equation.

$$E_o = \frac{\delta}{\delta + \gamma} * \frac{h_o - G}{HV} + \frac{\gamma}{\delta + \gamma} * f(V) * (e_a - e_d) \quad A.57$$

E_o is the potential evaporation (mm), δ is the slope of the saturation vapor pressure curve ($\text{kPa } ^\circ\text{C}^{-1}$), γ is a psychrometer constant ($\text{kPa } ^\circ\text{C}^{-1}$), h_o is the net radiation (MJ m^{-2})

²), G is the soil heat flux (MJ m^{-2}), HV is the latent heat of vaporization (MJ kg^{-1}), $f(V)$ is a wind speed function ($\text{mm d}^{-1} \text{ kPa}^{-1}$), e_a is the saturation vapor pressure at mean air temperature (kPa), and e_d is the vapor pressure at mean air temperature (kPa).

$$HV = 2.5 - 0.0022 * T \quad \text{A.58}$$

$$e_a = 0.1 * e^{\left(\frac{54.88 - 5.03 * \ln(T+273) - 6791}{T+273}\right)} \quad \text{A.59}$$

$$e_d = e_a * RH \quad \text{A.60}$$

T is the mean daily air temperature ($^{\circ}\text{C}$), and RH is the relative humidity expressed as a fraction.

$$\delta = \frac{e_a}{T+273} * \left(\frac{6791}{T+273} - 5.03\right) \quad \text{A.61}$$

$$\gamma = 6.6 * 10^{-4} * PB \quad \text{A.62}$$

PB is the barometric pressure (kPa).

$$PB = 101 - 0.0115 * ELEV + 5.44 * 10^{-7} * ELEV^2 \quad \text{A.63}$$

$ELEV$ is the elevation of the site (m).

Soil heat flux is estimated based upon air temperature on the day of interest as well as the air temperature for the previous 3 days.

$$G = 0.12 * \left(T_i - \frac{T_{i-1} + T_{i-2} + T_{i-3}}{3}\right) \quad \text{A.64}$$

Solar radiation is adjusted to obtain net radiation.

$$h_{0i} = RA_i * (1.0 - AB_i) - RAB_i * \left(\frac{0.9 * RA_i}{RAMX_i} + 0.1\right) \quad \text{A.65}$$

RA is the solar radiation (MJ m^{-2}), AB is the albedo, RAB is the net outgoing long wave radiation (MJ m^{-2}) for clear days, and RAMX is the maximum solar radiation possible (MJ m^{-2}) for the location on day i.

$$\text{RAB}_i = 4.9 \times 10^{-9} * (0.34 - 0.14 * \sqrt{e_d}) * (T_i + 273)^4 \quad \text{A.66}$$

$$\text{RAMX} = 30 * (1.0 + 0.0335 * \sin(\frac{2\pi}{365} * (i + 88.2))) * (\text{XT} * \sin(\frac{2\pi}{365} * \text{LAT}) * \sin\text{SD} + \cos(\frac{2\pi}{365} * \text{LAT}) * \cos\text{SD} * \sin\text{XT}) \quad \text{A.67}$$

$$\text{XT} = \cos^{-1} * (-\tan(\frac{2\pi}{365} * \text{LAT}) * \tan\text{SD}), \quad 0 \leq \text{XT} \leq \pi \quad \text{A.68}$$

LAT is the latitude in degrees, and SD is the angle of the sun's declination (radians).

$$\text{SD}_i = 0.4102 * \sin(\frac{2\pi}{365} * (i - 80.25)) \quad \text{A.69}$$

The wind function of the Penman equation is approximated with the following equation.

$$f(V) = 2.7 + 1.63 * V \quad \text{A.70}$$

The Priestly-Taylor (1972) method provides estimates of potential evaporation without wind and relative humidity inputs.

$$E_o = 30.6 * h_o * \frac{\delta}{\delta + 0.68} \quad \text{A.71}$$

$$h_{oi} = \frac{2\pi}{365} * \text{RA}_i * (1 - \text{AB}_i) \quad \text{A.72}$$

$$\delta = e^{(21.3 - \frac{5304}{T+273}) * (\frac{5304}{(T+273)^2})} \quad \text{A.73}$$

Both the Penman and Priestly-Taylor methods estimate albedo by the following process (Williams et al 1990). If snow cover exists with 5 mm or greater water content, the value of albedo is set to 0.6. If snow cover is less than 5 mm water content and no

crop is growing, the input soil albedo value is used. When crops are growing, albedo is estimated by the following equation.

$$AB = 0.23 * (1.0 - EA) + AB_s * EA \quad A.74$$

Where 0.23 is the albedo for plants, AB_s is the soil albedo, and EA is a soil cover index ranging from 0.0 to 1.0.

$$EA = e^{-0.1 * CV} \quad A.75$$

CV is the sum of aboveground biomass and crop residue ($t \text{ ha}^{-1}$).

Plant Water Evaporation. Potential plant water evaporation is estimated as follows.

$$E_p = \frac{E_o * LAI}{3.0}, \quad 0 \leq LAI \leq 3.0 \quad A.76$$

$$E_p = E_o, \quad LAI > 3.0 \quad A.77$$

E_p is the predicted plant water evaporation rate (mm d^{-1}).

Soil Water Evaporation. Potential soil water evaporation is simulated by the following equation.

$$E_s = \min[E_o * EA, E_o - E_p] \quad A.78$$

E_s is the potential soil water evaporation rate (mm d^{-1}), and E_o is potential evaporation.

Actual soil water evaporation is estimated considering only the top 0.2 m of the soil profile. Williams et al. (1990) state that soil water evaporation in the absence of

snow cover is governed by soil depth and water content according to the following equation.

$$EV_Z = E_s \left(\frac{\frac{Z}{0.2}}{\frac{Z}{0.2} + e^{-2.92 - 1.43 \frac{Z}{0.2}}} \right) \quad A.79$$

EV is the total soil water evaporation (mm) from the soil profile to depth Z (m). Potential soil water evaporation for a given soil layer is estimated as the difference between EV's at the layer boundaries.

$$SEV_x = EV_{Z(x)} - DV_{Z(x-1)} \quad A.80$$

SEV is the potential soil water evaporation for layer x (mm). SEV is reduced if soil water is limiting.

$$SEV_x^* = SEV_x \cdot e^{\frac{2.5 \cdot (SW_x - FC_x)}{FC_x - WP_x}}, \quad SW_x < FC_x \quad A.81$$

$$SEV_x^* = SEV_x, \quad SW_x \geq FC_x \quad A.82$$

SEV_x^{*} is the adjusted soil water evaporation estimate (mm). In order to assure that the soil water supply is adequate to meet the estimated soil water evaporation estimate the following process is utilized.

$$SEV_x^* = \min(SEV_x^*, SW_x - 0.5 \cdot WP_x) \quad A.83$$

Equation A.83 allows soil in the top 0.2 m to dry half the soil water content corresponding to the wilting point (Williams et al. 1990).

Erosion

When erosion occurs during an EPIC simulation, soil is removed from the soil surface. Recall that the first soil layer must be 10 mm in depth. In order to maintain the thickness of the first soil layer at 10 mm during erosion, the first soil layer is moved into the second soil layer and the properties of the first layer are adjusted by interpolation according to the distance the first layer moves into the second. If the first layer is completely eroded, then the first layer essentially becomes the first 10 mm of the second layer.

EPIC simulates water-induced erosion by one or more of six methods. Only one of the six methods can be selected to interact with other model components during a given simulation, but erosion estimates from all six methods can be obtained. Soil erosion models incorporated into EPIC are the Universal Soil Loss Equation (USLE) (Wischmeier and Smith 1978), the Modified Universal Soil Loss Equation (MUSLE) (Williams 1975), the Onstead-Foster (AOF) equation (Onstead and Foster 1975), the small watershed version of MUSLE (MUSS), a version of MUSLE that allows the user to input four principal coefficients (MUSI), and a version of MUSLE that is derived theoretically and is not empirically fit (MUST) (Dumesnil 1993).

Only the USLE, MUSLE, and AOF soil erosion models are discussed in the model documentation (Williams 1990). The main difference between MUSLE and the other two soil erosion models is that MUSLE does not contain a rainfall variable (Laflen et al. 1990). MUSLE uses runoff variables to simulate erosion and sediment yield, USLE depends strictly upon rainfall as an indicator of erosive energy, and AOF utilizes a combination of the USLE and MUSLE energy factors. In the absence of runoff, MUSLE will predict no erosion, and AOF will predict 63.6% as much as the USLE.

The water-induced soil erosion model in EPIC uses an equation of the following form.

$$Y = \chi * K * CE * PE * LS * ROKF \quad \text{A.84}$$

$$\chi = EI \quad \text{for USLE}$$

$$\chi = 11.8 * (Q^* * q_p)^{0.56} \quad \text{for MUSLE}$$

$$\chi = 0.646 * EI + 0.45 * (Q * q_p^*)^{0.33} \quad \text{for AOF}$$

Where Y is the sediment yield ($t \text{ ha}^{-1}$), χ is chosen by the user, K is the soil erodibility factor, CE is the crop management factor, PE is the erosion control practice factor, LS is the slope length and steepness factor, ROKF is the coarse fragment factor, EI is the rainfall energy factor, Q^* is the runoff volume (m^3), q_p is the peak runoff rate ($mm \text{ s}^{-1}$), Q is the runoff volume (mm), and q_p^* is the peak runoff rate ($mm \text{ h}^{-1}$).

EI is found as the product of the maximum 0.5-h rainfall intensity ($r_{0.5}$) and the rainfall energy realized during a given storm.

$$EI = \frac{R * (12.1 + 8.9 * (\log r_p - 0.434)) * r_{0.5}}{1000} \quad \text{A.85}$$

R is the daily rainfall amount (mm), r_p is the peak rainfall intensity ($mm \text{ h}^{-1}$), $r_{0.5}$ is the maximum 0.5-h rainfall intensity. A problem arises when estimating r_p because time-distributed rainfall is not available. EPIC estimates rainfall intensity based upon the assumption that rainfall intensity is exponentially distributed (Williams et al. 1990).

$$r_t = r_p * e^{-\frac{t}{\kappa}} \quad \text{A.86}$$

Where r is the rainfall intensity at time t ($mm \text{ h}^{-1}$), and κ is the decay constant (h).

Rainfall energy, RE, is computed as follows.

$$RE = \Delta R * (12.1 + 8.9 * \log \frac{R}{\Delta t}) \quad \text{A.87}$$

ΔR is the rainfall amount (mm) during the time interval Δt (h). Analytically, the rainfall energy equation is expressed as follows.

$$RE = 12.1 * \int_0^{\infty} r dt + 8.9 * \int_0^{\infty} r * \log r dt \quad A.88$$

Substituting equation A.86 into equation A.87 and integrating gives the equation for estimating daily rainfall energy.

$$RE = R * [12.1 + 8.9 * (\log r_p - 0.434)] \quad A.89$$

To compute values for r_p , equation A.88 is integrated.

$$R = r_p * \kappa \quad A.90$$

$$R_t = R * (1 - e^{-\frac{t}{\kappa}}) \quad A.91$$

$R_{0.5}$ is estimated by using $\alpha_{0.5}$, as mentioned in the hydrology section.

$$R_{0.5} = \alpha_{0.5} * R \quad A.92$$

To determine the value of r_p , equations A.90 and A.92 are substituted into equation A.91.

$$r_p = -2 * R * \ln(1 - \alpha_{0.5}) \quad A.93$$

The frequency, F , with which the maximum 0.5-h rainfall amount occurs is estimated by using the Hazen plotting position equation.

$$F = \frac{1}{2\tau} \quad A.94$$

The total number of rainfall events for each month, τ , is the product of the number of years of record and the average number of rainfall events for the month. To estimate the mean value of $\alpha_{0.5}$, it is first necessary to estimate the mean value of $R_{0.5}$. In order

to compute $R_{0.5}$ the maximum 0.5-h rainfall amounts are assumed to be exponentially distributed (Williams et al. 1990).

$$\bar{R}_{0.5,k} = \frac{R_{0.5F,k}}{-\ln F_k} \quad \text{A.95}$$

$\bar{R}_{0.5,k}$ is the mean maximum 0.5-h rainfall amount, $R_{0.5F,k}$ is the maximum 0.5-h rainfall amount for frequency F , and the subscript k refers to the month. Mean $\alpha_{0.5}$ is computed with the following equation.

$$\alpha_{0.5,k} = \frac{\bar{R}_{0.5,k}}{R_k} \quad \text{A.96}$$

\bar{R} is the mean amount of rainfall for each event (average monthly rainfall / average number of days of rainfall). Daily values of $\alpha_{0.5}$ are generated from a two-parameter gamma distribution which has a base defined by the upper and lower limits of $\alpha_{0.5}$. The lower limit, $\alpha_{0.5l}$, determined assuming a uniform rainfall rate is as follows.

$$\alpha_{0.5l} = \frac{0.5}{24} = 0.0208 \quad \text{A.97}$$

The upper limit of a $\alpha_{0.5}$ is estimated by substituting a high value for r_p (250 mm h⁻¹ is generally used) into equation A.98.

$$\alpha_{0.5u} = 1 - e^{\frac{-125}{R}} \quad \text{A.98}$$

The peak of the $\alpha_{0.5}$ gamma distribution is calculated as follows.

$$\alpha_{0.5P,k} = \frac{\alpha_{0.5,k} * (\nu - 1)}{\nu} \quad \text{A.99}$$

Where $\alpha_{0.5P,k}$ is the $\alpha_{0.5}$ value at the peak of the gamma distribution, and ν is the gamma distribution shape parameter.

The soil erodibility factor, K, is determined for the first soil layer at the start of each year of simulation.

$$K = (0.2 + 0.3 * e^{-0.0256 * SAN * (\frac{1-SIL}{100})}) * (\frac{SIL}{CLA + SIL})^{0.3} * (1.0 - \frac{0.25 * C}{C + e^{3.72 - 2.95 * C}}) * (1.0 - \frac{0.7 * SN_1}{SN_1 + e^{-5.51 + 22.9 * SN_1}})$$

A.100

SAN, SIL, CLA, and C are the sand, silt, clay, and organic carbon contents of the soil layer (%), respectively.

$$SN_1 = 1 - \frac{SAN}{100}$$

A.101

According to Williams et al. (1990), equation A.107 is utilized because it allows K to vary from about 0.1 to 0.5. The first term gives low K values for soils with high coarse-sand contents and high K values for soils with little sand. The fine sand content is estimated as the product of sand and silt divided by 100. The expression for coarse sand in the first term is simply the difference between sand and the estimated fine sand. The second term reduces K for soils that have high clay to silt ratios. The third term reduces K for soils with high organic carbon contents. The fourth term reduces K for soils with extremely high sand contents (SAN > 70%) (Williams et al. 1990).

CE is evaluated for all days when surface runoff occurs.

$$CE = e^{[(\ln 0.8 - \ln CE_{mn,j}) * (e^{-1.15CV}) + \ln CE_{mn,j}]}$$

A.102

Where CE_{mnj} is the minimum value of the crop management factor for crop j and CV is the sum of above ground biomass and crop residue ($t\ ha^{-1}$). The role of CE in EPIC is also discussed by Laflen et al. (1990).

The PE value is determined initially by considering the conservation practices to be applied to the watershed. LS is calculated in the following manner.

$$LS = \left(\frac{\lambda}{22.1}\right)^{\xi} * (65.41 * S^2 + 4.56S + 0.065) \quad A.103$$

S is the land surface slope ($m\ m^{-1}$), λ is the slope length (m), and ξ is a parameter dependent upon slope.

$$\xi = \frac{0.3S}{(S + e^{-1.47-61.09S}) + 0.2} \quad A.104$$

The coarse fragment factor is estimated following Simanton et al. (1984).

$$ROKF = e^{-0.03 * ROK} \quad A.105$$

Where ROK is the percent of coarse fragments (> 3 in. diameter) in the surface soil layer.

Nutrients

Nitrogen

Nitrate Loss in Surface Runoff. NO_3 -N loss in surface runoff is estimated considering only the first soil layer (10 mm thickness). The total amount of water leaving the first soil layer is the sum of Q , SSF_1 , and O .

$$QT = Q + O_1 + SSF_1 \quad A.106$$

QT is the total water lost from the first soil layer (mm). The amount of NO₃-N lost from the first layer is found as:

$$VNO_3 = QT * C_{NO3} \quad A.107$$

VNO₃ is the amount of NO₃-N lost from the first layer and C_{NO3} is the NO₃-N concentration of the first layer. At the end of the day the amount of NO₃-N left in the first layer is:

$$WNO_3 = WNO_{30} - QT * C_{NO3} \quad A.108$$

WNO₃₀ and WNO₃ are the weights of NO₃-N (kg) contained in the first layer at the beginning and the end of the day, respectively. NO₃-N concentration in the first soil layer can be estimated by dividing the weight of NO₃-N by the water storage volume.

$$C'_{NO3} = C_{NO3} - C_{NO3} * \frac{QT}{PO_1 - WP_1} \quad A.109$$

Where C'_{NO3} is the concentration of NO₃-N at the end of the day, PO₁ is the porosity of the first soil layer, and WP₁ is the wilting point water content (mm) of the first soil layer. Equation A.109 is a finite difference approximation for the following exponential equation.

$$C'_{NO3} = C_{NO3} * e^{\frac{-QT}{PO_1 - WP_1}} \quad A.110$$

VNO₃ is computed for any QT value by integrating equation A.110.

$$VNO_3 = W_{NO3} * \left(1 - e^{\frac{-QT}{PO_1 - WP_1}}\right) \quad A.111$$

The average concentration of QT for the day is found from the following.

$$C_{NO3} = \frac{VNO_3}{QT} \quad A.112$$

The amounts of NO₃-N lost to surface runoff, lateral subsurface flow, and percolation are estimated as the products of the volume of water passing through each pathway and the concentration calculated by equation A.112. NO₃-N loss is reported in kg ha⁻¹.

Nitrate Leaching. Leaching and lateral subsurface flow in lower soil layers are treated by the same approach used for the first soil layer except that surface runoff is not considered.

Nitrate Transport by Soil Water Evaporation. When soil water is evaporated from the soil, NO₃-N is moved upward into the first soil layer by mass flow. The equation for estimating upward NO₃-N transport is as follows.

$$ENO_3 = \sum_{x=2}^M (SEV_x * C_{NO3x}) \quad A.113$$

Where ENO₃ is the amount of NO₃-N (kg ha⁻¹) moved from lower soil layers to the first layer by soil water evaporation E_s (mm), the subscript x refers to soil layer, and M is the number of soil layers contributing to soil water evaporation (maximum depth is 0.2 m).

EPIC accounts for organic N transport by sediment, denitrification, mineralization, and immobilization. The procedures used to estimate these processes will not be discussed, and the reader is referred to Williams et al. 1990). Nitrogen contribution from rainfall is calculated based upon an average rainfall N concentration at a location for all storms. The amount of N contributed to the watershed by each rainfall is estimated as the product of rainfall amount and concentration.

Phosphorus

Soluble P Loss in Surface Runoff. EPIC follows the assumption that majority of phosphorus is associated with the sediment phase (Williams et al. 1990). The soluble P runoff equation used in EPIC is as follows.

$$YSP = \frac{0.01 * c_{LP1} * Q}{k_d} \quad A.114$$

YSP is the soluble P (kg ha^{-1}) lost in surface runoff of volume Q (mm), c_{LP1} is the concentration of labile P in the first soil layer (g t^{-1}), and k_d is the P concentration of the sediment divided by that of the soil solution ($\text{m}^3 \text{t}^{-1}$). EPIC assigns a value of 175 to k_d .

Phosphorus Transport by Sediment. Sediment transport of P is simulated as follows.

$$YP = 0.001 * Y * c_p * ER \quad A.115$$

Where YP is the sediment phase P lost in surface runoff (kg ha^{-1}) and c_p is the P concentration of sediment in the first soil layer (g t^{-1}).

The model documentation also discusses the procedures utilized by EPIC to estimate P mineralization, immobilization, and mineral P cycling. These components will not be discussed. The reader is referred to Williams et al. (1990).

APPENDIX II

**CLEAR CUT WATERSHED: RESULTS OF MODEL
PERFORMANCE EVALUATIONS**

Results of Model Performance Evaluation
 Daily Model Output
 Calibration for Total Suspended Solids (TSS)
 Recovery Year 1
 WS-I

Statistics for Linear Regression Analysis

Statistic	Value
Multiple R	0.519
R Square	0.270
Adj. R Square	0.268
Standard Error	0.017
Observations	365

ANOVA for Linear Regression Analysis

	df	SS	MS	F	Significance of F
Regression	1	0.0395592	0.039559	134.0302	1.35735E-26
Residual	363	0.10714	0.000295		
Total	364	0.1466992			

Coefficients

	Intercept	TSS ^a
Coefficient	0.00200765	0.6616669
Standard Error	0.00090648	0.0571529
Lower 95% CI	0.00022503	0.5492747
Upper 95% CI	0.00379026	0.7740591

Let alpha = 0.05

Test statistic = 1.96

Ho: a equal to 0 ; Ha: a not equal to 0

$t = (0.0020076 - 0) / 0.0009065 = 2.21$

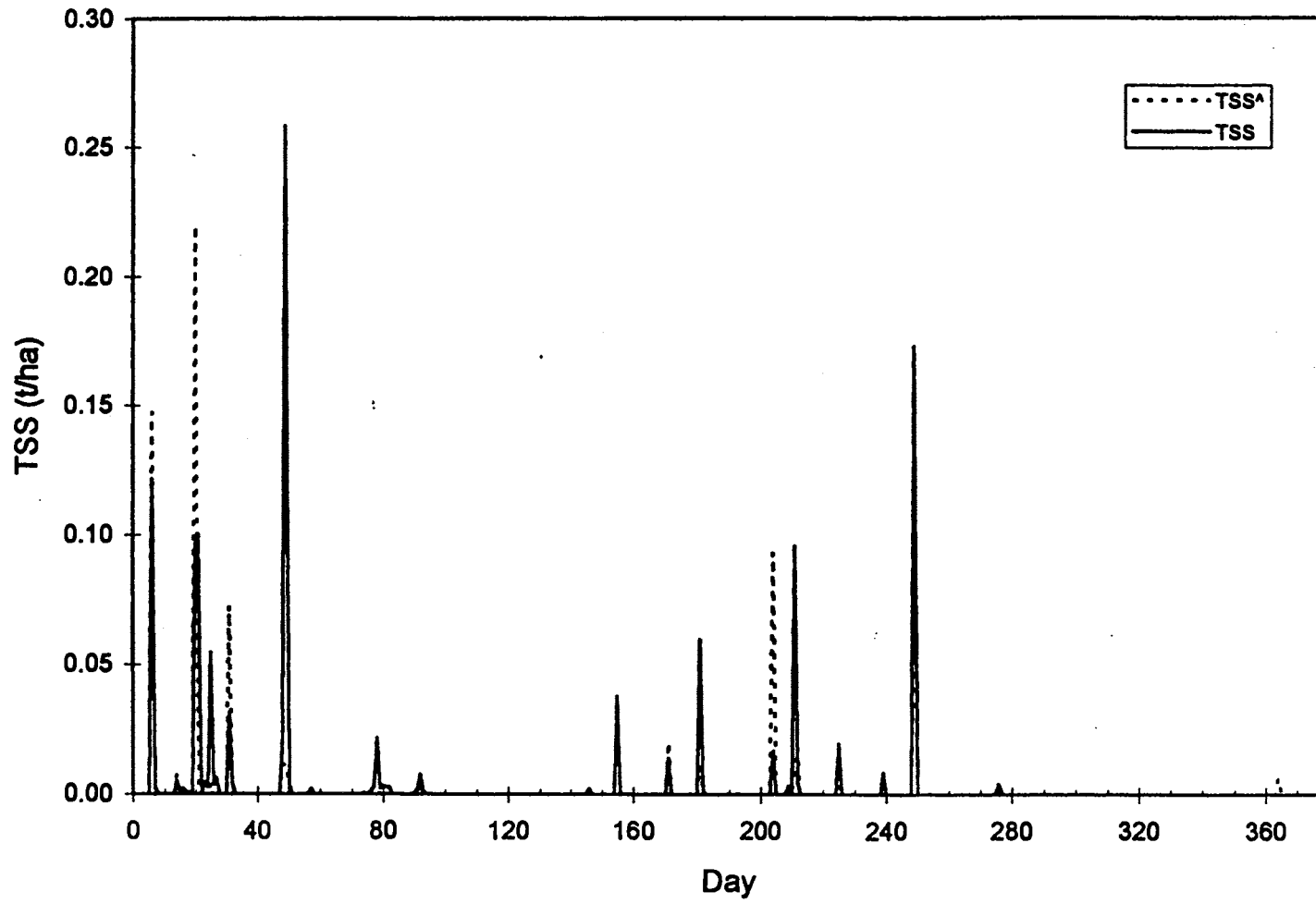
reject Ho: a equal to 0

Ho: b equal to 1 ; Ha: b not equal to 1

$t = (0.661667 - 1) / 0.057153 = -5.92$

reject Ho: b equal to 1

Daily TSS; Year R1; WS-I



Results of Model Performance Evaluation
 Daily Model Output
 Calibration for Total Suspended Solids (TSS)
 Recovery Year 2
 WS-I

Statistics for Linear Regression Analysis

Statistic	Value
Multiple R	0.842
R Square	0.708
Adj. R Square	0.707
Standard Error	0.004
Observations	365

ANOVA for Linear Regression Analysis

	df	SS	MS	F	Significance of F
Regression	1	0.0131304	0.01313	881.1862	3.9579E-99
Residual	363	0.005409	1.49E-05		
Total	364	0.0185394			

Coefficients

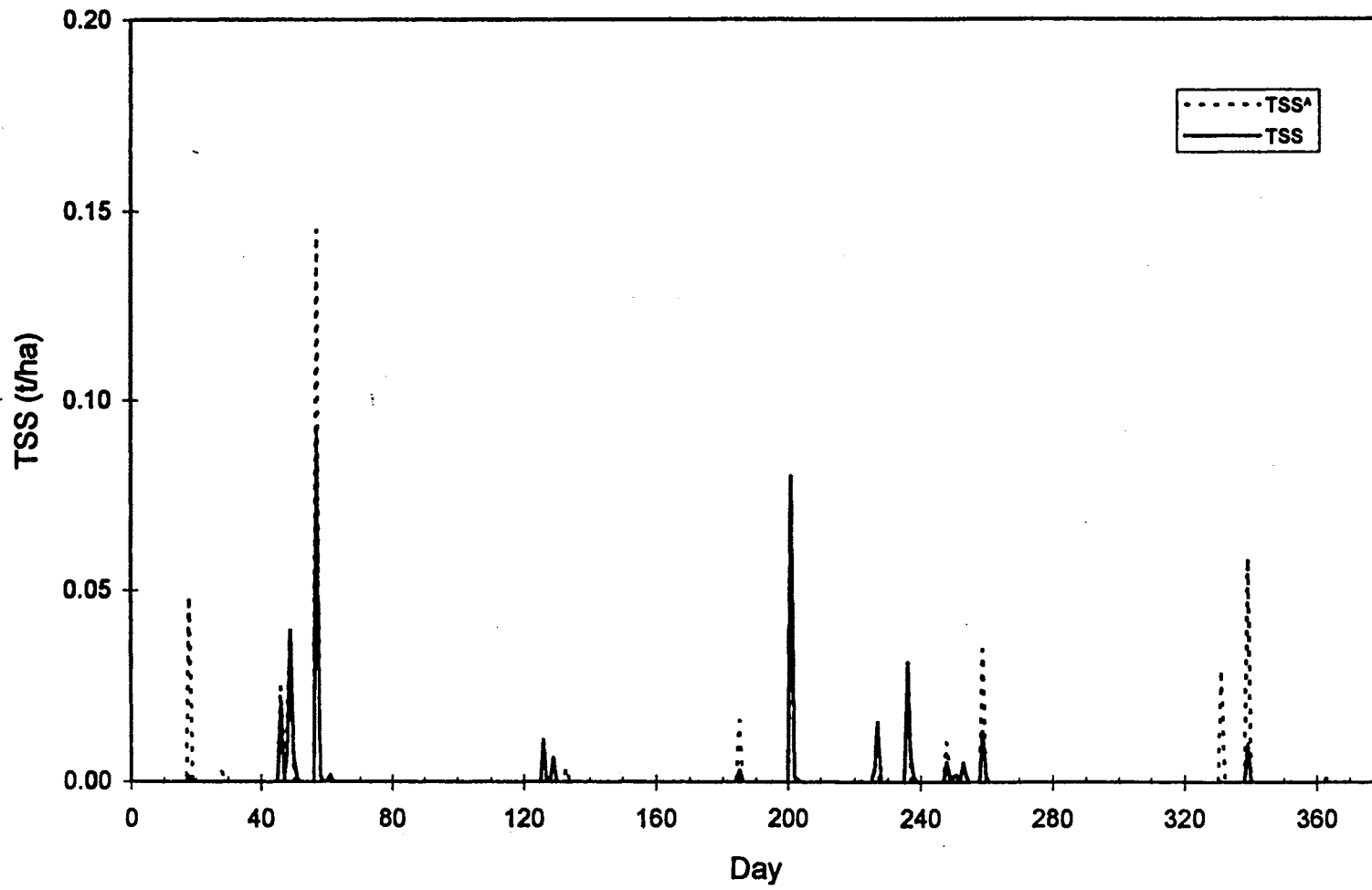
	Intercept	TSS^
Coefficient	0.00014391	0.6189568
Standard Error	0.00020424	0.020851
Lower 95% CI	-0.0002577	0.577953
Upper 95% CI	0.00054555	0.6599607

Let alpha = 0.05
 Test statistic = 1.96

Ho: a equal to 0 ; Ha: a not equal to 0
 $t = (0.0001439 - 0) / 0.0002042 = 0.70$
 fail to reject Ho: a equal to 0

Ho: b equal to 1 ; Ha: b not equal to 1
 $t = (0.618957 - 1) / 0.020851 = -18.27$
 reject Ho: b equal to 1

Daily TSS; Year R2; WS-I



Results of Model Performance Evaluation
 Daily Model Output
 Calibration for Total Suspended Solids (TSS)
 Recovery Year 3
 WS-I

Statistics for Linear Regression Analysis

Statistic	Value
Multiple R	0.180
R Square	0.032
Adj. R Square	0.030
Standard Error	0.004
Observations	365

ANOVA for Linear Regression Analysis

	df	SS	MS	F	Significance of F
Regression	1	0.0001567	0.000157	12.10508	0.000563973
Residual	363	0.0046989	1.29E-05		
Total	364	0.0048556			

Coefficients

	Intercept	TSS ^a
Coefficient	0.00036747	0.1414851
Standard Error	0.00019001	0.0406656
Lower 95% CI	-6.187E-06	0.0615155
Upper 95% CI	0.00074113	0.2214546

Let alpha = 0.05

Test statistic = 1.96

Ho: a equal to 0 ; Ha: a not equal to 0

$t = (0.0003675 - 0) / 0.00019 = 1.93$

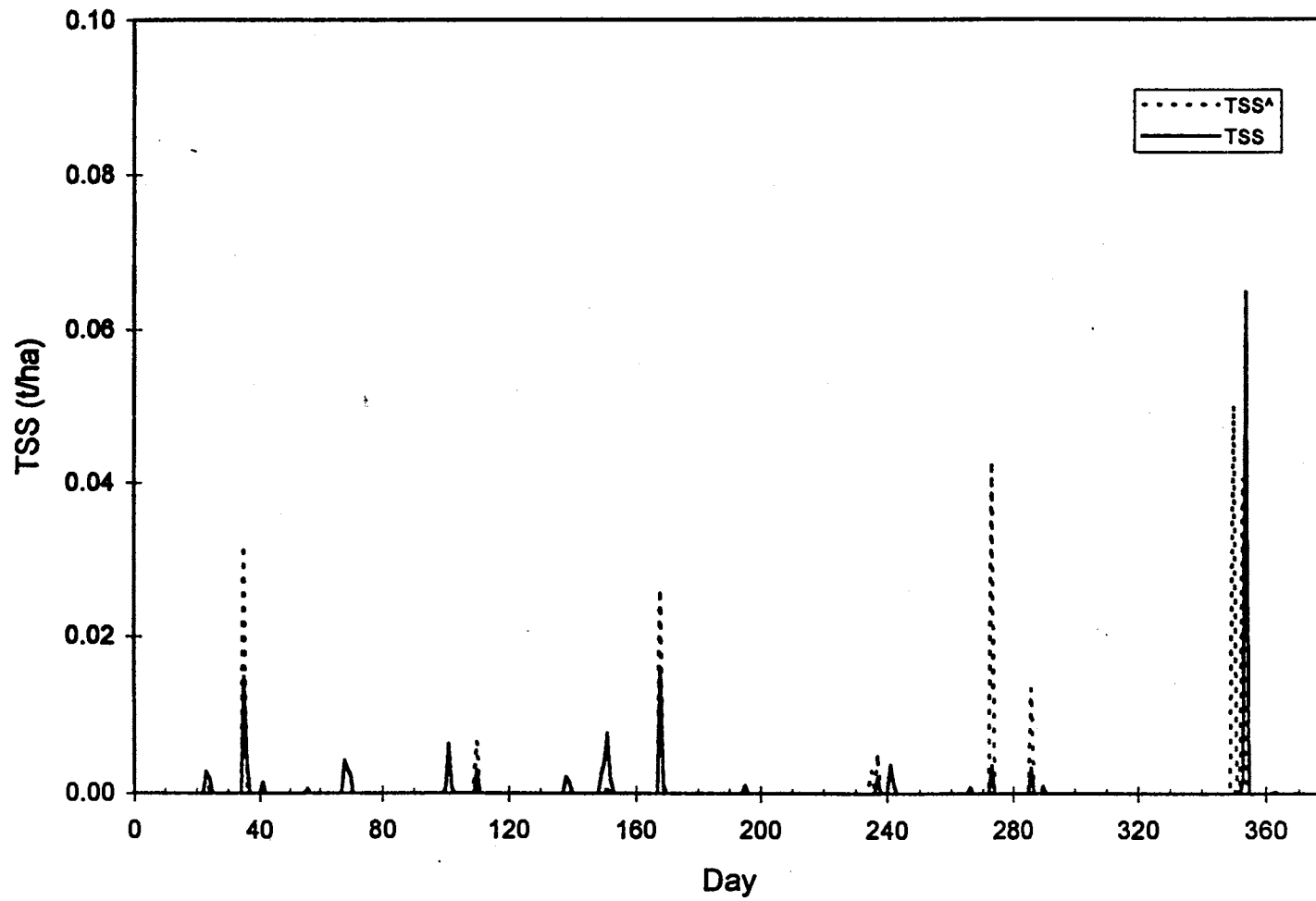
reject Ho: a equal to 0

Ho: b equal to 1 ; Ha: b not equal to 1

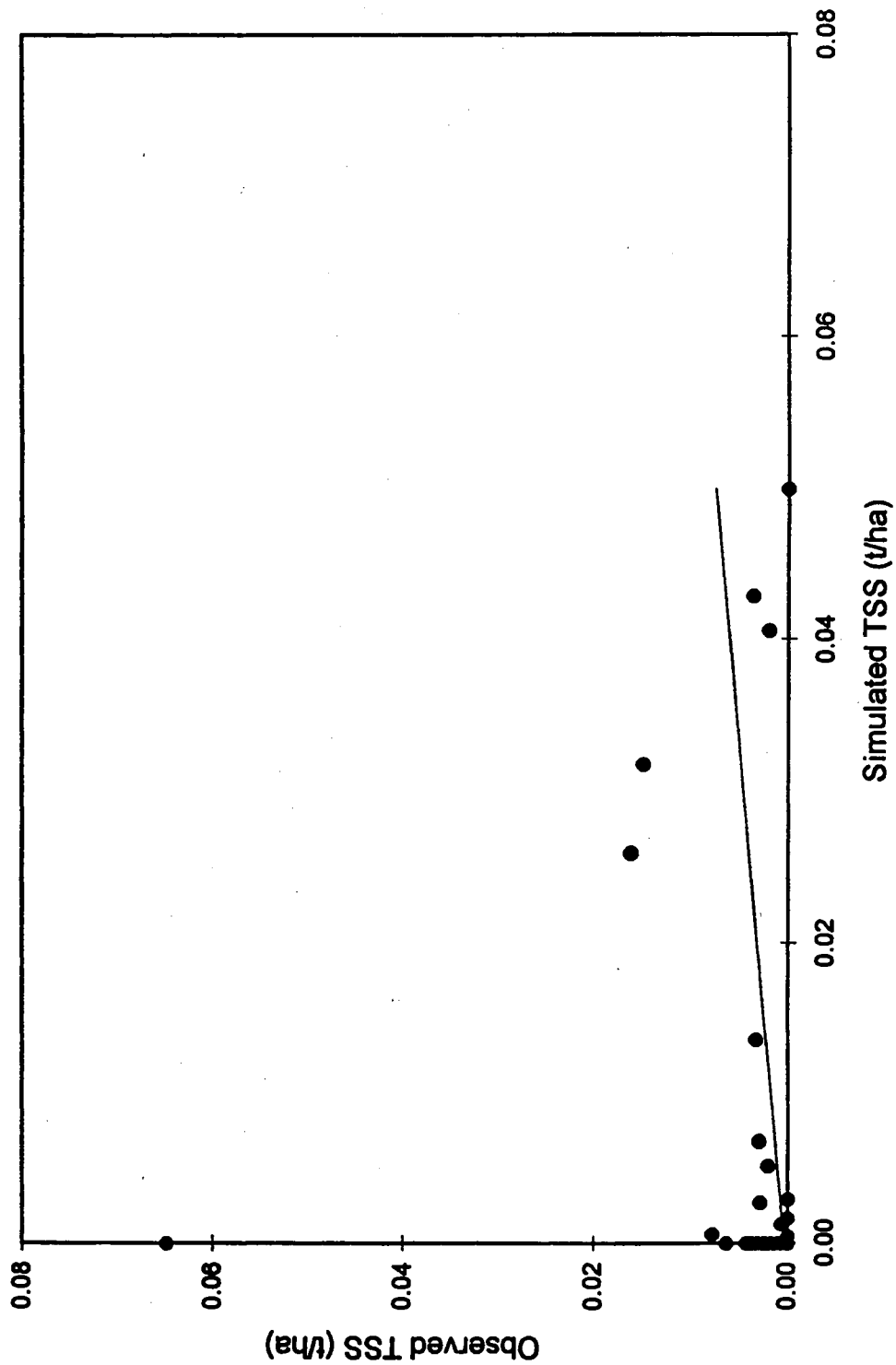
$t = (0.141485 - 1) / 0.040666 = -21.11$

reject Ho: b equal to 1

Daily TSS; Year R3; WS-I



Daily TSS; Year R3; WS-I



Results of Model Performance Evaluation
 Daily Model Output
 Calibration for Total Suspended Solids (TSS)
 Recovery Year 4
 WS-I

Statistics for Linear Regression Analysis

Statistic	Value
Multiple R	0.716
R Square	0.513
Adj. R Square	0.512
Standard Error	0.001
Observations	365

ANOVA for Linear Regression Analysis

	df	SS	MS	F	Significance of F
Regression	1	0.0004189	0.000419	382.2312	1.16891E-58
Residual	364	0.0003978	1.1E-06		
Total	365	0.0008166			

Coefficients

	Intercept	TSS^
Coefficient	0.00020227	0.4917033
Standard Error	5.5388E-05	0.0251501
Lower 95% CI	9.3349E-05	0.4422451
Upper 95% CI	0.00031119	0.5411615

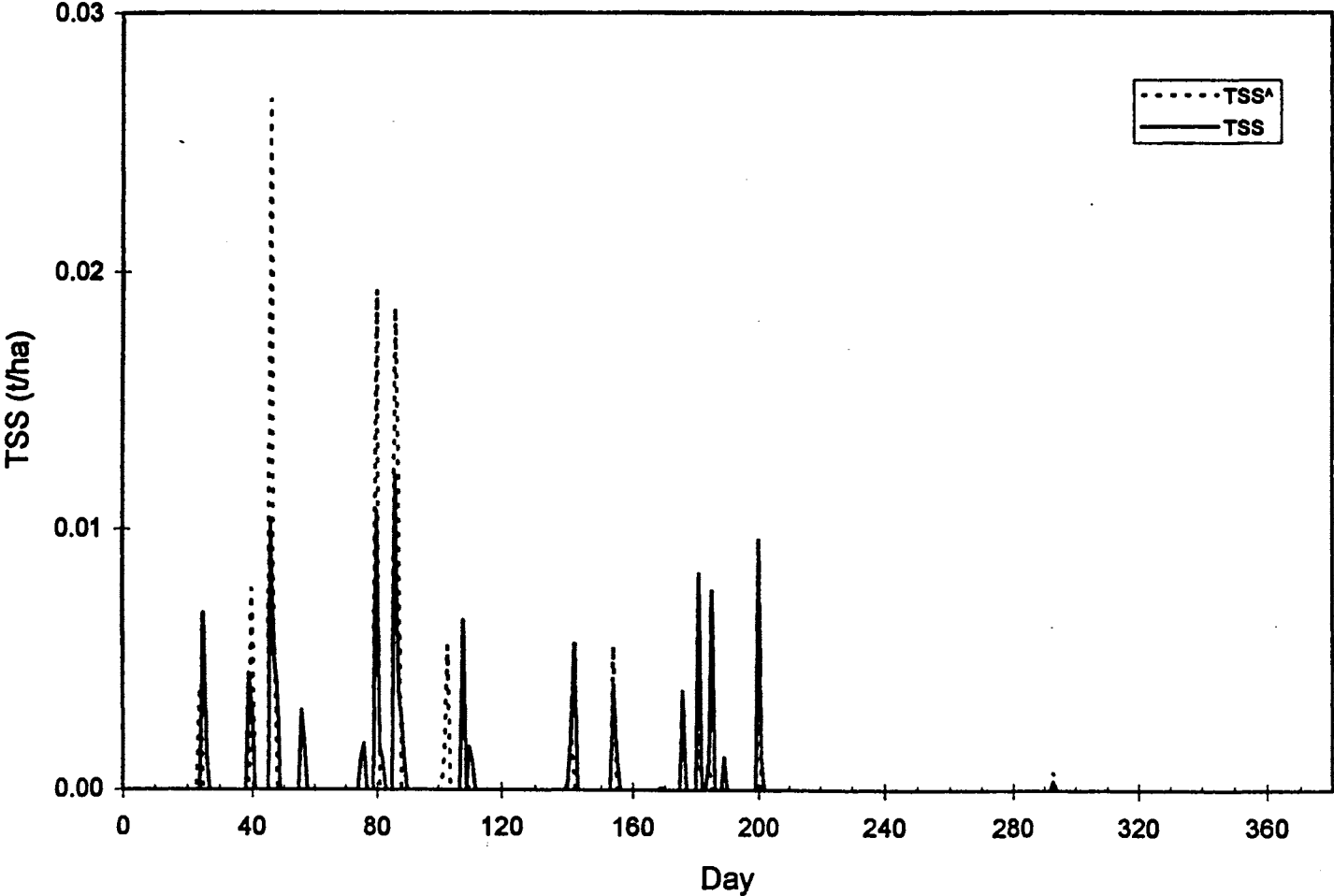
Let alpha = 0.05

Test statistic = 1.96

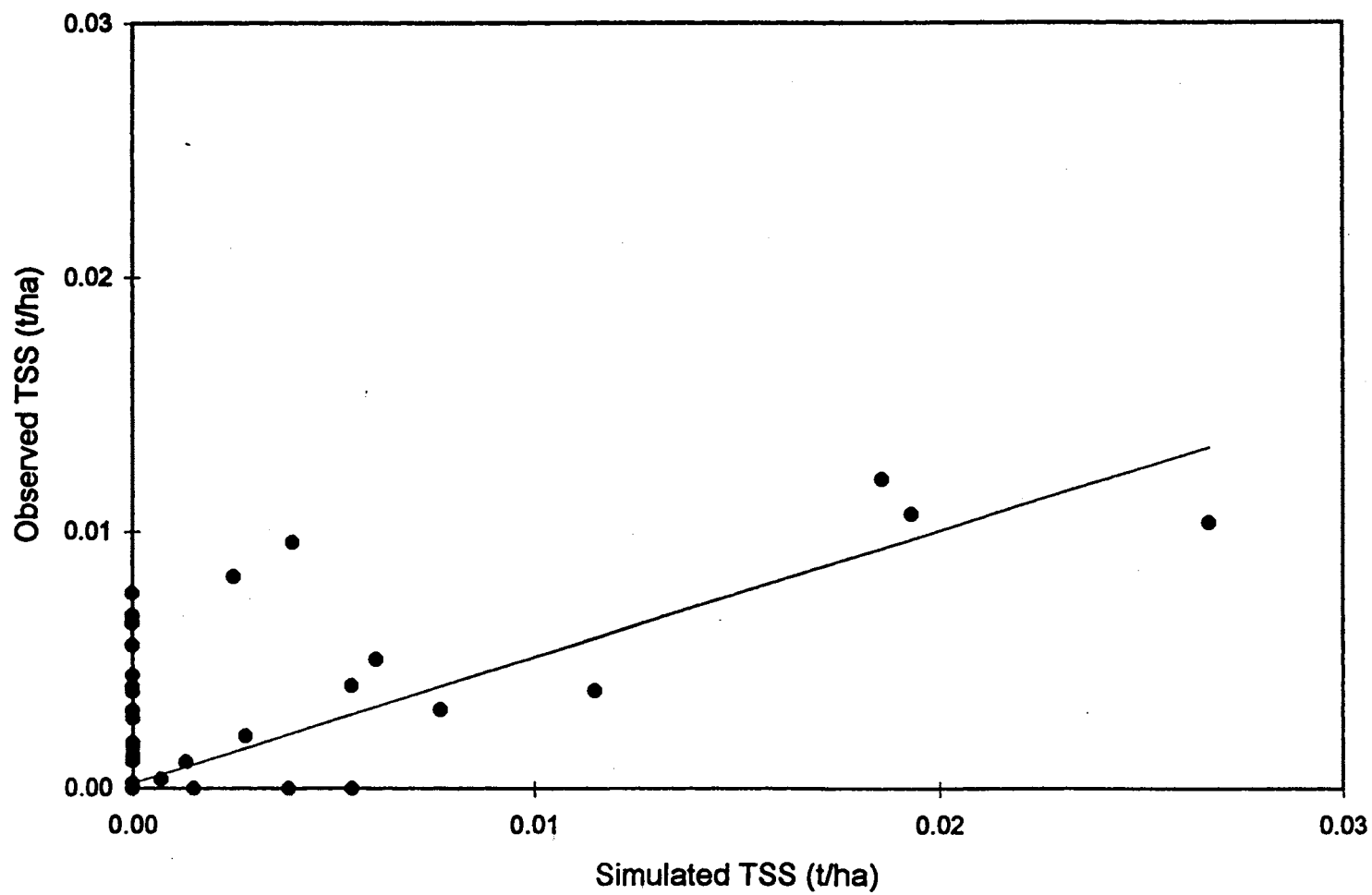
Ho: a equal to 0 ; Ha: a not equal to 0
 $t = (0.0002023 - 0) / 0.00005539 = 3.65$.
 reject Ho: a equal to 0

Ho: b equal to 1 ; Ha: b not equal to 1
 $t = (0.491703 - 1) / 0.02515 = -20.21$
 reject Ho: b equal to 1

Daily TSS; Year R4; WS-I



Daily TSS; Year R4; WS-I



Results of Model Performance Evaluation
 Daily Model Output
 Calibration for Total Phosphorus (PHOS)
 Recovery Year 1
 WS-I

Statistics for Linear Regression Analysis

Statistic	Value
Multiple R	0.698
R Square	0.487
Adj. R Square	0.486
Standard Error	0.014
Observations	365

ANOVA for Linear Regression Analysis

	df	SS	MS	F	Significance of F
Regression	1	0.0720496	0.07205	345.2081	1.24547E-54
Residual	363	0.075763	0.000209		
Total	364	0.1478126			

Coefficients

	Intercept	PHOS ^a
Coefficient	0.00169844	0.8458748
Standard Error	0.00076314	0.0455266
Lower 95% CI	0.0001977	0.7563459
Upper 95% CI	0.00319918	0.9354038

Let alpha = 0.05

Test statistic = 1.96

Ho: a equal to 0 ; Ha: a not equal to 0

$t = (0.0016984 - 0) / 0.0007631 = 2.23$

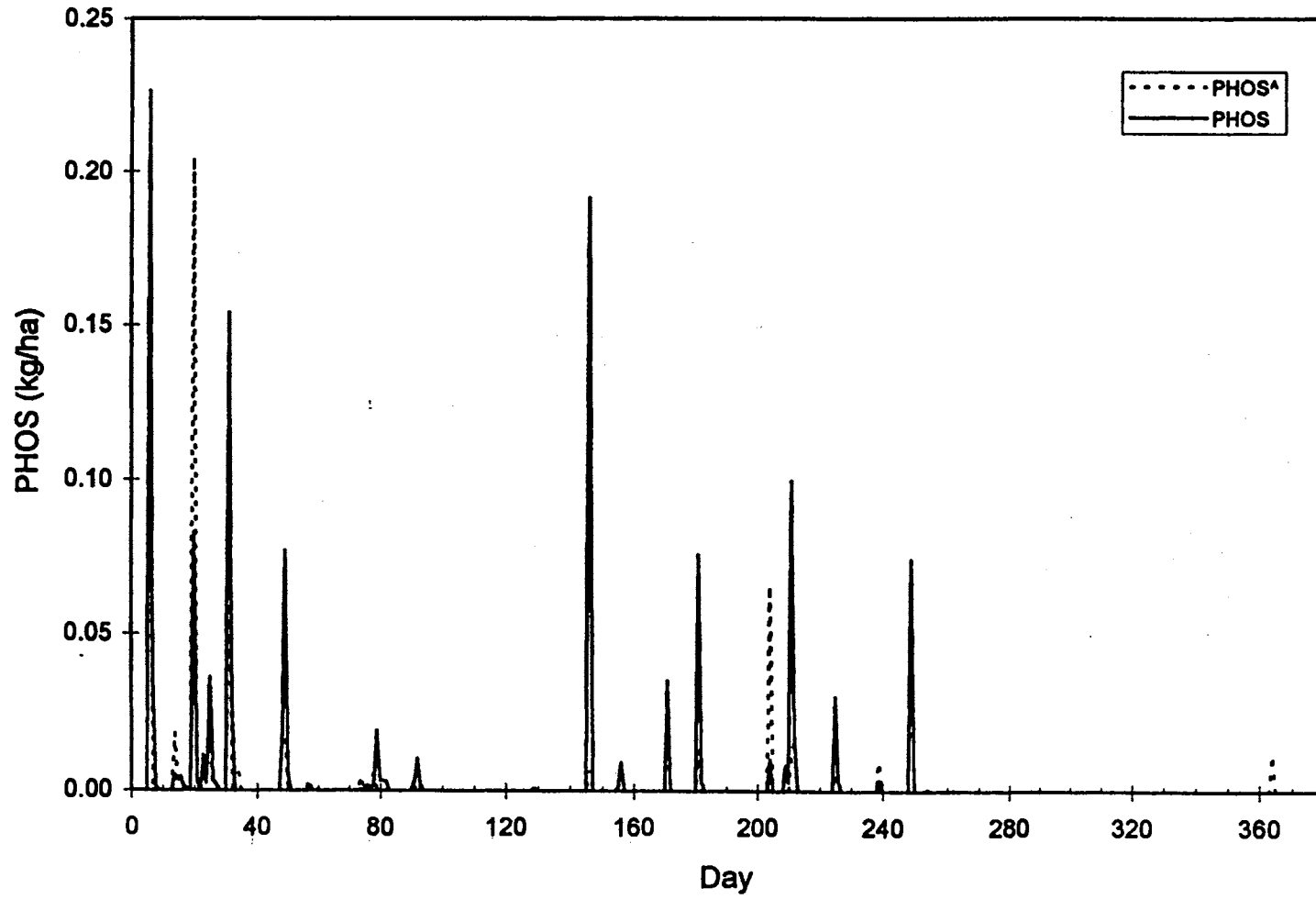
reject Ho: a equal to 0

Ho: b equal to 1 ; Ha: b not equal to 1

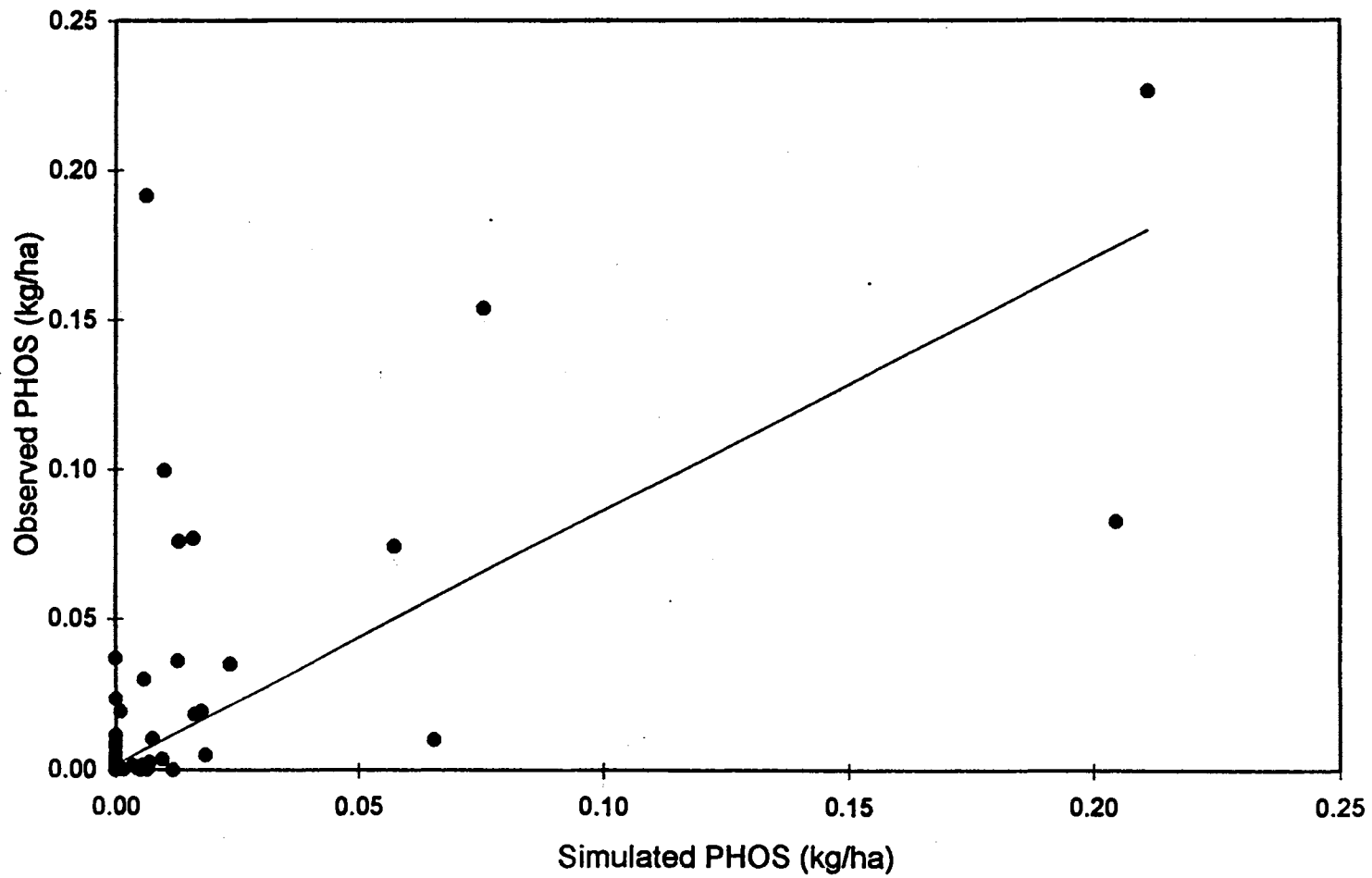
$t = (0.845875 - 1) / 0.045527 = -3.39$

reject Ho: b equal to 1

Daily PHOS; Year R1; WS-I



Daily PHOS; Year R1; WS-I



Results of Model Performance Evaluation
 Daily Model Output
 Calibration for Total Phosphorus (PHOS)
 Recovery Year 2
 WS-I

Statistics for Linear Regression Analysis

Statistic	Value
Multiple R	0.640
R Square	0.410
Adj. R Square	0.408
Standard Error	0.005
Observations	365

ANOVA for Linear Regression Analysis

	df	SS	MS	F	Significance of F
Regression	1	0.0061375	0.006138	251.909	1.85207E-43
Residual	363	0.0088441	2.44E-05		
Total	364	0.0149816			

Coefficients

	Intercept	PHOS ^A
Coefficient	0.00017444	0.6247284
Standard Error	0.00026277	0.0393613
Lower 95% CI	-0.0003423	0.5473237
Upper 95% CI	0.00069118	0.7021332

Let alpha = 0.05

Test statistic = 1.96

Ho: a equal to 0 ; Ha: a not equal to 0

$t = (0.0001744 - 0) / 0.0002628 = 0.67$

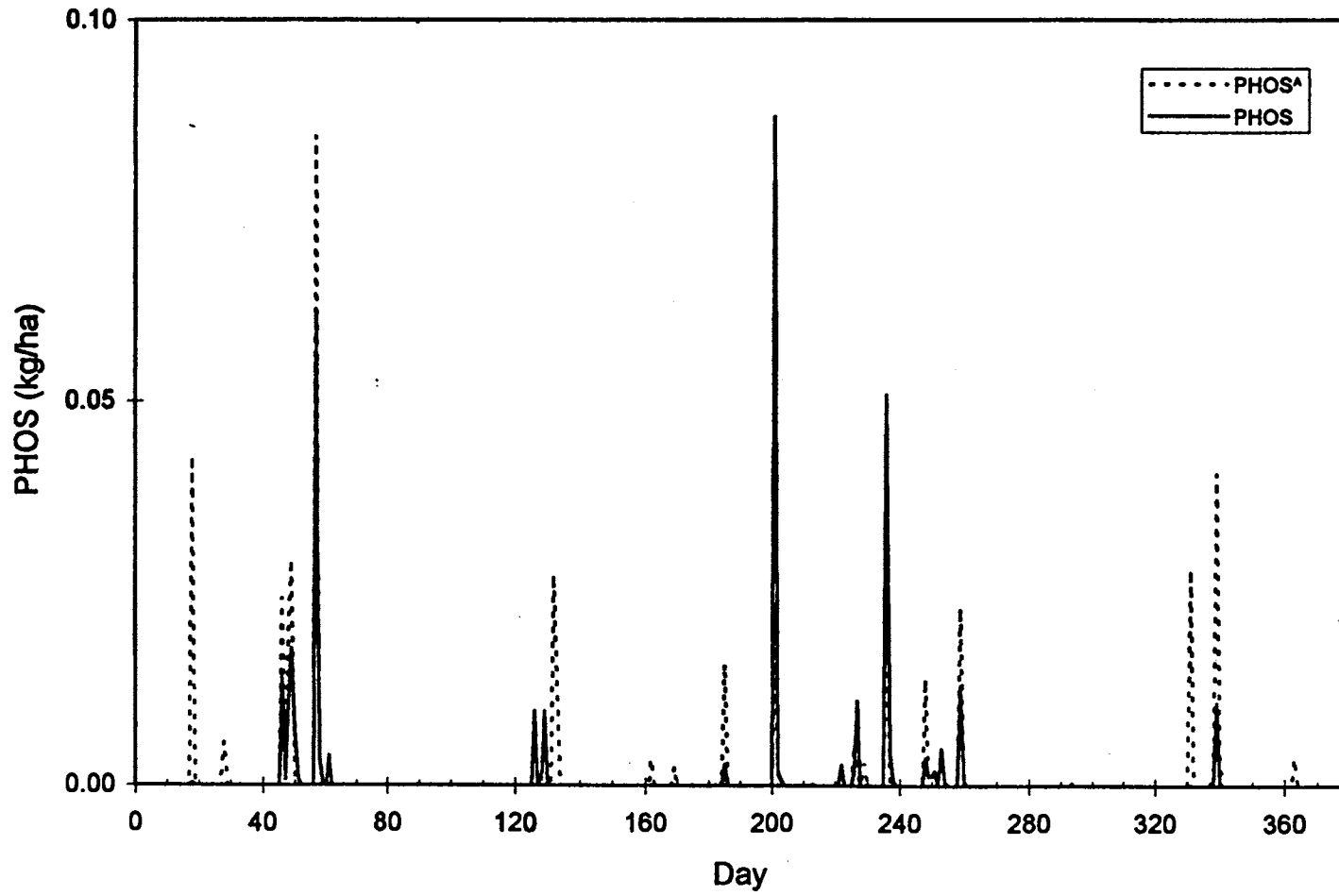
fail to reject Ho: a equal to 0

Ho: b equal to 1 ; Ha: b not equal to 1

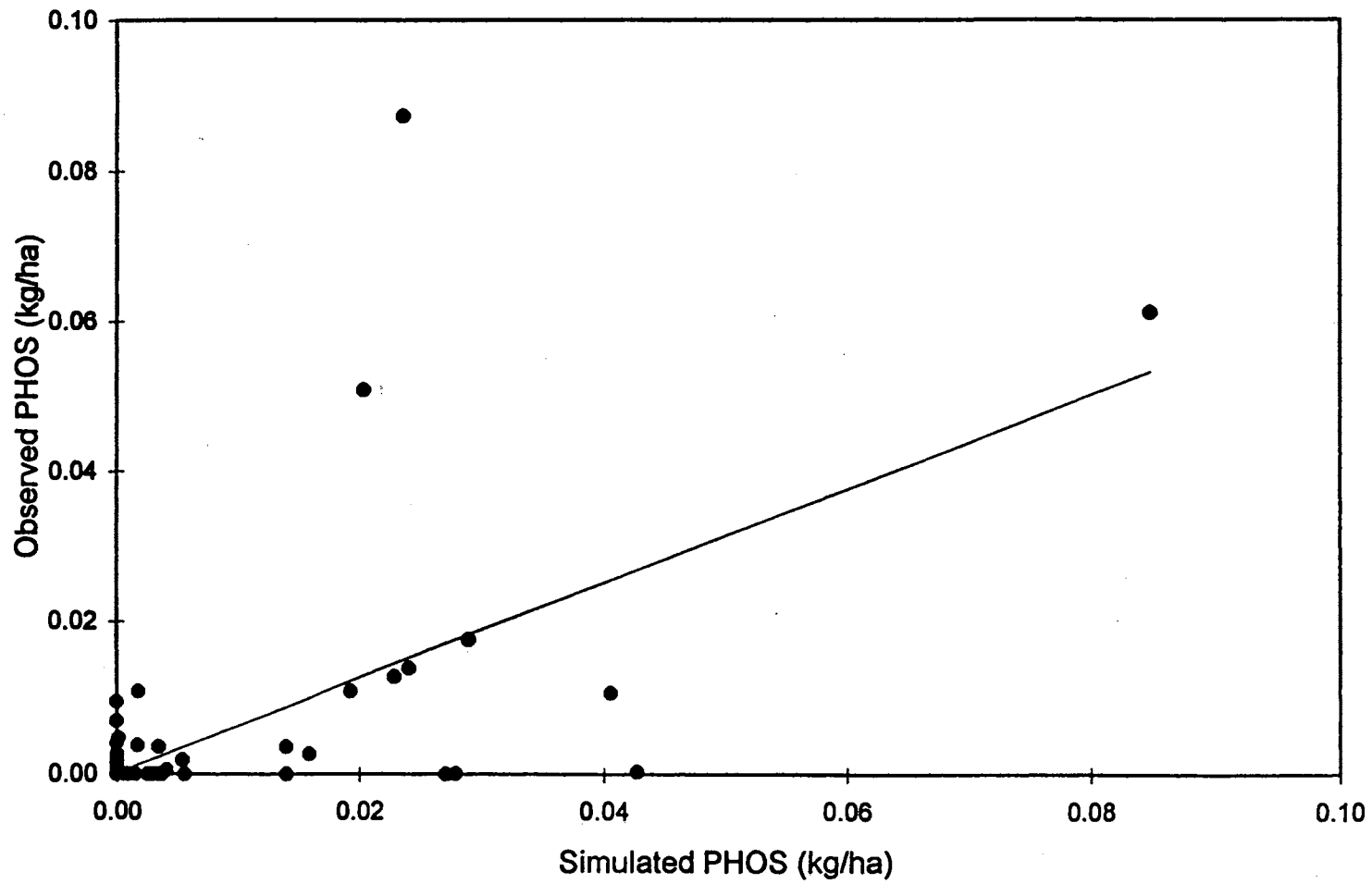
$t = (0.624728 - 1) / 0.039361 = -9.53$

reject Ho: b equal to 1

Daily PHOS; Year R2; WS-I.



Daily PHOS; Year R2; WS-I



Results of Model Performance Evaluation
 Daily Model Output
 Calibration for Total Phosphorus (PHOS)
 Recovery Year 3
 WS-I

Statistics for Linear Regression Analysis

Statistic	Value
Multiple R	0.393
R Square	0.155
Adj. R Square	0.152
Standard Error	0.001
Observations	365

ANOVA for Linear Regression Analysis

	df	SS	MS	F	Significance of F
Regression	1	9.503E-05	9.5E-05	66.42179	5.9606E-15
Residual	363	0.0005193	1.43E-06		
Total	364	0.0006143			

Coefficients

	Intercept	PHOS ^A
Coefficient	0.00018296	0.0915805
Standard Error	6.3331E-05	0.0112345
Lower 95% CI	5.8416E-05	0.0694677
Upper 95% CI	0.0003075	0.1136534

Let alpha = 0.05

Test statistic = 1.96

Ho: a equal to 0 ; Ha: a not equal to 0

$t = (0.000183 - 0) / 0.00006333 = 2.89$

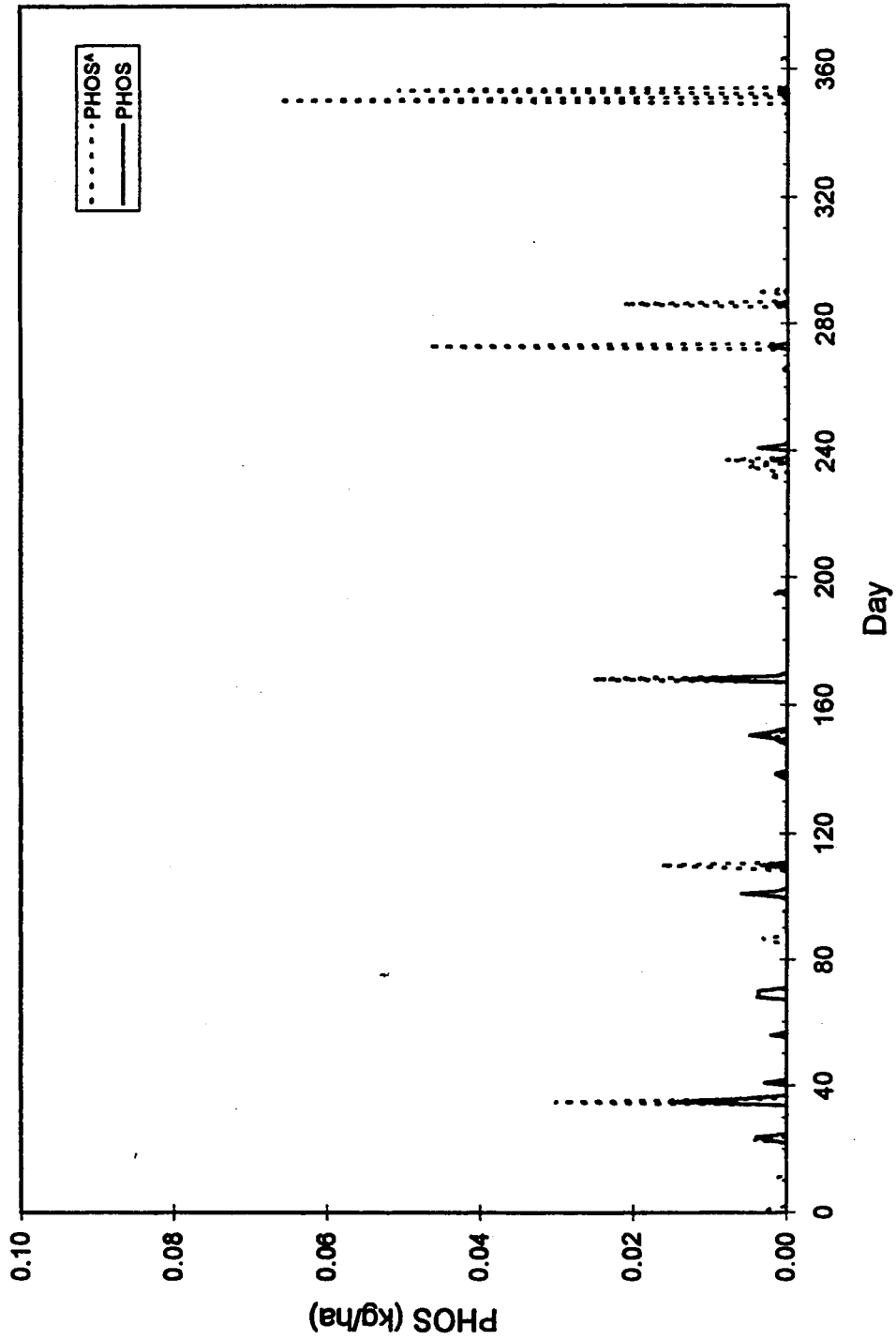
reject Ho: a equal to 0

Ho: b equal to 1 ; Ha: b not equal to 1

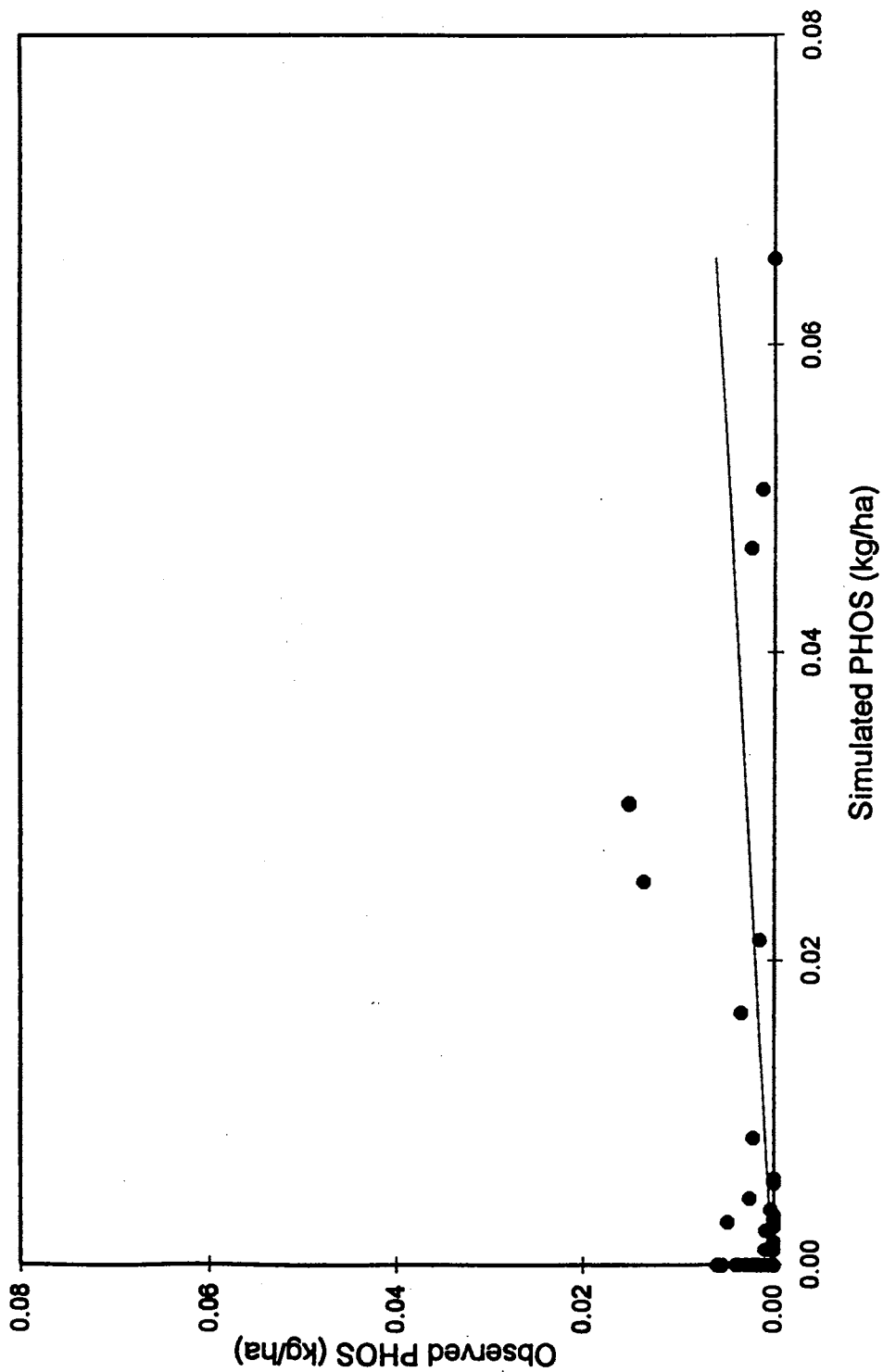
$t = (0.091581 - 1) / 0.011234 = -80.87$

reject Ho: b equal to 1

Daily PHOS; Year R3; WS-I



Daily PHOS; Year R3; WS-I



Results of Model Performance Evaluation
 Daily Model Output
 Calibration for Total Phosphorus (PHOS)
 Recovery Year 4
 WS-I

Statistics for Linear Regression Analysis

Statistic	Value
Multiple R	0.81791268
R Square	0.66898116
Adj. R Square	0.66806926
Standard Error	0.00059447
Observations	365

ANOVA for Linear Regression Analysis

	df	SS	MS	F	Significance of F
Regression	1	0.0002593	0.000259	733.6143	3.6447E-89
Residual	363	0.0001283	3.53E-07		
Total	364	0.0003875			

Coefficients

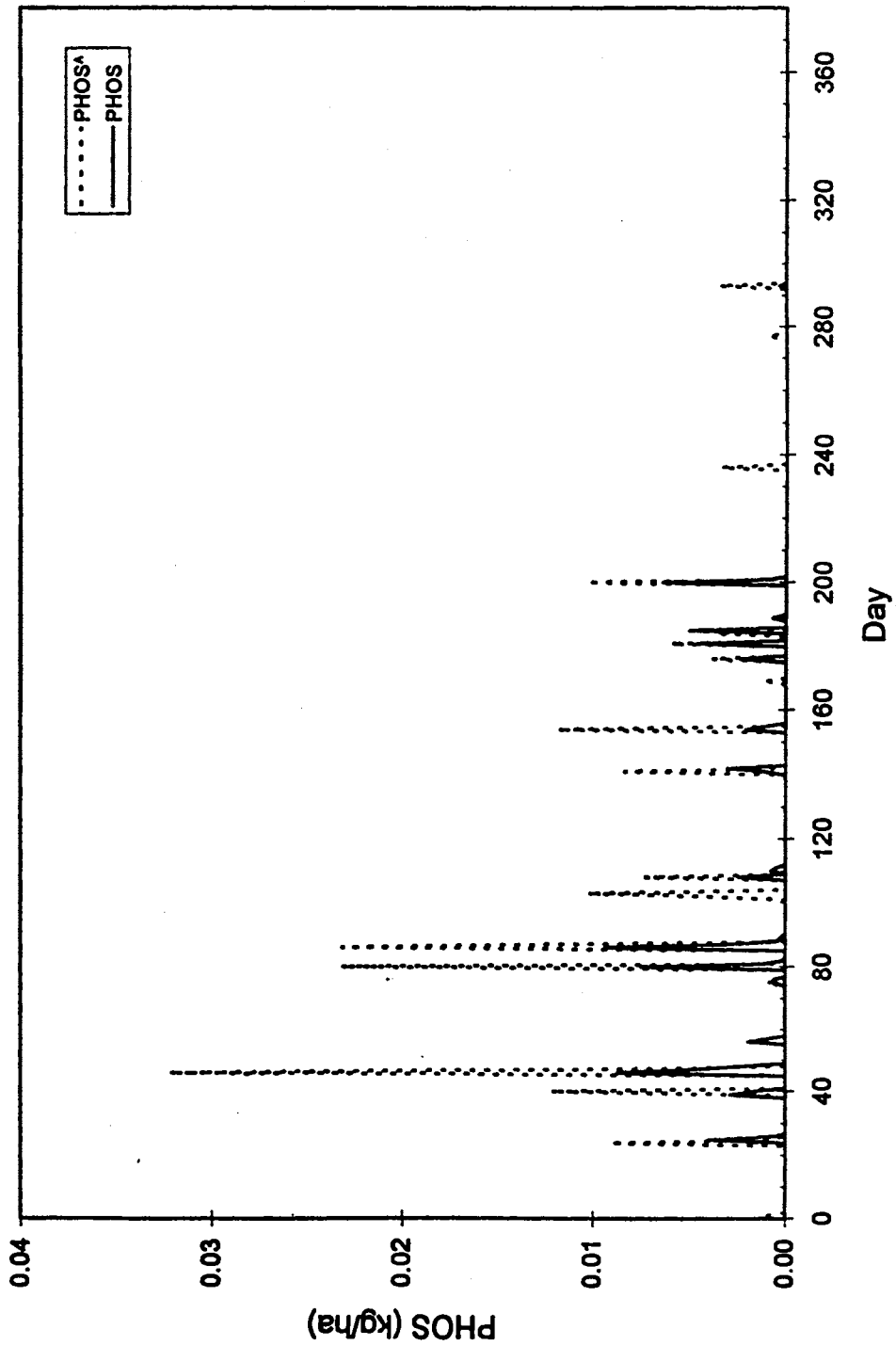
	Intercept	PHOS ^A
Coefficient	6.6961E-05	0.2922583
Standard Error	3.1666E-05	0.0107903
Lower 95% CI	4.6889E-06	0.271039
Upper 95% CI	0.00012923	0.3134776

Let alpha = 0.05
 Test statistic = 1.96

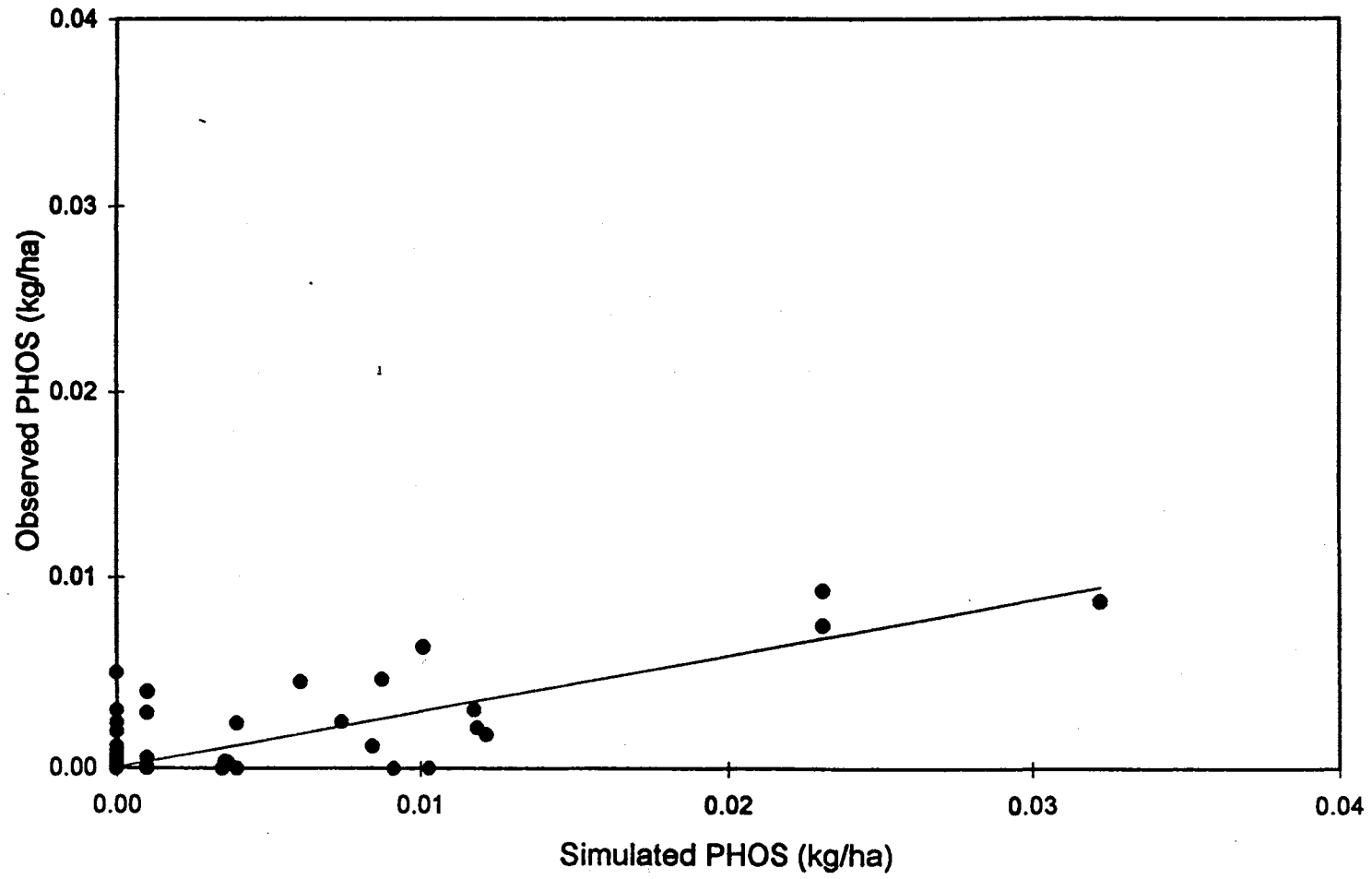
Ho: a equal to 0 ; Ha: a not equal to 0
 $t = (0.00006696 - 0) / 0.00003167 = 2.11$
 reject Ho: a equal to 0

Ho: b equal to 1 ; Ha: b not equal to 1
 $t = (0.292258 - 1) / 0.01079 = -65.59$
 reject Ho: b equal to 1

Year R4; WS-I



Daily PHOS; Year R4; WS-I



Results of Model Performance Evaluation
 Daily Model Output
 Calibration for Nitrate-Nitrogen (NO₃N)
 Recovery Year 1
 WS-I

Statistics for Linear Regression Analysis

Statistic	Value
Multiple R	0.649
R Square	0.421
Adj. R Square	0.419
Standard Error	0.047
Observations	365

ANOVA for Linear Regression Analysis

	df	SS	MS	F	Significance of F
Regression	1	0.5874524	0.587452	263.7654	5.70826E-45
Residual	363	0.8084655	0.002227		
Total	364	1.3959179			

Coefficients

	Intercept	NO ₃ N ^a
Coefficient	0.00254804	0.8199974
Standard Error	0.0026222	0.0504898
Lower 95% CI	-0.0026086	0.7207083
Upper 95% CI	0.00770464	0.9192865

Let alpha = 0.05

Test statistic = 1.96

Ho: a equal to 0 ; Ha: a not equal to 0

$t = (0.002548 - 0) / 0.0026222 = 0.97$

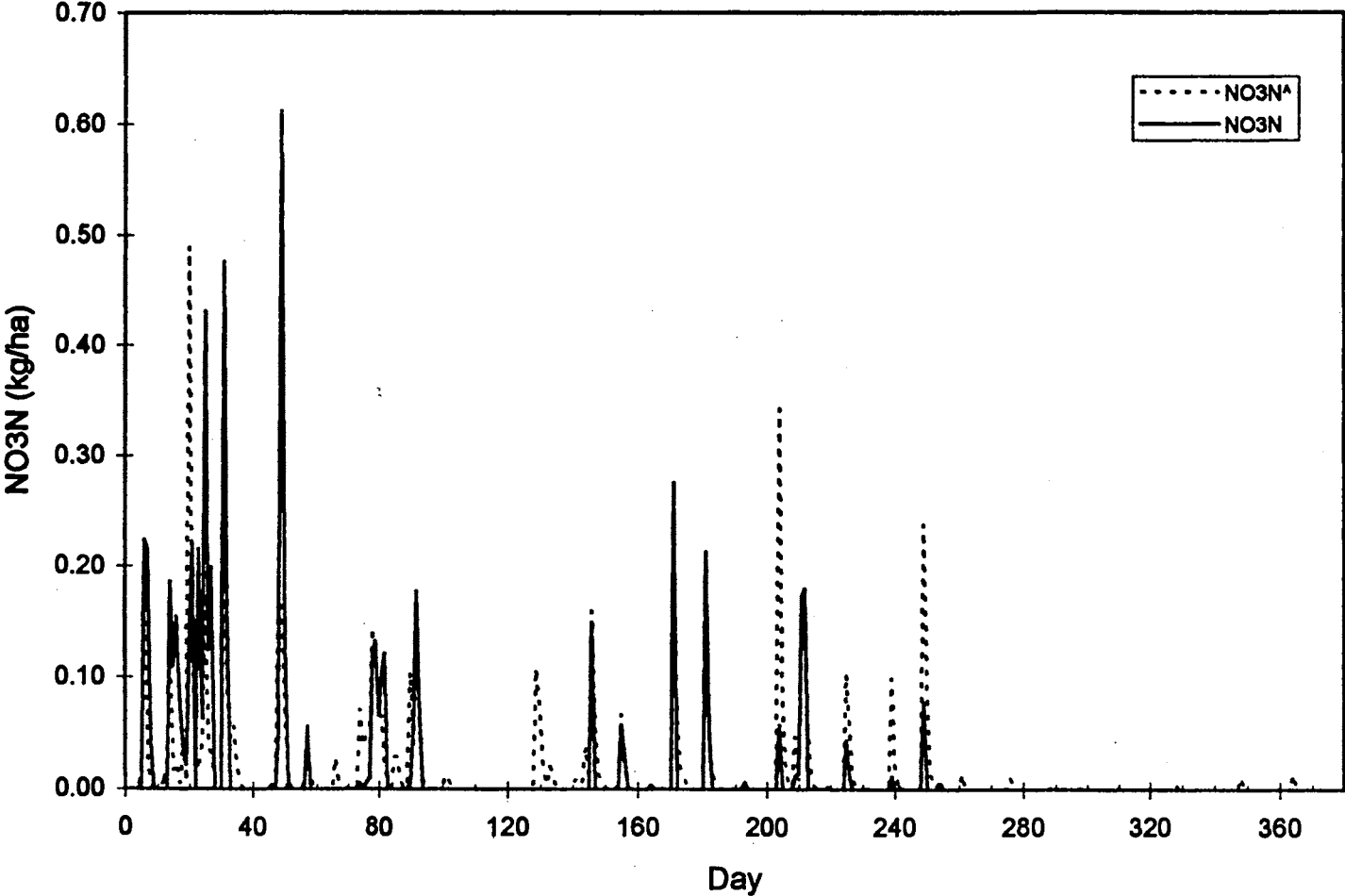
fail to reject Ho: a equal to 0

Ho: b equal to 1 ; Ha: b not equal to 1

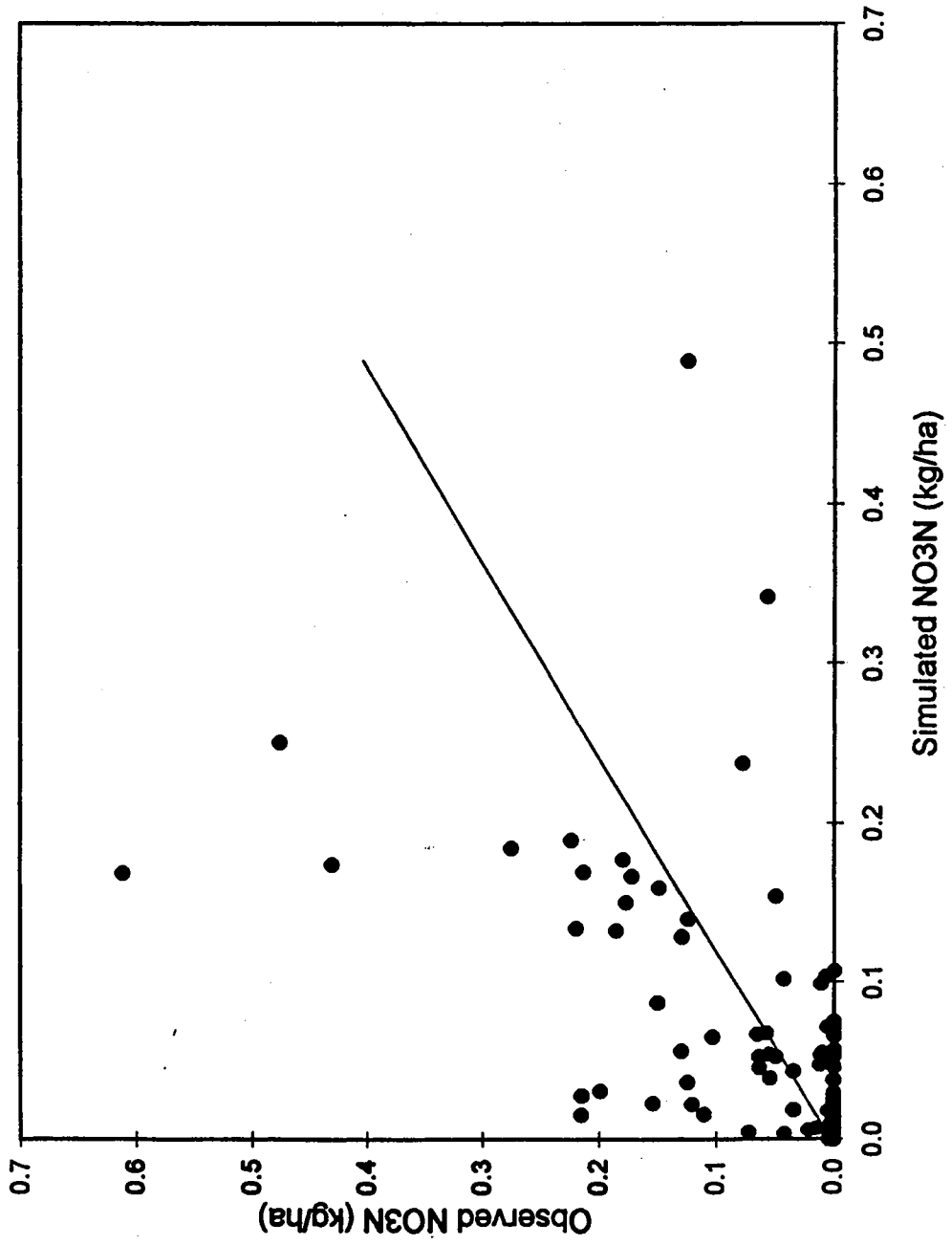
$t = (0.819997 - 1) / 0.05049 = -3.57$

reject Ho: b equal to 1

Daily NO3N; Year R1; WS-I



Daily NO3N; Year R1; WS-I



Results of Model Performance Evaluation
 Daily Model Output
 Calibration for Nitrate-Nitrogen (NO3N)
 Recovery Year 2
 WS-I

Statistics for Linear Regression Analysis

Statistic	Value
Multiple R	0.435
R Square	0.189
Adj. R Square	0.187
Standard Error	0.015
Observations	365

ANOVA for Linear Regression Analysis

	df	SS	MS	F	Significance of F
Regression	1	0.0179832	0.017983	84.67175	2.83275E-18
Residual	363	0.077011	0.000212		
Total	364	0.0949743			

Coefficients

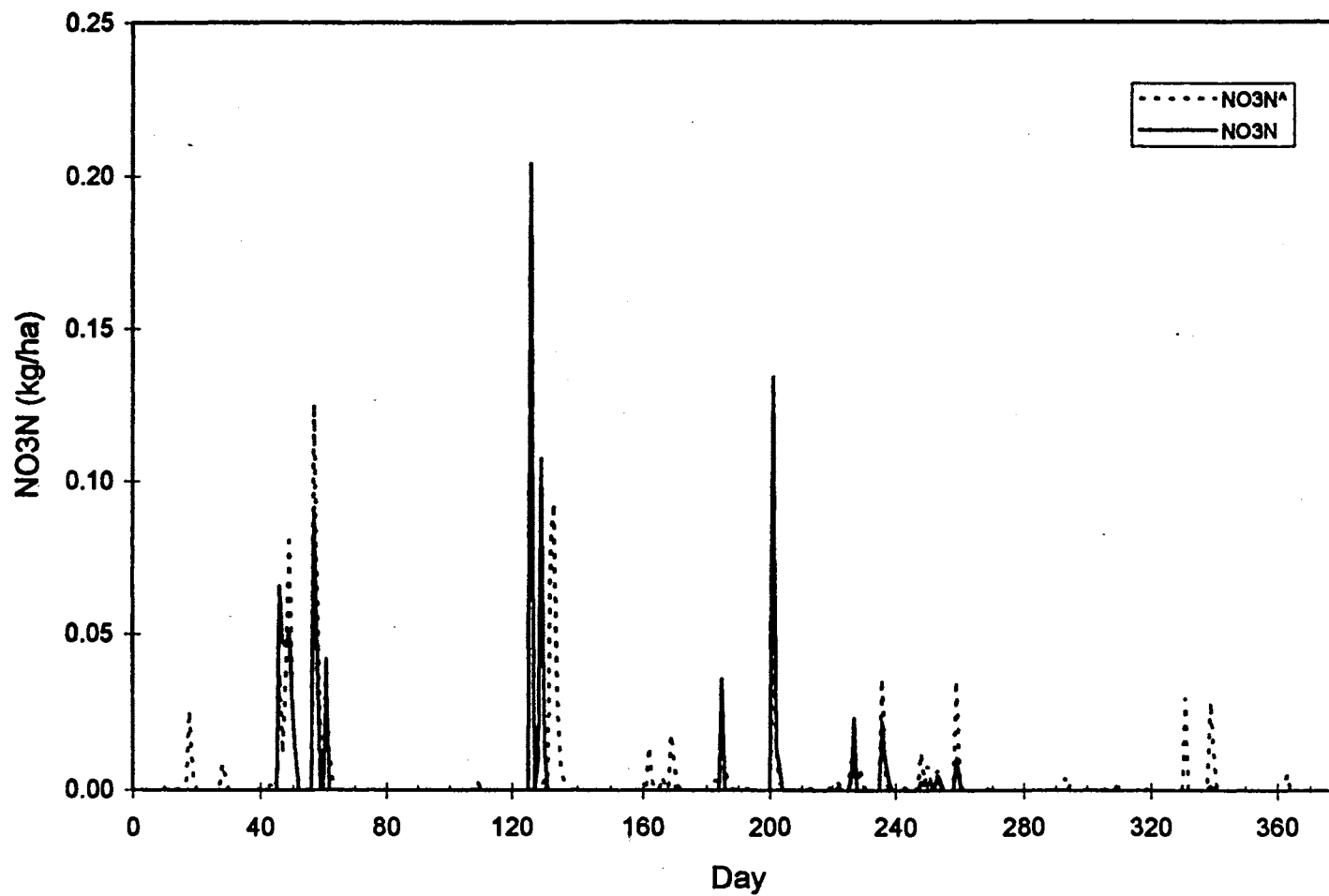
	Intercept	NO3N ^a
Coefficient	0.0010322	0.577353
Standard Error	0.00078736	0.062744
Lower 95% CI	-0.0005162	0.4539658
Upper 95% CI	0.00258056	0.7007403

Let alpha = 0.05
 Test statistic = 1.96

Ho: a equal to 0 ; Ha: a not equal to 0
 $t = (0.0010322 - 0) / 0.0007874 = 1.31$
 fail to reject Ho: a equal to 0

Ho: b equal to 1 ; Ha: b not equal to 1
 $t = (0.577353 - 1) / 0.062744 = -6.74$
 reject Ho: b equal to 1

Daily NO3N; Year R2; WS-I



Results of Model Performance Evaluation
 Daily Model Output
 Calibration for Nitrate-Nitrogen (NO3N)
 Recovery Year 3
 WS-I

Statistics for Linear Regression Analysis

Statistic	Value
Multiple R	0.304
R Square	0.092
Adj. R Square	0.090
Standard Error	0.002
Observations	365

ANOVA for Linear Regression Analysis

	df	SS	MS	F	Significance of F
Regression	1	0.0001291	0.000129	36.91801	3.11438E-09
Residual	363	0.0012696	3.5E-06		
Total	364	0.0013988			

Coefficients

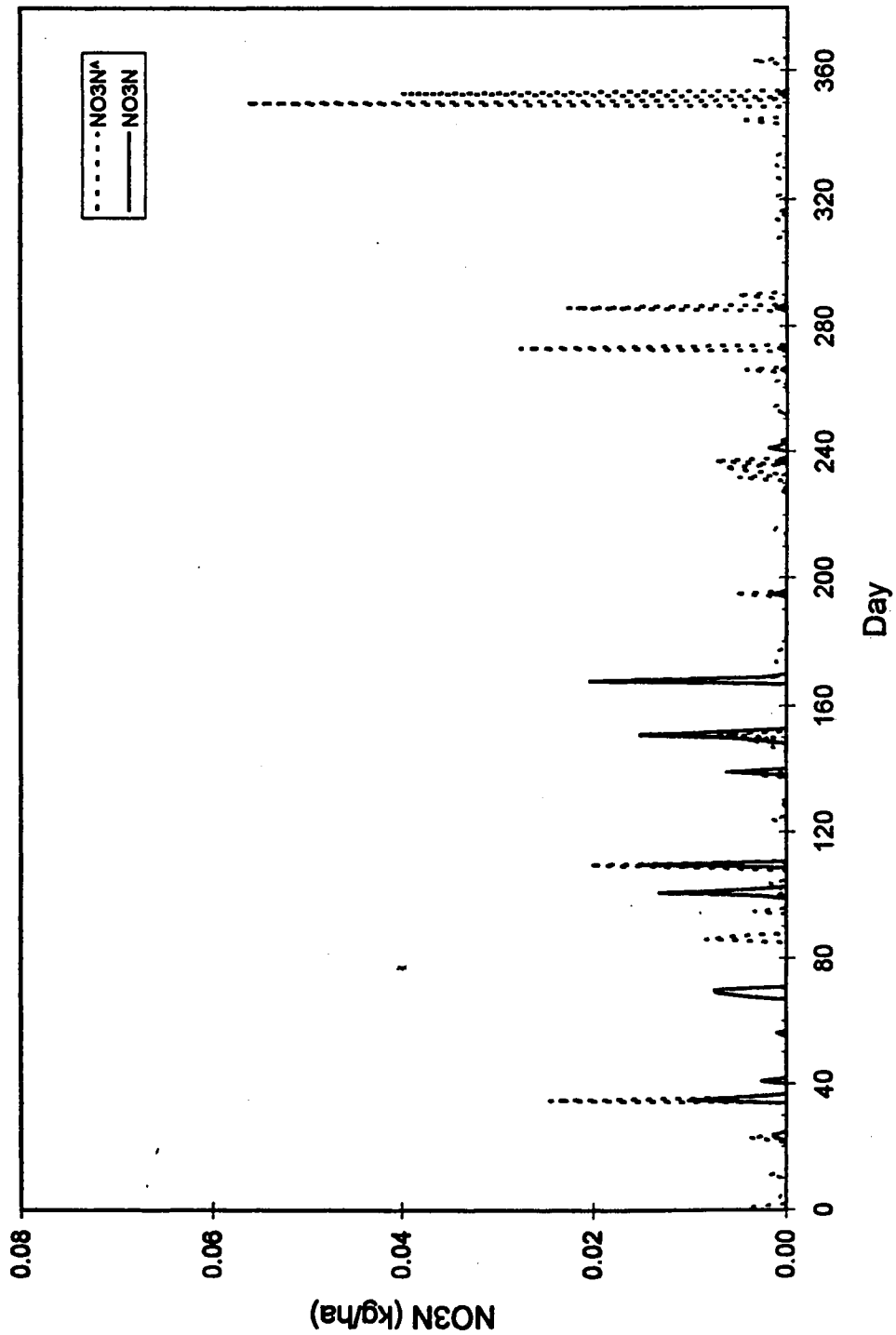
	Intercept	NO3N^
Coefficient	0.00026359	0.1299897
Standard Error	0.00010006	0.0213939
Lower 95% CI	6.6813E-05	0.0879182
Upper 95% CI	0.00046037	0.1720612

Let alpha = 0.05
 Test statistic = 1.96

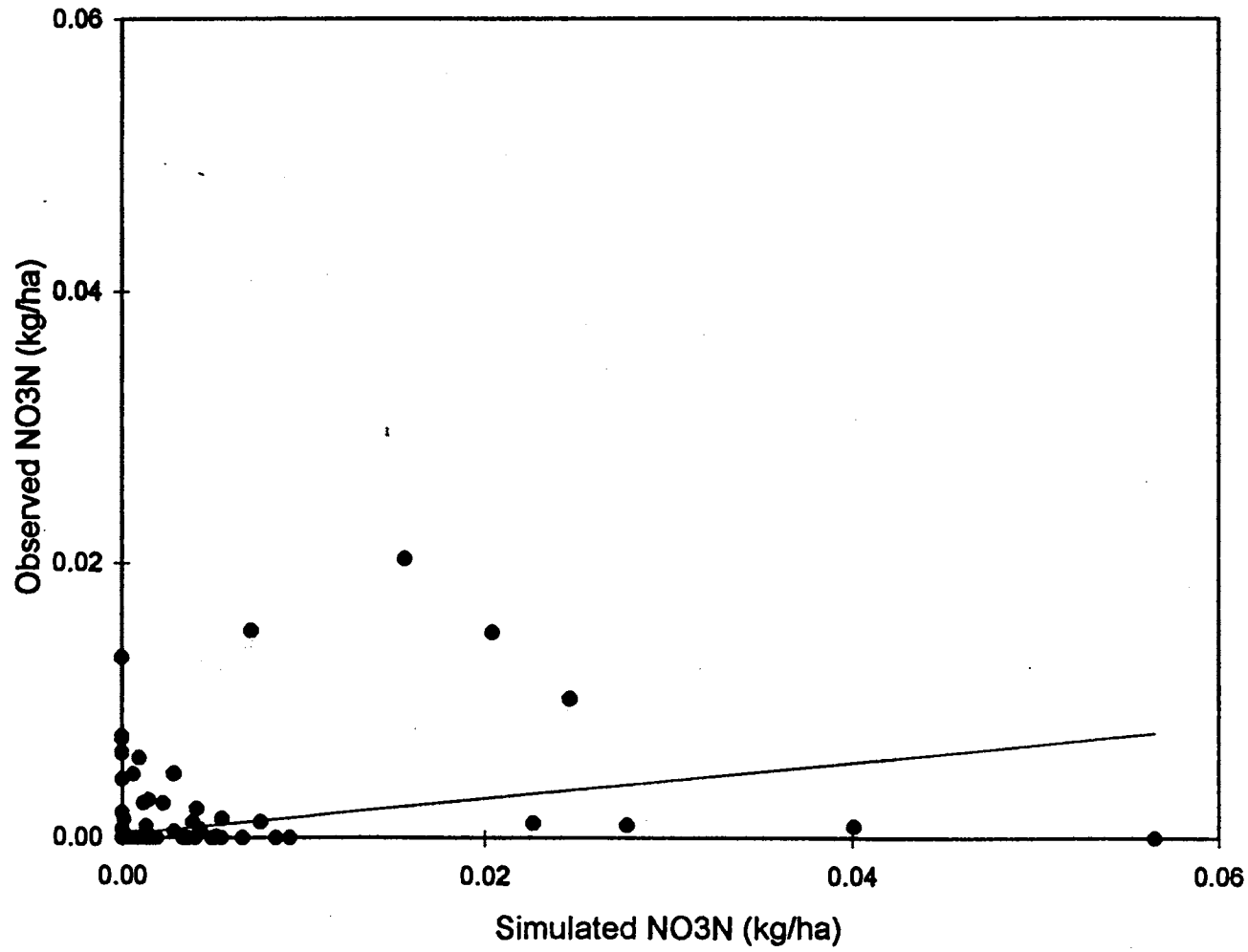
Ho: a equal to 0 ; Ha: a not equal to 0
 $t = (0.0002636 - 0) / 0.0001001 = 2.63$
 reject Ho: a equal to 0

Ho: b equal to 1 ; Ha: b not equal to 1
 $t = (0.12999 - 1) / 0.021394 = -40.67$
 reject Ho: b equal to 1

Daily NO3N; Year R3; WS-I



Daily NO3N; Year R3; WS-I



Results of Model Performance Evaluation
 Daily Model Output
 Calibration for Nitrate-Nitrogen (NO3N)
 Recovery Year 4
 WS-I

Statistics for Linear Regression Analysis

Statistic	Value
Multiple R	0.571
R Square	0.328
Adj. R Square	0.324
Standard Error	0.001
Observations	365

ANOVA for Linear Regression Analysis

	df	SS	MS	F	Significance of F
Regression	1	0.0001071	0.000107	175.1876	6.6307E-33
Residual	363	0.0002219	6.11E-07		
Total	364	0.000329			

Coefficients

	Intercept	NO3N^
Coefficient	9.2217E-05	0.1649934
Standard Error	4.2159E-05	0.0124656
Lower 95% CI	9.3112E-06	0.1404795
Upper 95% CI	0.00017512	0.1895073

Let alpha = 0.05

Test statistic = 1.96

Ho: a equal to 0 ; Ha: a not equal to 0

$t = (0.00009222 - 0) / 0.00004216 = 2.18$

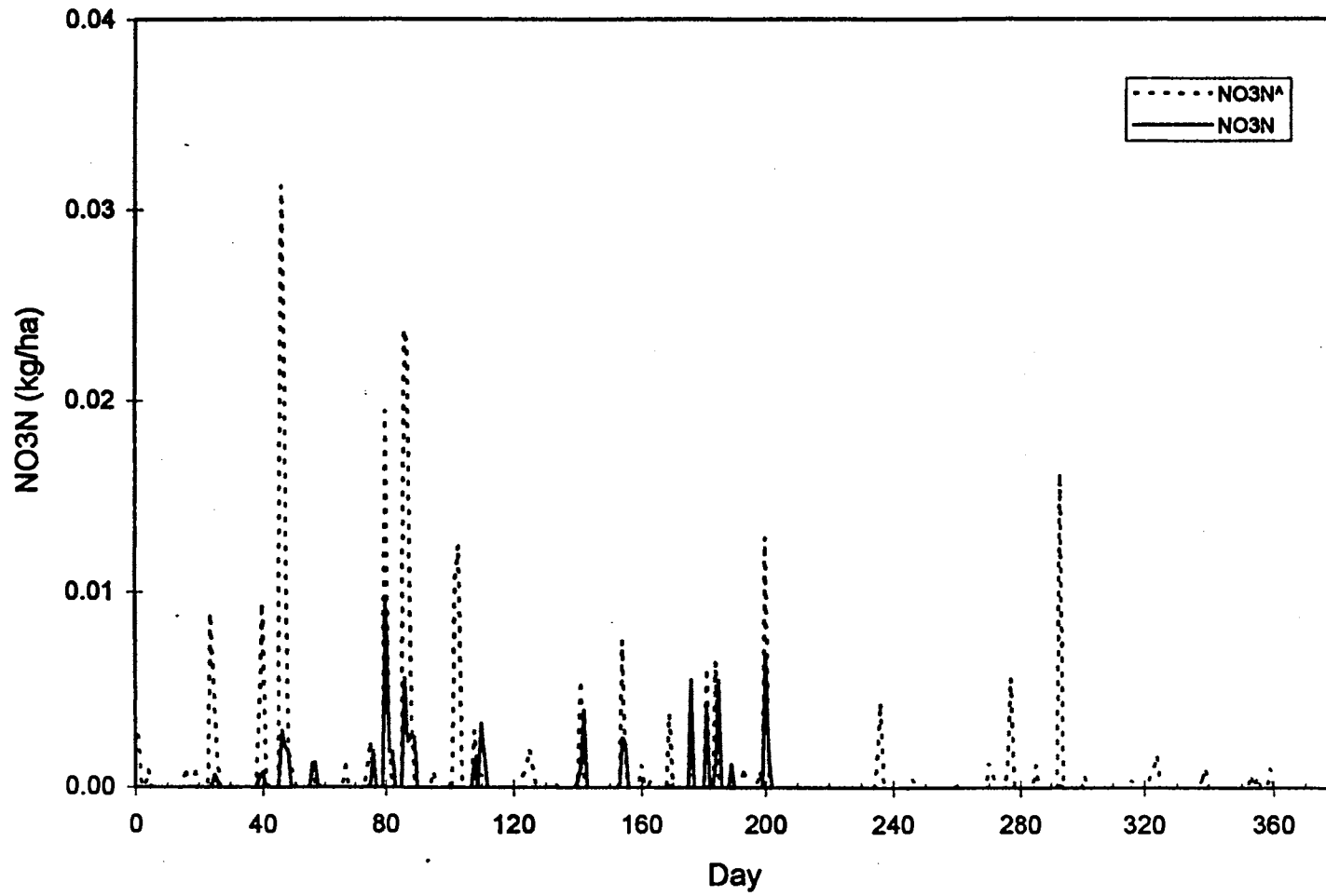
reject Ho: a equal to 0

Ho: b equal to 1 ; Ha: b not equal to 1

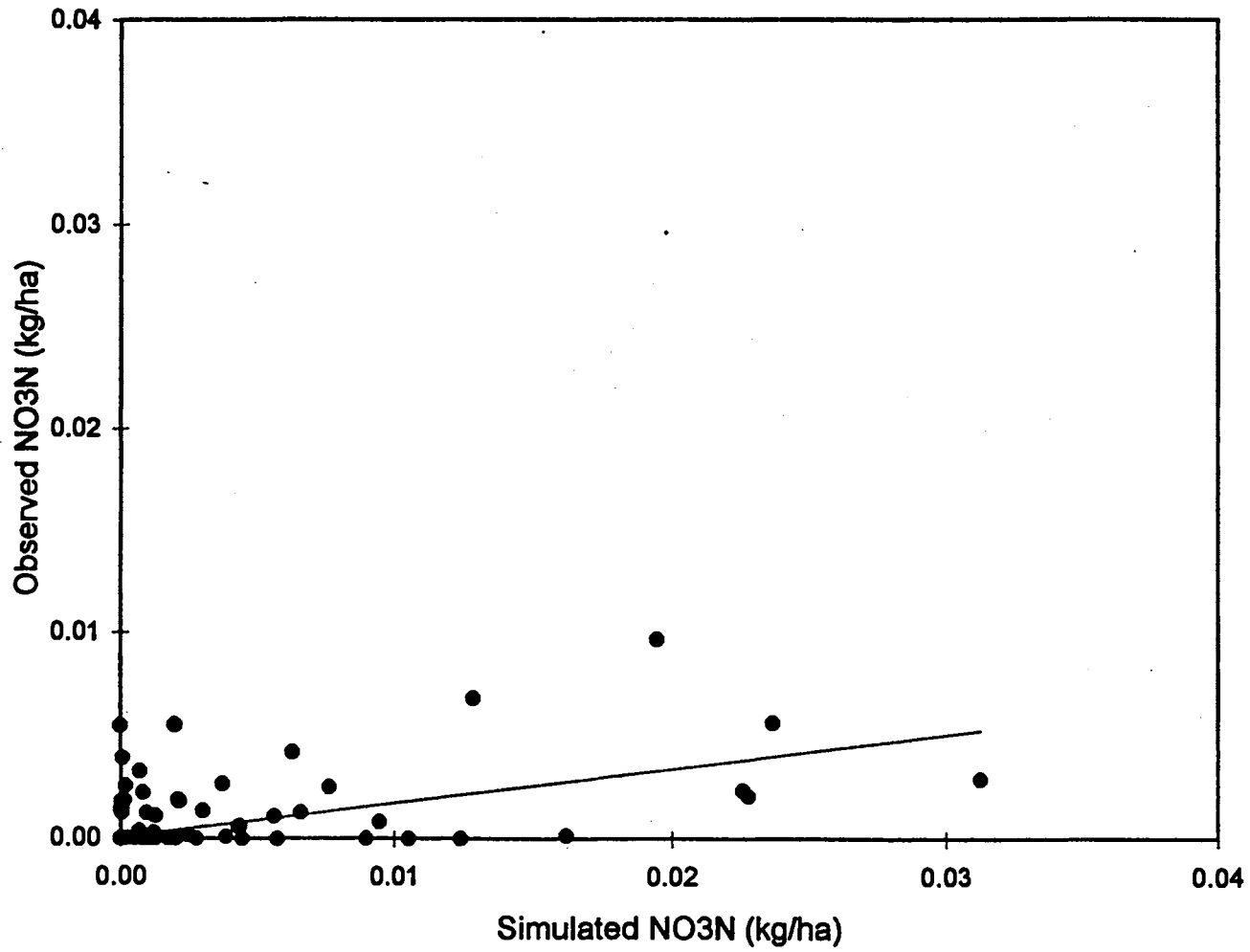
$t = (0.164993 - 1) / 0.012466 = -66.98$

reject Ho: b equal to 1

Daily NO3N; Year R4; WS-I



Daily NO3N; Year R4; WS-I



APPENDIX III
**UNDISTURBED WATERSHED: RESULTS OF MODEL
PERFORMANCE EVALUATIONS**

Results of Model Performance Evaluation
 Calibration for Total Suspended Solids (TSS)
 Daily Model Output
 Entire Data Set
 WS-III

Statistics for Linear Regression Analysis

Statistic	Value
Multiple R	0.52165478
R Square	0.27212371
Adj. R Square	0.27172487
Standard Error	0.0007612
Observations	1827

ANOVA for Linear Regression Analysis

	df	SS	MS	F	Significance of F
Regression	1	0.0003953	0.000395	682.2942	4.7948E-128
Residual	1825	0.0010575	5.79E-07		
Total	1826	0.0014528			

Coefficients

	Intercept	TSS^
Coefficient	0.00012863	0.768035
Standard Error	1.7965E-05	0.0294032
Lower 95% CI	9.3396E-05	0.7103674
Upper 95% CI	0.00016386	0.8257026

Let alpha = 0.05

Test statistic = 1.96

Ho: a equal to 0 ; Ha: a not equal to 0

$t = (0.0001286 - 0) / 0.00001797 = 7.16$

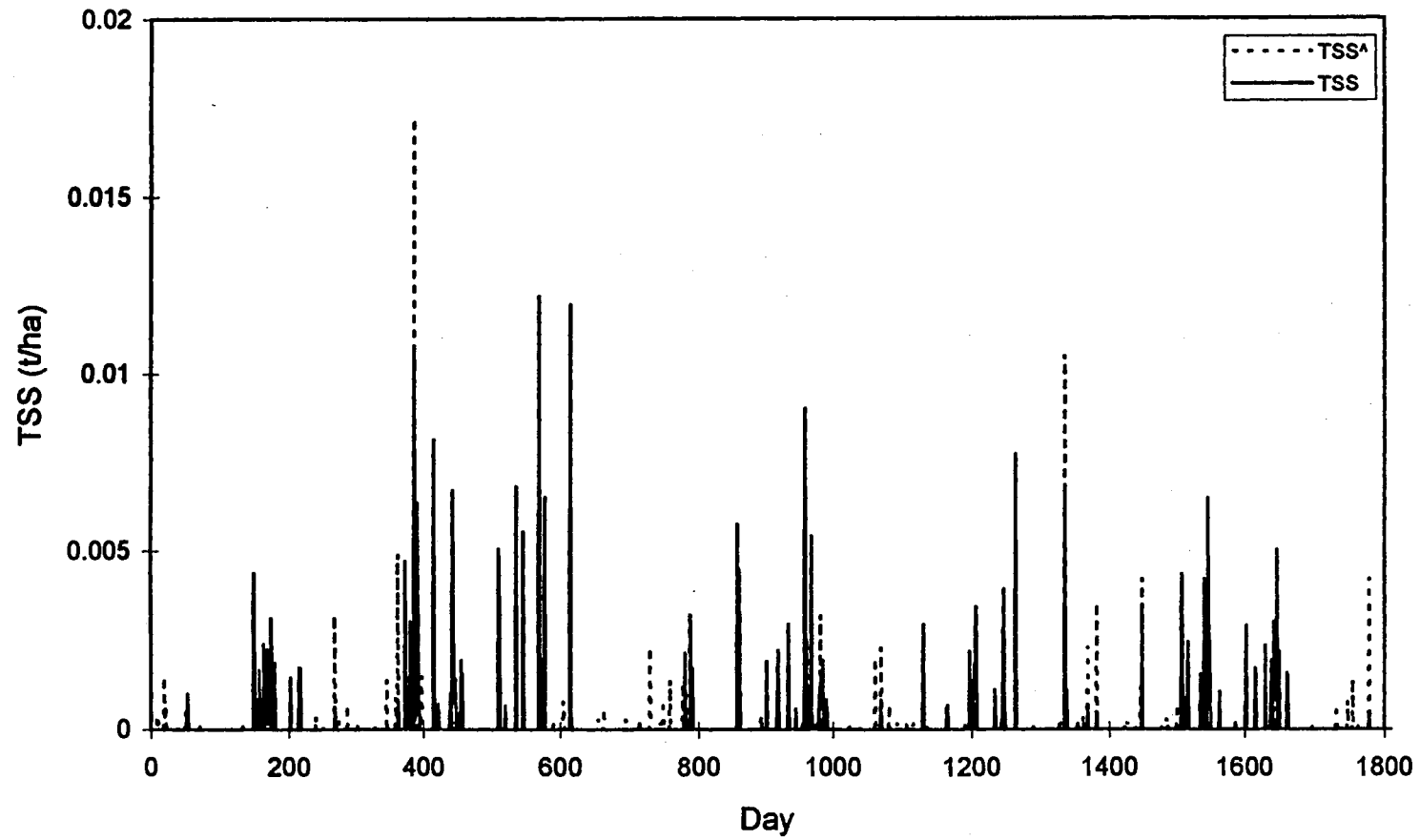
reject Ho: a equal to 0

Ho: b equal to 1 ; Ha: b not equal to 1

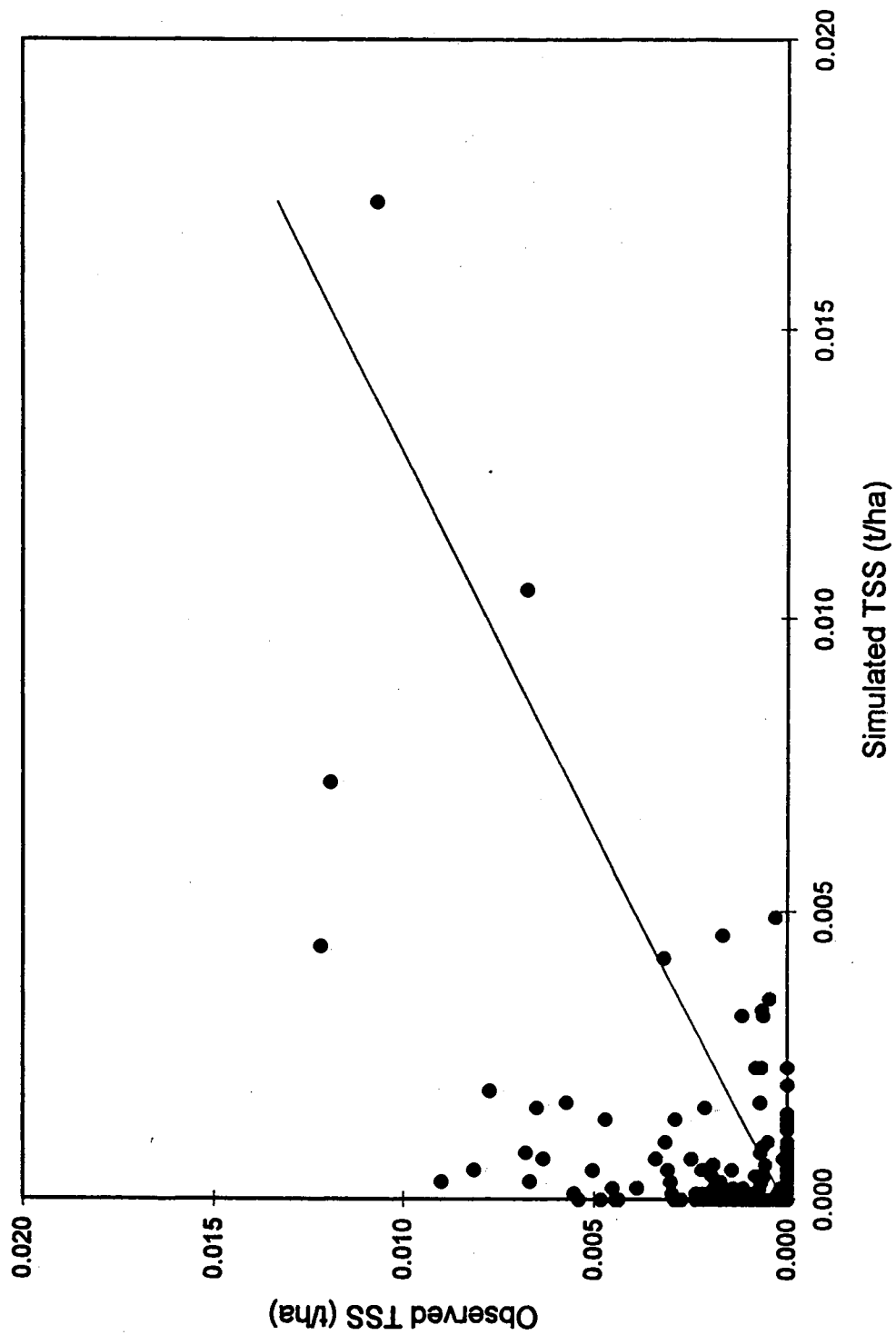
$t = (0.768035 - 1) / 0.029403 = -7.89$

reject Ho: b equal to 1

Daily TSS; 83-88; WS-III



Daily TSS; 83-88; WS-III



Results of Model Performance Evaluation
 Calibration for Total Phosphorus (PHOS)
 Daily Model Output
 Entire Data Set
 WS-III

Statistics for Linear Regression Analysis

Statistic	Value
Multiple R	0.74332477
R Square	0.55253172
Adj. R Square	0.55228653
Standard Error	0.00121186
Observations	1827

ANOVA for Linear Regression Analysis

	df	SS	MS	F	Significance of F
Regression	1	0.0033095	0.00331	2253.501	0
Residual	1825	0.0026802	1.47E-06		
Total	1826	0.0059897			

Coefficients

	Intercept	PHOS^
Coefficient	0.00014465	0.7864023
Standard Error	2.8443E-05	0.0165659
Lower 95% CI	8.8863E-05	0.7539121
Upper 95% CI	0.00020043	0.8188925

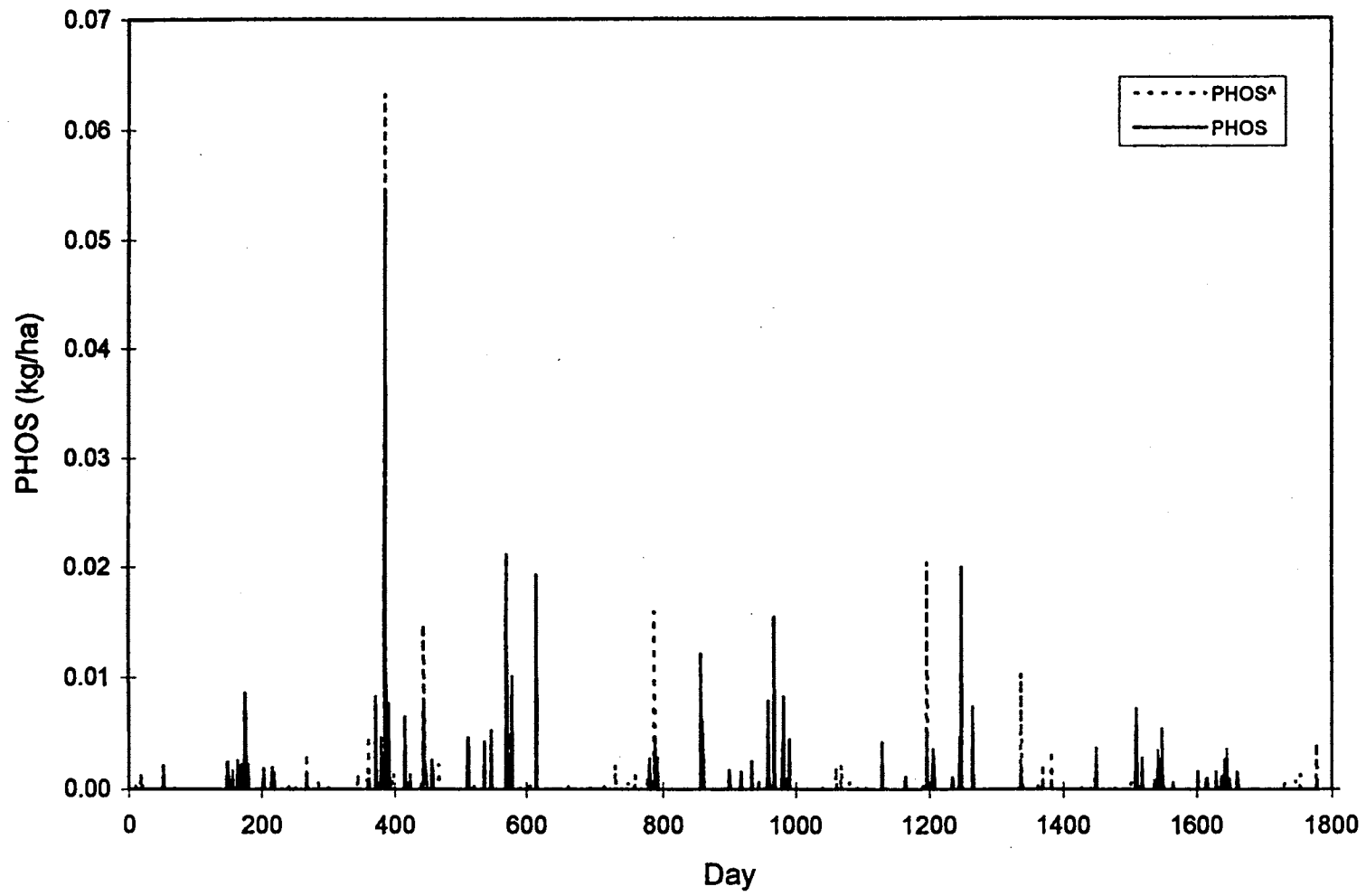
Let alpha = 0.05

Test statistic = 1.96

Ho: a equal to 0 ; Ha: a not equal to 0
 $t = (0.0001446 - 0) / 0.00002844 = 5.08$
 reject Ho: a equal to 0

Ho: b equal to 1 ; Ha: b not equal to 1
 $t = (0.786402 - 1) / 0.016566 = -12.89$
 reject Ho: b equal to 1

Daily PHOS; 83-88; WS-III



Results of Model Performance Evaluation
 Calibration for Nitrate-Nitrogen (NO3N)
 Daily Model Output
 Entire Data Set
 WS-III

Statistics for Linear Regression Analysis

Statistic	Value
Multiple R	0.38687448
R Square	0.14967186
Adj. R Square	0.14920593
Standard Error	0.00027919
Observations	1827

ANOVA for Linear Regression Analysis

	df	SS	MS	F	Significance of F
Regression	1	2.504E-05	2.5E-05	321.2303	2.69194E-66
Residual	1825	0.0001423	7.79E-08		
Total	1826	0.0001673			

Coefficients

	Intercept	NO3N ^A
Coefficient	2.1777E-05	0.410213
Standard Error	6.6458E-06	0.0228877
Lower 95% CI	8.7432E-06	0.3653243
Upper 95% CI	3.4811E-05	0.4551018

Let alpha = 0.05

Test statistic = 1.96

Ho: a equal to 0 ; Ha: a not equal to 0

$t = (0.00002178 - 0) / 0.000006646 = 3.28$

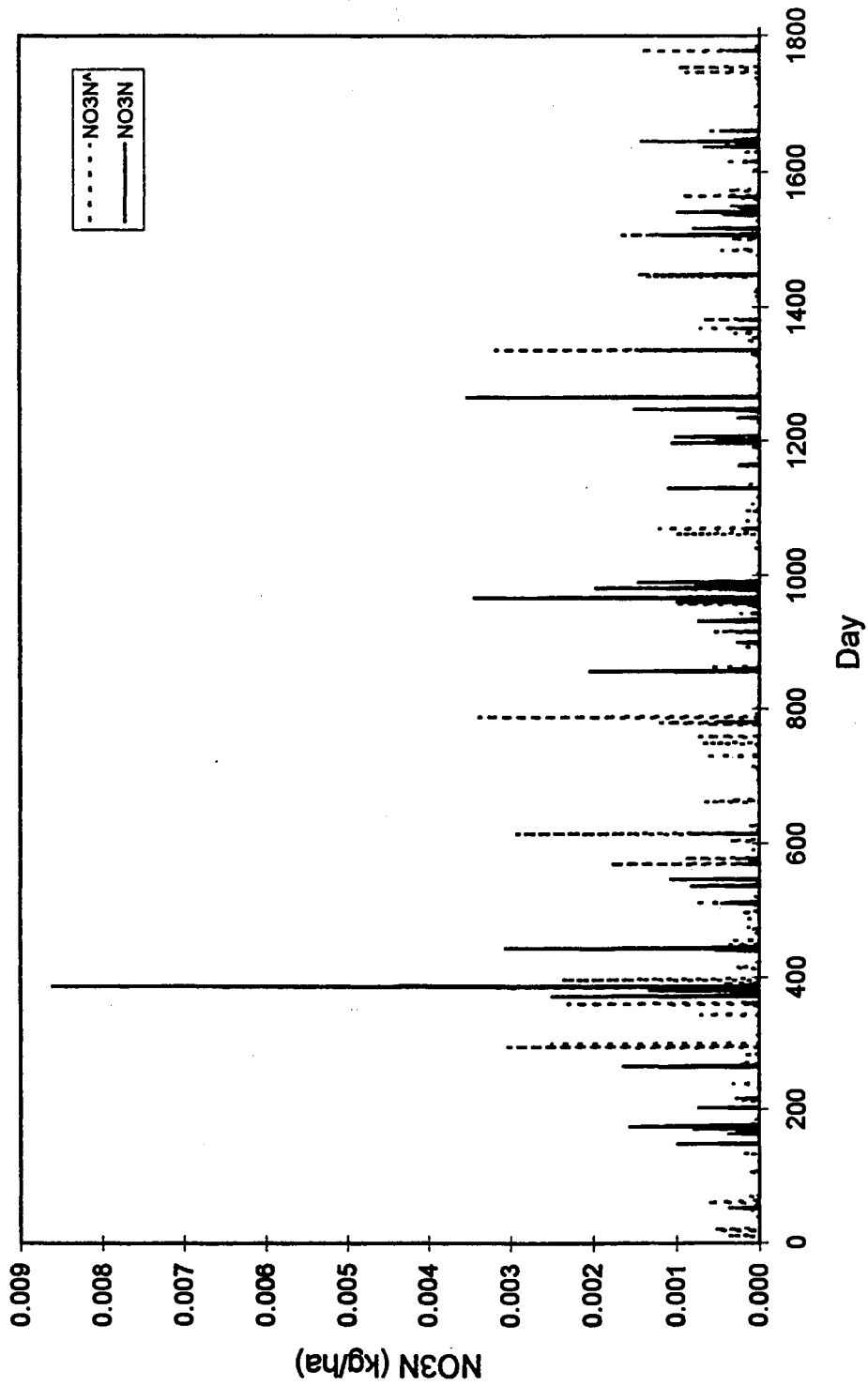
reject Ho: a equal to 0

Ho: b equal to 1 ; Ha: b not equal to 1

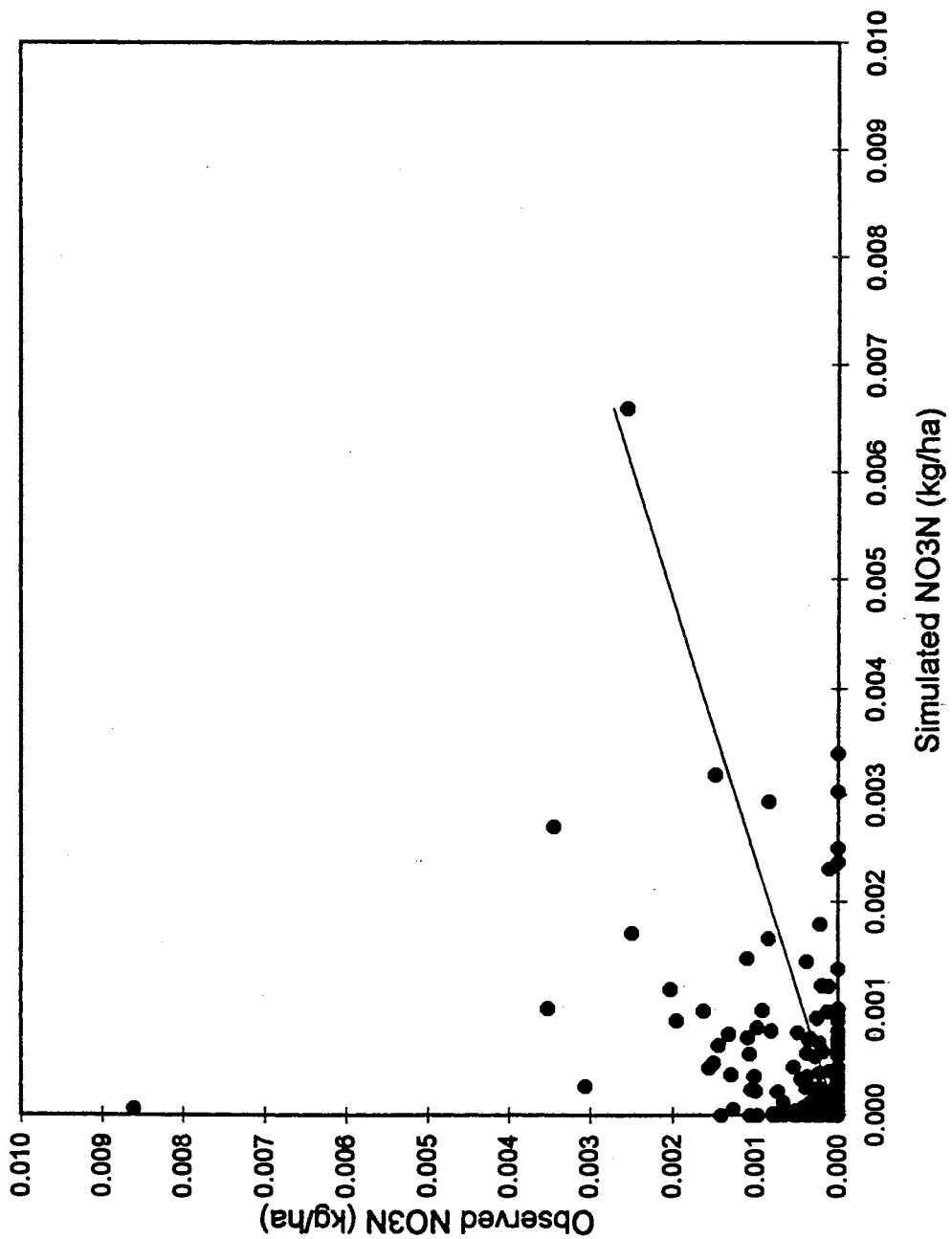
$t = (0.410213 - 1) / 0.022888 = -25.77$

reject Ho: b equal to 1

Daily NO3N; 83-88; WS-III



Daily NO3N; 83-88; WS-III



VITA 

Kenneth Wilburn Tate

Candidate for the Degree of

Doctor of Philosophy

Thesis: A STOCHASTIC FRAMEWORK FOR EVALUATING FOREST
MANAGEMENT IMPACTS ON WATER QUALITY FROM
WATERSHEDS IN THE OUACHITA MOUNTAINS

Major Field: Environmental Science

Biographical:

Personal Data: Born in Castro Valley, California, on May 27, 1967, the son
of Kenneth E. and Carolyn J. Tate.

Education: Graduated from Norman High School, Norman, OK in May 1985;
received Bachelor of Science and Master of Science degree in Agronomy
from Oklahoma State University, Stillwater, Oklahoma in May 1989 and
December 1991, respectively. Completed the requirements for the Doctor of
Philosophy degree with a major in Environmental Science at Oklahoma
State University in May 1995.

Professional Experience: Senior Agriculturist, Department of Agronomy,
Oklahoma State University, August 1989 to November 1991.

Professional Memberships: Society for Range Management